AD-A151 908 MULTIVARIABLE CONTROL LAW DESIGN FOR THE AFTI/F-16 WITH A FAILED CONTROL SURFACE(U) AIR FORCE INST OF TECH WRIGHT-PATTERSON AFB OH SCHOOL OF ENGI.. R A ESLINGER 1/4

UNCLASSIFIED DEC 84 AFIT/GE/ENG/84D-28 F/G 1/2 NL

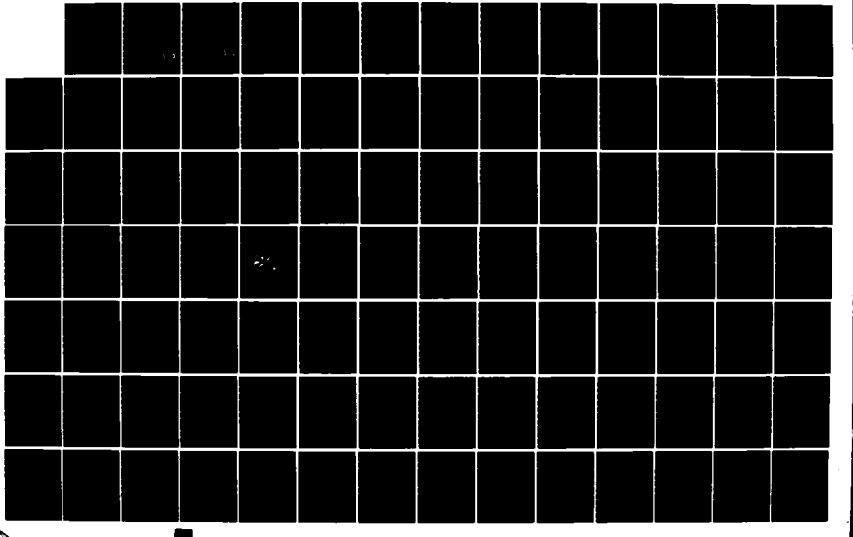

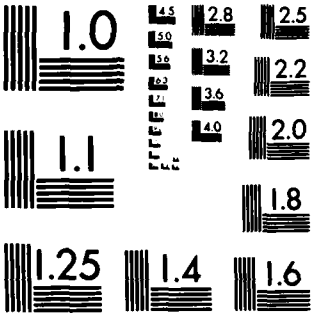

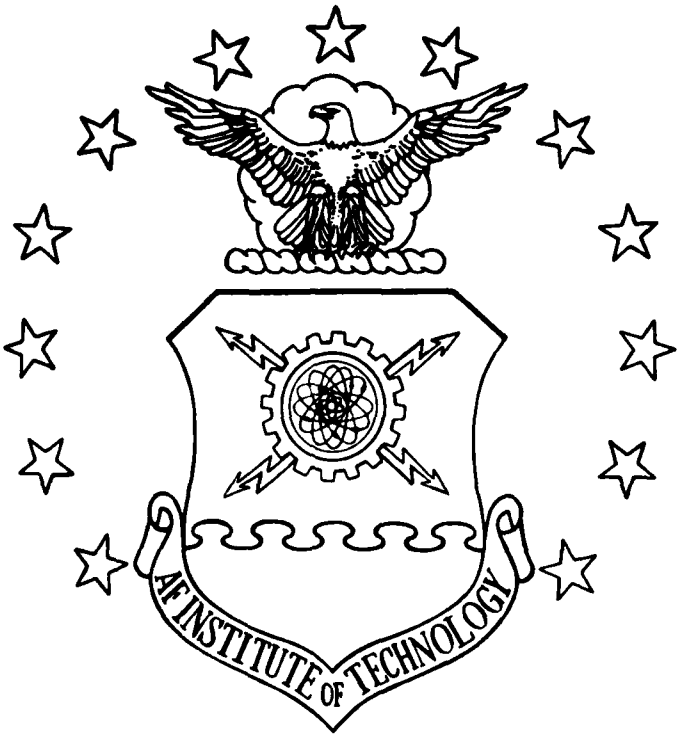

MULTIVARIABLE CONTROL LAW DESIGN FOR THE AFTI/F-16 WITH A FAILED CONTROL SURFACE

THESIS

AFIT/GE/ENG/84D-28 Robert A. Eslinger
2nd Lt USA

DEPARTMENT OF THE AIR FORCE
AIR UNIVERSITY
AIR FORCE INSTITUTE OF TECHNOLOGY

Wright-Patterson Air Force Base, Ohio

AFIT/GE/ENG/84D-28

MULTIVARIABLE CONTROL LAW DESIGN FOR THE AFTI/F-16 WITH A FAILED CONTROL SURFACE

THESIS

AFIT/GE/ENG/84D-28 Robert A. Eslinger
2nd Lt USAF

Approved for public release; distribution unlimited

AFIT/GE/ENG/84D-28

MULTIVARIABLE CONTROL LAW DESIGN FOR THE AFTI/F-16 WITH A FAILED CONTROL SURFACE

THESIS

Presented to the Faculty of the School of Engineering
of the Air Force Institute of Technology
Air University
In Partial Fulfillment of the
Requirements for the Degree of
Master of Science in Electrical Engineering

by
Robert A. Eslinger, B.S.
2nd Lt USAF
Graduate Electrical Engineer
December 1984

Preface

In searching for a thesis topic I found that there is a great interest within the Air Force Flight Dynamics Laboratory at Wright-Patterson AFB in the concept of self-repairing flight control. This concept not only holds promise for a more efficient and cost effective fighting force, but also has the potential for saving the lives of many pilots. It is hoped that the results of this thesis can be of use to the Flight Dynamics Laboratory in reaching the goal of designing self-repairing flight control systems.

There are several people who deserve thanks for providing guidance, expertise, and their time in helping with this thesis effort. These people include: my thesis reader, Dr. Robert Calico, of the Air Force Institute of Technology; Mr. Brian VanVliet of the AFTI/F-16 Program Office; Captain Mike Masi of the Flight Dynamics Laboratory; and Lieutenant Brian Mayhew of the Foreign Technology Division (a recent graduate of the Air Force Institute of Technology). I would especially like to thank my advisor, Dr. John D'Azzo, and my sponsor, Mr. A. Finley Barfield, for the excellent help and guidance they provided.

Finally, I would like to pay tribute to my family. My wife, Tammi, supported me throughout the thesis effort and spent many hours in helping to prepare the final draft. Our three month old son, Allen, has been a joy and has provided

many happy diversions form the thesis work. I wish to express my love and thanks to both of them.

Robert A. Eslinger

Table of Contents

List of Figures

List of Tables

List of Symbols

$\underline{A}$	Continuous-time plant matrix
$A_{n_{CG}}$	Normal acceleration at center of gravity
A_{n_p}	Normal acceleration at pilot's station
$A_{y_{CG}}$	Side acceleration at center of gravity
A_{y_p}	Side acceleration at pilot's station
$A_{z_{CG}}$	Normal acceleration at center of gravity in z direction
α	angle of attack
α_T	Trim angle of attack
$\bar{\alpha}$	Ratio of proportional to integral feedback
$\underline{B}$	Continuous-time input matrix
b	Wing span
β	sideslip angle
$\underline{C}$	Continuous-time output matrix
c	Mean aerodynamic cord
CG	Center of gravity
C_D	Nondimensional coefficient of drag along velocity vector
C_{D_α}	Nondimensional variation of drag with angle of attack
C_{D_δ}	Nondimensional variation of drag with control surface deflections
C_{D_u}	Nondimensional variation of drag with forward velocity
C_L	Nondimensional variation of lift normal to velocity vector

C_{L_α} Nondimensional variation of lift with angle of attack

$C_{L_{\dot{\alpha}}}$ Nondimensional variation of lift with rate of change of angle of attack

C_{L_δ} Nondimensional variation of lift with control surface deflections

C_{L_0} Nondimensional coefficient of lift at zero angle of attack

C_{L_q} Nondimensional variation of lift with pitch rate

C_{L_β} Nondimensional variation of rolling moment with sideslip angle

C_{ℓ_δ} Nondimensional variation of rolling moment with control surface deflections

C_{ℓ_p} Nondimensional variation of rolling moment with roll rate

C_{ℓ_r} Nondimensional variation of rolling moment with yaw rate

C_m Nondimensional coefficient of pitching moment

C_{m_α} Nondimensional variation of pitching moment with angle of attack

C_{m_δ} Nondimensional variation of pitching moment with control surface deflections

C_{m_0} Nondimensional coefficient of pitching moment at zero angle of attack

C_{m_q} Nondimensional variation of pitching moment with pitch rate

C_{m_u} Nondimensional variation of pitching moment with forward velocity

C_{n_β} Nondimensional variation of yawing moment with sideslip angle

C_{n_δ} Nondimensional variation of yawing moment with control surface deflections

C_{n_p} Nondimensional variation of yawing moment with roll rate

cos	Cosine
C_x	Nondimensional x-force coefficient
C_{x_α}	Nondimensional variation of x-force with angle of attack
C_{x_δ}	Nondimensional variation of x-force with control surface deflections
C_{x_q}	Nondimensional variation of x-force with pitch rate
C_{x_u}	Nondimensional variation of x-force with forward velocity
C_{y_β}	Nondimensional variation of y-force with sideslip angle
C_{y_δ}	Nondimensional variation of y-force with control surface deflections
C_{y_p}	Nondimensional variation of y-force with roll rate
C_{y_r}	Nondimensional variation of y-force with yaw rate
C_z	Nondimensional z-force coefficient
C_{z_α}	Nondimensional variation of z-force with angle of attack
$C_{z_{\dot\alpha}}$	Nondimensional variation of z-force with rate of change of angle of attack
C_{z_δ}	Nondimensional variation of z-force with control surface deflections
C_{z_q}	Nondimensional variation of z-force with pitch rate
C_{z_u}	Nondimensional variation of z-force with forward velocity
$\underline{D}$	Continuous-time feedforward matrix
δa	Aileron deflection
δc	Canard deflection
δDF	Differential flaperon deflection

δDT	Differential horizontal tail deflection
δe	Elevator (symmetric horizontal tail) deflection
δf	Flap (symmetric flaperon) deflection
δr	Rudder deflection
δT	Change in thrust
ϵ	Weighting matrix multiplier
ft	Feet
F_y	Sideforce in y-body axis
F_z	Force in z-body axis
$F_{z_{CG}}$	z-force at center of gravity
g	Gravity constant (32.2 ft/sec^2)
I_x	Moment of inertia about x-axis
I_y	Moment of inertia about y-axis
I_z	Moment of inertia about z-axis
I_{xz}	Product of inertia about xz-axis
$\underline{K}_0$	Proportional control law feedback matrix
$\underline{K}_1$	Integral control law feedback matrix
Lat	Lateral
lbs	Pounds
Long	Longitudinal
ℓ	Number of outputs, left
ℓ_x	Distance form CG to sensor location along x-axis
ℓ_y	Distance from CG to sensor location along y-axis
ℓ_z	Distance from CG to sensor location along z-axis
L_β	Dimensional variation of rolling moment with sideslip angle

L_δ Dimensional variation of rolling moment with control surface deflections

L_p Dimensional variation of rolling moment with roll rate

L_r Dimensional variation of rolling moment with yaw rate

$\underline{M}$ Measurement matrix

m Aircraft mass, number of inputs

M_α Dimensional variation of pitching moment with angle of attack

$M_{\dot{\alpha}}$ Dimensional variation of pitching moment with rate of change of angle of attack

M_q Dimensional variation of pitching moment with pitch rate

M_θ Dimensional variation of pitching moment with pitch angle

n Number of states

N_β Dimensional variation of yawing moment with sideslip angle

N_δ Dimensional variation of yawing moment with control surface deflections

N_r Dimensional variation of yawing moment with yaw rate

N_p Dimensional variation of yawing moment with roll rate

p Roll rate

q Pitch rate

$\bar{q}$ Dynamic pressure

r Yaw rate

S Surface area

s Laplace operator

sec Seconds

sin Sine

σ Elements of the weighting matrix

$\underline{\Sigma}$ Gain weighting matrix

t Total control surface

T Sampling period, Thrust

U Velocity along x-axis

$\underline{u}$ Input vector

$\underline{v}$ Command input vector

V_T Trimmed Forward Velocity

W Aircraft weight

$\underline{x}$ State vector

X_α Dimensional variation of x-force with angle of attack

$X_{\dot{\alpha}}$ Dimensional variation of x-force with rate of change of angle of attack

X_δ Dimensional variation of x-force with control surface deflections

X_q Dimensional variation of x-force with pitch rate

X_u Dimensional variation of x-force with forward velocity

$\underline{Y}$ Output vector

Y_β Dimensional variation of y-force with sideslip angle

Y_δ Dimensional variation of y-force with control surface deflections

Y_p Dimensional variation of y-force with roll rate

Y_r Dimensional variation of y-force with yaw rate

Z_α Dimensional variation of z-force with angle of attack

$Z_{\dot{\alpha}}$ Dimensional variation of z-force with rate of change of angle of attack

Z_δ Dimensional variation of z-force with control surface deflections

Z_q Dimensional variation of z-force with pitch rate

Z_u Dimensional variation of z-force with forward velocity

Z_t	Transmission zeros
$Z_{1,2}$	Finite system roots
Z_3	Infinite system roots
θ	Pitch angle
ϕ	Roll angle
ψ	Yaw angle
γ	Flight path angle

Abstract

Two linearized models containing coupled aircraft equations are developed for the AFTI/F-16. The first is a model of the healthy aircraft with all control surfaces intact, and the second is a model of the aircraft with a free-floating right horizontal tail and all other surfaces operational.

The multivariable design technique of Professor Brian Porter and the computer program MULTI are first used to design control laws for the healthy model. The control laws are tailored to perform seven maneuvers at four flight conditions. Maximum maneuvers are commanded to yield maximum control surface deflections.

The same control law designs are then applied to the model with a failed right horizontal tail, and the performance is evaluated. Some maneuvers require modifications to the designs or lowered maximum maneuver requirements to avoid overshooting the deflection limits of the operational control surfaces.

Simulation responses are presented for both the healthy and failure aircraft models. Generally, when the right horizontal tail fails, the left horizontal tail assumes primary pitch control and the flaperons take over complete roll control. The flaperons, rudder, and canards deflect to counter the rolling and yawing moments produced by the left

horizontal tail deflection.

The design process used in the study is applicable to other control surface failures. Recommendations are presented for future study.

MULTIVARIABLE CONTROL LAW DESIGN FOR THE AFTI/F-16 WITH A FAILED CONTROL SURFACE

I. Introduction

I-1. Background

In recent years much attention has been directed towards the design of flight control laws which maintain aircraft stability after a control surface failure. This topic is of special interest to the Air Force because its aircraft may be required to fly in hostile environments where ground fire, air-to-air missiles, or other hazards may damage control surfaces. More specifically, the Air Force Flight Dynamics Laboratory at Wright-Patterson Air Force Base has begun a program which stresses the need for control laws that can handle surface failures in future aircraft designs.

The concept behind the flight Dynamics Laboratory's program is called "self-repairing flight control". This concept promises benefits to the Air Force by improving safety for the pilots and by increasing aircraft availability in wartime. With self-repairing control an aircraft will be able to continue its primary mission, or take on a secondary mission, even with damaged control surfaces or failed actuators. Self-repairing control will greatly reduce the need for field maintenance, and allow deferment

of repair of minor damage. Self-repairing therefore increases aircraft availability and increases the possible number of sorties for each plane. Additionally, the concept will reduce the cost of aircraft systems by reducing the amount of hardware redundancy needed for safe flight (13:141-146).

As can be expected, self-repairing flight control is a broad concept that involves several engineering disciplines. Much work must be done in order to develop a self-repairing flight control system that performs the following necessary tasks. First, control surface failures must be detected and isolated in some way so that the system knows which surface has failed. Second, a way must be found to estimate the extent of the damage or failure. For example, damage to a surface can range from a small hole to complete destruction of the surface. Severe damage may threaten the safety of the pilot while slight damage may allow continuation of the mission but with degraded aircraft performance. Third, the flight control system must do something to minimize the effects of the damage. The system must at least keep the aircraft stable so that the pilot can fly back to friendly territory. Finally, the system must somehow inform the pilot of what has happened and what is the new status of the system (13:147).

Before too much time, effort, and money are spent on the first, second, and last tasks listed above, it is important to ascertain that the aircraft is capable of handling

control surface failures in the first place. Advanced aircraft designs, such as the AFTI/F-16, have Control Configured Vehicle (CCV) capabilities which enhance combat effectiveness by allowing the aircraft to perform unconventional maneuvers such as fuselage pointing and translation. The maneuvers are accomplished by the use of additional control surfaces, like canards, and by independent operation of left and right elevators and ailerons. In this way surfaces which previously could only affect longitudinal movements can now affect lateral motions, and vice versa. With these CCV capabilities, other control surfaces can apply the forces and moments needed for stability when one surface is missing or damaged.

While CCV capabilties offer outstanding payoffs in combat effectiveness and survivability, design of flight control laws for such aircraft becomes more difficult because of a large number of required feedback loops and the multiple input/output nature of the problem. Design is further complicated when considering the loss of a control surface because of cross-coupling between the longitudinal and lateral aircraft equations. The multivariable, high-gain, error actuated design technique of Professor Brian Porter from the University of Salford, England, is of interest to the Air Force Flight Dynamics Laboratory as a technique for handling CCV designs. Professor Porter's design method is outlined in Appendix A.

I-2. Problem

Loss of a control surface may cause instability and degraded performance in modern air superiority aircraft unless the flight control system is designed to handle such a change in the aircraft's configuration. The purpose of this research is to present a technique for evaluating the performance of an aircraft after a control surface failure has occurred. Control laws are developed for a healthy aircraft model using the Porter technique, and then new control laws are designed, also using the Porter technique, to provide maximum performance with a particular surface failure.

I-3. Scope

The control surface failure considered in this study is a free-floating right horizontal tail half. The failed surface is assumed free-floating so that it does not create forces and moments on the aircraft. Although this investigation is limited to one control surface failure, the modeling and design procedures used can be applied to other failed surfaces.

Aircraft performance is evaluated at four flight conditions: subsonic (0.6 Mach at 30,000 feet), transonic (0.9 Mach at 20,000 feet), supersonic (1.6 Mach at 30,000 feet), and landing approach (0.3 Mach at 30 feet). These flight conditions are chosen because they sample a variety of points in the aircraft's flight envelope. Seven

maneuvers are considered in this study for the evaluation of aircraft performance. The maneuvers are: g-command, pitch pointing, longitudinal translation, roll, sideforce, yaw pointing, and lateral translation. These maneuvers are described in detail in Chapter IV.

I-4. Assumptions

For most preliminary designs using linearized perturbation equations the longitudinal and lateral equations of motion are considered to be decoupled. However, in this study the lateral and longitudinal equations are coupled from the start because an unsymmetrical control surface failure causes cross-coupling between the two sets of equations.

The engine thrust model, discussed in Chapter II, is assumed to be a first order lag and is included only to hold the forward velocity constant during maneuvering. Although two vertical canards are present on the AFTI/F-16, the canards are considered to be one surface in order to simplify the designs. The remaining assumptions are similar to those used in a recent thesis by Mr. Finley Barfield (4:6) and are listed below.

* The aircraft is a rigid body with constant mass.
* The atmosphere is fixed with respect to the earth.
* The earth's surface is an inertial reference frame.
* Linearization about an operating condition is valid for preliminary aircraft models.

* Aerodynamics are constant for Mach and altitude.

The constant mass assumption is valid because the system responses occur over a relatively short period of time. The rigid body assumption is valid as long as the resulting design bandwidths sufficiently limit noise due to structural interactions. The other assumptions greatly simplify the design and are widely accepted in preliminary design efforts. Further investigations can take into account the effects of noise and wind gusts, but these effects are not considered in this study.

I-5. Approach

The AFTI/F-16 is chosen for this study because some control laws for the healthy aircraft have been developed in Barfield's thesis (4), and because most of the needed information on the aircraft is readily available from the Flight Dynamics Laboritory (1). Two linear models, one for the healthy aircraft and one for the aircraft with a failed right horizontal tail, are developed for the AFTI/F-16 and placed in state space form.

Control laws are designed, using the Porter technique and the computer program MULTI, for the healthy aircraft model at the four flight conditions. The designs are tailored to the maneuvers performed at each flight condition. The designs are then applied to the failure model, and the aircraft performance is evaluated. If necessary, the control laws are redesigned to achieve optimal

performance and to keep surface deflections within the appropriate limits.

I-6. Overview

Appendix A summarizes the theory of the multivariable design technique of Professor Porter, and Appendix B lists the equations used in developing the aircraft models. The actual models used for each flight condition are given in Appendix C which also presents data files used with the computer program MULTI.

Chapter II begins with a description of the AFTI/F-16 aircraft and developes the healthy and failed models used in this study. Actuator and thrust models are also discussed in Chapter II. Chapter III describes in detail the process used in designing the control laws for this study, and Chapter IV describes the maneuvers considered.

The simulation responses for the transonic flight condition are presented in Chapter V, and the simulation responses for the remaining flight conditions are given in Appendix D. Chapter VI concludes the study with a general discussion of results and recommendations for future study.

II. Aircraft Description and Models

II-1. AFTI/F-16 Description

The AFTI (Advanced Fighter Technology Integration)/F-16 aircraft, shown in Figure 2-1, is an F-16A air superiority fighter modified to be a testbed for evaluating new technologies (3:1). The modifications include: addition of two vertical canards mounted on the engine inlet; modifications to the functions of existing control surfaces by allowing independent motion of the trailing edge flaps and independent motion of the horizontal tail halves; and addition of a redundant, digital fly-by-wire flight control system. The AFTI/F-16 is not an operational fighter, but the technologies tested on it will be employed in the Air Force's future Advanced Tactical Fighter (ATF) aircraft.

By design the unaugmented aircraft is statically unstable in the longitudinal axis for subsonic flight. This

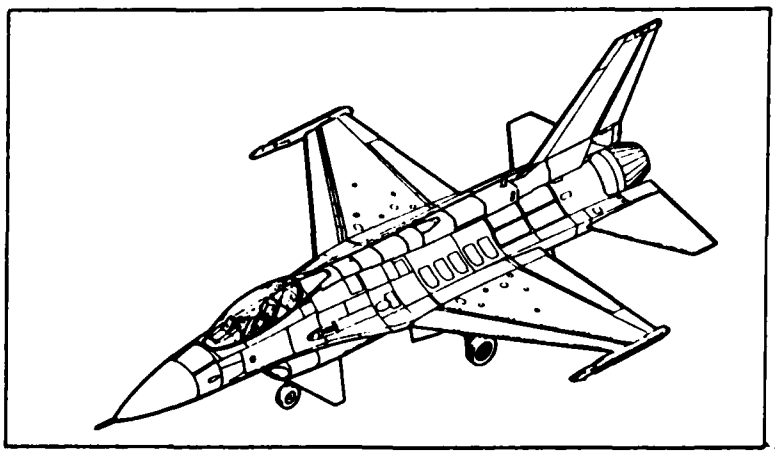

Figure 2-1: The AFTI/F-16
Source: (1)

is because the center of gravity is located behind the aerodynamic center of the aircraft. The instability, manifested by an unstable short period root, allows the aircraft to withstand higher load factors and reduces drag. Also, the Dutch roll mode of the aircraft is lightly damped. It is the primary purpose of the flight control system to stabilize the aircraft longitudinally and improve the Dutch roll damping (4:29-31).

Like other fighters in the Air Force inventory, the AFTI/F-16 can perform conventional maneuvers, such as pitching longitudinally, rolling laterally, and turning with zero sideslip (coordinated turn). AFTI/F-16 pilots can also command maneuvers that require decoupling of the aircraft's forces and moments which cannot be commanded in conventional fighters, like pitch-pointing, yaw pointing, and lateral and longitudinal translation. Conventional and decoupled maneuvers can be blended to give the AFTI/F-16 a versatile inventory of maneuvers.

The control surfaces used in maneuvering the aircraft are shown in Figure 2-2. The surfaces that this thesis is concerned with are shown in heavy black and include the left and right horizontal tail halves, left and right flaperons, the rudder, and the left and right canards. The horizontal tail halves can deflect symmetrically as elevators to pitch the aircraft, or deflect asymmetrically to augment rolling. Similarly, the flaperons also have a dual function. They can deflect symmetrically as flaps or asymmetrically as

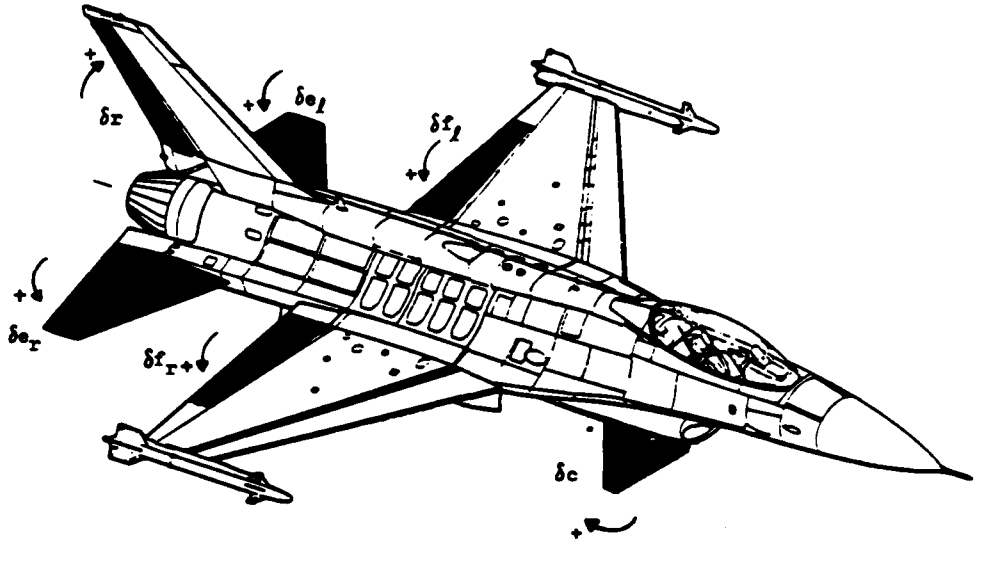

+δDF is defined as: δf_r down, δf_ℓ up

+δDT is defined as: δe_r down, δe_ℓ up

Figure 2-2: AFTI/F-16 Control Surfaces and Definition of Positive Deflections

Source: (1)

ailerons for primary roll control (4:29). For the purposes of this study, the canards are considered to be one surface that provides sideforces on the aircraft. Actually, the canards can also be used in a snowplow configuration as a speed brake. The rudder is used for yawing as on conventional aircraft. Figure 2-2 defines the positive direction of surface deflections.

The AFTI/F-16's maneuvers are tailored to primary mission tasks which are divided into four major configurations of the flight control system. The first configuration is the normal mode which is used for takeoff, cruise, landing, and air refueling. The second, air-to-air gunnery mode, lets the pilot command precise pointing to targets and evasive maneuvering. The air-to-surface gunnery mode, the third configuration, provides pointing for strafing ground targets as well as evasive maneuvering for greater survivability. The last configuration of the flight control system, air-to-surface bombing mode, allows the pilot to precisely control the aircraft's velocity vector for accurate bombing (3:4). This study investigates the design of control laws for the air-to-air gunnery mode.

The many advanced technologies incorporated into the AFTI/F-16 set it apart from conventional fighters. Lessons learned through the use of the AFTI/F-16 testbed will aid the Air Force in developing its next generation of fighter aircraft.

II-2. Aircraft Models

Reference 4 is the main source of information for the development of the aircraft model for this study. The aircraft is modeled by a set of first order differential equations in the state space form

$$\dot{\underline{x}} = \underline{A}\underline{x} + \underline{B}\underline{u} \qquad (2\text{-}1)$$

The state equations are derived from the aircraft equations of motion which consist of forces at the center of gravity (CG) and moments. The detailed derivations of the state perturbation equations are given in Reference 4.

Equation (2-2) is the state space model for the healthy aircraft, where the primed terms are dimensionalized derivatives in the body axis. The equations used for calculating the primed derivatives are listed in Appendix B. The body axis reference frame is chosen for the design because all accelerations and rates measured for feedback signals are sensed in the body axis, and because pilots desire to command body accelerations and rates that they can feel (6:10). Figure 2-3 defines the body axis as well as positive directions of forces, moments, and angles.

For the healthy aircraft model of Equation (2-2) the surfaces are defined as follows:

δe_t is the total elevator where both horizontal tail halves deflect symmetrically

δf_t is the total flap where both flaperons deflect symmetrically

$$
\begin{bmatrix} \dot{\theta} \\ \dot{u} \\ \dot{\alpha} \\ \dot{q} \\ \dot{\phi} \\ \dot{\beta} \\ \dot{p} \\ \dot{r} \end{bmatrix} =
\begin{bmatrix}
0 & 0 & 0 & 1 & 0 & 0 & 0 & 0 \\
X'_\theta & X'_u & X'_\alpha & X'_q & 0 & 0 & 0 & 0 \\
Z'_\theta & Z'_u & Z'_\alpha & Z'_q & 0 & 0 & 0 & 0 \\
M'_\theta & M'_u & M'_\alpha & M'_q & 0 & 0 & 0 & 0 \\
0 & 0 & 0 & 0 & 0 & 0 & 1 & 0 \\
0 & 0 & 0 & 0 & Y'_\phi & Y'_\beta & Y'_p & Y'_r \\
0 & 0 & 0 & 0 & 0 & L'_\beta & L'_p & L'_r \\
0 & 0 & 0 & 0 & 0 & N'_\beta & N'_p & N'_r
\end{bmatrix}
\begin{bmatrix} \theta \\ u \\ \alpha \\ q \\ \phi \\ \beta \\ p \\ r \end{bmatrix}
+
\begin{bmatrix}
0 & 0 & 0 & 0 & 0 & 0 \\
X'_{\delta e_t} & X'_{\delta f_t} & 0 & 0 & 0 & X'_{\delta T} \\
Z'_{\delta e_t} & Z'_{\delta f_t} & 0 & 0 & 0 & 0 \\
M'_{\delta e_t} & M'_{\delta f_t} & 0 & 0 & M'_{\delta c} & 0 \\
0 & 0 & 0 & 0 & 0 & 0 \\
0 & 0 & Y'_{\delta a} & Y'_{\delta r} & Y'_{\delta c} & 0 \\
0 & 0 & L'_{\delta a} & L'_{\delta r} & L'_{\delta c} & 0 \\
0 & 0 & N'_{\delta a} & N'_{\delta r} & N'_{\delta c} & 0
\end{bmatrix}
\begin{bmatrix} \delta e_t \\ \delta f_t \\ \delta a \\ \delta r \\ \delta c \\ \delta T \end{bmatrix}
\qquad (2\text{-}2)
$$

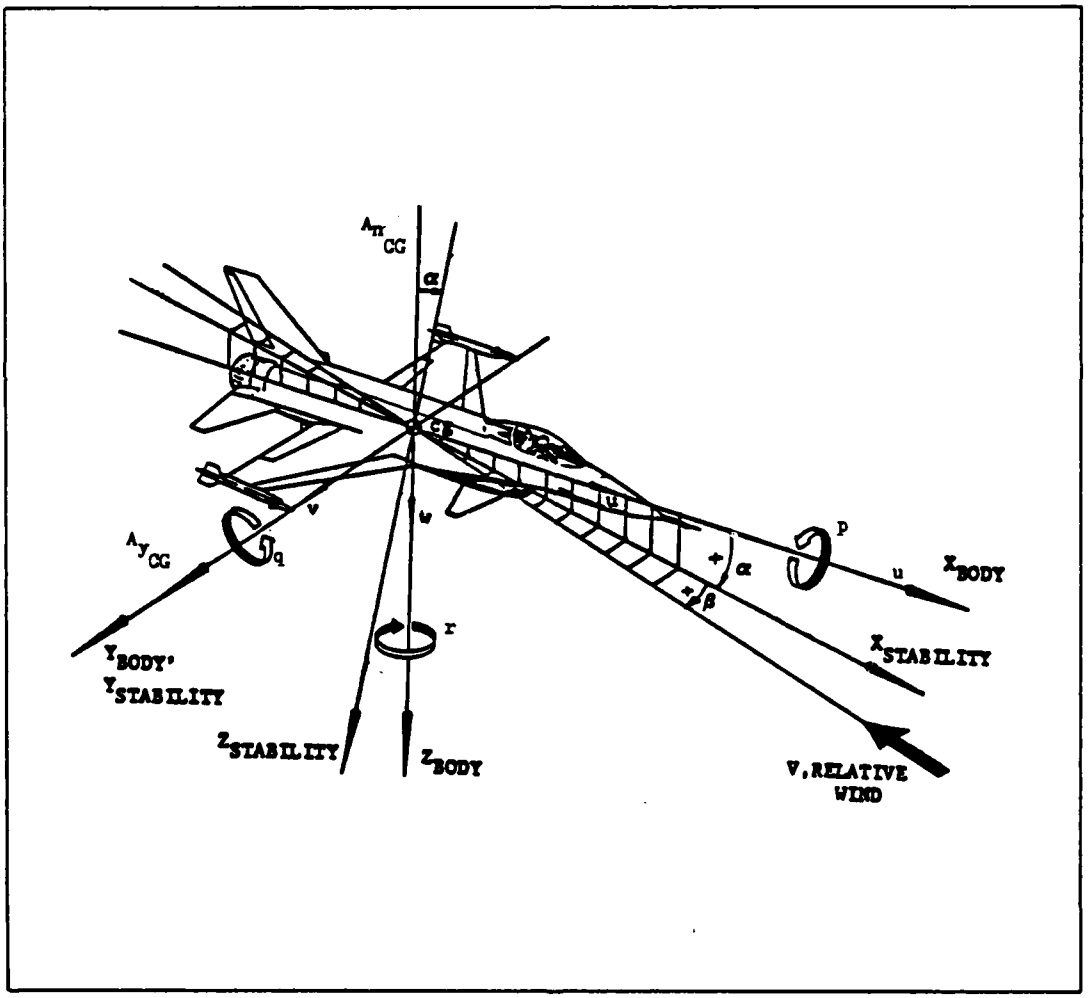

Figure 2-3: Positive Directions of Forces, Moments, and Angles in the Body Reference Frame

Source: (1)

δa is the combination of differential flaperon (δDF) and differential tail (δDT) deflections

δr is the rudder deflection

δc is the total symmetrical canard deflection

The aileron deflection, δa, demonstrates that the differential tail augments the flaperons in rolling the aircraft. The equation governing the aileron deflection is

$$a = \delta DF + 0.25(\delta DT) \qquad (2\text{-}3)$$

where 0.25 is an arbitrary constant corresponding to the reciprocal of a gain on the differential horizontal tail actuators. If the constant is decreased the actuator gain increases, which increases the contribution of the differential tail in rolling the aircraft. The reason for modeling the aileron in this way, and not splitting the flaperons and tail, is due to a lack of necessary feedback signals. This is discussed in detail in the next chapter.

Equation (2-4) is the model for the aircraft with a failed right horizontal tail half. In this model the flaperons and tail are split with the control surfaces defined as follows:

δe_ℓ is the left elevator (left horizontal tail half) deflection

δf_r is the right flaperon deflection

δf_ℓ is the left flaperon deflection

δr is the rudder deflection

δc is the total symmetrical canard deflection

$$\begin{bmatrix} \dot{\theta} \\ \dot{u} \\ \dot{\alpha} \\ \dot{q} \\ \dot{\phi} \\ \dot{\beta} \\ \dot{p} \\ \dot{r} \end{bmatrix} = \begin{bmatrix} 0 & 0 & 0 & 1 & 0 & 0 & 0 & 0 \\ X'_\theta & X'_u & X'_\alpha & X'_q & 0 & 0 & 0 & 0 \\ Z'_\theta & Z'_u & Z'_\alpha & Z'_q & 0 & 0 & 0 & 0 \\ M'_\theta & M'_u & M'_\alpha & M'_q & 0 & 0 & 0 & 0 \\ 0 & 0 & 0 & 0 & 0 & 0 & 1 & 0 \\ 0 & 0 & 0 & 0 & Y'_\phi & Y'_\beta & Y'_p & Y'_r \\ 0 & 0 & 0 & 0 & 0 & L'_\beta & L'_p & L'_r \\ 0 & 0 & 0 & 0 & 0 & N'_\beta & N'_p & N'_r \end{bmatrix} \begin{bmatrix} \theta \\ u \\ \alpha \\ q \\ \phi \\ \beta \\ p \\ r \end{bmatrix} + \begin{bmatrix} 0 & 0 & 0 & 0 & 0 & 0 \\ X'_{\delta e_\ell} & X'_{\delta f_r} & X'_{\delta f_\ell} & 0 & 0 & X'_{\delta T} \\ Z'_{\delta e_\ell} & Z'_{\delta f_r} & Z'_{\delta f_\ell} & 0 & 0 & 0 \\ M'_{\delta e_\ell} & M'_{\delta f_r} & M'_{\delta f_\ell} & 0 & M'_{\delta c} & 0 \\ 0 & 0 & 0 & 0 & 0 & 0 \\ Y'_{\delta e_\ell} & Y'_{\delta f_r} & Y'_{\delta f_\ell} & Y'_{\delta r} & Y'_{\delta c} & 0 \\ L'_{\delta e_\ell} & L'_{\delta f_r} & L'_{\delta f_\ell} & L'_{\delta r} & L'_{\delta c} & 0 \\ N'_{\delta e_\ell} & N'_{\delta f_r} & N'_{\delta f_\ell} & N'_{\delta r} & N'_{\delta c} & 0 \end{bmatrix} \begin{bmatrix} \delta e_\ell \\ \delta f_r \\ \delta f_\ell \\ \delta r \\ \delta c \\ \delta T \end{bmatrix} \qquad (2\text{-}4)$$

A simple model for engine thrust is included in both the healthy aircraft and failure models to prevent the aircraft velocity from bleeding off during maneuvers. It is assumed that the thrust is aligned with the x-axis so that no moments are created, and that the engine response is modeled by a simple first order lag, $1/(s + 1)$.

Table 2-1 lists thrust data for each of the flight conditions considered in this thesis. The dimensionalized derivative, $X'_{\delta T}$, is calculated by subtracting the thrust required to trim the aircraft from the maximum thrust available at a given flight condition, and then dividing by the mass of the aircraft. For example, at 0.9 Mach, 20,000 feet

$$X'_{\delta T} = \frac{(16{,}500 - 3{,}932.6)}{652.733} \frac{\text{pounds}}{\text{slugs}} = 19.254 \text{ feet/second}^2$$

The change in thrust, δT, is measured in pounds of thrust.

TABLE 2-1

Thrust Data

Flight Condition (Mach/feet)	Maximum Thrust (pounds)	Trim Thrust (pounds)	$X'_{\delta T}$ (feet/sec^2)
0.3 / 30	19,000	4,449.7	22.291
0.6 / 30,000	9,000	2,110.7	10.555
0.9 / 20,000	16,500	3,932.6	19.254
1.6 / 30,000	20,500	15,780.8	7.230

Source: (1)

II-3. Output Vector

An output vector, $\underline{y}$, must be added to the models of Equations (2-2) and (2-4) in order to command maneuvers. The output vector used in Reference 4 is also chosen for this study because the vector elements are naturally commanded by the pilot when performing maneuvers, and because all the outputs can either be accurately measured or easily calculated from other measurements, which is necessary for feedback signals. The three longitudinal outputs commanded are forward velocity, pitch rate, and normal acceleration at the pilot's station, and the three lateral outputs are yaw rate, roll rate, and lateral acceleration at the pilot's station. Six outputs are required since there are six control element inputs in the aircraft models. Forward velocity is chosen as an output because it is directly affected by thrust.

The output vector is added to the state space aircraft models with an output matrix, $\underline{C}$, and a feed-forward matrix, $\underline{D}$. The aircraft models then take the form

$$\dot{\underline{x}} = \underline{Ax} + \underline{Bu}$$

$$\underline{y} = \underline{Cx} + \underline{Du} \qquad (2\text{-}5)$$

Because forward velocity, pitch rate, roll rate, and yaw rate are already state variables, they are easily added to the models by placing ones in the appropriate positions in the $\underline{C}$ matrix. The normal and lateral accelerations, however, are linear combinations of state equations and require

some derivation. Reference 4 is the source of information for deriving the acceleration equations.

An expression for the acceleration along the z axis at the center of gravity is found from the aircraft force equation

$$F_{z_{CG}} = m(\dot{W} + pV - qU - g\cos\theta\cos\phi) \tag{2-6}$$

thus

$$A_{z_{CG}} = \frac{F_{z_{CG}}}{m} = \dot{W} + pV - qU - g\cos\theta\cos\phi \tag{2-7}$$

Equation (2-7) is written as a perturbation equation

$$A_{z_{CG}} = Z_\alpha\alpha + Z_{\dot{\alpha}}\dot{\alpha} + Z_q q + Z_u u + (Z_{\delta e_t})\delta e_t + (Z_{\delta f_t})\delta f_t \tag{2-8}$$

where

$$Z_\alpha = \frac{\bar{q}S}{m} C_{z_\alpha} \tag{2-9}$$

$$Z_{\dot{\alpha}} = \frac{\bar{q}Sc}{2Um} C_{z_{\dot{\alpha}}} \approx 0 \tag{2-10}$$

$$Z_q = \frac{\bar{q}Sc}{2Um} C_{z_q} \tag{2-11}$$

$$Z_u = \frac{\bar{q}S}{mU} C_{z_u} \tag{2-12}$$

$$Z_{\delta e_t} = \frac{\bar{q}S}{m} C_{z_{\delta e_t}} \tag{2-13}$$

$$Z_{\delta f_t} = \frac{\bar{q}S}{m} C_{z_{\delta f_t}} \tag{2-14}$$

The two control surface derivatives, $Z_{\delta e_t}$ and $Z_{\delta f_t}$, are for the healthy aircraft model. For the failed right elevator model the control surface derivatives are $Z_{\delta e_\ell}$, $Z_{\delta f_r}$, and $Z_{\delta f_\ell}$ where

$$Z_{\delta e_\ell} = 0.5\ Z_{\delta e_t} \tag{2-15}$$

$$Z_{\delta f_r} = Z_{\delta f_\ell} = 0.5\ Z_{\delta f_t} \tag{2-16}$$

Equation (2-8) gives the acceleration in the z direction at the center of gravity, but the normal acceleration at the pilot's station is desired. Normal acceleration is in the minus z direction

$$A_{n_{CG}} = - A_{z_{CG}} \tag{2-17}$$

and acceleration at the pilot's station is determined from

$$A_{n_p} = A_{n_{CG}} - (\ell_x)(pr - \dot{q}) - (\ell_y)(rq + \dot{p}) + (\ell_z)(p^2 + q^2) \tag{2-18}$$

where ℓ_x, ℓ_y, and ℓ_z are distances in the body axis from the center of gravity to the pilot's station. Assuming small values for ℓ_y and ℓ_z, and a small contribution from lateral terms, Equation (2-18) reduces to

$$A_{n_p} = A_{n_{CG}} + (\ell_x)\dot{q} \tag{2-19}$$

or, from Equation (2-17),

$$A_{n_p} = (\ell_x)\dot{q} - A_{z_{CG}} \tag{2-20}$$

Substituting Equation (2-8) and the state equation for $\dot{q}$ into Equation (2-20), the normal acceleration at the pilot's station is given by

$$\begin{aligned} A_{n_p} = {} & (\ell_x M'_\theta)\theta + (\ell_x M'_u - Z_u)u + (\ell_x M'_\alpha - Z_\alpha)\alpha \\ & + (\ell_x M'_q - Z_q)q + (\ell_x M'_{\delta e_t} - Z_{\delta e_t})\delta e_t \\ & + (\ell_x M'_{\delta f_t} - Z_{\delta f_t})\delta f_t + (\ell_x M'_{\delta c})\delta c \end{aligned} \tag{2-21}$$

where the primed terms are defined in Appendix B, and ℓ_x is equal to 13.95 feet for the AFTI/F-16. Similarly, for the failed right elevator model

$$\begin{aligned} A_{n_p} = {} & (\ell_x M'_\theta)\theta + (\ell_x M'_u - Z_u)u + (\ell_x M'_\alpha - Z_\alpha)\alpha \\ & + (\ell_x M'_q - Z_q)q + (\ell_x M'_{\delta e_\ell} - Z_{\delta e_\ell})\delta e_\ell \\ & + (\ell_x M'_{\delta f_r} - Z_{\delta f_r})\delta f_r + (\ell_x M'_{\delta f_\ell} - Z_{\delta f_\ell})\delta f_\ell \\ & + (\ell_x M'_{\delta c})\delta c \end{aligned} \tag{2-22}$$

The equation for the lateral acceleration at the pilot's station is developed in a similar manner where

$$A_{y_p} = A_{y_{CG}} - (\ell_x)(pq - \dot{r}) - (\ell_y)(p^2 + r^2) + (\ell_z)(qr - \dot{p}) \quad (2\text{-}23)$$

can be reduced to

$$A_{y_p} = A_{y_{CG}} + (\ell_x)\dot{r} \quad (2\text{-}24)$$

For the healthy aircraft model the lateral acceleration at the pilot's station is given by

$$A_{y_p} = (\ell_x N'_\beta + Y_\beta)\beta + (\ell_x N'_p + Y_p)p + (\ell_x N'_r + Y_r)r + (\ell_x N'_{\delta a} + Y_{\delta a})\delta a + (\ell_x N'_{\delta r} + Y_{\delta r})\delta r + (\ell_x N'_{\delta c} + Y_{\delta c})\delta c \quad (2\text{-}25)$$

and for the failed right elevator

$$A_{y_p} = (\ell_x N'_\beta + Y_\beta)\beta + (\ell_x N'_p + Y_p)p + (\ell_x N'_r + Y_r)r + (\ell_x N'_{\delta e_\ell} + Y_{\delta e_\ell})\delta e_\ell + (\ell_x N'_{\delta f_r} + Y_{\delta f_r})\delta f_r + (\ell_x N'_{\delta f_\ell} + Y_{\delta f_\ell})\delta f_\ell + (\ell_x N'_{\delta r} + Y_{\delta r})\delta r + (\ell_x N'_{\delta c} + Y_{\delta c})\delta c \quad (2\text{-}26)$$

where the primed terms are defined in Appendix B, and the Y derivatives are given by

$$Y_\beta = \frac{\bar{q}S}{m} C_{Y_\beta} \quad (2\text{-}27)$$

$$Y_p = \frac{\bar{q}Sb}{2Um} C_{y_p} \quad (2\text{-}28)$$

$$Y_r = \frac{\bar{q}Sb}{2Um} C_{y_r} \quad (2\text{-}29)$$

$$Y_{\delta a} = \frac{\bar{q}S}{m} C_{y_{\delta a}} \quad (2\text{-}30)$$

$$Y_{\delta r} = \frac{\bar{q}S}{m} C_{y_{\delta r}} \quad (2\text{-}31)$$

$$Y_{\delta c} = \frac{\bar{q}S}{m} C_{y_{\delta c}} \quad (2\text{-}32)$$

$$Y_{\delta e_\ell} = -0.5\ (0.25)\ Y_{\delta DT} \quad (2\text{-}33)$$

$$Y_{\delta f_r} = 0.5\ Y_{\delta DF} \quad (2\text{-}34)$$

$$Y_{\delta f_\ell} = -0.5\ Y_{\delta DF} \quad (2\text{-}35)$$

Equations (2-21) and (2-25) are used to form the state space model of the output equation for the healthy aircraft given by Equation (2-36). The output equation for the failed right elevator model is given by Equation (2-37) which contains Equations (2-22) and (2-26).

The output state equations include a feed-forward matrix, $\underline{D}$, but the design technique does not allow for the feed-forward matrix. The $\underline{D}$ matrix is eliminated by including actuator states in the state space models. Reference 2 gives a fourth-order actuator model for all of the control surfaces (2: A-19, A-20):

$$\begin{bmatrix} u \\ A_{n_p} \\ q \\ A_{y_p} \\ p \\ r \end{bmatrix} = \begin{bmatrix} 0 & 1 & 0 & 0 & 0 & 0 & 0 & 0 \\ A_{n_\theta} & A_{n_u} & A_{n_\alpha} & A_{n_q} & 0 & 0 & 0 & 0 \\ 0 & 0 & 0 & 1 & 0 & 0 & 0 & 0 \\ 0 & 0 & 0 & 0 & 0 & A_{y_\beta} & A_{y_p}^* & A_{y_r} \\ 0 & 0 & 0 & 0 & 0 & 0 & 1 & 0 \\ 0 & 0 & 0 & 0 & 0 & 0 & 0 & 1 \end{bmatrix} \begin{bmatrix} \theta \\ u \\ \alpha \\ q \\ \phi \\ \beta \\ p \\ r \end{bmatrix} + \begin{bmatrix} 0 & 0 & 0 & 0 & 0 & 0 \\ A_{n_{\delta e_t}} & A_{n_{\delta f_t}} & 0 & 0 & A_{n_{\delta c}} & 0 \\ 0 & 0 & 0 & 0 & 0 & 0 \\ 0 & 0 & A_{y_{\delta a}} & A_{y_{\delta r}} & A_{y_{\delta c}} & 0 \\ 0 & 0 & 0 & 0 & 0 & 0 \\ 0 & 0 & 0 & 0 & 0 & 0 \end{bmatrix} \begin{bmatrix} \delta e_t \\ \delta f_t \\ \delta a \\ \delta r \\ \delta c \\ \delta T \end{bmatrix} \quad (2\text{-}36)$$

Note: The A_n and A_y terms in the matricies correspond to the expressions in parentheses in Equations (2-21) and (2-25). The starred term, $A_{y_p}^*$, is the coefficient of p, and is not the lateral acceleration at the pilot's station.

$$\begin{bmatrix} u \\ A_{n_p} \\ q \\ A_{y_p} \\ p \\ r \end{bmatrix} = \begin{bmatrix} 0 & 1 & 0 & 0 & 0 & 0 & 0 & 0 \\ A_{n_\theta} & A_{n_u} & A_{n_\alpha} & A_{n_q} & 0 & 0 & 0 & 0 \\ 0 & 0 & 0 & 1 & 0 & 0 & 0 & 0 \\ 0 & 0 & 0 & 0 & 0 & A_{y_\beta} & A_{y_p}^* & A_{y_r} \\ 0 & 0 & 0 & 0 & 0 & 0 & 1 & 0 \\ 0 & 0 & 0 & 0 & 0 & 0 & 0 & 1 \end{bmatrix} \begin{bmatrix} \theta \\ u \\ \alpha \\ q \\ \phi \\ \beta \\ p \\ r \end{bmatrix} + \begin{bmatrix} 0 & 0 & 0 & 0 & 0 & 0 \\ A_{n_{\delta e_\ell}} & A_{n_{\delta f_r}} & A_{n_{\delta f_\ell}} & 0 & A_{n_{\delta c}} & 0 \\ 0 & 0 & 0 & 0 & 0 & 0 \\ A_{y_{\delta e_\ell}} & A_{y_{\delta f_r}} & A_{y_{\delta f_\ell}} & A_{y_{\delta r}} & A_{y_{\delta c}} & 0 \\ 0 & 0 & 0 & 0 & 0 & 0 \\ 0 & 0 & 0 & 0 & 0 & 0 \end{bmatrix} \begin{bmatrix} \delta e_\ell \\ \delta f_r \\ \delta f_\ell \\ \delta r \\ \delta c \\ \delta T \end{bmatrix} \quad (2\text{-}37)$$

Note: The A_n and A_y terms in the matricies correspond to the expressions in parentheses in Equations (2-22) and (2-26). The starred term, $A_{y_p}^*$, is the coefficient of p, and is not the lateral acceleration at the pilot's station.

$$\frac{(20.2)(144.8)(71.4)^2}{(s + 20.2)(s + 144.8)[s^2 + 2(0.736)(71.4)s + 71.4^2]} \quad (2\text{-}38)$$

For this study, Equation (2-38) is approximated by a second-order model:

$$\frac{(20)(72)}{(s + 20)(s + 72)} \quad (2\text{-}39)$$

As shown in Figure 2-4, the frequency response of the second-order model agrees closely with that of the fourth-order model for frequencies less than 50 radians/second.

In order to add just one state to the model for each actuator, the simplified actuator model is split up with the 20/(s + 20) portion included in the state space aircraft model and the 72/(s + 72) portion added to the model externally with the program MULTI. The new actuator inputs are marked with a subscript, i, for "intermediate." Equation (2-40) forms the new state space model for the healthy aircraft. The new actuator inputs and an intermediate thrust input have been added to the original models in order to eliminate the feed-forward matrix. Equation (2-41) forms the new model for the aircraft with a failed right elevator.

The next chapter discusses in detail the design procedure using the two aircraft models developed here. Problems encountered in the design process are also discussed.

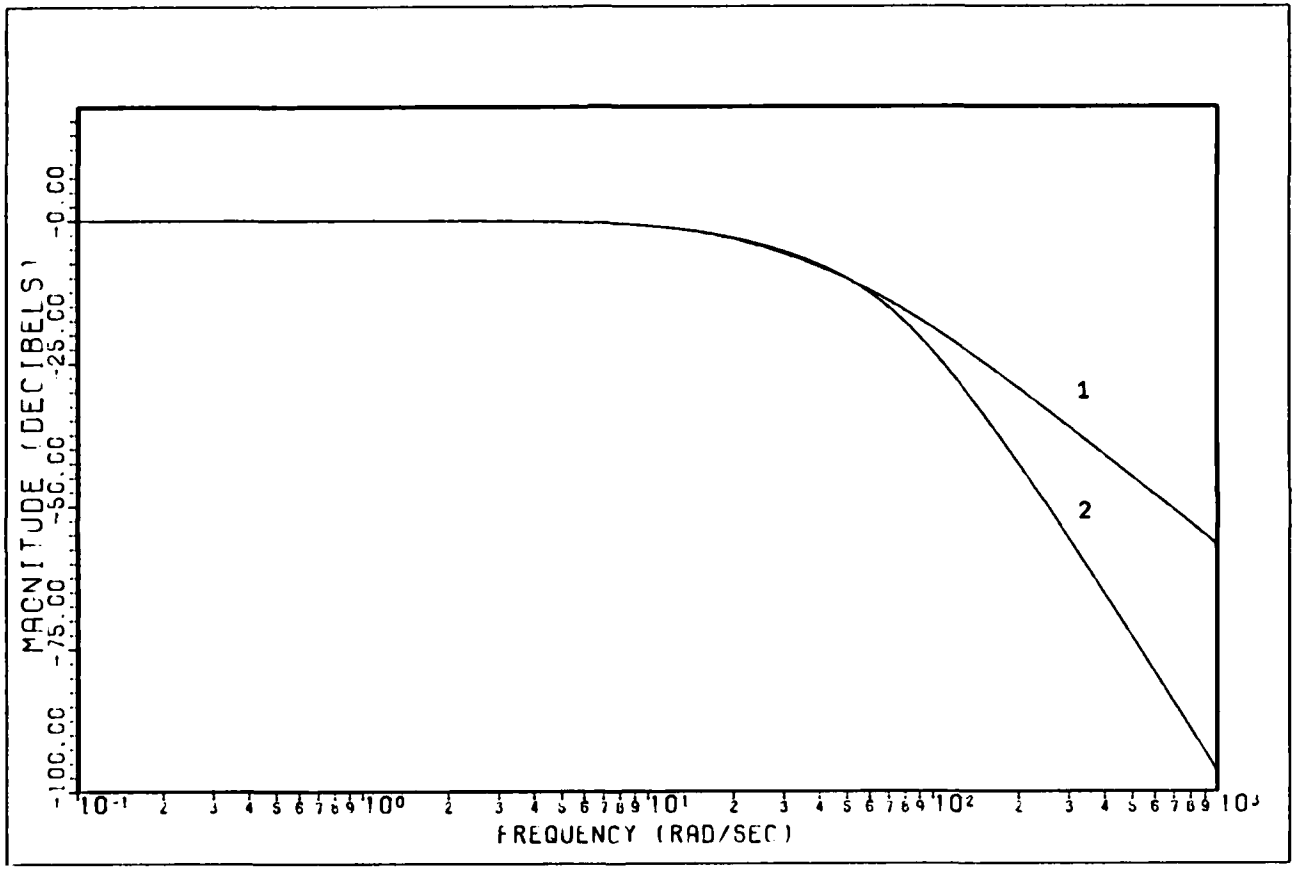

1 = Second-order actuator model
2 = Fourth-order actuator model

Figure 2-4: Frequency Responses of Actuator Models

$$
\begin{bmatrix} \dot{\theta} \\ \dot{u} \\ \dot{\alpha} \\ \dot{q} \\ \dot{\phi} \\ \dot{\beta} \\ \dot{p} \\ \dot{r} \\ \dot{\delta e_t} \\ \dot{\delta f_t} \\ \dot{\delta a} \\ \dot{\delta r} \\ \dot{\delta c} \\ \dot{\delta T} \end{bmatrix} =
\begin{bmatrix}
0 & 0 & 0 & 1 & 0 & 0 & 0 & 0 & 0 & 0 & 0 & 0 & 0 & 0 \\
X'_\theta & X'_u & X'_\alpha & X'_q & 0 & 0 & 0 & 0 & X'_{\delta e_t} & X'_{\delta f_t} & 0 & 0 & 0 & X'_{\delta T} \\
Z'_\theta & Z'_u & Z'_\alpha & Z'_q & 0 & 0 & 0 & 0 & Z'_{\delta e_t} & Z'_{\delta f_t} & 0 & 0 & 0 & 0 \\
M'_\theta & M'_u & M'_\alpha & M'_q & 0 & 0 & 0 & 0 & M'_{\delta e_t} & M'_{\delta f_t} & 0 & 0 & M'_{\delta c} & 0 \\
0 & 0 & 0 & 0 & 0 & 0 & 1 & 0 & 0 & 0 & 0 & 0 & 0 & 0 \\
0 & 0 & 0 & 0 & Y'_\phi & Y'_\beta & Y'_p & Y'_r & 0 & 0 & Y'_{\delta a} & Y'_{\delta r} & Y'_{\delta c} & 0 \\
0 & 0 & 0 & 0 & 0 & L'_\beta & L'_p & L'_r & 0 & 0 & L'_{\delta a} & L'_{\delta r} & L'_{\delta c} & 0 \\
0 & 0 & 0 & 0 & 0 & N'_\beta & N'_p & N'_r & 0 & 0 & N'_{\delta a} & N'_{\delta r} & N'_{\delta c} & 0 \\
0 & 0 & 0 & 0 & 0 & 0 & 0 & 0 & -20 & 0 & 0 & 0 & 0 & 0 \\
0 & 0 & 0 & 0 & 0 & 0 & 0 & 0 & 0 & -20 & 0 & 0 & 0 & 0 \\
0 & 0 & 0 & 0 & 0 & 0 & 0 & 0 & 0 & 0 & -20 & 0 & 0 & 0 \\
0 & 0 & 0 & 0 & 0 & 0 & 0 & 0 & 0 & 0 & 0 & -20 & 0 & 0 \\
0 & 0 & 0 & 0 & 0 & 0 & 0 & 0 & 0 & 0 & 0 & 0 & -20 & 0 \\
0 & 0 & 0 & 0 & 0 & 0 & 0 & 0 & 0 & 0 & 0 & 0 & 0 & -1
\end{bmatrix}
\begin{bmatrix} \theta \\ u \\ \alpha \\ q \\ \phi \\ \beta \\ p \\ r \\ \delta e_t \\ \delta f_t \\ \delta a \\ \delta r \\ \delta c \\ \delta T \end{bmatrix}
+
\begin{bmatrix}
0 & 0 & 0 & 0 & 0 & 0 \\
0 & 0 & 0 & 0 & 0 & 0 \\
0 & 0 & 0 & 0 & 0 & 0 \\
0 & 0 & 0 & 0 & 0 & 0 \\
0 & 0 & 0 & 0 & 0 & 0 \\
0 & 0 & 0 & 0 & 0 & 0 \\
0 & 0 & 0 & 0 & 0 & 0 \\
0 & 0 & 0 & 0 & 0 & 0 \\
20 & 0 & 0 & 0 & 0 & 0 \\
0 & 20 & 0 & 0 & 0 & 0 \\
0 & 0 & 20 & 0 & 0 & 0 \\
0 & 0 & 0 & 20 & 0 & 0 \\
0 & 0 & 0 & 0 & 20 & 0 \\
0 & 0 & 0 & 0 & 0 & 1
\end{bmatrix}
\begin{bmatrix} \delta e_{ti} \\ \delta f_{ti} \\ \delta a_i \\ \delta r_i \\ \delta c_i \\ \delta T_i \end{bmatrix}
$$

$$
\begin{bmatrix} u \\ A_{n_p} \\ q \\ A_{y_p} \\ p \\ r \end{bmatrix} = \begin{bmatrix} 0 & 1 & 0 & 0 & 0 & 0 & 0 & 0 & 0 & 0 & 0 & 0 & 0 & 0 \\ A_{n_\theta} & A_{n_u} & A_{n_\alpha} & A_{n_q} & 0 & 0 & 0 & 0 & A_{n_{\delta e_t}} & A_{n_{\delta f_t}} & 0 & 0 & A_{n_{\delta c}} & 0 \\ 0 & 0 & 0 & 1 & 0 & 0 & 0 & 0 & 0 & 0 & 0 & 0 & 0 & 0 \\ 0 & 0 & 0 & 0 & 0 & A_{y_\beta} & A_{y_p}^* & A_{y_r} & 0 & 0 & A_{y_{\delta a}} & A_{y_{\delta r}} & A_{y_{\delta c}} & 0 \\ 0 & 0 & 0 & 0 & 0 & 0 & 1 & 0 & 0 & 0 & 0 & 0 & 0 & 0 \\ 0 & 0 & 0 & 0 & 0 & 0 & 0 & 1 & 0 & 0 & 0 & 0 & 0 & 0 \end{bmatrix} \begin{bmatrix} \theta \\ u \\ \alpha \\ q \\ \phi \\ \beta \\ p \\ r \\ \delta e_t \\ \delta f_t \\ \delta a \\ \delta r \\ \delta c \\ \delta T \end{bmatrix} \qquad (2\text{-}40)
$$

Note: The A_n and A_y terms in the matricies correspond to the expressions in parentheses in Equations (2-21) and (2-25). The starred term, $A_{y_p}^*$, is the coefficient of p and is not the lateral acceleraton at the pilot's station.

$$
\begin{bmatrix} \dot{\theta} \\ \dot{u} \\ \dot{\alpha} \\ \dot{q} \\ \dot{\phi} \\ \dot{\beta} \\ \dot{p} \\ \dot{r} \\ \dot{\delta e}_{\ell} \\ \dot{\delta f}_{r} \\ \dot{\delta f}_{\ell} \\ \dot{\delta r} \\ \dot{\delta c} \\ \dot{\delta T} \end{bmatrix} =
\begin{bmatrix}
0 & 0 & 0 & 1 & 0 & 0 & 0 & 0 & 0 & 0 & 0 & 0 & 0 & 0 \\
X'_{\theta} & X'_{u} & X'_{\alpha} & X'_{q} & 0 & 0 & 0 & 0 & X'_{\delta e_{\ell}} & X'_{\delta f_{r}} & X'_{\delta f_{\ell}} & 0 & 0 & X'_{\delta T} \\
Z'_{\theta} & Z'_{u} & Z'_{\alpha} & Z'_{q} & 0 & 0 & 0 & 0 & Z'_{\delta e_{\ell}} & Z'_{\delta f_{r}} & Z'_{\delta f_{\ell}} & 0 & 0 & 0 \\
M'_{\theta} & M'_{u} & M'_{\alpha} & M'_{q} & 0 & 0 & 0 & 0 & M'_{\delta e_{\ell}} & M'_{\delta f_{r}} & M'_{\delta f_{\ell}} & 0 & M'_{\delta c} & 0 \\
0 & 0 & 0 & 0 & 0 & 0 & 1 & 0 & 0 & 0 & 0 & 0 & 0 & 0 \\
0 & 0 & 0 & 0 & Y'_{\phi} & Y'_{\beta} & Y'_{p} & Y'_{r} & Y'_{\delta e_{\ell}} & Y'_{\delta f_{r}} & Y'_{\delta f_{\ell}} & Y'_{\delta r} & Y'_{\delta c} & 0 \\
0 & 0 & 0 & 0 & 0 & L'_{\beta} & L'_{p} & L'_{r} & L'_{\delta e_{\ell}} & L'_{\delta f_{r}} & L'_{\delta f_{\ell}} & L'_{\delta r} & L'_{\delta c} & 0 \\
0 & 0 & 0 & 0 & 0 & N'_{\beta} & N'_{p} & N'_{r} & N'_{\delta e_{\ell}} & N'_{\delta f_{r}} & N'_{\delta f_{\ell}} & N'_{\delta r} & N'_{\delta c} & 0 \\
0 & 0 & 0 & 0 & 0 & 0 & 0 & 0 & -20 & 0 & 0 & 0 & 0 & 0 \\
0 & 0 & 0 & 0 & 0 & 0 & 0 & 0 & 0 & -20 & 0 & 0 & 0 & 0 \\
0 & 0 & 0 & 0 & 0 & 0 & 0 & 0 & 0 & 0 & -20 & 0 & 0 & 0 \\
0 & 0 & 0 & 0 & 0 & 0 & 0 & 0 & 0 & 0 & 0 & -20 & 0 & 0 \\
0 & 0 & 0 & 0 & 0 & 0 & 0 & 0 & 0 & 0 & 0 & 0 & -20 & 0 \\
0 & 0 & 0 & 0 & 0 & 0 & 0 & 0 & 0 & 0 & 0 & 0 & 0 & -1
\end{bmatrix}
\begin{bmatrix} \theta \\ u \\ \alpha \\ q \\ \phi \\ \beta \\ p \\ r \\ \delta e_{\ell} \\ \delta f_{r} \\ \delta f_{\ell} \\ \delta r \\ \delta c \\ \delta T \end{bmatrix} +
\begin{bmatrix}
0 & 0 & 0 & 0 & 0 & 0 \\
0 & 0 & 0 & 0 & 0 & 0 \\
0 & 0 & 0 & 0 & 0 & 0 \\
0 & 0 & 0 & 0 & 0 & 0 \\
0 & 0 & 0 & 0 & 0 & 0 \\
0 & 0 & 0 & 0 & 0 & 0 \\
0 & 0 & 0 & 0 & 0 & 0 \\
0 & 0 & 0 & 0 & 0 & 0 \\
20 & 0 & 0 & 0 & 0 & 0 \\
0 & 20 & 0 & 0 & 0 & 0 \\
0 & 0 & 20 & 0 & 0 & 0 \\
0 & 0 & 0 & 20 & 0 & 0 \\
0 & 0 & 0 & 0 & 20 & 0 \\
0 & 0 & 0 & 0 & 0 & 1
\end{bmatrix}
\begin{bmatrix} \delta e_{\ell i} \\ \delta f_{r i} \\ \delta f_{\ell i} \\ \delta r_{i} \\ \delta c_{i} \\ \delta T_{i} \end{bmatrix}
$$

$$
\begin{bmatrix} u \\ A_{n_p} \\ q \\ A_{y_p} \\ p \\ r \end{bmatrix} = \begin{bmatrix} 0 & 1 & 0 & 0 & 0 & 0 & 0 & 0 & 0 & 0 & 0 & 0 & 0 & 0 \\ A_{n_\theta} & A_{n_u} & A_{n_\alpha} & A_{n_q} & 0 & 0 & 0 & 0 & A_{n_{\delta e_\ell}} & A_{n_{\delta f_r}} & A_{n_{\delta f_\ell}} & 0 & A_{n_{\delta c}} & 0 \\ 0 & 0 & 0 & 1 & 0 & 0 & 0 & 0 & 0 & 0 & 0 & 0 & 0 & 0 \\ 0 & 0 & 0 & 0 & 0 & A_{y_\beta} & A_{y_p}^* & A_{y_r} & A_{y_{\delta e_\ell}} & A_{y_{\delta f_r}} & A_{y_{\delta f_\ell}} & A_{y_{\delta r}} & A_{y_{\delta c}} & 0 \\ 0 & 0 & 0 & 0 & 0 & 0 & 1 & 0 & 0 & 0 & 0 & 0 & 0 & 0 \\ 0 & 0 & 0 & 0 & 0 & 0 & 0 & 1 & 0 & 0 & 0 & 0 & 0 & 0 \end{bmatrix} \begin{bmatrix} \theta \\ u \\ \alpha \\ q \\ \phi \\ \beta \\ p \\ r \\ \delta e_\ell \\ \delta f_r \\ \delta f_\ell \\ \delta r \\ \delta c \\ \delta T \end{bmatrix} \qquad (2\text{-}41)
$$

Note: The A_n and A_y terms in the matricies correspond to the expressions in parentheses in Equations (2-22) and (2-26). The starred term, $A_{y_p}^*$, is the coefficient of p and is not the lateral acceleraton at the pilot's station.

III. Design Process

The aircraft models used in this study are developed in Chapter II. Equation (2-40) is the model for the healthy aircraft, and Equation (2-41) is the model for the aircraft with a failed right elevator. This chapter describes how control laws are designed for the two models using the computer program, MULTI. Appendix A outlines the theory behind the design process, while this chapter describes in detail the practical aspects of the design.

III-1. MULTI

Because the multivariable design method of Professor Porter involves the manipulation of matrices and vectors, a computer program can be a great aid to the designer. MULTI is an interactive program made up of approximately 70 numbered options that allow the user to perform a digital, multivariable design (8:2). The program is currently running on a CDC CYBER computer with the NOS operating system. Writing of MULTI was begun by Douglas Porter in 1981 as part of his thesis research at the Air Force Institute of Technology (10). Several other AFIT students have made modifications and additions to the program, and improvements are still being made.

The latest additions to MULTI were written by Major Terry Courtheyn as part of his AFIT thesis requirements (5). His additions include the formation of an open-loop transfer function matrix and a conversion routine to change

simulation responses from radians to degress. The unit conversion routine is used extensively for the designs in this thesis.

Reference 8 is the MULTI User's Manual which describes the use of MULTI and all of its options; however, the designer should be aware of subtle details that are not discussed in the manual. These details are discussed later in this chapter when needed.

III-2. Plant Zeros

For this study, the plant consists of either one of the aircraft models (Equations (2-40) and (2-41)). Before the plant is entered into MULTI the system zeros are checked for the presence of decoupling zeros and the locations of transmission zeros. The check is made by using another interactive computer program called ZERO (7:85-136). If no decoupling zeros are present, the system is completely controllable and observable as required by the design method. As discussed in Appendix A, the transmission zeros are not altered by output feedback and must be located in a stable region of the complex plane.

For the plants of this study the program ZERO indicates that there are no decoupling zeros present; therefore, the plants are completely controllable and observable. However, the system has four transmission zeros located at the origin. Because the presence of four transmission zeros at the origin implies the system is unstable regardless of

output feedback, more discussion is required on this point.

As pointed out by Barfield (4:83-85), the four transmission zeros are located at the origin because of assumptions made in forming the aircraft models. First it is assumed that

$$q = \dot{\theta} \tag{3-1}$$

and

$$p = \dot{\phi} \tag{3-2}$$

The two integrations implied by these equations account for two of the transmission zeros at the origin. If q and p were commanded with step functions, θ and ϕ would ramp to infinity, thus some of the system responses are unbounded for bounded inputs. However, for any practical maneuver, q and p are commanded with functions that resemble pulses more than steps so that θ and ϕ reach steady-state values.

The remaining two transmission zeros are accounted for by two other assumptions made in the model development. The acceleration along the z axis at the center of gravity is given by the same equation (Equation (2-8)) as the $\dot{\alpha}$ state equation. The normal acceleration at the pilot's station is therefore equal to a linear combination of $\dot{\alpha}$ and $\dot{q}$. As with the q and p inputs above, a bounded command of A_{n_p} can yield unbounded responses for the α and q states. Similarly, the lateral acceleration at the pilot's station is a linear combination of $\dot{\beta}$ and $\dot{r}$, so if A_{y_p} is commanded by a step, the

β and r responses ramp to infinity. In practice, though, acceleration commands resemble pulses which yield steady-state values for the other system responses.

III-3. Entering Actuator Models into MULTI

As discussed in Chapter II, a second-order model is used for the control surface actuators. Part of the second-order model is included in Equations (2-40) and (2-41) in order to avoid having a feed-forward matrix in the aircraft models. The remaining portion of the actuator model is implemented using MULTI Option #4 (8:6) and is external to the plant.

MULTI Option #4 requires an external model for every control input. Because the first-order thrust model is already included in the plant, a transfer function of $1000/(s + 1000)$ is used for the external thrust model for Option #4. This external thrust model approximates unity.

The controllable and observable plant information and external actuator models are stored in data files for use by MULTI Option #9 (8:7). The data files for this study are listed in Appendix C.

III-4. Measurement Matrix

The plants used in this thesis are irregular as described in Appendix A. It is therefore necessary to feed back the derivatives of certain states through a measurement matrix, M. The measurement matrix should be chosen such that its nonzero elements are as sparce as possible and so

that FB, when formed, has full rank. The measurement matrix is also required to yield stable transmission zeros for the system.

As mentioned in Chapter II it would have been desirable to model the healthy aircraft with left and right differential tails and left and right flaperons rather than the combinations used in Equation (2-40). It would have then been possible to model a failed surface by eliminating that surface from the state equations. Modeling in this way would greatly simplify the interperation of control surface responses when comparing healthy and failed aircraft simulations.

The problem in trying to model the healthy aircraft with split tails and flaperons is that there are not enough independent feedback sources in the plant. The healthy model would have required seven inputs and seven outputs, and CB would have had a rank deficiency of five. The measurement matrix would then be required to feed back five independent derivatives of states. Because the lateral acceleration, A_{n_p}, is a linear combination of the α and q equations, $\dot{\alpha}$ and $\dot{q}$ cannot be fed back together through M. Similarly, because A_{y_p} is included in the output vector, $\dot{\beta}$ and $\dot{r}$ cannot be fed back together. Also, because θ and ϕ are dependent on q and p respectively, $\dot{\theta}$ and $\dot{\phi}$ cannot be fed back through M. With these limitations, only four independent derivatives of states are available to be fed back through M instead of the required five.

Modeling the healthy aircraft as in Equation (2-40) reduces the number of inputs and outputs by one, and the rank deficiency of $\underline{CB}$ is four. Keeping in mind the limitations described above, the four derivatives fed back through $\underline{M}$ are $\dot{u}$, $\dot{q}$, $\dot{p}$, and $\dot{r}$. These derivatives are easily measured or calculated from aircraft sensor output signals. The same derivatives are also fed back for the failed right elevator model. The measurement matrix used with both the healthy and failed aircraft models is

$$\underline{M} = \begin{bmatrix} 0 & 0.1 & 0 & 0 & 0 & 0 & 0 & 0 \\ 0 & 0 & 0 & 0 & 0 & 0 & 0 & 0 \\ 0 & 0 & 0 & 0.1 & 0 & 0 & 0 & 0 \\ 0 & 0 & 0 & 0 & 0 & 0 & 0 & 0 \\ 0 & 0 & 0 & 0 & 0 & 0 & 0.25 & 0 \\ 0 & 0 & 0 & 0 & 0 & 0 & 0 & 0.25 \end{bmatrix} \quad (3\text{-}3)$$

The choices of the nonzero values are somewhat arbitrary, but the values are less than one in order to avoid large gains in $\underline{K}_0$ and $\underline{K}_1$ which may cause instabilities. Also, the locations of the transmission zeros due to the measurement matrix are approximately equal to minus the reciprocal of the matrix elements. From Equation (3-3), two transmission zeros are added near -10, and two more are added near -4 on the real axis.

III-5. Design Parameters

Appendix A describes the formation of the gain

matrices, $\underline{K}_0$ and $\underline{K}_1$, for an irregular plant. After the measurement matrix, $\underline{M}$, and the design parameters, $\bar{\alpha}$, $\underline{\Sigma}$, and ε, have been entered into MULTI, the program calculates the gain matrices. There are no rules that tell how to choose any of the design parameters. The design of control laws reduces to a trial and error process; however, the design steps discussed below help speed up the process.

Because the longitudinal and lateral equations of the healthy aircraft model (Equation (2-40)) are coupled only by the $M'_{\delta C}$ term, which always has a small value, the equations are considered to be decoupled for purposes of choosing design parameters. The designs of Reference 4 were achieved for separate longitudinal and lateral aircraft models. Since the healthy aircraft model in this thesis is essentially decoupled, the design parameters used in Reference 4 are used as starting points for the designs of this thesis. When designing a control law for a longitudinal maneuver, the σ values (elements of the diagonal weighting matrix, $\underline{\Sigma}$) corresponding to lateral quantities are held constant, while σ values corresponding to longitudinal quantities are varied with successive trials. Similarly, when designing for lateral maneuvers, longitudinal σ's are held constant while lateral σ's are varied.

For preliminary design trails the ratio of proportional to integral control, $\bar{\alpha}$, and the weighting matrix multiplier, ε, are set to one while the diagonal weighting matrix elements are varied. The σ values are adjusted so that the

system is stable and the corresponding elements of the output vector, $\underline{y}$, closely follow the input commands.

If satisfactory responses cannot be achieved by changing the elements of $\underline{\Sigma}$ alone, $\bar{\alpha}$ is varied while holding the other design parameters constant. Increasing the value of $\bar{\alpha}$ tends to shorten the settling time of the system responses. Originally, the $\bar{\alpha}$ parameter in MULTI was implimented as the reciprocal of the definition in Appendix A, which meant that the proportional gains, $\underline{K}_0$, were changed while the integral gains, $\underline{K}_1$, were held constant. It is desired, however, to hold $\underline{K}_0$ constant while varying $\underline{K}_1$; therefore, the MULTI program has been modified to do this.

During the design process the weighting matrix multiplier, ϵ, is useful for finding the maximum gain values that still permit stable operation. It is normally set back to one, with the σ's adjusted accordingly, for the final designs.

III-6. Design Simulation

Each design iteration is checked with the simulation routine in MULTI. Before a simulation can be run an input command vector, $\underline{v}$, must be supplied to MULTI. The elements of the input command vector are the same as those of the output vector, $\underline{y}$; therefore,

$$\underline{v} = \{u,\ A_{n_p},\ q,\ A_{y_p},\ p,\ r\}^T \qquad (3\text{-}2)$$

The command inputs can be either ramp or step commands but

cannot be left floating. Because each element of $\underline{v}$ must be commanded, some calculations are necessary when performing certain maneuvers. The maneuvers considered in this study are described in the next chapter along with the development of the corresponding command vectors.

It is extremely important that any control law design results in stable system responses. It would have been faster and less costly in computer time to check the closed-loop transfer functions of the system responses for stability before running a simulation; however, the factoring routine in MULTI Option #6 (8:6) becomes error prone when transfer functions are greater than fifth order. Large systems, like the ones in this study, may in fact be stable even though Option #6 indicates poles in the far right half plane. It is suggested that the problem be corrected in a future research effort.

After running a simulation on MULTI, stability is first checked by examining the figures of merit of the output responses. Large peak values in the figures of merit usually indicate an unstable system. Attempting to plot an unstable response with a MULTI plotting routine may lead to a fatal error and loss of data due to an arithmetic overflow. If the peak values are close to the commanded steady state values, the system may be stable. The time responses of the system's states and outputs are then plotted for the time interval desired and checked for diverging ramps or oscillations. It may be necessary to increase the time interval

and rerun the simulation to ensure that instabilities do not become evident after a longer period of time.

III-7. Final Designs

The trial and error design process ends when desirable system responses are achieved. Desirable responses are those the that reach a steady state value quickly without an excessive overshoot and are free of oscillations. Control surface responses must remain within the rate and maximum deflection limits shown in Table 3-1. To avoid exceeding the rate limits the input commands are ramped to steady state values rather than stepped. The duration of the ramp is determined by examining the control surface responses. The ramp time is increased until all the surface responses are within their respective rate limits.

When an acceptable control law is finally achieved for a maneuver using the healthy aircraft model, the same design parameters are tried for the same maneuver and flight condition using the failed right elevator model of Equation (2-41). New gain matrices are calculated because the control surfaces are represented differently in the failure model than in the healthy aircraft model. Changing the gains implies that the aircraft must be able to detect a failure and then reconfigure the flight control system accordingly. If the new gains result in unacceptable responses for the failed system, the design parameters are varied until acceptable responses are finally achieved. If

Table 3-1

Surface Position and Rate Limits

Surface	Position Limit (degrees)	No Load Rate Limit (degrees/second)
Elevators	± 25	60
Flaperons	± 20	52
Rudder	± 30	120
Canards	± 27	100

Source: (4:93)

control surface limits are exceeded, it may be necessary to redefine the maximum maneuvers that the aircraft can perform with the failed surface.

The next chapter describes in detail the maneuvers considered in this study.

IV. Maneuvers

Chapter III discusses the design method used in developing control laws for the aircraft. Each control law is tailored for a specific maneuver at a specific flight condition. This chapter describes the maneuvers considered in this study and discusses the development of a command vector, $\underline{v}$, for each maneuver.

IV-1. Longitudinal Maneuvers

The three longitudinal maneuvers considered in this thesis are: g-command (constant-g pullup), pitch pointing, and longitudinal translation.

The g-command, or constant-g pullup, maneuver is used to climb from wings level flight. The pilot commands a constant normal acceleration that he feels with his body, and the aircraft pitches and climbs while generating the constant acceleration. The flight path angle, γ, changes as the pitch angle and angle of attack change, and is governed by the equation

$$\gamma = \theta - \alpha \tag{4-1}$$

The command vector, $\underline{v}$, for the g-command maneuver includes a step command on A_{n_p} in order to achieve a constant normal acceleration at the pilot's station. Because none of the elements of $\underline{v}$ can be left floating, the pitch rate, q, must also be commanded with a step. The magnitude of the step is developed as follows (4:107). For trimmed, wings

level flight Equation (2-7) can be written as

$$A_{z_{CG}} = \dot{\alpha}U - qU \tag{4-2}$$

Substituting Equation (4-2) into Equations (2-17) and (2-19)

$$A_{n_p} = qU - \dot{\alpha}U + (\ell_x)\dot{q} \tag{4-3}$$

For constant acceleration and pitch rate commands, the value of α reaches a constant and thus $\dot{\alpha}$ and $\dot{q}$ equal zero; therefore

$$A_{n_p}(g) = [U\ (ft/sec)]\left[\frac{1}{32.2}\ \frac{g}{ft/sec}\right] q\ (radian/sec) \tag{4-4}$$

The magnitude of the step command on q is then given by

$$q = \frac{32.2}{U} A_{n_p} \tag{4-5}$$

A step command on A_{n_p} and q implies mathematically that the commands are applied for infinite time. For a practical maneuver, the commands are cut off after a finite time; therefore, the simulation responses are observed for only a few seconds.

As with the rest of the maneuvers in this study, the change in forward velocity, u, is commanded to zero. Also, when performing a longitudinal maneuver, the lateral elements of $\underline{v}$ are commanded to zero.

Although not attempted in this study, the g-command maneuver can be combined with the roll maneuver, discussed later, to perform a coordinated turn. The pilot still commands a constant normal acceleration, but the direction

of the acceleration is at an angle equal to the roll angle with respect to a flat earth reference frame.

The pitch pointing maneuver is used to precisely aim the fuselage of the aircraft longitudinally at a target. The maneuver gives the pilot a great advantage in air-to-air combat. When performing a pitch pointing maneuver, the aircraft pitches without changing its flight path angle. From Equation (4-1) the angle of attack must be equal to the pitch angle. Also, for a pitch pointing maneuver, no normal acceleration is developed.

It is desirable to command pitch angle to demonstrate a pitch pointing maneuver; however, pitch rate, q, is an element of the command vector and θ is not. The pitch rate is therefore commanded with a pulse. The integral, or area, of the pulse determines the pitch angle commanded. All other elements of $\underline{v}$ are commanded to zero.

Like the g-command maneuver, pitch pointing can also be combined with a roll maneuver. This combination is valuable for air-to-air combat, but is not attempted in this thesis. It is suggested, though, that the combination of maneuvers be investigated in future research.

The longitudinal translation maneuver involves the development of a constant normal velocity without changing the aircraft's pitch angle. The flight path angle does change and, for wings level flight, is equal to the change in angle of attack. The longitudinal translation maneuver is useful in air-to-air combat and air refueling.

In order to command a constant normal velocity, the normal acceleration, A_{n_p}, is commanded with a pulse. The integral of the pulse determines the steady state value of the normal velocity. The other elements of $\underline{v}$ are commanded to zero.

IV-2. Lateral Maneuvers

Four lateral maneuvers are considered in this study. They are: roll, sideforce (flat turn), yaw pointing, and lateral translation.

The roll maneuver involves developing a roll rate about the aircraft's velocity vector without accelerating laterally or normally and without changing the fight path angle. The reason for rolling about the velocity vector and not the aircraft's x axis is due to the modeling of the aircraft in the body reference frame (4:36). At high angles of attack, rolling about the x axis results in large sideslip angles.

In order to properly command a roll about the velocity vector, two problems arise. The first problem involves commanding sideslip, β, to zero, when it is not an element of the command vector, and, at the same time, commanding yaw rate, r, to the proper value. As developed in Reference 4, an estimate for sideslip rate is derived from the y axis force equation

$$F_{y_{CG}} = m(\dot{V} + Ur - pW) - gm\cos\theta\sin\phi \qquad (4\text{-}6)$$

Rearranging Equation (4-6) and dividing by mass, m,

$$A_{y_{CG}} = \frac{F_{y_{CG}}}{m} = U(\dot{\beta} + r - p\alpha - \frac{g}{U}\cos\theta\sin\phi) \qquad (4\text{-}7)$$

Solving for $\dot{\beta}$ and inserting Equation (2-24)

$$\dot{\beta} = \frac{A_{y_p}}{U} - \frac{(\ell_x)\dot{r}}{U} - r + p\alpha + \frac{g}{U}\cos\theta\sin\phi \qquad (4\text{-}8)$$

For constant roll rates, $\dot{r}$ is zero. The equation that approximates sideslip rate is finally written by neglecting the gravity terms in Equation (4-8)

$$\dot{\beta} \approx \frac{A_{y_p}}{U} - r + p\alpha_T \qquad (4\text{-}9)$$

The lateral acceleration in Equation (4-9) is commanded to zero; therefore, for the roll maneuver Equation (4-9) becomes

$$\dot{\beta} = p\alpha_T - r \qquad (4\text{-}10)$$

To overcome the problem of commanding β to zero, the command and output vectors for the aircraft models are changed to

$$\underline{v} = \underline{y} = \{u, A_{n_p}, q, A_{y_p}, p, (r - p\alpha_T)\}^T \qquad (4\text{-}11)$$

The output matrix, $\underline{C}$, in Equation (2-40) then becomes the matrix in Equation (4-12). A similar change is made for the output matrix in Equation (2-41). By then commanding

$(r - p\alpha_T)$ to zero, $\dot{\beta}$, and therefore β, is commanded to zero also. The roll rate, p, is commanded with a pulse so that the steady-state roll angle is equal to the integral of the pulse.

$$\underline{C} = \begin{bmatrix} 0 & 1 & 0 & 0 & 0 & 0 & 0 & 0 & 0 & 0 & 0 & 0 & 0 & 0 \\ A_{n_\theta} & A_{n_u} & A_{n_\alpha} & A_{n_q} & 0 & 0 & 0 & 0 & A_{n_{\delta e_t}} & A_{n_{\delta f_t}} & 0 & 0 & A_{n_{\delta c}} & 0 \\ 0 & 0 & 0 & 1 & 0 & 0 & 0 & 0 & 0 & 0 & 0 & 0 & 0 & 0 \\ 0 & 0 & 0 & 0 & 0 & A_{y_\beta} & A_{y_p} & A_{y_r} & 0 & 0 & A_{y_{\delta a}} & A_{y_{\delta r}} & A_{y_{\delta c}} & 0 \\ 0 & 0 & 0 & 0 & 0 & 0 & 1 & 0 & 0 & 0 & 0 & 0 & 0 & 0 \\ 0 & 0 & 0 & 0 & 0 & 0 & -\alpha_T & 1 & 0 & 0 & 0 & 0 & 0 & 0 \end{bmatrix} \quad (4\text{-}12)$$

The second problem stems from neglecting the gravity terms in Equation (4-8). If the steady-state roll angle is less than ten degrees, the approximation is valid, but for large roll angles a change in the model is required. As the aircraft rolls, the direction of gravity changes with respect to the aircraft body axis. In order to maintain a constant altitude, the normal and lateral accelerations must combine to cancel gravity. Unfortunately, to command the accelerations properly requires sinusoidal inputs to the command vector. At this time, MULTI does not allow for sinusoidal commands. To overcome this problem, the Y'_ϕ term in the aircraft models (Equations (2-40) and (2-41)) is replaced by zero. By doing this, the lateral equations in the models do not include a roll angle term; therefore, the

orientation of the gravity vector is not taken into account when rolling the aircraft. With this change, acceptable roll maneuver responses are achieved.

The sideforce (flat turn) maneuver is used for changing the heading angle of the aircraft without developing a roll angle or sideslip. To command the maneuver, the lateral acceleration is commanded with a step function. The yaw rate, r, is also commanded with a step function, but a with magnitude determined by the acceleration command and aircraft velocity. The equation governing the r command magnitude is developed from Equation (4-9). Assuming that no sideslip or roll angle is generated with the maneuver, $\dot{\beta}$ and p are set to zero and Equation (4-9) becomes

$$r = \frac{32.2}{U} A_{y_p} \qquad (4\text{-}13)$$

where the proper unit conversion is included as in Equation (4-4). The command vector for the sideforce maneuver consists of step commands on lateral acceleration and yaw rate, and the remaining vector elements are commanded to zero.

The yaw pointing maneuver is similar to pitch pointing, but in the lateral direction. Yaw pointing is used to aim the fuselage laterally at a target without rolling or accelerating laterally. Equation (4-9) is used in forming the command vector for this maneuver. By commanding the lateral acceleration and roll rate to zero, Equation (4-9) reduces to

$$\dot{\beta} \approx - r \qquad (4\text{-}14)$$

A desired sideslip angle, or pointing angle for this maneuver, can be developed by commanding r with a pulse of the opposite sign. The command vector for the yaw pointing maneuver therefore consists of a pulse on r and zero commands on the other vector elements. The area of the pulse on r determines the pointing angle commanded.

Lateral translation is similar to longitudinal translation, but in the lateral direction. When commanding this maneuver, it is desired to develop a constant lateral velocity without rolling or yawing. To perform the maneuver, the lateral acceleration is commanded with a pulse. The integral of the pulse approximates the lateral velocity developed. The other elements of the command vector are set to zero.

Table 4-1 summarizes the command vectors for the maneuvers considered in this study.

The next chapter discusses the simulation responses of the maneuvers described in this chapter at the four flight conditions.

Table 4-1

Maneuver Commands

Maneuvers	COMMAND VECTOR ELEMENTS					
	Longitudinal			Lateral		
	u	A_{n_p}	q	A_{y_p}	p	r
G-Command (Constant-G Pullup)	0	step	$\frac{32.2}{U} A_{n_p}$	0	0	0
Pitch Pointing	0	0	pulse	0	0	0
Longitudinal Translation	0	pulse	0	0	0	0
Roll About Velocity Vector	0	0	0	0	pulse	0*
Sideforce (Flat Turn)	0	0	0	step	0	$\frac{32.2}{U} A_{y_p}$
Yaw Pointing	0	0	0	0	0	pulse
Lateral Translation	0	0	0	pulse	0	0

* Actually commanding $r - p\alpha_T$ for roll maneuver.

V. Design Responses

This chapter presents the simulation responses for the control laws developed in this thesis. Chapter III describes in detail the process used in designing the control laws, and Chapter IV discusses the maneuvers considered. Appendix C lists the data used in the aircraft models for each flight condition. The four flight conditions considered in this study are: transonic flight (0.9 Mach at 20,000 feet), subsonic flight (0.6 Mach at 30,000 feet), supersonic flight (1.6 Mach at 30,000 feet), and landing approach (0.3 Mach at 30 feet). This chapter lists the resonses for the transonic flight condition only. The simulation responses for the remaining three flight conditions are presented in Appendix D.

The main concern for this study is that the control surface responses are within the rate and angular deflection limits listed in Table 3-1 for both the healthy and failed right elevator models. The command vector elements, listed in Table 4-1, are therefore commanded with magnitudes that yield maximum control surface deflections in order to determine the maximum capabilities of the aircraft. In some cases large roll and pitch angles are generated which contradict the small angle assumptions made when developing the aircraft perturbation equations. Although this invalidates the linear aircraft models, a general idea of the control surface deflections needed to perform the maneuvers is

obtained. The commanded magnitudes are decreased from the maximum values if a large angle of attack or sideslip is generated.

For each of the flight conditions, when simulating a longitudinal maneuver the elements of the diagonal weighting matrix $\underline{\Sigma}$ corresponding to lateral quantities are set to the values used in the sideforce maneuver design. Similarly, when simulating a lateral maneuver the elements of $\underline{\Sigma}$ corresponding to longitudinal quantities are set to the values used in the g-command maneuver design. This is done because all elements of $\underline{\Sigma}$ affect the gain matrices $\underline{K}_0$ and $\underline{K}_1$ and because the sideforce and g-command maneuvers are conventional maneuvers.

This chapter is divided into seven sections corresponding to each maneuver at the transonic flight condition. Each section includes tables that list the design parameters and simulation response plots generated with the program MULTI. Appendix D is organized in a similar manner.

Air-to-air combat often begins in the transonic region of the flight envelope. Because of this, the transonic flight condition (0.9 Mach at 20,000 feet) is an important condition for demonstrating the maneuverability of the aircraft. Because of a relatively high dynamic pressure ($\bar{q}$ = 552 lbs/ft^2) at this flight condition, the control surfaces are extremely effective in maneuvering the aircraft, and designs at this flight condition are fairly easy.

V-1. G-Command Maneuver

Tables 5-1 and 5-2 list the design parameters for the g-command maneuver for the healthy and failed right elevator models. As shown in the tables, the same design parameters, $\bar{\alpha}$, $\underline{\Sigma}$, and ϵ, are used for both aircraft models.

Figures 5-1 through 5-7 show the simulation responses for the g-command maneuver. For this maneuver the healthy aircraft longitudinal responses change very little when the right horizontal tail fails. Also, the healthy aircraft lateral responses are zero and are very small with the failed model. For these reasons Figures 5-1 through 5-3 give simulation responses for both the healthy and failed aircraft models.

The maximum normal acceleration commanded (9g) is limited by the flaperon deflection, as shown in Figures 5-4 and 5-5. A comparison of Figures 5-4 and 5-5 shows that, for the failure case, the left elevator deflects approximately twice the amount required when both tail halves are working. Figure 5-5 indicates that the flaperon deflection is slightly asymmetric for the failure case. This asymmetry compensates for the rolling moment created by the left elevator deflection. Also, Figure 5-7 shows that the rudder and canard compensate for the adverse yaw caused by a difference in drag between the left and right halves of the aircraft.

Table 5-1

G-Command: Healthy Model, 0.9 Mach at 20,000 Feet

Sampling Time: T = 0.02 second

$\bar{\alpha} = 1.0$

$\epsilon = 1.0$

$\underline{\Sigma} = \text{diag}\ \{2.0,\ 0.1,\ 2.35,\ 1.0,\ 2.3,\ 1.0\}$

$$\underline{K}_0 = \begin{bmatrix} 0.0 & -0.2267E-03 & -0.3534E-01 & -0.1370E-02 & 0.5821E-04 & 0.1407E-02 \\ 0.0 & 0.8425E-03 & -0.5018E-01 & 0.8348E-03 & -0.3546E-04 & -0.8572E-03 \\ 0.0 & 0.0 & 0.0 & 0.6581E-02 & -0.7018E-02 & -0.1200E-01 \\ 0.0 & 0.0 & 0.0 & 0.2548E-01 & 0.1858E-02 & -0.5830E-01 \\ 0.0 & 0.0 & 0.0 & 0.2794E-01 & -0.1187E-02 & -0.2870E-01 \\ 0.1039E+01 & -0.1555E-02 & 0.1944E+00 & 0.8464E-03 & -0.3595E-04 & -0.8691E-03 \end{bmatrix}$$

$\underline{K}_1 = \underline{K}_0$

Input Ramp Time: 0.4 second

Command Vector:

$u = 0.0$

$A_{n_p} = 9.0$ g (step)

$q = 0.3105$ radian/second (step)

$A_{y_p} = 0.0$

$p = 0.0$

$r = 0.0$

Table 5-2

G-Command: Failed Model, 0.9 Mach at 20,000 Feet

Sampling Time: T = 0.02 second

$\bar{\alpha} = 1.0$

$\varepsilon = 1.0$

$\underline{\Sigma} = \text{diag}\ \{2.0,\ 0.1,\ 2.35,\ 1.0,\ 2.3,\ 1.0\}$

$$\underline{K}_0 = \begin{bmatrix} 0.0 & -0.4529E-03 & -0.7062E-01 & -0.2750E-02 & 0.1285E-03 & 0.2833E-02 \\ 0.0 & 0.7775E-03 & -0.6031E-01 & 0.8910E-02 & -0.9049E-02 & -0.1590E-01 \\ 0.0 & 0.9072E-03 & -0.4008E-01 & -0.7235E-02 & 0.8970E-02 & 0.1417E-01 \\ 0.0 & -0.4018E-04 & -0.6264E-02 & 0.2640E-01 & 0.6243E-03 & -0.6018E-01 \\ 0.0 & -0.4012E-05 & -0.6256E-03 & 0.2804E-01 & -0.1310E-02 & -0.2888E-01 \\ 0.1039E+01 & -0.1554E-02 & 0.1946E+00 & 0.8576E-03 & -0.4007E-04 & -0.8835E-03 \end{bmatrix}$$

$\underline{K}_1 = \underline{K}_0$

Input Ramp Time: 0.4 second

Command Vector:

$u = 0.0$

$A_{n_p} = 9.0$ g (step)

$q = 0.3105$ radian/second (step)

$A_{y_p} = 0.0$

$p = 0.0$

$r = 0.0$

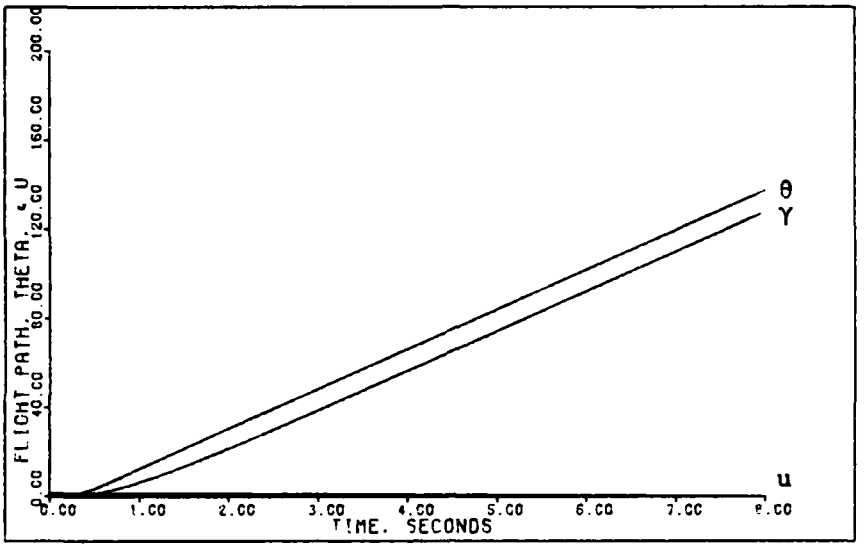

Figure 5-1: 0.9M Healthy/Failed G-Command -- Flight Path Angle, Pitch Angle, and Forward Velocity

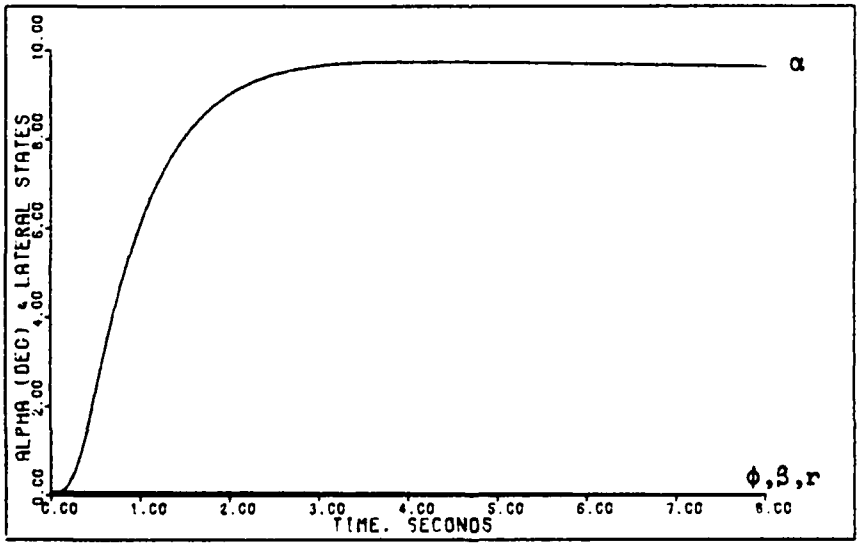

Figure 5-2: 0.9M Healthy/Failed G-Command -- Angle of Attack, Roll Angle, Sideslip Angle, and Yaw Rate

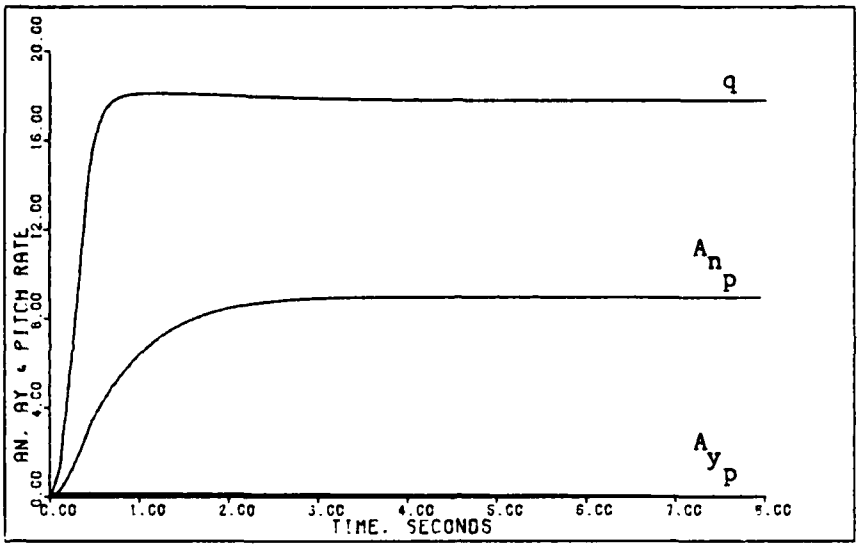

Figure 5-3: 0.9M Healthy/Failed G-Command -- Pitch Rate, Normal Acceleration, and Lateral Acceleration

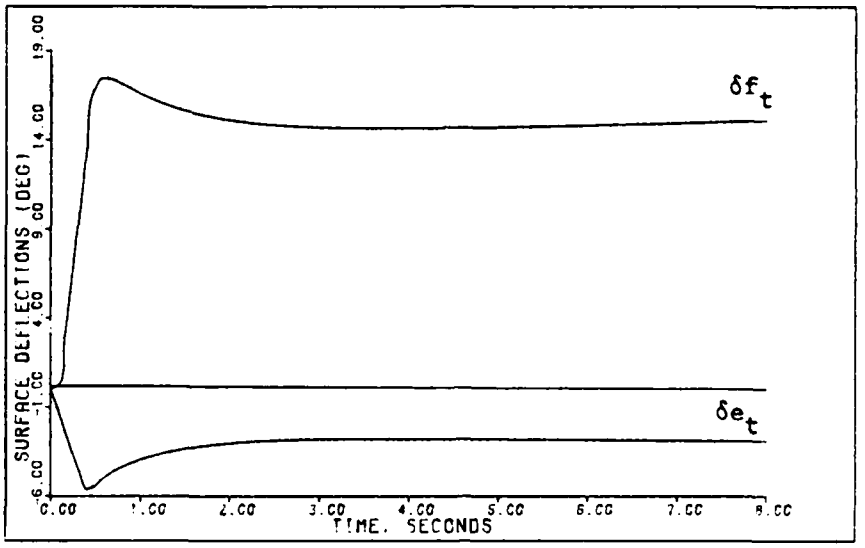

Figure 5-4: 0.9M Healthy G-Command -- Elevator and Flap Deflections

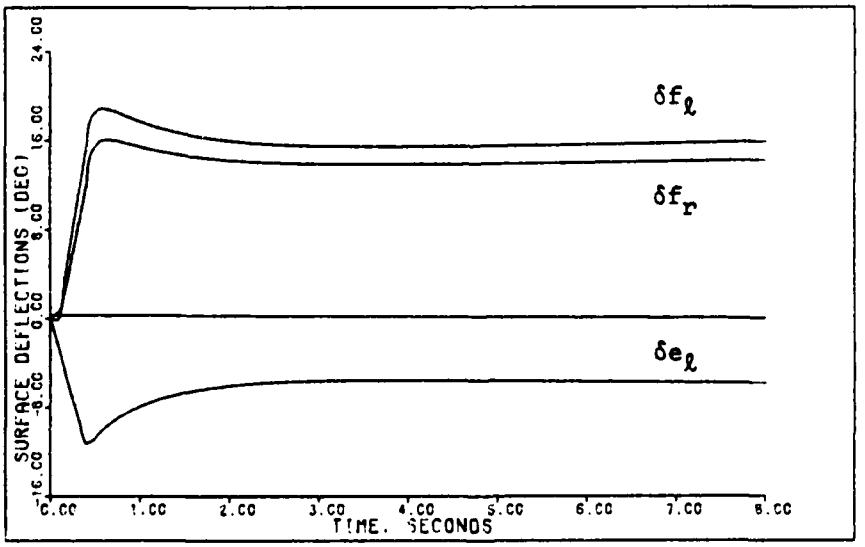

Figure 5-5: 0.9M Failed G-Command -- Left Elevator and Flaperon Deflections

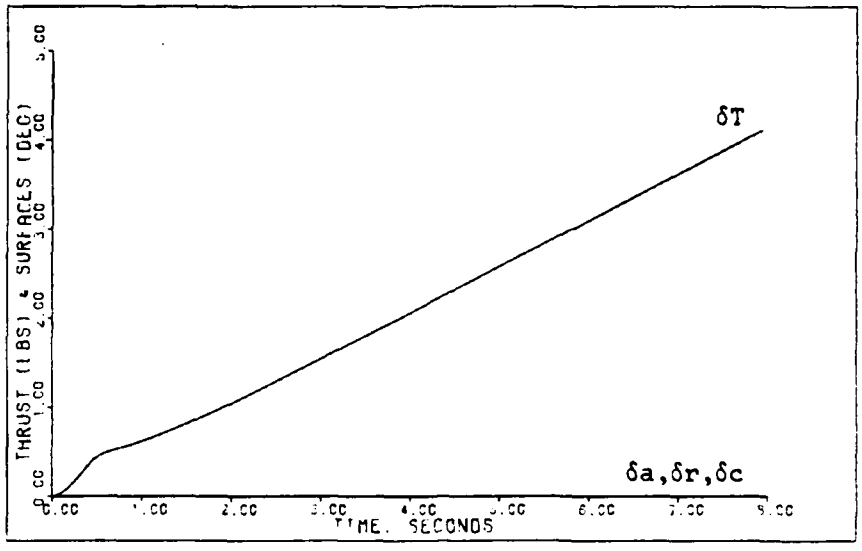

Figure 5-6: 0.9M Healthy G-Command -- Aileron, Rudder, and Canard Deflections and Thrust

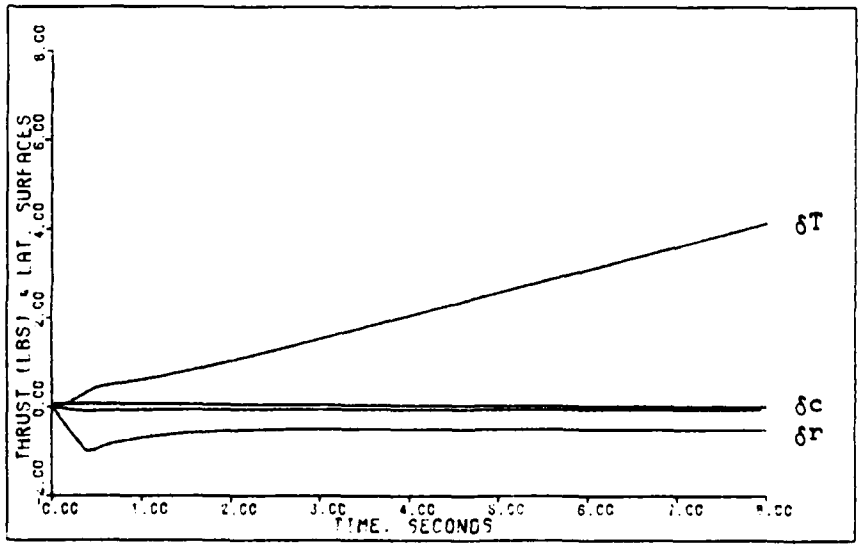

Figure 5-7: 0.9M Failed G-Command -- Rudder and Canard Deflections and Thrust

V-2. Pitch Pointing Maneuver

Tables 5-3 and 5-4 give the design parameters for the pitch pointing maneuver. As with the g-command maneuver the design parameters $\bar{\alpha}$, $\underline{\Sigma}$, and ε are the same for the healthy and failed models.

The simulation responses for the pitch pointing maneuver are given in Figures 5-8 through 5-14. For the same reasons discussed in the g-command maneuver section, Figures 5-8 through 5-10 give simulation responses for both the healthy and failed aircraft models. The failure model requires that the left elevator must deflect approximately twice the angle of the healthy elevator deflection. Also, for the failure model, the flaperons deflect asymmetrically to counter the roll induced by the failed right horizontal tail, and the rudder and canard deflect to compensate for adverse yaw.

AD-A151 908 MULTIVARIABLE CONTROL LAW DESIGN FOR THE AFTI/F-16 WITH A FAILED CONTROL SURFACE(U) AIR FORCE INST OF TECH WRIGHT-PATTERSON AFB OH SCHOOL OF ENGI.. R A ESLINGER 2/4

UNCLASSIFIED DEC 84 AFIT/GE/ENG/84D-28 F/G 1/2 NL

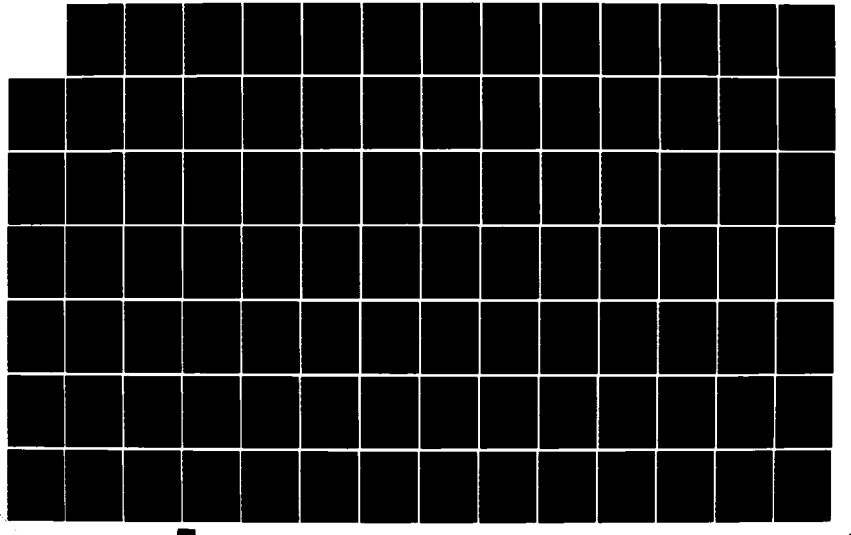

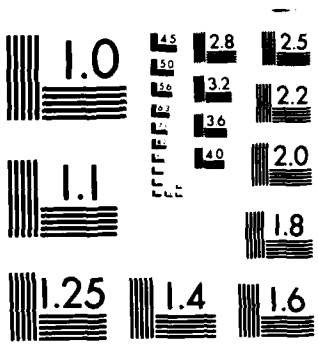

Table 5-3

Pitch Pointing: Healthy Model, 0.9 Mach at 20,000 Feet

Sampling Time: T = 0.02 second

$\bar{\alpha} = 2.0$

$\epsilon = 1.0$

$\underline{\Sigma} = \text{diag}\{2.0, 3.0, 2.35, 1.0, 2.3, 1.0\}$

$$\underline{K}_0 = \begin{bmatrix} 0.0 & -0.6800E-02 & -0.3534E-01 & -0.1370E-02 & 0.5821E-04 & 0.1407E-02 \\ 0.0 & 0.2527E-01 & -0.5018E-01 & 0.8348E-03 & -0.3546E-04 & -0.8572E-03 \\ 0.0 & 0.0 & 0.0 & 0.6581E-02 & -0.7018E-02 & -0.1200E-01 \\ 0.0 & 0.0 & 0.0 & 0.2548E-01 & 0.1858E-02 & -0.5830E-01 \\ 0.0 & 0.0 & 0.0 & 0.2794E-01 & -0.1187E-02 & -0.2870E-01 \\ 0.1039E+01 & -0.4666E-01 & 0.1944E+00 & 0.8464E-03 & -0.3595E-04 & -0.8691E-03 \end{bmatrix}$$

$$\underline{K}_1 = \begin{bmatrix} 0.0 & -0.1360E-01 & -0.7068E-01 & -0.2741E-02 & 0.1164E-03 & 0.2814E-02 \\ 0.0 & 0.5055E-01 & -0.1004E+00 & 0.1670E-02 & -0.7092E-04 & -0.1714E-02 \\ 0.0 & 0.0 & 0.0 & 0.1316E-01 & -0.1404E-01 & -0.2400E-01 \\ 0.0 & 0.0 & 0.0 & 0.5095E-01 & 0.3715E-02 & -0.1166E+00 \\ 0.0 & 0.0 & 0.0 & 0.5589E-01 & -0.2374E-02 & -0.5739E-01 \\ 0.2077E+01 & -0.9331E-01 & 0.3888E+00 & 0.1693E-02 & -0.7190E-04 & -0.1738E-02 \end{bmatrix}$$

Input Ramp Time: 0.2 second

Command Vector:

$u = 0.0$

$A_{n_p} = 0.0$

$q = 0.03491$ radian/second (1 second pulse)

$A_{y_p} = 0.0$

$p = 0.0$

$r = 0.0$

Table 5-4

Pitch Pointing: Failed Model, 0.9 Mach at 20,000 Feet

Sampling Time: T = 0.02 second

$\bar{\alpha} = 2.0$

$\epsilon = 1.0$

$\underline{\Sigma} = \text{diag}\{2.0, 3.0, 2.35, 1.0, 2.3, 1.0\}$

$$\underline{K}_0 = \begin{bmatrix} 0.0 & -0.1359E-02 & -0.7062E-01 & -0.2750E-02 & 0.1285E-03 & 0.2833E-02 \\ 0.0 & 0.2332E-01 & -0.6031E-01 & 0.8910E-02 & -0.9049E-02 & -0.1590E-01 \\ 0.0 & 0.2722E-01 & -0.4008E-01 & -0.7235E-02 & 0.8970E-02 & 0.1417E-01 \\ 0.0 & -0.1205E-02 & -0.6264E-02 & 0.2640E-01 & 0.6243E-03 & -0.6018E-01 \\ 0.0 & -0.1204E-03 & -0.6256E-03 & 0.2804E-01 & -0.1310E-02 & -0.2888E-01 \\ 0.1039E+01 & -0.4662E-01 & 0.1946E+00 & 0.8576E-03 & -0.4007E-04 & -0.8835E-03 \end{bmatrix}$$

$$\underline{K}_1 = \begin{bmatrix} 0.0 & -0.2718E-01 & -0.1412E+00 & -0.5499E-02 & 0.2569E-03 & 0.5665E-02 \\ 0.0 & 0.4665E-01 & -0.1206E+00 & 0.1782E-01 & -0.1810E-01 & -0.3179E-01 \\ 0.0 & 0.5443E-01 & -0.8017E-01 & -0.1447E-01 & 0.1794E-01 & 0.2834E-01 \\ 0.0 & -0.2411E-02 & -0.1253E-01 & 0.5280E-01 & 0.1249E-02 & -0.1204E+00 \\ 0.0 & -0.2407E-03 & -0.1251E-02 & 0.5607E-01 & -0.2620E-02 & -0.5777E-01 \\ 0.2077E+01 & -0.9324E-01 & 0.3892E+00 & 0.1715E-02 & -0.8013E-04 & -0.1767E-02 \end{bmatrix}$$

Input Ramp Time: 0.2 second

Command Vector:

$u = 0.0$

$A_{n_p} = 0.0$

$q = 0.03491$ radian/second (1 second pulse)

$A_{y_p} = 0.0$

$p = 0.0$

$r = 0.0$

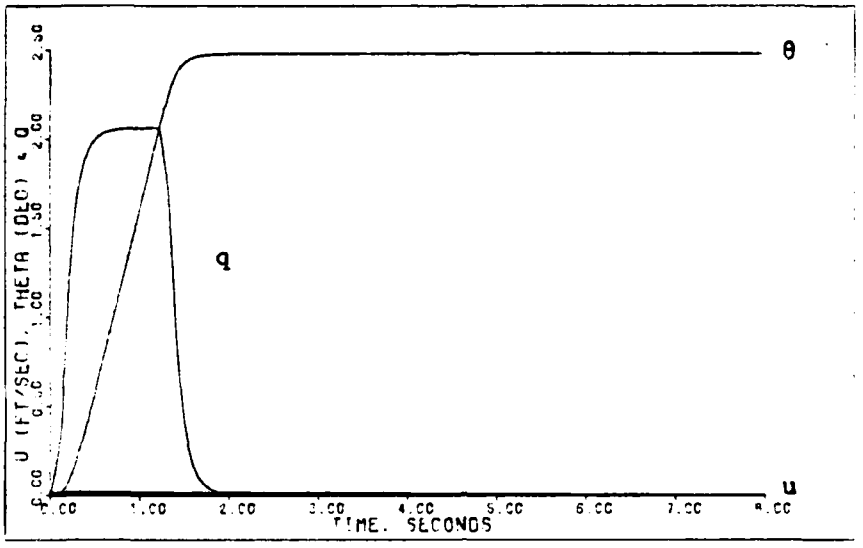

Figure 5-8: 0.9M Healthy/Failed Pitch Pointing -- Pitch Rate, Pitch Angle, and Forward Velocity

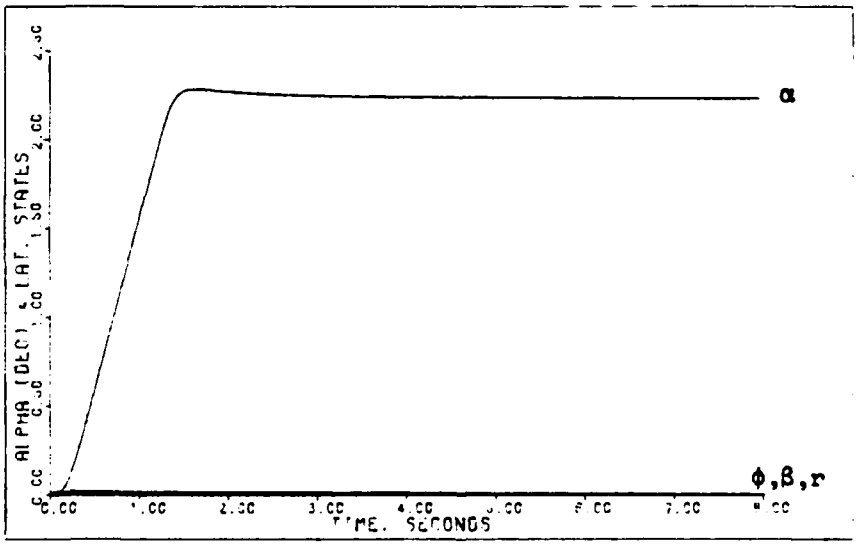

Figure 5-9: 0.9M Healthy/Failed Pitch Pointing -- Angle of Attack, Roll Angle, Sideslip Angle, and Yaw Rate

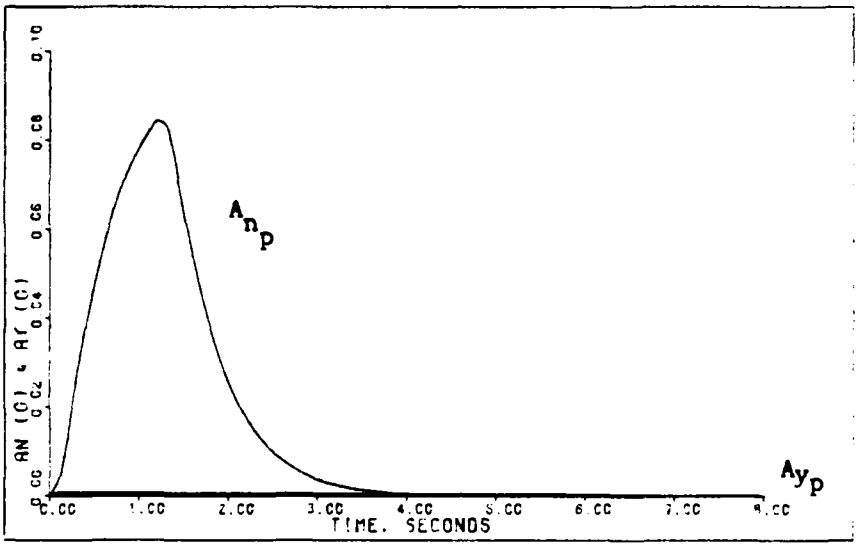

Figure 5-10: 0.9M Healthy/Failed Pitch Pointing -- Normal Acceleration and Lateral Acceleration

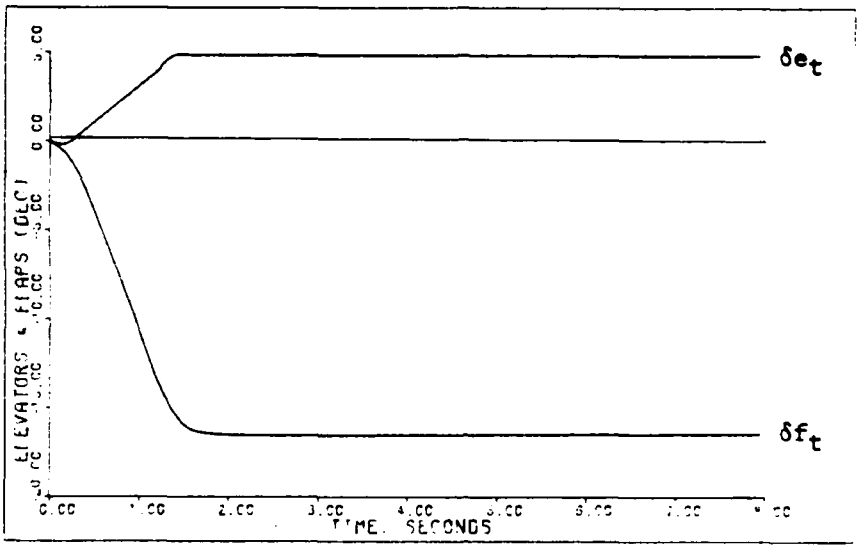

Figure 5-11: 0.9M Healthy Pitch Pointing -- Elevator and Flap Deflections

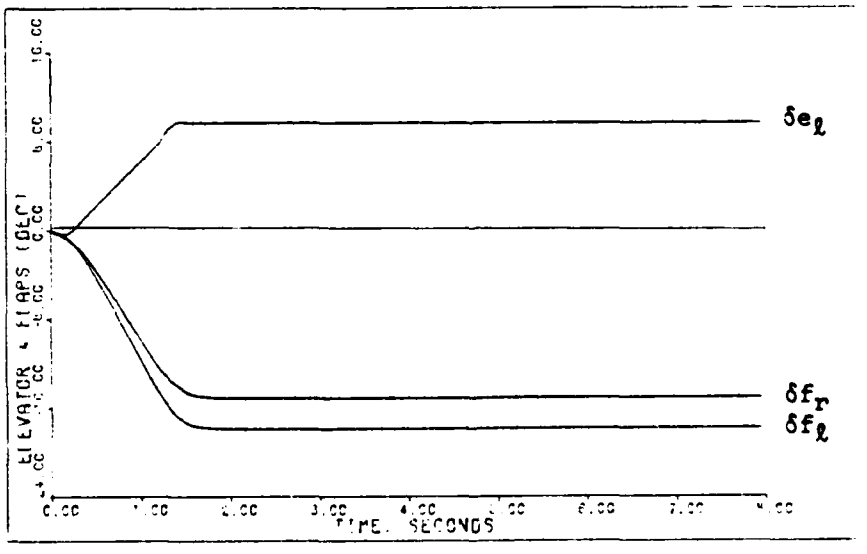

Figure 5-12: 0.9M Failed Pitch Pointing -- Left Elevator and Flaperon Deflections

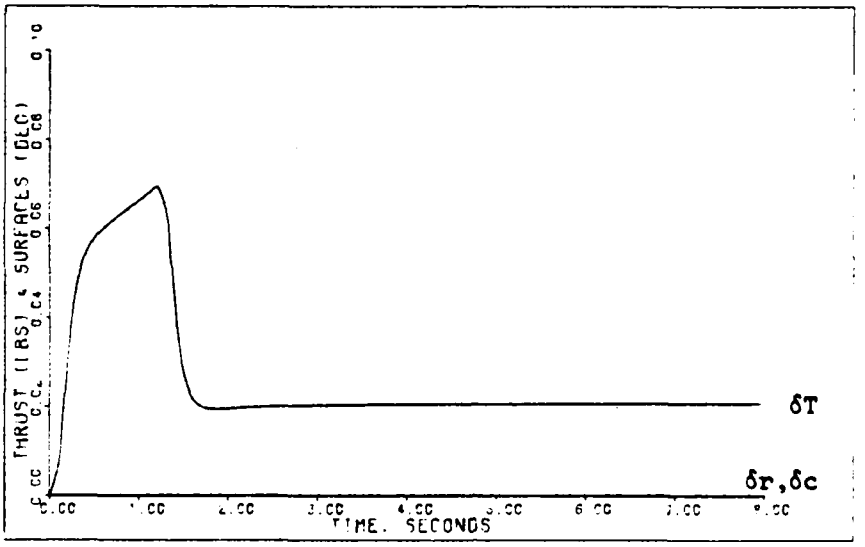

Figure 5-13: 0.9M Healthy Pitch Pointing -- Aileron, Rudder, and Canard Deflections and Thrust

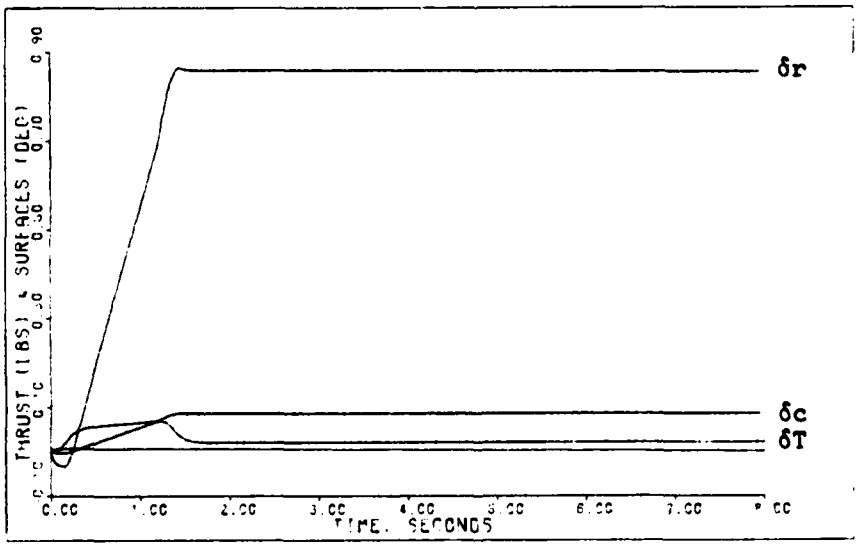

Figure 5-14: 0.9M Failed Pitch Pointing -- Rudder and Canard Deflections and Thrust

V-3. Longitudinal Translation Maneuver

Tables 5-5 and 5-6 give the design parameters for the longitudinal translation maneuver. Once again the design parameters $\bar{\alpha}$, $\underline{\Sigma}$, and ϵ are the same for the healthy and failed models.

The simulation responses for the longitudinal translation maneuver are given in Figures 5-15 through 5-21. As discussed in the g-command maneuver section Figures 5-15 through 5-17 give simulation responses for both the healthy and failed aircraft models. The maximum longitudinal translation command of 0.9g for one second, which yields a normal velocity of approximately 29 feet/second, is limited by the flaperon deflection.

As with the previous two longitudinal maneuvers the failure model requires that the left elevator must deflect approximately twice the angle of the healthy elevator deflection. Also, for the failure model, the flaperons deflect asymmetrically to counter the roll induced by the failed right horizontal tail, and the rudder and canard deflect to compensate for adverse yaw.

Table 5-5

Longitudinal Translation: Healthy Model,
0.9 Mach at 20,000 Feet

Sampling Time: T = 0.02 second

$\bar{\alpha} = 1.0$

$\varepsilon = 1.0$

$\underline{\Sigma} = \text{diag}\ \{2.0,\ 2.0,\ 2.35,\ 1.0,\ 2.3,\ 1.0\}$

$$\underline{K}_0 = \begin{bmatrix} 0.0 & -0.4533E-02 & -0.3534E-01 & -0.1370E-02 & 0.5821E-04 & 0.1407E-02 \\ 0.0 & 0.1685E-01 & -0.5018E-01 & 0.8348E-03 & -0.3546E-04 & -0.8572E-03 \\ 0.0 & 0.0 & 0.0 & 0.6581E-02 & -0.7018E-02 & -0.1200E-01 \\ 0.0 & 0.0 & 0.0 & 0.2548E-01 & 0.1858E-02 & -0.5830E-01 \\ 0.0 & 0.0 & 0.0 & 0.2794E-01 & -0.1187E-02 & -0.2870E-01 \\ 0.1039E+01 & -0.3110E-01 & 0.1944E+00 & 0.8464E-03 & -0.3595E-04 & -0.8691E-03 \end{bmatrix}$$

$\underline{K}_1 = \underline{K}_0$

Input Ramp Time: 0.2 second

Command Vector:

$u = 0.0$

$A_{n_p} = 0.9$ g (1 second pulse)

$q = 0.0$

$A_{y_p} = 0.0$

$p = 0.0$

$r = 0.0$

Table 5-6

Longitudinal Translation: Failed Model,
0.9 Mach at 20,000 Feet

Sampling Time: T = 0.02 second

$\bar{\alpha} = 1.0$

$\epsilon = 1.0$

$\underline{\Sigma} = \text{diag}\ \{2.0,\ 2.0,\ 2.35,\ 1.0,\ 2.3,\ 1.0\}$

$$\underline{K}_0 = \begin{bmatrix} 0.0 & -0.9059E-02 & -0.7062E-01 & -0.2750E-02 & 0.1285E-03 & 0.2833E-02 \\ 0.0 & 0.1555E-01 & -0.6031E-01 & 0.8910E-02 & -0.9049E-02 & -0.1590E-01 \\ 0.0 & 0.1814E-01 & -0.4008E-01 & -0.7235E-02 & 0.8970E-02 & 0.1417E-01 \\ 0.0 & -0.8036E-03 & -0.6264E-02 & 0.2640E-01 & 0.6243E-03 & -0.6018E-01 \\ 0.0 & -0.8025E-04 & -0.6256E-03 & 0.2804E-01 & -0.1310E-02 & -0.2888E-01 \\ 0.1039E+01 & -0.3108E-01 & 0.1946E+00 & 0.8576E-03 & -0.4007E-04 & -0.8835E-03 \end{bmatrix}$$

$\underline{K}_1 = \underline{K}_0$

Input Ramp Time: 0.2 second

Command Vector:

$u = 0.0$

$A_{n_p} = 0.9\ g$ (1 second pulse)

$q = 0.0$

$A_{y_p} = 0.0$

$p = 0.0$

$r = 0.0$

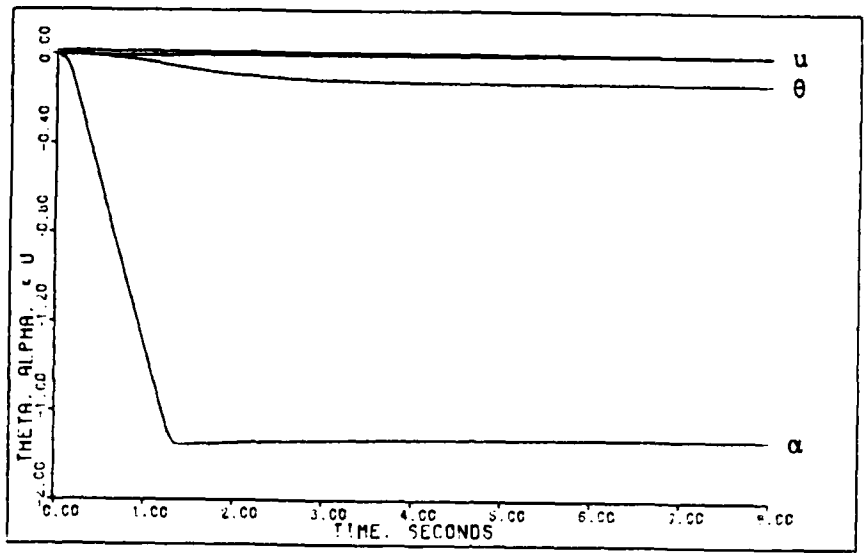

Figure 5-15: 0.9M Healthy/Failed Longitudinal Translation -- Pitch Angle, Angle of Attack, and Forward Velocity

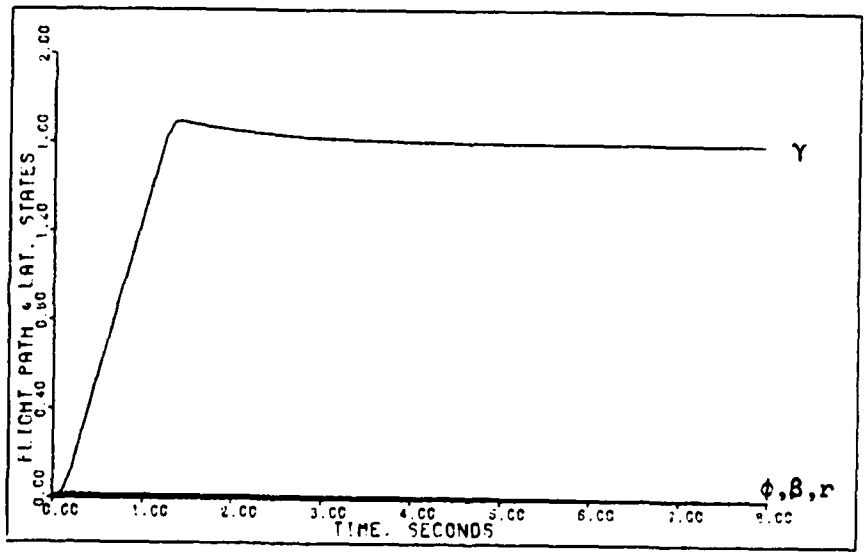

Figure 5-16: 0.9M Healthy/Failed Longitudinal Translation -- Flight Path Angle, Roll Angle, Sideslip Angle, and Yaw Rate

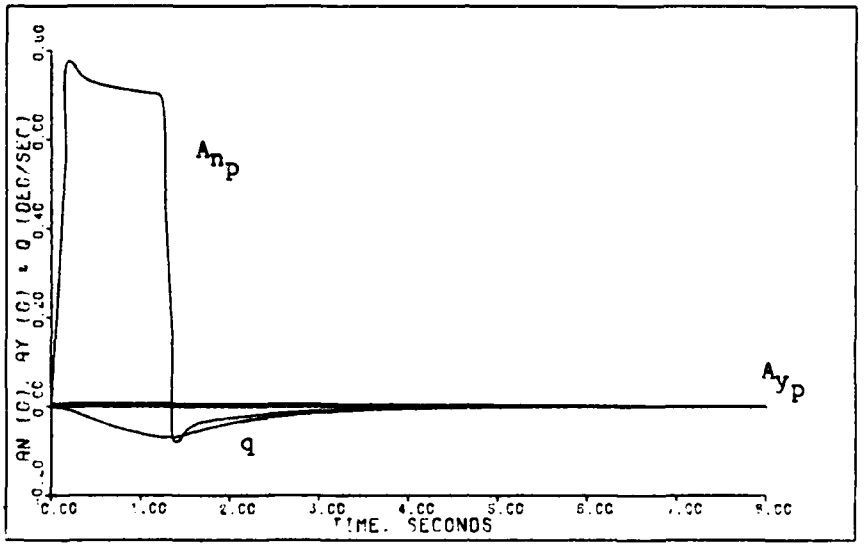

Figure 5-17: 0.9M Healthy/Failed Longitudinal Translation -- Pitch Rate, Normal Acceleration, and Lateral Acceleration

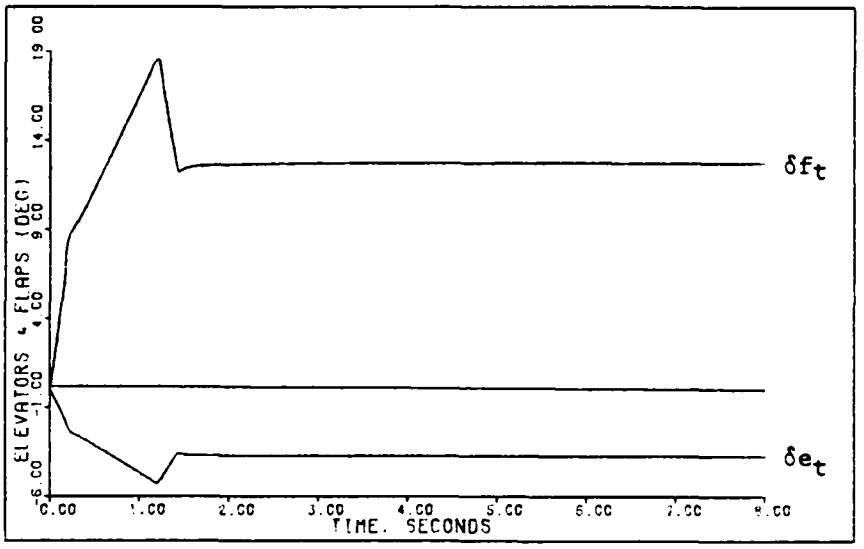

Figure 5-18: 0.9M Healthy Longitudinal Translation -- Elevator and Flap Deflections

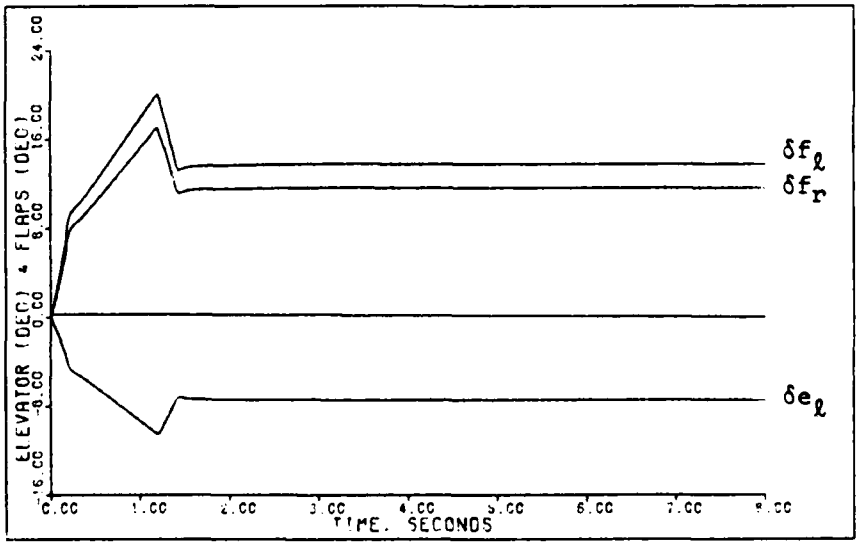

Figure 5-19: 0.9M Failed Longitudinal Translation -- Left Elevator and Flaperon Deflections

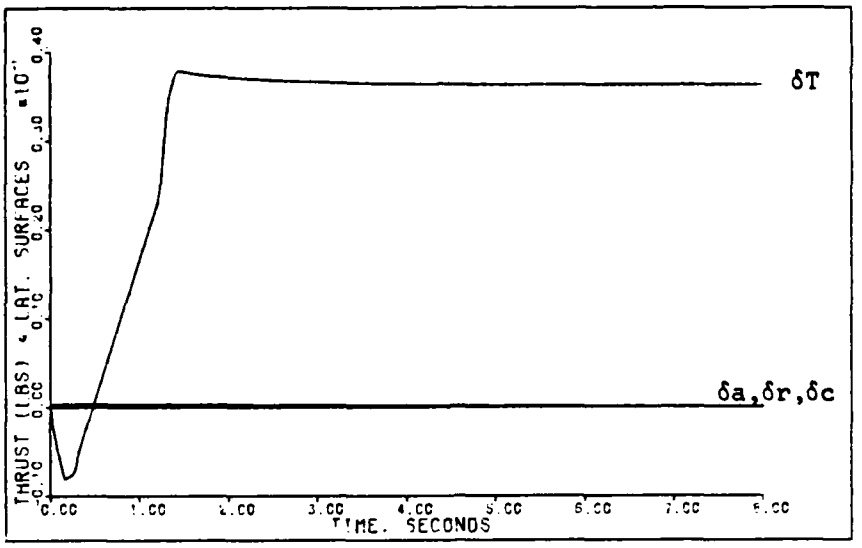

Figure 5-20: 0.9M Healthy Longitudinal Translation -- Aileron, Rudder, and Canard Deflections and Thrust

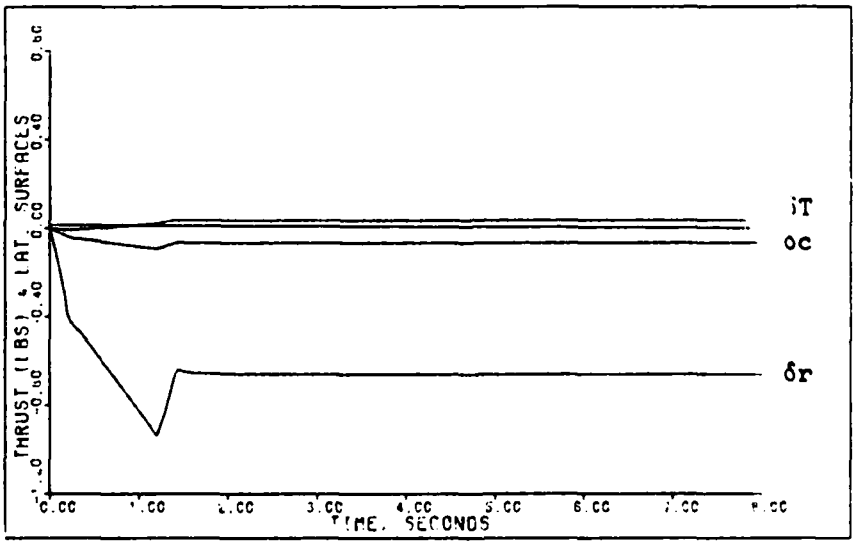

Figure 5-21: 0.9M Failed Longitudinal Translation -- Rudder and Canard Deflections and Thrust

V-4. Roll About Velocity Vector Maneuver

The roll maneuver requires some modifications to the healthy and failure models. These modifications are discussed in Chapter IV and are included in Tables 5-7 and 5-8, which give the design parameters $\bar{\alpha}$, $\underline{\Sigma}$, and ϵ for the roll maneuver. The parameters are the same for the healthy and failed models.

The simulation responses for the roll maneuver are given in Figures 5-22 through 5-28. For this maneuver the longitudinal responses are very small for both the healthy and failure models. Also, the healthy aircraft lateral responses change very little when the right horizontal tail fails. For these reasons Figures 5-22 through 5-24 give simulation responses for both the healthy and failed aircraft models.

The roll rate commanded is limited to 308 degrees per second for three seconds in order to avoid generating too large a sideslip angle. The large roll rate command creates a steady-state roll angle of approximately 1000 degrees which corresponds to rolling the aircraft 2.8 times. This large roll angle contradicts the small angle assumptions made when developing the linear aircraft models; however, approximations of the surface deflections required to obtain the commanded roll rate are obtained. This maneuver should be simulated with a full nonlinear model in the future.

The aileron deflection for the healthy aircraft (Figure 5-27) is less than the flaperon deflections for the failure

case (Figure 5-26) because the aileron deflection includes a contribution from the horizontal tail. When the right horizontal tail fails the flaperons must deflect more to achieve the commanded roll rate. The rudder and canard deflections are unaffected by the failure of the right horizontal tail.

Table 5-7

Roll About Velocity Vector: Healthy Model,
0.9 Mach at 20,000 Feet

Sampling Time: T = 0.02 second

$\bar{\alpha} = 1.0$

$\epsilon = 1.0$

$\underline{\Sigma} = \text{diag}\{2.0, 1.0, 2.35, 1.0, 1.0, 1.0\}$

$$\underline{K}_0 = \begin{bmatrix} 0.0 & -0.2267E-03 & -0.3534E-01 & -0.1370E-02 & 0.2531E-04 & 0.1407E-02 \\ 0.0 & 0.8425E-03 & -0.5018E-01 & 0.8348E-03 & -0.1542E-04 & -0.8572E-03 \\ 0.0 & 0.0 & 0.0 & 0.6581E-02 & -0.3051E-02 & -0.1200E-01 \\ 0.0 & 0.0 & 0.0 & 0.2548E-01 & 0.8077E-03 & -0.5830E-01 \\ 0.0 & 0.0 & 0.0 & 0.2794E-01 & -0.5161E-03 & -0.2870E-01 \\ 0.1039E+01 & -0.1555E-02 & 0.1944E+00 & 0.8464E-03 & -0.1563E-04 & -0.8691E-03 \end{bmatrix}$$

$\underline{K}_1 = \underline{K}_0$

Input Ramp Time: 0.4 second

Command Vector:

$u = 0.0$

$A_{n_p} = 0.0$

$q = 0.0$

$A_{y_p} = 0.0$

$p = 5.376$ radians/second (3 second pulse)

$r\text{-}\alpha_T = 0.0$

Table 5-8

Roll About Velocity Vector: Failed Model,
0.9 Mach at 20,000 Feet

Sampling Time: T = 0.02 second

$\bar{\alpha} = 1.0$

$\epsilon = 1.0$

$\underline{\Sigma} = \text{diag}\ \{2.0, 1.0, 2.35, 1.0, 1.0, 1.0\}$

$$\underline{K}_0 = \begin{bmatrix} 0.0 & -0.4529E-03 & -0.7062E-01 & -0.2750E-02 & 0.5585E-04 & 0.2833E-02 \\ 0.0 & 0.7775E-03 & -0.6031E-01 & 0.8910E-02 & -0.3934E-02 & -0.1590E-01 \\ 0.0 & 0.9072E-03 & -0.4008E-01 & -0.7235E-02 & 0.3900E-02 & 0.1417E-01 \\ 0.0 & -0.4018E-04 & -0.6264E-02 & 0.2640E-01 & 0.2715E-03 & -0.6018E-01 \\ 0.0 & -0.4012E-05 & -0.6256E-03 & 0.2804E-01 & -0.5695E-03 & -0.2888E-01 \\ 0.1039E+01 & -0.1554E-02 & 0.1946E+00 & 0.8576E-03 & -0.1742E-04 & -0.8835E-03 \end{bmatrix}$$

$\underline{K}_1 = \underline{K}_0$

Input Ramp Time: 0.4 second

Command Vector:

$u = 0.0$

$A_{n_p} = 0.0$

$q = 0.0$

$A_{y_p} = 0.0$

$p = 5.376$ radians/second (3 second pulse)

$r-\alpha_T = 0.0$

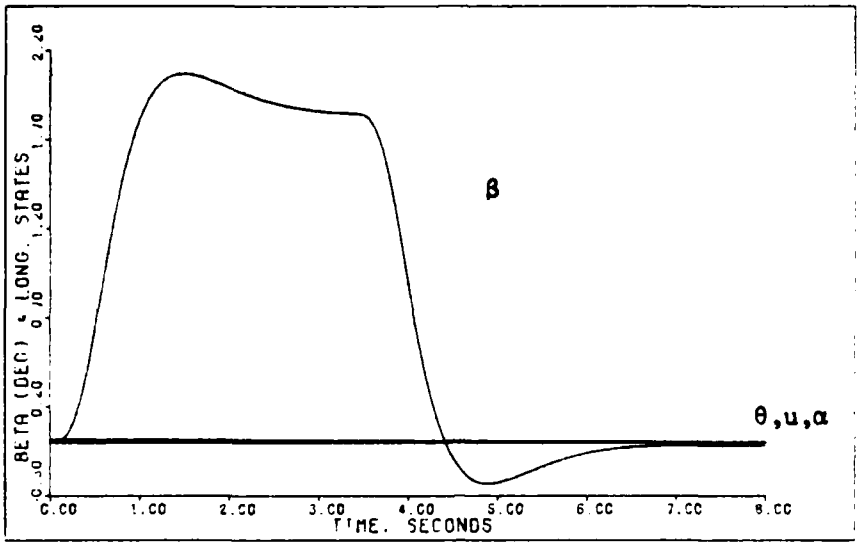

Figure 5-22: 0.9M Healthy/Failed Roll -- Sideslip Angle, Pitch Angle, Angle of Attack, and Forward Velocity

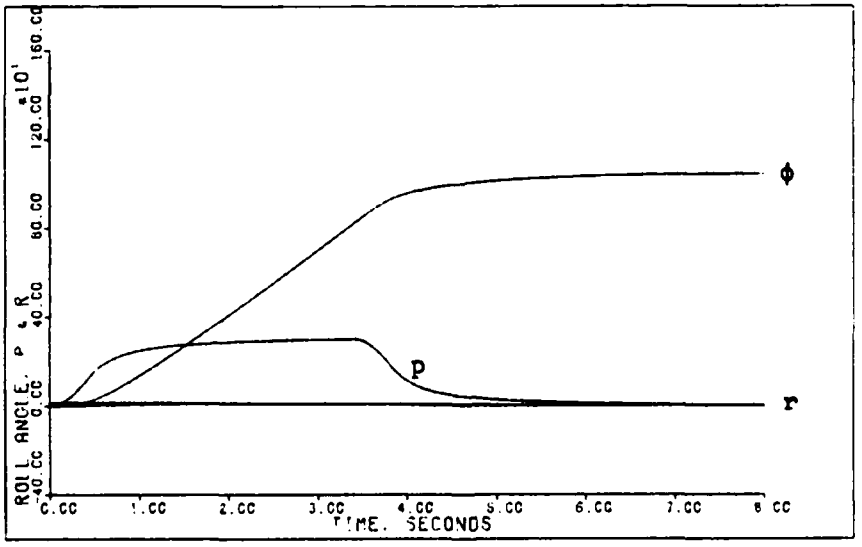

Figure 5-23: 0.9M Healthy/Failed Roll -- Roll Angle, Roll Rate, and Yaw Rate

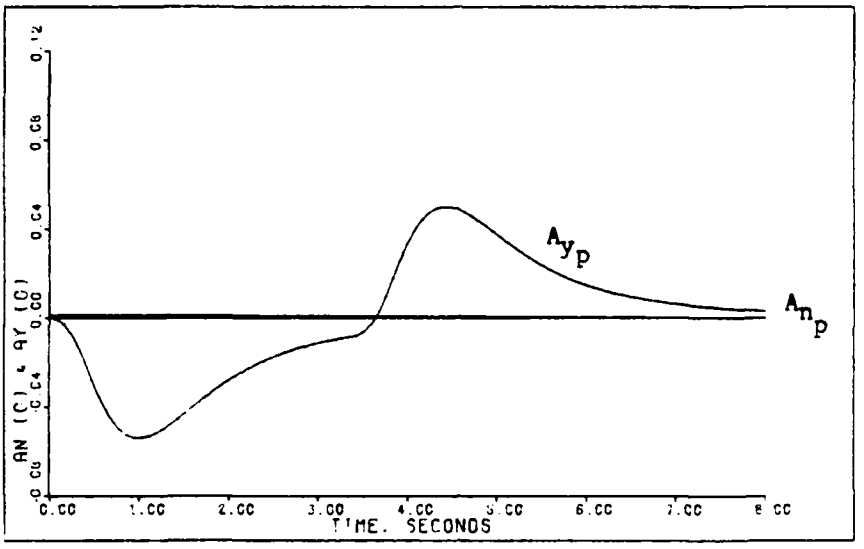

Figure 5-24: 0.9M Healthy/Failed Roll -- Normal Acceleration and Lateral Acceleration

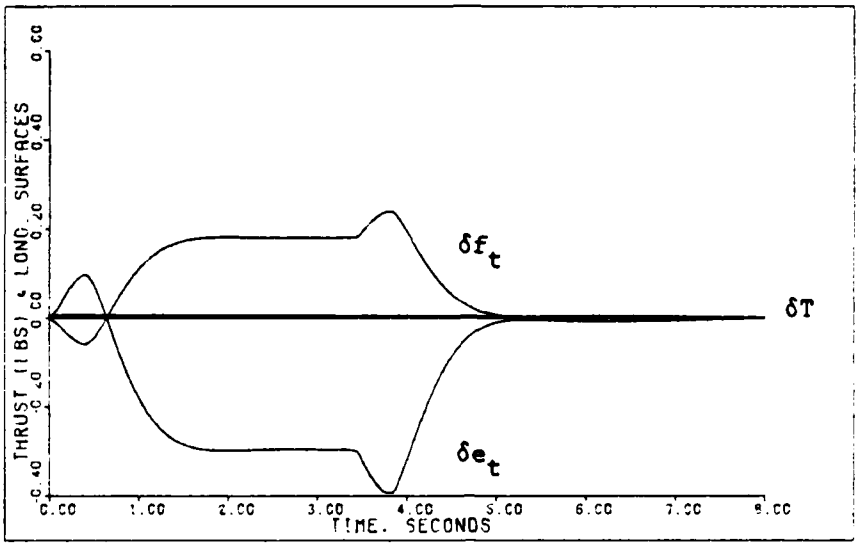

Figure 5-25: 0.9M Healthy Roll -- Elevator and Flap Deflections and Thrust

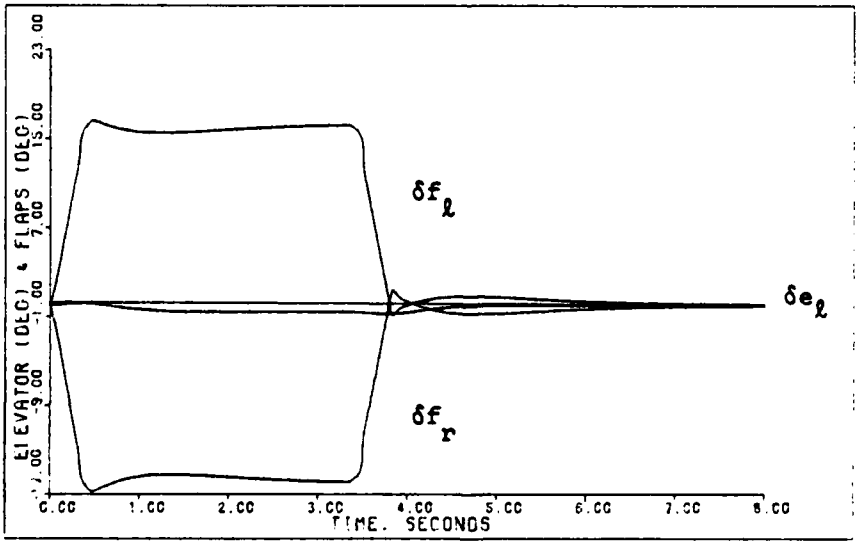

Figure 5-26: 0.9M Failed Roll -- Left Elevator and Flaperon Deflections

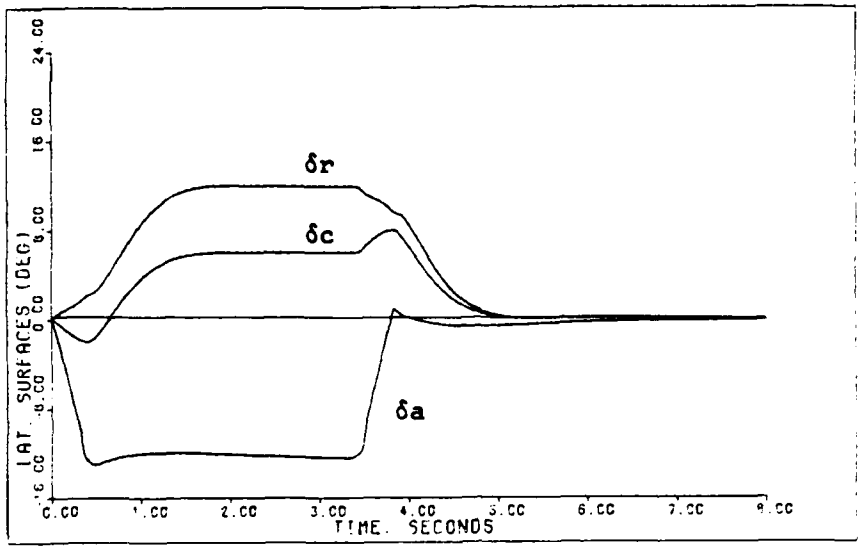

Figure 5-27: 0.9M Healthy Roll -- Aileron, Rudder, and Canard Deflections

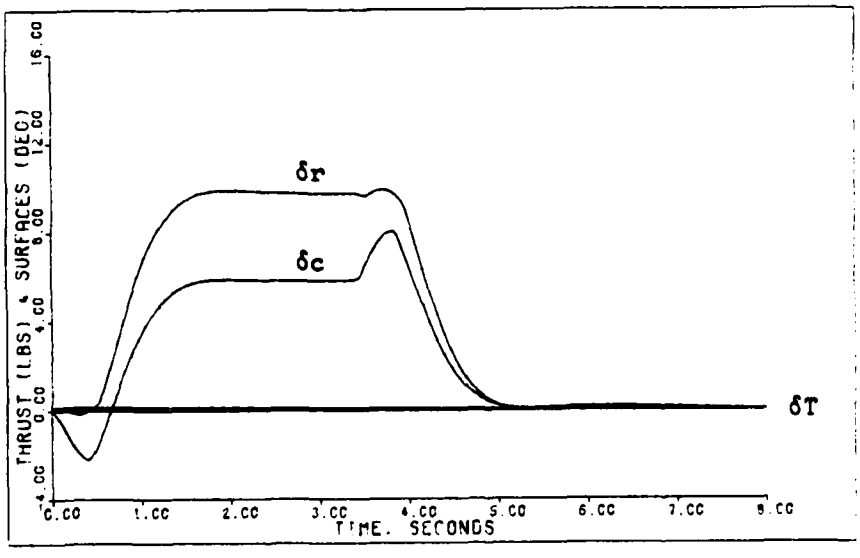

Figure 5-28: 0.9M Failed Roll -- Rudder and Canard Deflections and Thrust

V-5. Sideforce (Flat Turn) Maneuver

Tables 5-9 and 5-10 give the design parameters $\bar{\alpha}$, $\underline{\Sigma}$, and ε for both the healthy and failed cases of the sideforce maneuver. The same parameters are used for both cases.

Figures 5-29 through 5-35 present the simulation responses for a 0.8g sideforce command. The maximum value commanded is limited by the canard deflection. As with the roll maneuver the healthy and failed longitudinal responses are very small, and the lateral responses change very little when the right horizontal tail fails; therefore, Figures 5-29 through 5-31 give simulation responses for both the healthy and failed models.

For this maneuver the horizontal tail is mainly used to counter the longitudinal pitching moment produced by the canard deflection although it also contributes to roll control for the healthy aircraft case. When the right horizontal tail fails the left horizontal tail deflects approximately twice the deflection of the healthy elevators. The flaperons deflect slightly asymmetrically to compensate for the roll created by the failed right horizontal tail. The rudder and canard deflections change only slightly for the failure case.

Table 5-9

Sideforce Maneuver: Healthy Model,
0.9 Mach at 20,000 Feet

Sampling Time: T = 0.02 second

$\bar{\alpha} = 1.0$

$\epsilon = 1.0$

$\Sigma = \text{diag}\{2.0, 1.0, 2.35, 1.0, 2.3, 1.0\}$

$$\underline{K}_0 = \begin{bmatrix} 0.0 & -0.2267E-03 & -0.3534E-01 & -0.1370E-02 & 0.5821E-04 & 0.1407E-02 \\ 0.0 & 0.8425E-03 & -0.5018E-01 & 0.8348E-03 & -0.3546E-04 & -0.8572E-03 \\ 0.0 & 0.0 & 0.0 & 0.6581E-02 & -0.7018E-02 & -0.1200E-01 \\ 0.0 & 0.0 & 0.0 & 0.2548E-01 & 0.1858E-02 & -0.5830E-01 \\ 0.0 & 0.0 & 0.0 & 0.2794E-01 & -0.1187E-02 & -0.2870E-01 \\ 0.1039E+01 & -0.1555E-02 & 0.1944E+00 & 0.8464E-03 & -0.3595E-04 & -0.8691E-03 \end{bmatrix}$$

$\underline{K}_1 = \underline{K}_0$

Input Ramp Time: 0.5 second

Command Vector:

$u = 0.0$

$A_{n_p} = 0.0$

$q = 0.0$

$A_{y_p} = 0.8$ g (step)

$p = 0.0$

$r = 0.02760$ radian/second (step)

Table 5-10

Sideforce Maneuver: Failed Model,
0.9 Mach at 20,000 Feet

Sampling Time: T = 0.02 second

$\bar{\alpha} = 1.0$

$\epsilon = 1.0$

$\underline{\Sigma} = \text{diag}\ \{2.0, 1.0, 2.35, 1.0, 2.3, 1.0\}$

$$\underline{K}_0 = \begin{bmatrix} 0.0 & -0.4529E-03 & -0.7062E-01 & -0.2750E-02 & 0.1285E-03 & 0.2833E-02 \\ 0.0 & 0.7775E-03 & -0.6031E-01 & 0.8910E-02 & -0.9049E-02 & -0.1590E-01 \\ 0.0 & 0.9072E-03 & -0.4008E-01 & -0.7235E-02 & 0.8970E-02 & 0.1417E-01 \\ 0.0 & -0.4018E-04 & -0.6264E-02 & 0.2640E-01 & 0.6243E-03 & -0.6018E-01 \\ 0.0 & -0.4012E-05 & -0.6256E-03 & 0.2804E-01 & -0.1310E-02 & -0.2888E-01 \\ 0.1039E+01 & -0.1554E-02 & 0.1946E+00 & 0.8576E-03 & -0.4007E-04 & -0.8835E-03 \end{bmatrix}$$

$\underline{K}_1 = \underline{K}_0$

Input Ramp Time: 0.5 second

Command Vector:

$u = 0.0$

$A_{n_p} = 0.0$

$q = 0.0$

$A_{y_p} = 0.8$ g (step)

$p = 0.0$

$r = 0.02760$ radian/second (step)

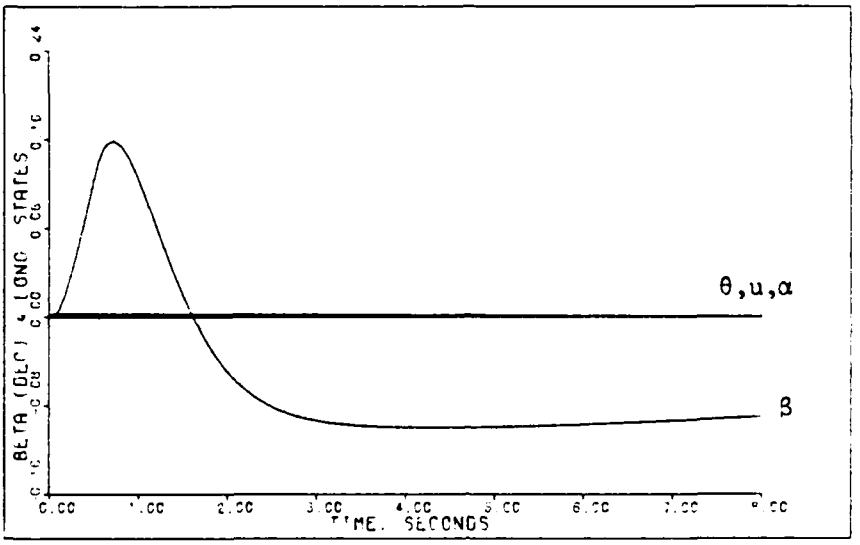

Figure 5-29: 0.9M Healthy/Failed Sideforce -- Sideslip Angle, Pitch Angle, Angle of Attack, and Forward Velocity

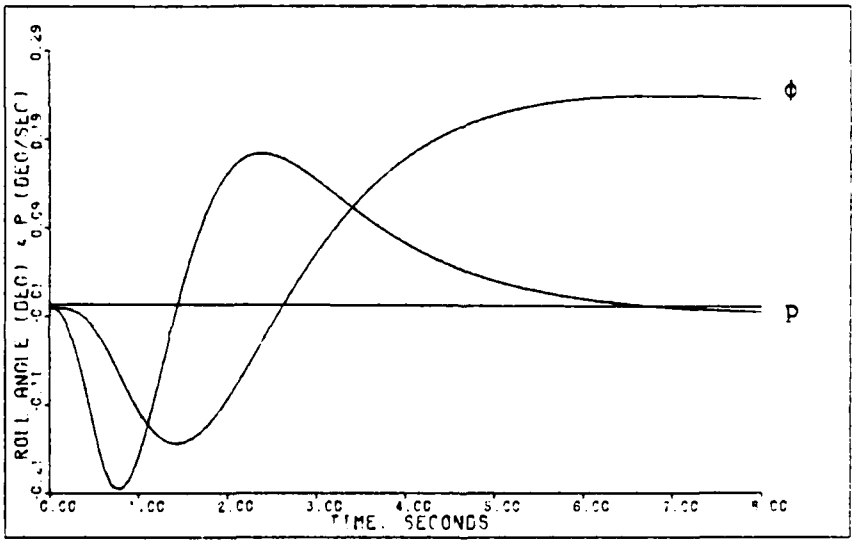

Figure 5-30: 0.9M Healthy/Failed Sideforce -- Roll Angle and Roll Rate

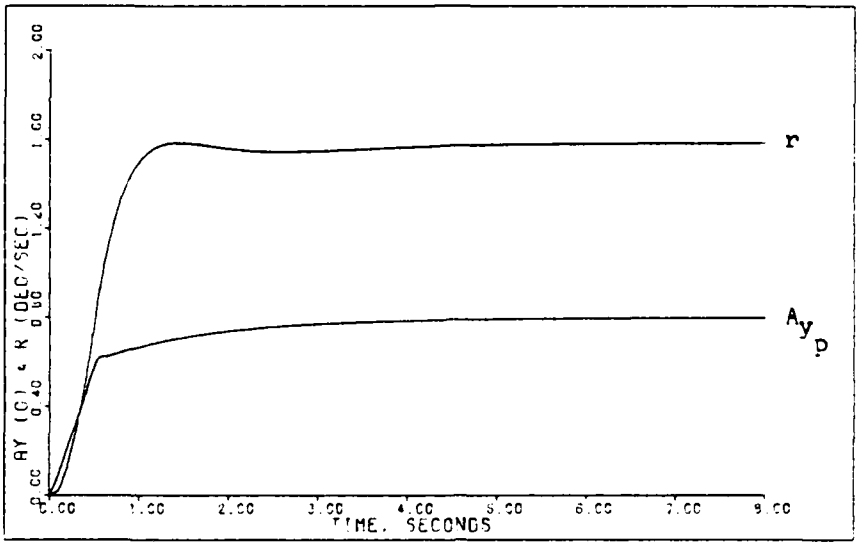

Figure 5-31: 0.9M Healthy/Failed Sideforce -- Lateral Acceleration and Yaw Rate

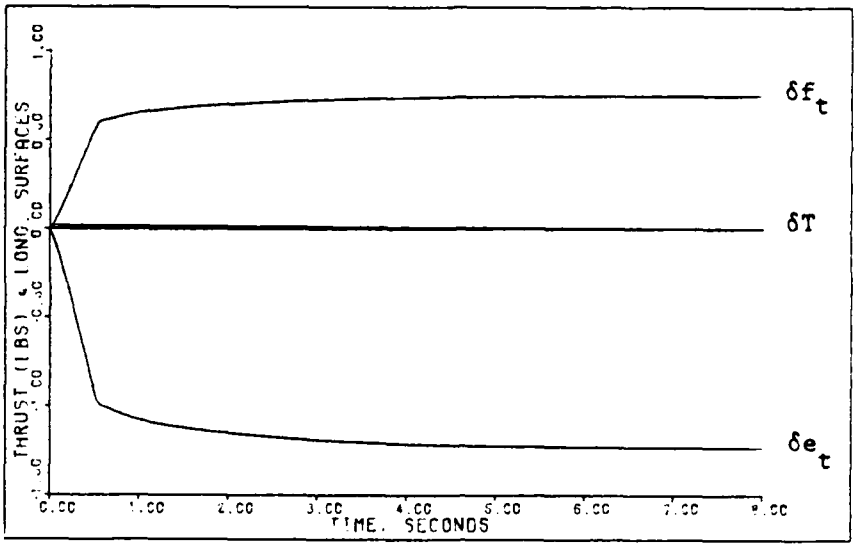

Figure 5-32: 0.9M Healthy Sideforce -- Elevator and Flap Deflections and Thrust

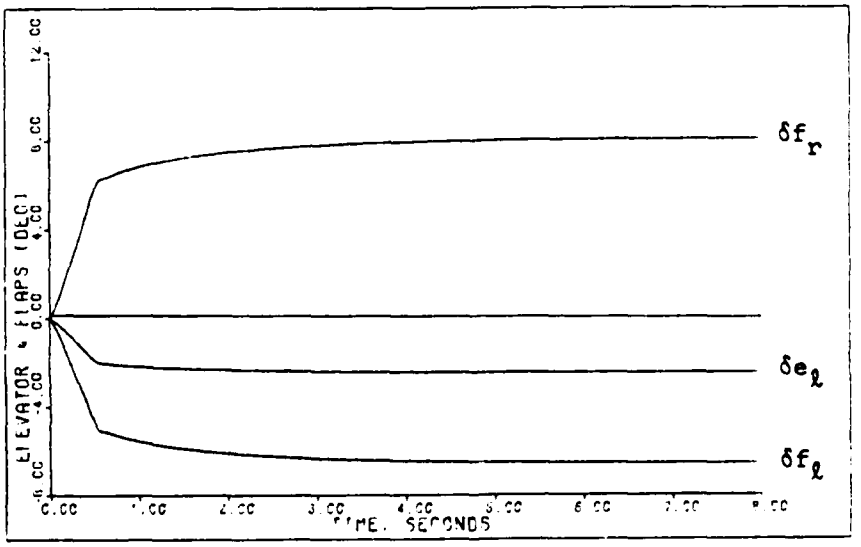

Figure 5-33: 0.9M Failed Sideforce -- Left Elevator and Flaperon Deflections

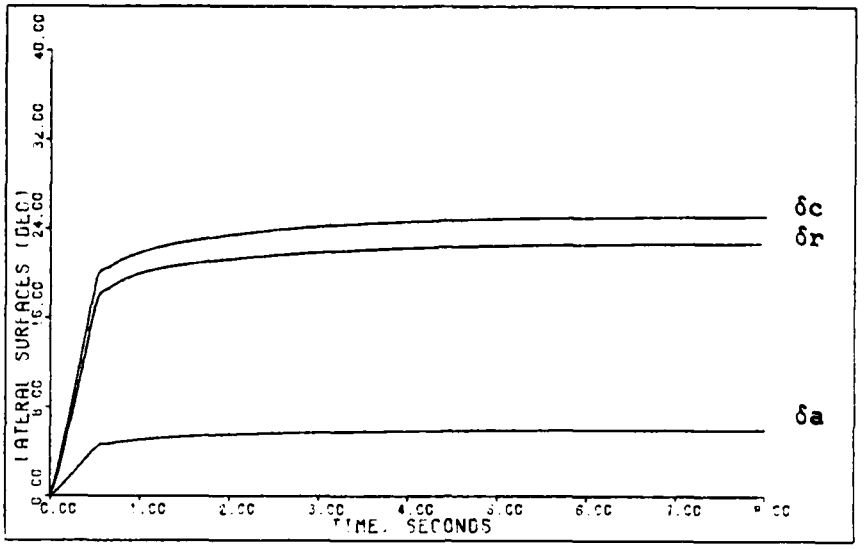

Figure 5-34: 0.9M Healthy Sideforce -- Aileron, Rudder, and Canard Deflections

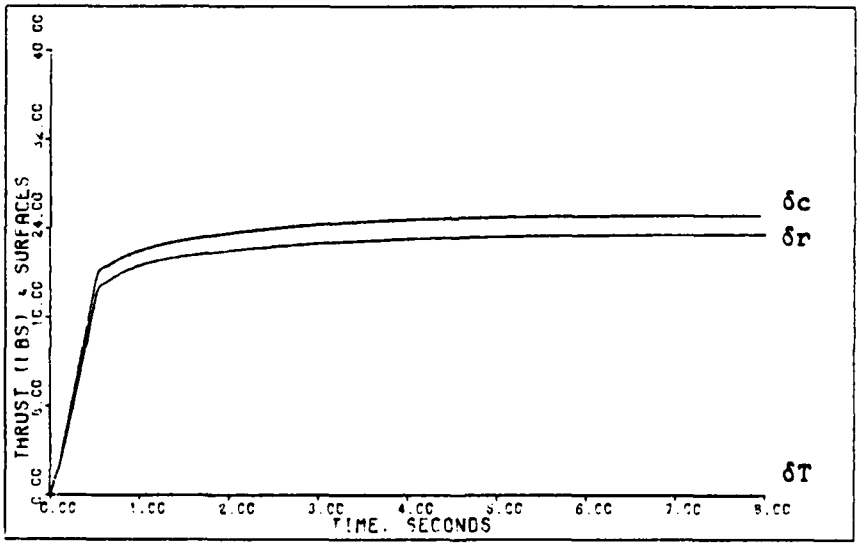

Figure 5-35: 0.9M Failed Sideforce -- Rudder and Canard Deflections and Thrust

V-6. Yaw Pointing Maneuver

The design parameters $\bar{\alpha}$, $\underline{\Sigma}$, and ϵ for the yaw pointing maneuver are given in Tables 5-11 and 5-12 for both the healthy and failed models. The parameters are the same for both cases.

Figures 5-36 through 5-42 present the simulation responses for a four degree yaw pointing command. The maximum angle commanded for this maneuver is limited by the ability to hold the roll angle to a small value. As with the roll and sideforce maneuvers, Figures 5-36 through 5-38 give simulation responses for both the healthy and failed aircraft models.

For the yaw pointing maneuver the horizontal tail is used for both pitch and roll control. When the right horizontal tail fails the flaperons take over the roll control and deflect asymmetrically to counter the rolling moment of the left horizontal tail, which deflects for pitch control. The rudder and canard responses are not affected much by the failure for this maneuver.

Table 5-11

Yaw Pointing: Healthy Model, 0.9 Mach at 20,000 Feet

Sampling Time: T = 0.02 second

$\bar{\alpha}$ = 6.0

ε = 1.0

$\underline{\Sigma}$ = diag {2.0, 1.0, 2.35, 3.0, 3.25, 3.0}

$$\underline{K}_0 = \begin{bmatrix} 0.0 & -0.2267E-03 & -0.3534E-01 & -0.4111E-02 & 0.8225E-04 & 0.4222E-02 \\ 0.0 & 0.8425E-03 & -0.5018E-01 & 0.2504E-02 & -0.5011E-04 & -0.2572E-02 \\ 0.0 & 0.0 & 0.0 & 0.1974E-01 & -0.9916E-02 & -0.3600E-01 \\ 0.0 & 0.0 & 0.0 & 0.7643E-01 & 0.2625E-02 & -0.1749E+00 \\ 0.0 & 0.0 & 0.0 & 0.8383E-01 & -0.1677E-02 & -0.8609E-01 \\ 0.1039E+01 & -0.1555E-02 & 0.1944E+00 & 0.2539E-02 & -0.5080E-04 & -0.2607E-02 \end{bmatrix}$$

$$\underline{K}_1 = \begin{bmatrix} 0.0 & -0.1360E-02 & -0.2120E+00 & -0.2467E-01 & 0.4935E-01 & 0.2533E-01 \\ 0.0 & 0.5055E-02 & -0.3011E+00 & 0.1503E-01 & -0.3006E-03 & -0.1543E-01 \\ 0.0 & 0.0 & 0.0 & 0.1185E+00 & -0.5950E-01 & -0.2160E+00 \\ 0.0 & 0.0 & 0.0 & 0.4586E+00 & 0.1575E-01 & -0.1049E+01 \\ 0.0 & 0.0 & 0.0 & 0.5030E+00 & -0.1006E-01 & -0.5165E+00 \\ 0.6232E+01 & -0.9331E-02 & 0.1166E+01 & 0.1523E-01 & -0.3048E-03 & -0.1564E-01 \end{bmatrix}$$

Input Ramp Time: 0.2 second

Command Vector:

$u = 0.0$

$A_{n_p} = 0.0$

$q = 0.0$

$A_{y_p} = 0.0$

$p = 0.0$

$r = -0.05818$ radian/second (1 second pulse)

Table 5-12

Yaw Pointing: Failed Model, 0.9 Mach at 20,000 Feet

Sampling Time: T = 0.02 second

$\bar{\alpha} = 6.0$

$\varepsilon = 1.0$

$\underline{\Sigma} = \text{diag}\ \{2.0,\ 1.0,\ 2.35,\ 3.0,\ 3.25,\ 3.0\}$

$$\underline{K}_0 = \begin{bmatrix} 0.0 & -0.4529E-03 & -0.7062E-01 & -0.8249E-02 & 0.1815E-03 & 0.8498E-02 \\ 0.0 & 0.7775E-03 & -0.6031E-01 & 0.2673E-01 & -0.1279E-01 & -0.4769E-01 \\ 0.0 & 0.9072E-03 & -0.4008E-01 & -0.2170E-01 & 0.1268E-01 & 0.4251E-01 \\ 0.0 & -0.4018E-04 & -0.6264E-02 & 0.7920E-01 & 0.8822E-03 & -0.1805E+00 \\ 0.0 & -0.4012E-05 & -0.6256E-03 & 0.8411E-01 & -0.1851E-02 & -0.8665E-01 \\ 0.1039E+01 & -0.1554E-02 & 0.1946E+00 & 0.2573E-02 & -0.5662E-04 & -0.2651E-02 \end{bmatrix}$$

$$\underline{K}_1 = \begin{bmatrix} 0.0 & -0.2718E-02 & -0.4237E+00 & -0.4949E-01 & 0.1089E-02 & 0.5099E-01 \\ 0.0 & 0.4665E-02 & -0.3619E+00 & 0.1604E+00 & -0.7672E-01 & -0.2861E+00 \\ 0.0 & 0.5443E-02 & -0.2405E+00 & -0.1302E+00 & 0.7605E-01 & 0.2551E+00 \\ 0.0 & -0.2411E-03 & -0.3759E-01 & 0.4752E+00 & 0.5293E-02 & -0.1083E+01 \\ 0.0 & -0.2407E-04 & -0.3754E-02 & 0.5046E+00 & -0.1111E-01 & -0.5199E+00 \\ 0.6232E+01 & -0.9324E-02 & 0.1168E+01 & 0.1544E-01 & -0.3397E-03 & -0.1590E-01 \end{bmatrix}$$

Input Ramp Time: 0.2 second

Command Vector:

$u = 0.0$

$A_{n_p} = 0.0$

$q = 0.0$

$A_{y_p} = 0.0$

$p = 0.0$

$r = -0.05818$ radian/second (1 second pulse)

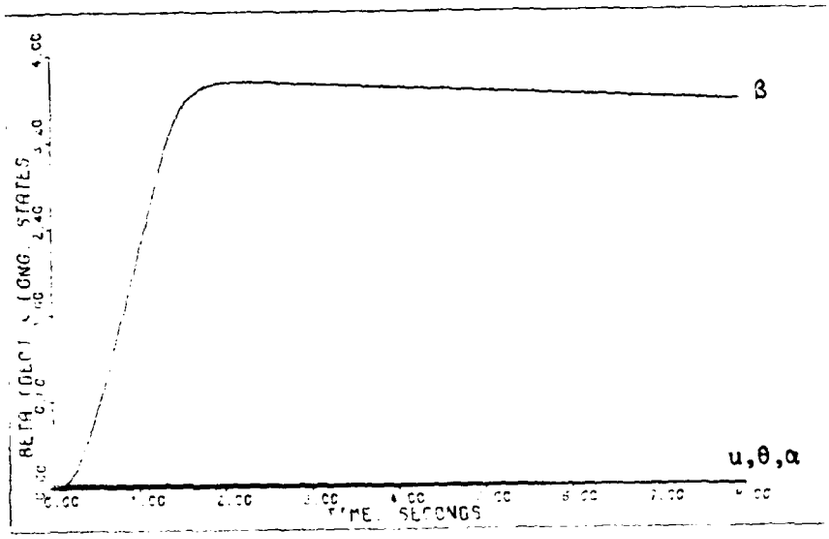

Figure 5-36: 0.9M Healthy/Failed Yaw Pointing -- Sideslip Angle, Pitch Angle, Angle of Attack, and Forward Velocity

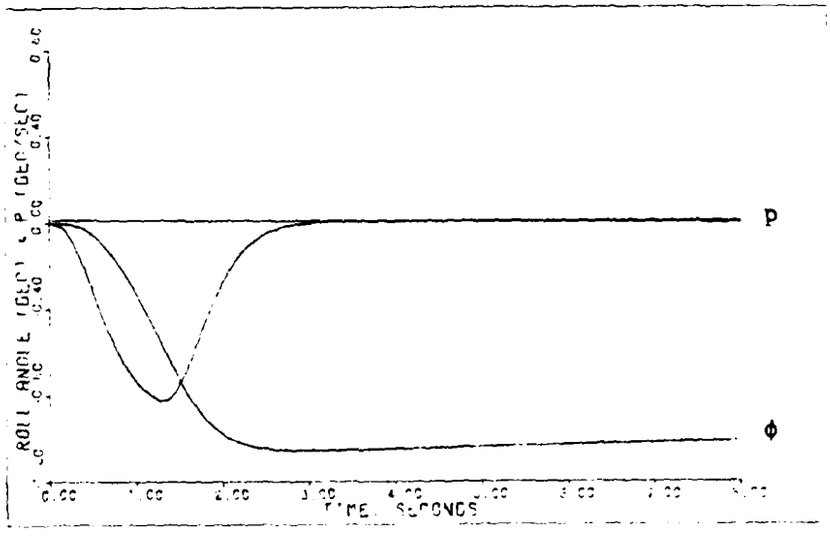

Figure 5-37: 0.9M Healthy/Failed Yaw Pointing -- Roll Angle and Roll Rate

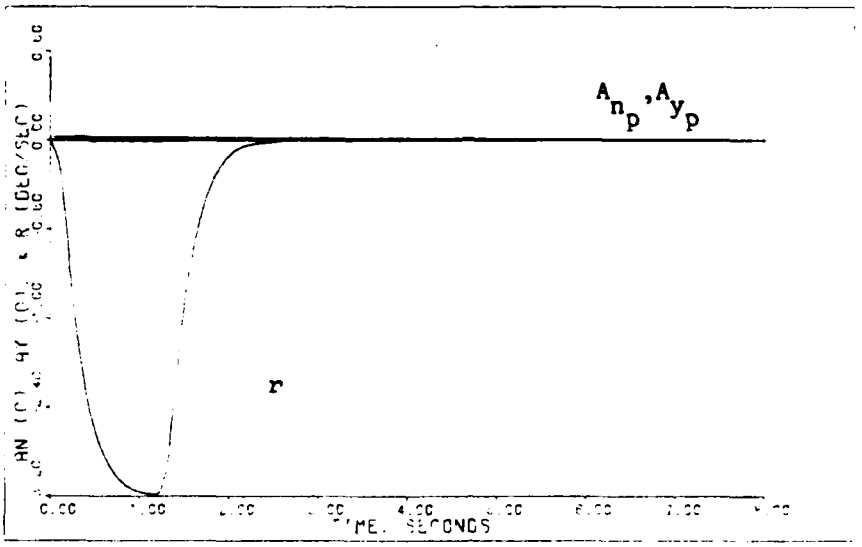

Figure 5-38: 0.9M Healthy/Failed Yaw Pointing -- Normal Acceleration, Lateral Acceleration, and Yaw Rate

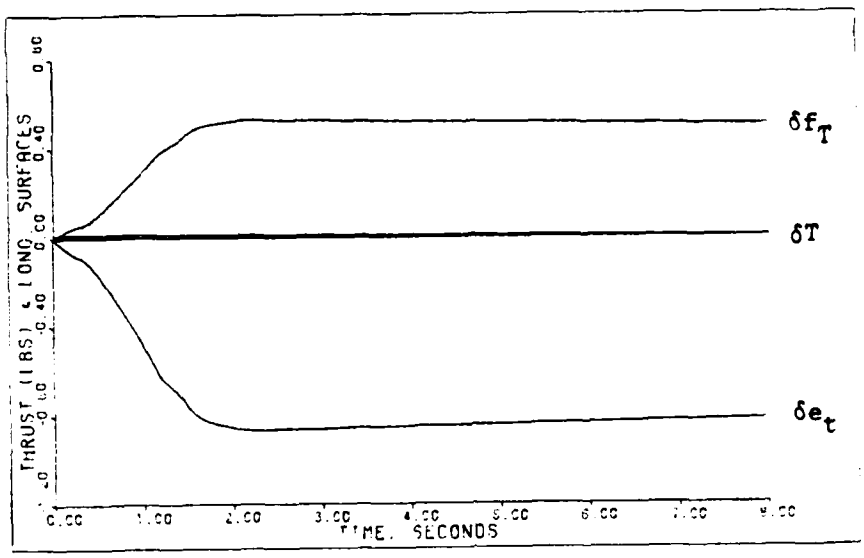

Figure 5-39: 0.9M Healthy Yaw Pointing -- Elevator and Flap Deflections and Thrust

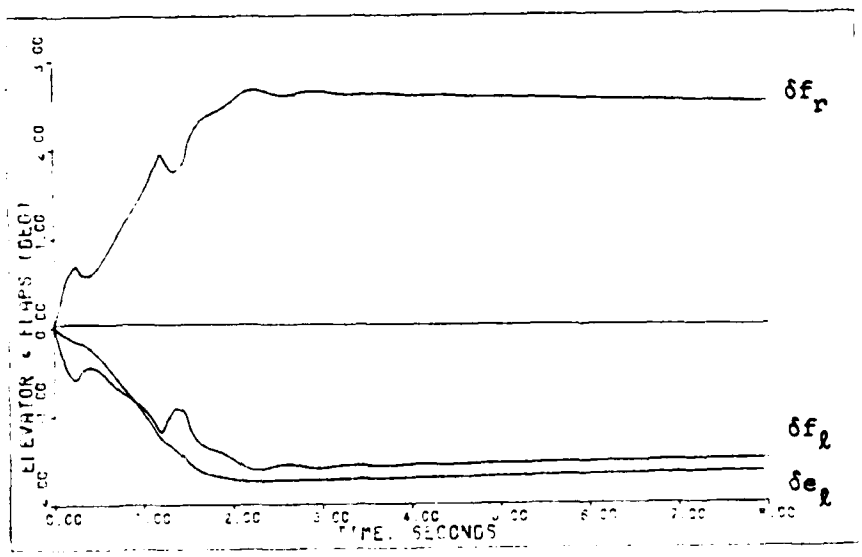

Figure 5-40: 0.9M Failed Yaw Pointing -- Left Elevator and Flaperon Deflections

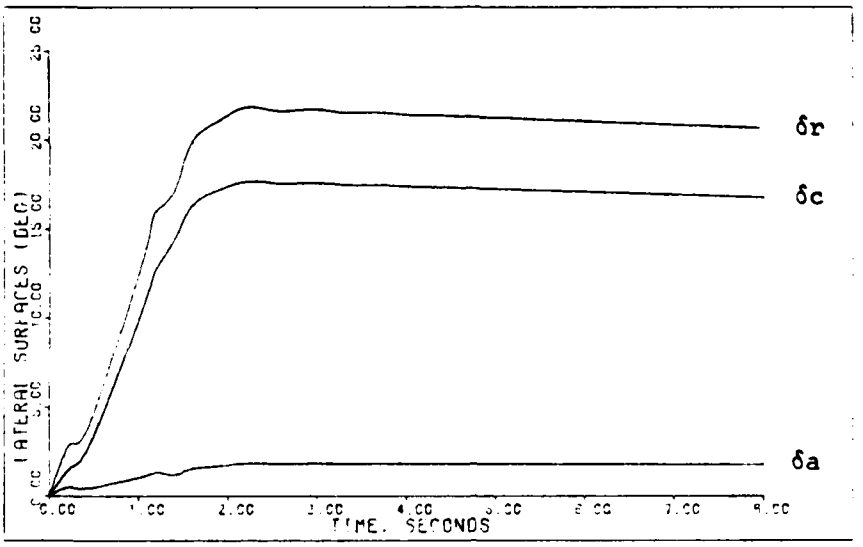

Figure 5-41: 0.9M Healthy Yaw Pointing -- Aileron, Rudder, and Canard Deflections

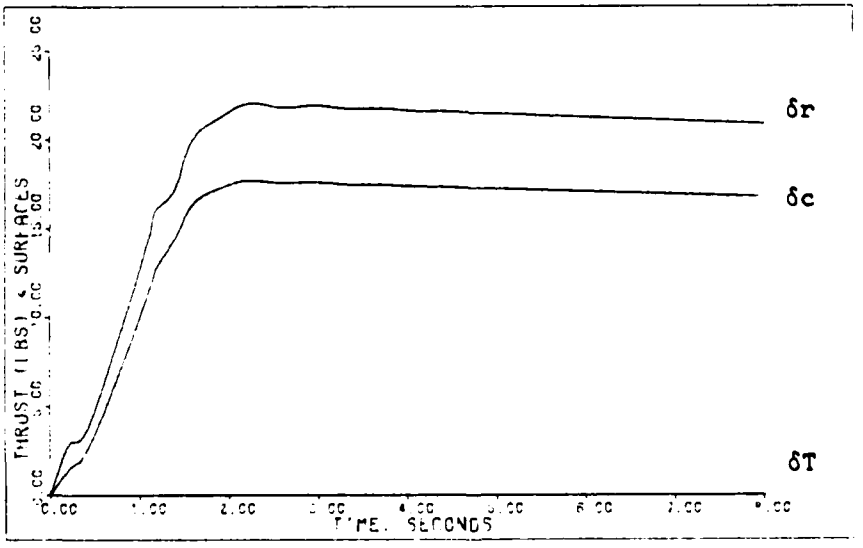

Figure 5-42: 0.9M Failed Yaw Pointing -- Rudder and Canard Deflections and Thrust

V-7. Lateral Translation Maneuver

Tables 5-13 and 5-14 give the design parameters $\bar{\alpha}$, $\underline{\Sigma}$, and ϵ for the lateral translation maneuver. As indicated in the tables the same design parameters are used for both the healthy and failed aircraft models.

The simulation responses for a 0.6g lateral acceleration command, which corresponds to a steady-state lateral velocity value of 25 feet/second, are given in Figures 5-43 through 5-49. The maximum lateral acceleration commanded for this maneuver is limited by the ability to hold the roll angle to a small value. As explained for the roll and side-force maneuvers, Figures 5-43 through 5-45 give simulation responses for both the healthy and failed aircraft models.

For the lateral translation maneuver the horizontal tail is used mainly as an elevator to counter the small pitch moment generated by the canard deflection. When the right horizontal tail fails the left horizontal tail deflects to approximately twice the elevator deflection of the healthy aircraft simulation, and the flaperons deflect asymmetrically to counter the rolling moment of the left horizontal tail. The rudder and canard responses are not affected much by the failure for this maneuver.

Table 5-13

Lateral Translation: Healthy Model,
0.9 Mach at 20,000 Feet

Sampling Time: T = 0.02 second

$\bar{\alpha}$ = 3.0

ε = 1.0

$\underline{\Sigma}$ = diag {2.0, 1.0, 2.35, 2.5, 3.0, 3.25}

$$\underline{K}_0 = \begin{bmatrix} 0.0 & -0.2267E-03 & -0.3534E-01 & -0.3426E-02 & 0.7593E-04 & 0.4573E-02 \\ 0.0 & 0.8425E-03 & -0.5018E-01 & 0.2087E-02 & -0.4625E-04 & -0.2786E-02 \\ 0.0 & 0.0 & 0.0 & 0.1645E-01 & -0.9154E-02 & -0.3900E-01 \\ 0.0 & 0.0 & 0.0 & 0.6369E-01 & 0.2423E-02 & -0.1895E+00 \\ 0.0 & 0.0 & 0.0 & 0.6986E-01 & -0.1548E-02 & -0.9326E-01 \\ 0.1039E+01 & -0.1555E-02 & 0.1944E+00 & 0.2116E-02 & -0.4689E-04 & -0.2825E-02 \end{bmatrix}$$

$$\underline{K}_1 = \begin{bmatrix} 0.0 & -0.6800E-03 & -0.1060E+00 & -0.1028E-01 & 0.2278E-03 & 0.1372E-01 \\ 0.0 & 0.2527E-02 & -0.1505E+00 & 0.6261E-02 & -0.1388E-03 & -0.8358E-02 \\ 0.0 & 0.0 & 0.0 & 0.4936E-01 & -0.2746E-01 & -0.1170E+00 \\ 0.0 & 0.0 & 0.0 & 0.1911E+00 & 0.7269E-02 & -0.5685E+00 \\ 0.0 & 0.0 & 0.0 & 0.2096E+00 & -0.4645E-02 & -0.2798E+00 \\ 0.3116E+01 & -0.4666E-02 & 0.5832E+00 & 0.6348E-02 & -0.1407E-03 & -0.8474E-02 \end{bmatrix}$$

Input Ramp Time: 0.3 second

Command Vector:

u = 0.0

A_{n_p} = 0.0

q = 0.0

A_{y_p} = 0.6 g (1 second pulse)

p = 0.0

r = 0.0

Table 5-14

Lateral Translation: Failed Model,
0.9 Mach at 20,000 Feet

Sampling Time: T = 0.02 second

$\bar{\alpha} = 3.0$

$\epsilon = 1.0$

$\underline{\Sigma} = \text{diag}\ \{2.0, 1.0, 2.35, 2.5, 3.0, 3.25\}$

$$\underline{K}_0 = \begin{bmatrix} 0.0 & -0.4529E-03 & -0.7062E-01 & -0.6874E-02 & 0.1676E-03 & 0.9206E-02 \\ 0.0 & 0.7775E-03 & -0.6031E-01 & 0.2227E-01 & -0.1180E-01 & -0.5166E-01 \\ 0.0 & 0.9072E-03 & -0.4008E-01 & -0.1809E-01 & 0.1170E-01 & 0.4605E-01 \\ 0.0 & -0.4018E-04 & -0.6264E-02 & 0.6600E-01 & 0.8144E-03 & -0.1956E+00 \\ 0.0 & -0.4012E-05 & -0.6256E-03 & 0.7009E-01 & -0.1708E-02 & -0.9387E-01 \\ 0.1039E+01 & -0.1554E-02 & 0.1946E+00 & 0.2144E-02 & -0.5226E-04 & -0.2871E-02 \end{bmatrix}$$

$$\underline{K}_1 = \begin{bmatrix} 0.0 & -0.1359E-02 & -0.2119E+00 & -0.2062E-01 & 0.5027E-03 & 0.2762E-01 \\ 0.0 & 0.2332E-02 & -0.1809E+00 & 0.6682E-01 & -0.3541E-01 & -0.1550E+00 \\ 0.0 & 0.2722E-02 & -0.1203E+00 & -0.5426E-01 & 0.3510E-01 & 0.1382E+00 \\ 0.0 & -0.1205E-03 & -0.1879E-01 & 0.1980E+00 & 0.2443E-02 & -0.5868E+00 \\ 0.0 & -0.1204E-04 & -0.1877E-02 & 0.2103E+00 & -0.5125E-02 & -0.2816E+00 \\ 0.3116E+01 & -0.4662E-02 & 0.5838E+01 & 0.6432E-02 & -0.1568E-03 & -0.8614E-02 \end{bmatrix}$$

Input Ramp Time: 0.3 second

Command Vector:

$u = 0.0$

$A_{n_p} = 0.0$

$q = 0.0$

$A_{y_p} = 0.6$ g (1 second pulse)

$p = 0.0$

$r = 0.0$

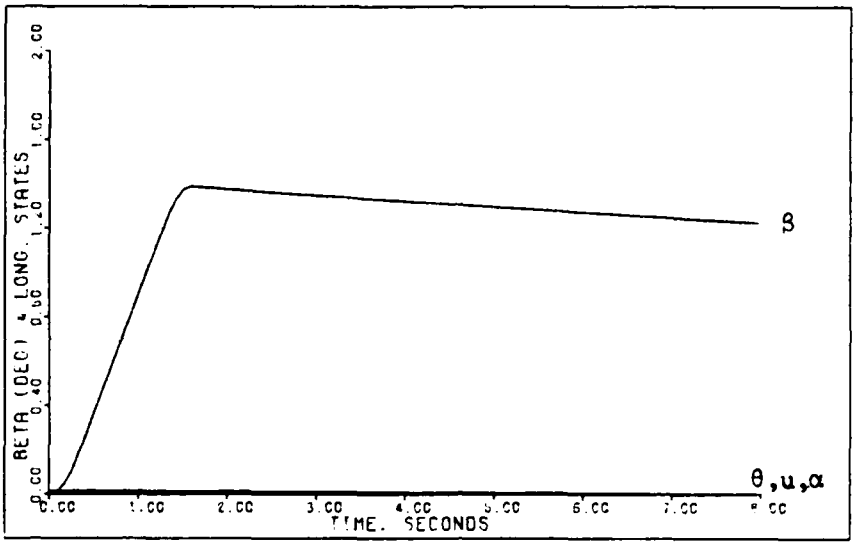

Figure 5-43: 0.9M Healthy/Failed Lateral Translation -- Sideslip Angle, Pitch Angle, Angle of Attack, and Forward Velocity

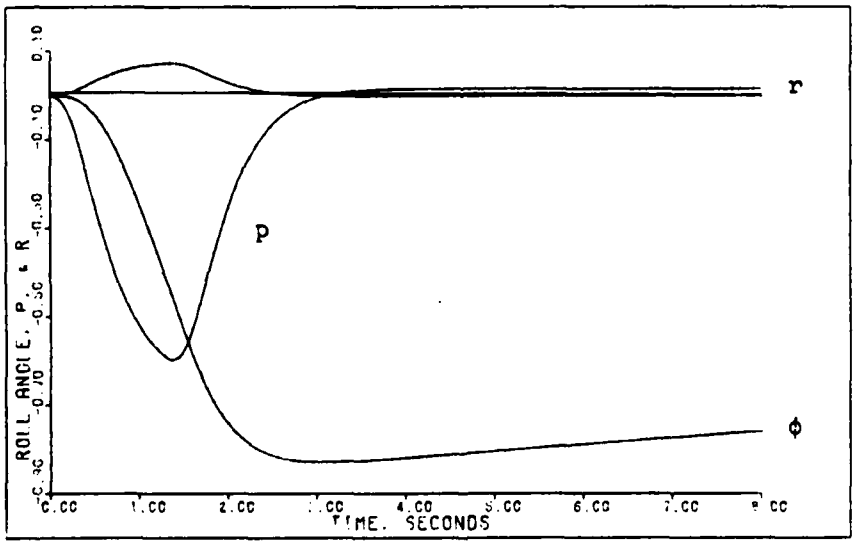

Figure 5-44: 0.9M Healthy/Failed Lateral Translation -- Roll Angle, Roll Rate, and Yaw Rate

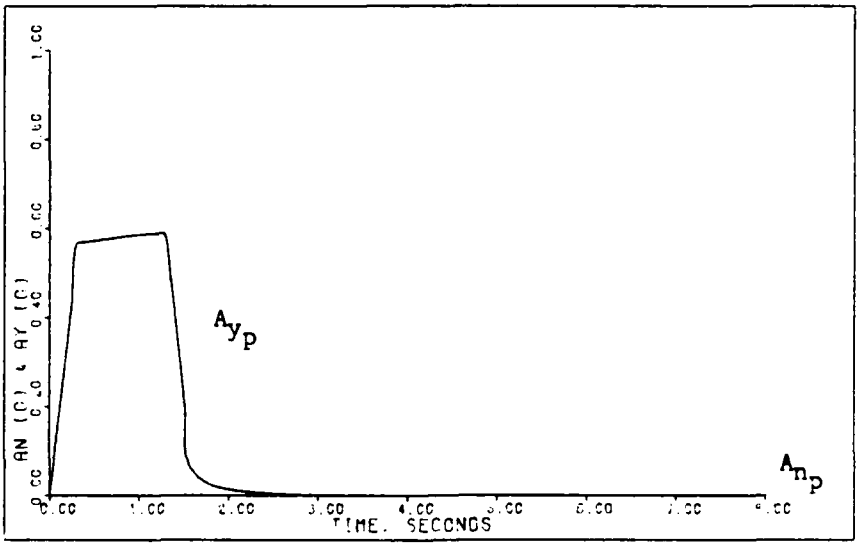

Figure 5-45: 0.9M Healthy/Failed Lateral Translation -- Normal Acceleration and Lateral Acceleration

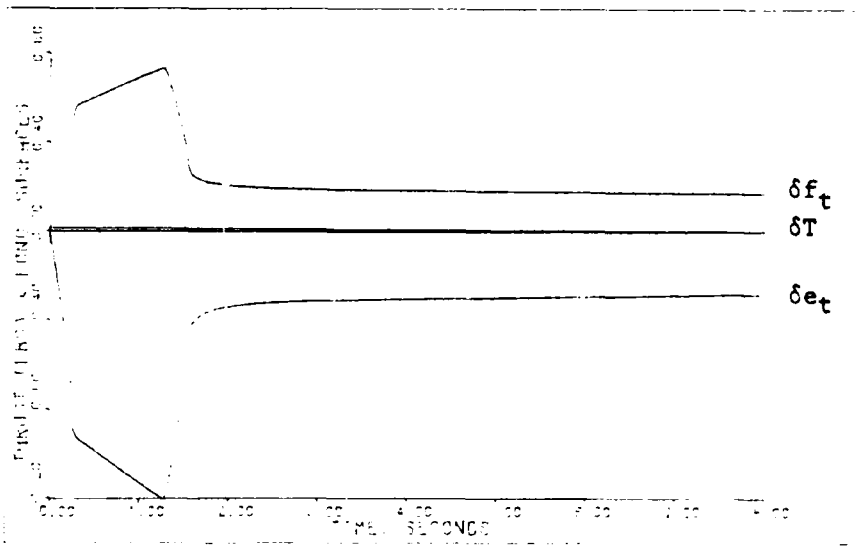

Figure 5-46: 0.9M Healthy Lateral Translation -- Elevator and Flap Deflections and Thrust

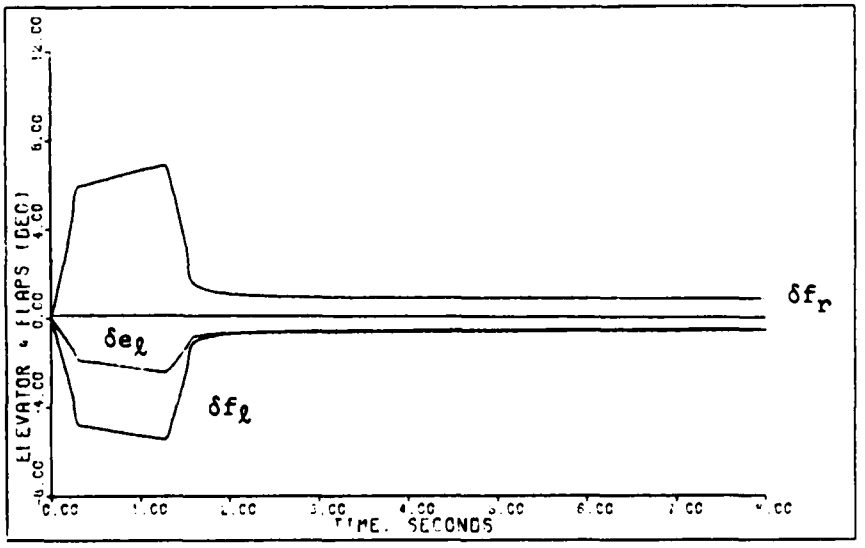

Figure 5-47: 0.9M Failed Lateral Translation -- Left Elevator and Flaperon Deflections

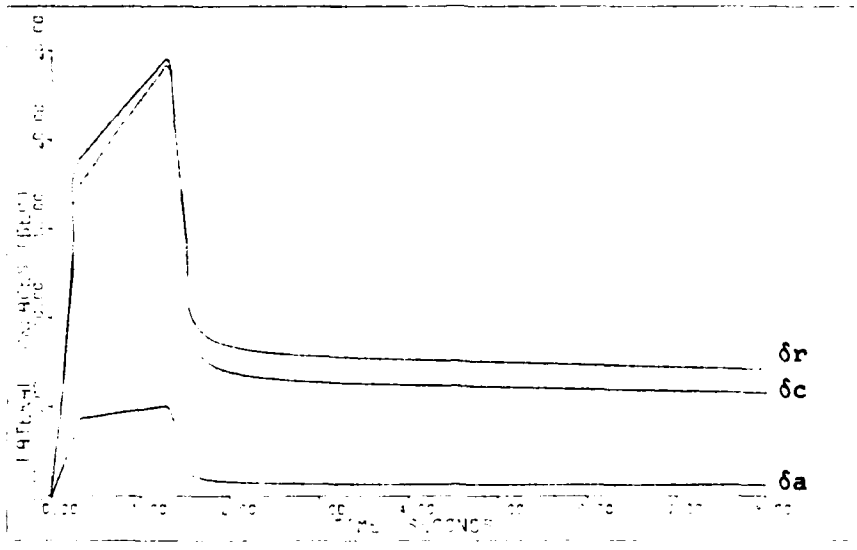

Figure 5-48: 0.9M Healthy Lateral Translation -- Aileron, Rudder, and Canard Deflections

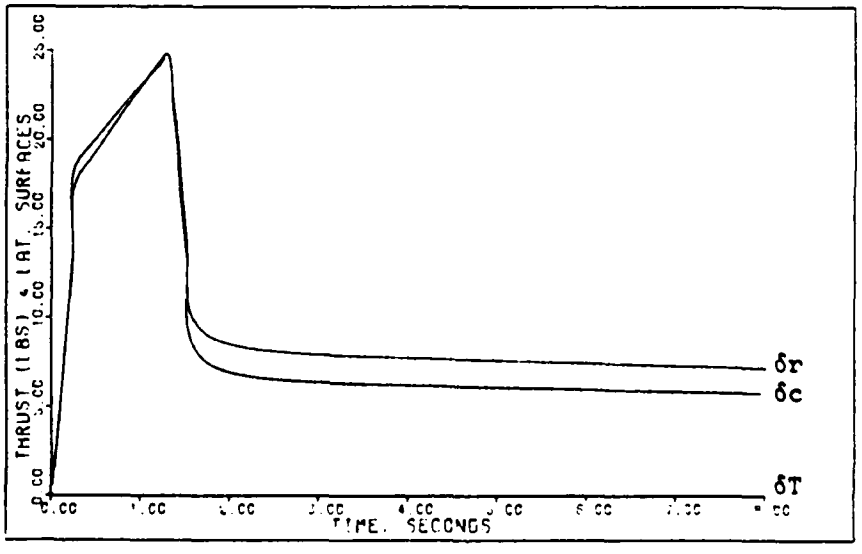

Figure 5-49: 0.9M Failed Lateral Translation -- Rudder and Canard Deflections and Thrust

Appendix D lists the remainder of the simulation responses generated in this study. As shown in this chapter the transonic flight condition simulation responses show that the aircraft is still able to perform the commanded maneuvers when the right horizontal tail is failed. Appendix D presents some cases where the aircraft performance is degraded when the right horizontal tail fails.

The next chapter discusses the results of this study in general terms and presents recomendations for further study.

VI. Conclusions and Recommendations

In this study control laws are developed for the AFTI/F-16 using the Porter method. Acceptable designs are achieved for a model of the healthy aircraft with all control surfaces operational and for a model with the right horizontal tail free-floating. Designs are accomplished for seven maneuvers at four key flight conditions within the aircraft's flight envelope. The control laws consist of the gain matrixes $\underline{K}_1$ and $\underline{K}_0$ which can be implemented in a digital flight control computer. Each control law is tailored to a specific maneuver at a particular flight condition. The maneuvers include both conventional and CCV maneuvers.

VI-1. Design Summary

Control laws are first developed for the healthy aircraft model with the aid of the computer program MULTI, which proves invaluable when utilizing the Porter method. The transonic and supersonic flight conditions (0.9 Mach at 20,000 and 1.6 Mach at 30,000) are the simplest cases to design because of the high dynamic pressure at these flight conditions.

Maximum inputs are commanded for each maneuver in order to estimate the control surface deflections required for maximum performance. Because commanding maximum maneuvers invalidates the small angle assumptions made in deriving the linearized perturbation models, some of the simulation responses are open to interpertation. A nonlinear simula-

tion of the designs would eliminate any problems due to the linearization assumptions.

After acceptable control laws are achieved for the healthy aircraft model, the same design parameters ($\underline{M}$, $\bar{\alpha}$, $\underline{\Sigma}$, and ϵ) are used to calulate gain matrices for the model with a failed right horizontal tail. The calculation of new gain matrices implies that the system must be able to detect the failure and reconfigure accordingly. The detection problem is beyond the scope of this study, but it is assumed that a failure detection scheme can be developed.

For most cases considered in this thesis, satisfactory simulation responses are achieved for the failure model without requiring further design trials. The four cases that do require changes in the design parameters or input command magnitudes are: pitch pointing at supersonic speed; longitudinal translation at supersonic speed; roll at supersonic speed; and roll at landing approach. In each of these four cases the failure of the right horizontal tail requires an increased deflection of the remaining control surfaces to compensate for the loss. For these cases, if changing the design parameters does not yield a satisfactory result, then the maximum maneuver commanded is decreased.

In general, when the right horizontal tail fails, the left horizontal tail assumes primary pitch control and the flaperons take over complete roll control. The flaperons also compensate for unwanted rolling and pitching moments created by the left horizontal tail deflection. The

deflection of the left horizontal tail also creates a yawing moment due to the difference in drag between the left and right halves of the aircraft. The rudder and canards compensate for this yawing moment.

The simulation results of this study indicate, for the linearized models used here, that the aircraft is capable of maneuvering with a free-floating right horizontal tail. Although much work must still be accomplished before these results are accepted in practice, the results do imply that it is worthwhile to continue research into the effects of a failed right horizontal tail. The procedures used in this study are applicable to other control surface failures, such as a failed flaperon.

VI-2. Recommendations for Future Study

Although the computer program MULTI has proved to be a great aid in performing multivariable designs with the Porter method, additional improvements can still be made in the program. As pointed out in Chapter III, the factoring routine in MULTI Option #6 becomes error prone when large order transfer functions are calculated. Correction of this problem will allow the user to check stabilty without running several time consuming simulation runs.

Even if MULTI Option #6 had the desired increased factoring accuracy, it is still desirable at times to check simulation responses over long periods of time. Currently the plotting routine in MULTI does not generate enough data

points for plotting long simulation times. If more data points are plotted then more details can be observed on the response plots, which may indicate limit cycles or slowly growing instabilities. This change should be readily achievable.

The addition of a nonlinear simulation block to MULTI is strongly recommended. Such an addition would allow for more realistic simulations of the control law designs. A nonlinear simulaion on MULTI is feasible because the differential equation solver subroutine (called ODE) currently used with MULTI is capable of handling nonlinear equations.

Other extentions of this thesis can be studied with MULTI in its current state. To add more realism to the simulations, a computational time delay and sensor models should be added to the models of this study. Other phenomena, like the effects of wind gusts and sensor noise, should also be studied.

The results of this thesis are a small step toward the goal of designing flight control systems that can compensate for battle damage or control surface failures. If, however, the control laws developed in this study are simulated under more realistic conditions and fine tuned, the results could make a significant contribution to the self-repairing flight control program undertaken by the Air Force Flight Dynamics Laboratory.

Bibliography

1. AFTI/F-16 Advanced Development Program Office, AFWAL/FII. Wright-Patterson AFB OH.

2. AFWAL-TR-83-3-1. AFTI/F-16 Development and Integration Program DFCS Phase Final Technical Report, Vol 3, Part 1. General Dynamics, Fort Worth Division, Fort Worth, Texas. December 1983.

3. Barfield, A. F., B. W. Van Vliet, and D. C. Anderson. "AFTI/F-16 Advanced Multimode Control System Design for Task-Tailored Operations," AIAA Aircraft Systems and Technology Conference. AIAA-81-1707. Dayton, Ohio, August 11-13, 1981.

4. Barfield, A. Finley. Multivariable Control Laws for the AFTI/F-16. MS Thesis, AFIT/GE/EE/83S-4. School of Engineering, Air Force Institute of Technology, Wright-Patterson AFB OH, July 1983.

5. Courtheyn, Major Terry. Multivariable Control Law Design for the X-29. MS Thesis, AFIT/GE/ENG/84D-21. School of Engineering, Air Force Institute of Technology, Wright-Patterson AFB OH, December 1984.

6. Hoffman, Lt. Marc L. Evaluation of a Digital Flight Controller for a Flexible-Fighter. MS Thesis, AFIT/GE/EE/83D-30. School of Engineering, Air Force Institute of Technology, Wright-Patterson AFB OH, December 1982.

7. Lewis, 2Lt. Thomas. High-Gain Error Actuated Flight Control System for Continuous Linear Multivariable Plants. MS Thesis, AFIT/GAE/EE/82D-1. School of Engineering, Air Force Institute of Technology, Wright-Patterson AFB OH, December 1982.

8. Masi, M., Russ, D. MULTI User's Manual. AFWAL-TM-83-182-FIGL, Air Force Flight Dynamics Laboratory, Wright-Patterson AFB OH (August 1984).

9. Porter, B. and Bradshaw, A. "Singular Perturbation Methods in the Design of Tracking Systems Incorporating High-Gain Error Actuated Controllers," International Journal of Systems Science, 12 (10): 1169-1220 (1981).

10. Porter, Capt. Douglas. Design and Analysis of a Multivariable, Digital Controller for the A-7D DIGITAC II Aircraft and the Development of an Interactive Computer Design Program. MS Thesis, AFIT/GE/EE/81D-48. School of Engineering, Air Force Institute of Technology, Wright-Patterson AFB OH, December 1981.

11. Pugh, A. C. "Transmission and System Zeros," International Journal of Control, 26 (2): 315-324 (1977).

12. Ridgely, B., Banda, S., and D'Azzo, J. "Decoupling of High-Gain Multivariable Tracking Systems," AIAA 21st Aerospace Sciences Conference, Reno, Nevada, January 1983, AIAA Paper No. 83-0280.

13. Rubertus, Duane P. "Self-repairing Digital Flight Control System," Restructurable Controls. 133-159. NASA conference Publication 2277, 1983.

Appendix A: Multivariable Control Theory

This thesis utilizes the multivariable design method of Professor Brian Porter of the University of Salford, England (9). The design method uses output feedback with high-gain error-actuated controllers. Output feedback is advantagous since state variables may be difficult to measure while system response data are more readily available.

System State Equations

Porter's method works equally well for either continuous or discrete systems, but it is often easier to first examine a system in the continous time domain. This is because designs can be more easily visualized in the s-plane than in the z-plane. A continuous time system is represented by the state space model:

$$\dot{\underline{x}} = \underline{A}\underline{x} + \underline{B}\underline{u}$$
$$\underline{y} = \underline{C}\underline{x} \qquad \text{(A-1)}$$

where

$\underline{A}$ = continuous plant matrix (n x n)

$\underline{B}$ = continuous input control matrix (n x m)

$\underline{C}$ = continuous output matrix (ℓ x n)

$\underline{x}$ = state variable vector with n states

$\underline{u}$ = input vector with m inputs

$\underline{y}$ = output vector with ℓ outputs

The system inputs for an aircraft are the control surface deflections or actuator input commands, and the system outputs are aircraft responses affected by the inputs.

The method does not allow for a feedforward, $\underline{D}$, matrix. If such a matrix is present in the original state space model, the control inputs must be redefined as states so that the $\underline{D}$ matrix is absorbed into the $\underline{C}$ matrix. This can be accomplished by incorporating the actuator dynamics into the plant model. Actuator inputs then become control inputs.

To employ Porter's method, it is desirable (but not necessary) to partition the system state equations as follows:

$$\begin{bmatrix} \dot{\underline{x}}_1 \\ \hline \dot{\underline{x}}_2 \end{bmatrix} = \left[\begin{array}{c|c} \underline{A}_{11} & \underline{A}_{12} \\ \hline \underline{A}_{21} & \underline{A}_{22} \end{array}\right] \begin{bmatrix} \underline{x}_1 \\ \hline \underline{x}_2 \end{bmatrix} + \begin{bmatrix} \underline{B}_1 \\ \hline \underline{B}_2 \end{bmatrix} \underline{u}$$

$$\underline{y} = \left[\begin{array}{c|c} \underline{C}_1 & \underline{C}_2 \end{array}\right] \begin{bmatrix} \underline{x}_1 \\ \hline \underline{x}_2 \end{bmatrix} \qquad \text{(A-2)}$$

The equations are partitioned so that $\underline{B}_2$ and $\underline{C}_2$ are square ($m \times m$) and ($\ell \times \ell$) matrices, respectively. The method requires that the number of inputs to the system equals the number of outputs which means $m = \ell$, and therefore the dimension of $\underline{B}_2$ equals the dimension of $\underline{C}_2$. It is often possible to form the state equations so that $\underline{B}_1 = \underline{0}$.

For the discrete case the system equations are written as follows:

$$\underline{x}[(k+1)T] = \underline{\phi x}(kT) + \underline{\psi u}(kT)$$

$$\underline{y}(kT) = \underline{\Gamma x}(kT) \qquad \text{(A-3)}$$

where

$\underline{\phi} = \exp(\underline{A}T)$ = discrete plant matrix

$\underline{\psi} = \int_0^T \exp(\underline{A}T)\underline{B}dt$ = discrete input control matrix

$\underline{\Gamma} = \underline{C}$ = discrete output matrix

In the above equations T is the sampling period, and k takes on integer values from zero to plus infinity.

System With Output Feedback

Figure A-1 shows the block diagram for a continuous output feedback system, where $\underline{v}$ is the command input vector, and $\underline{y}$ is the desired output vector. The blocks for the plant are derived directly from the system state equations, Equation (A-1). The proportional plus integral controller has three parameters, $\underline{K}_0$, $\underline{K}_1$ and g, which must be determined by the designer. The output signal of the controller, $\underline{u}$, is given in the following control law equation:

$$\underline{u} = g(\underline{K}_0\underline{e} + \int \underline{K}_1\ \underline{e}dt) \qquad \text{(A-4)}$$

where

$\underline{u}$ is the output signal of the controller

$\underline{e}$ is the error signal at the input of the controller

$\underline{K}_0$ is the proportional gain matrix

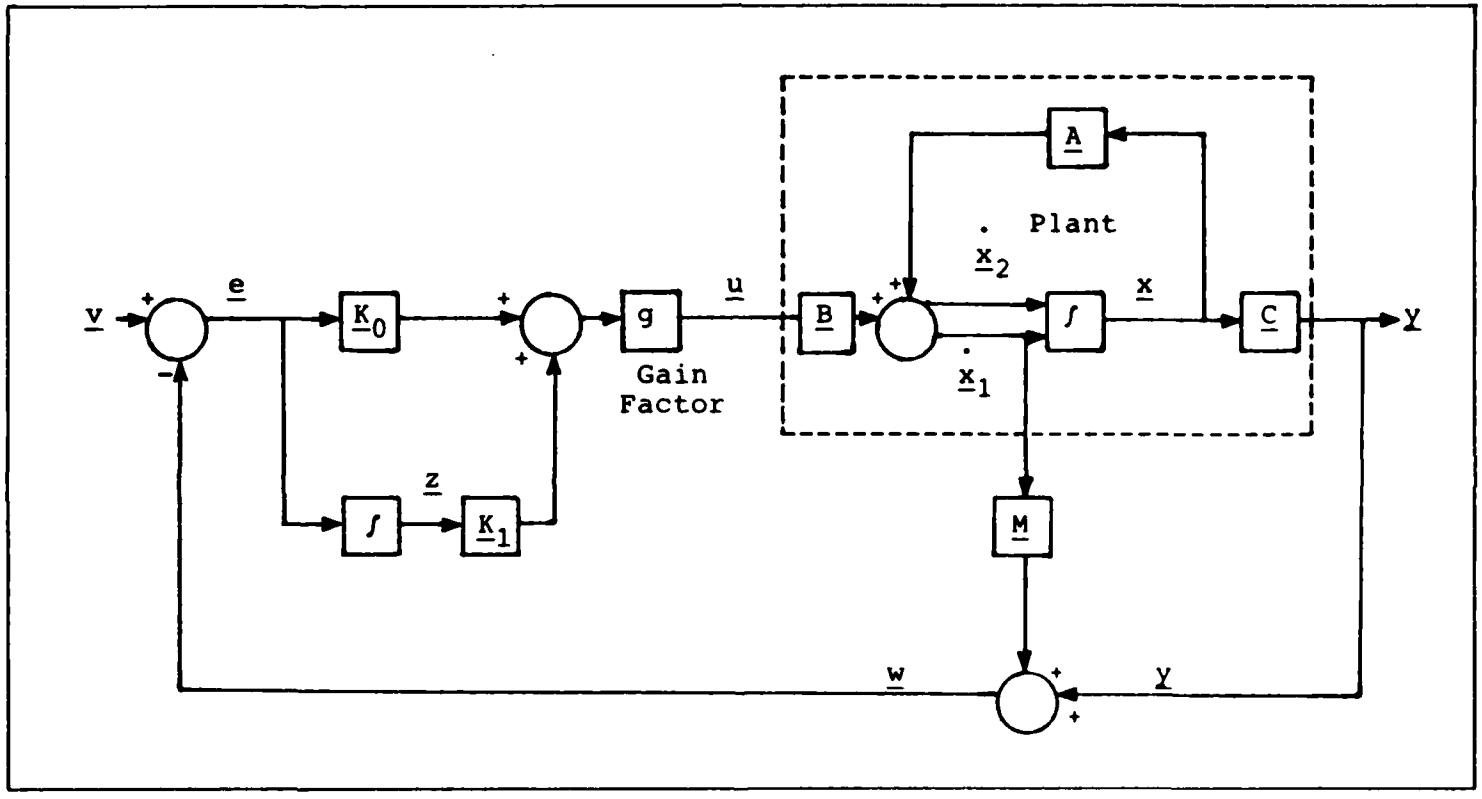

Figure A-1. System block Diagram -- Continuous Case

$\underline{K}_1$ is the gain matrix for the integral term

g is the scalar forward path gain

A measurement matrix $\underline{M}$ is included in the system if the plant is irregular. Regular and irregular plants are discussed later.

The discrete system block diagram, shown in Figure A-2, is similar to the continuous system, but Equation (A-4) becomes

$$\underline{u}(kT) = (1/T)[\underline{K}_0\underline{e}(kT) + \underline{K}_1\underline{z}(kT)] \qquad (A-5)$$

where the forward path gain g equals the sampling frequency, (1/T). The $\underline{z}(kT)$ matrix is derived from the backward difference equation,

$$\underline{z}[(k+1)T] = \underline{z}(kT) + T\underline{e}(kT) \qquad (A-6)$$

The steps to be taken next in the design method depend on whether or not [$\underline{CB}$] has full rank, i.e., does it have an inverse. If the matrix [$\underline{CB}$] has full rank, the plant is called "regular" and no measurement matrix $\underline{M}$ is needed. However, if [$\underline{CB}$] does not have full rank, the plant is called "irregular" and $\underline{M}$ is needed to form a new matrix [$\underline{FB}$] (see Equations (A-12) through (A-14)) which does have an inverse. This is explained in more detail in the next sections. When the partitioned $\underline{B}$ matrix in Equation (A-2) has the form

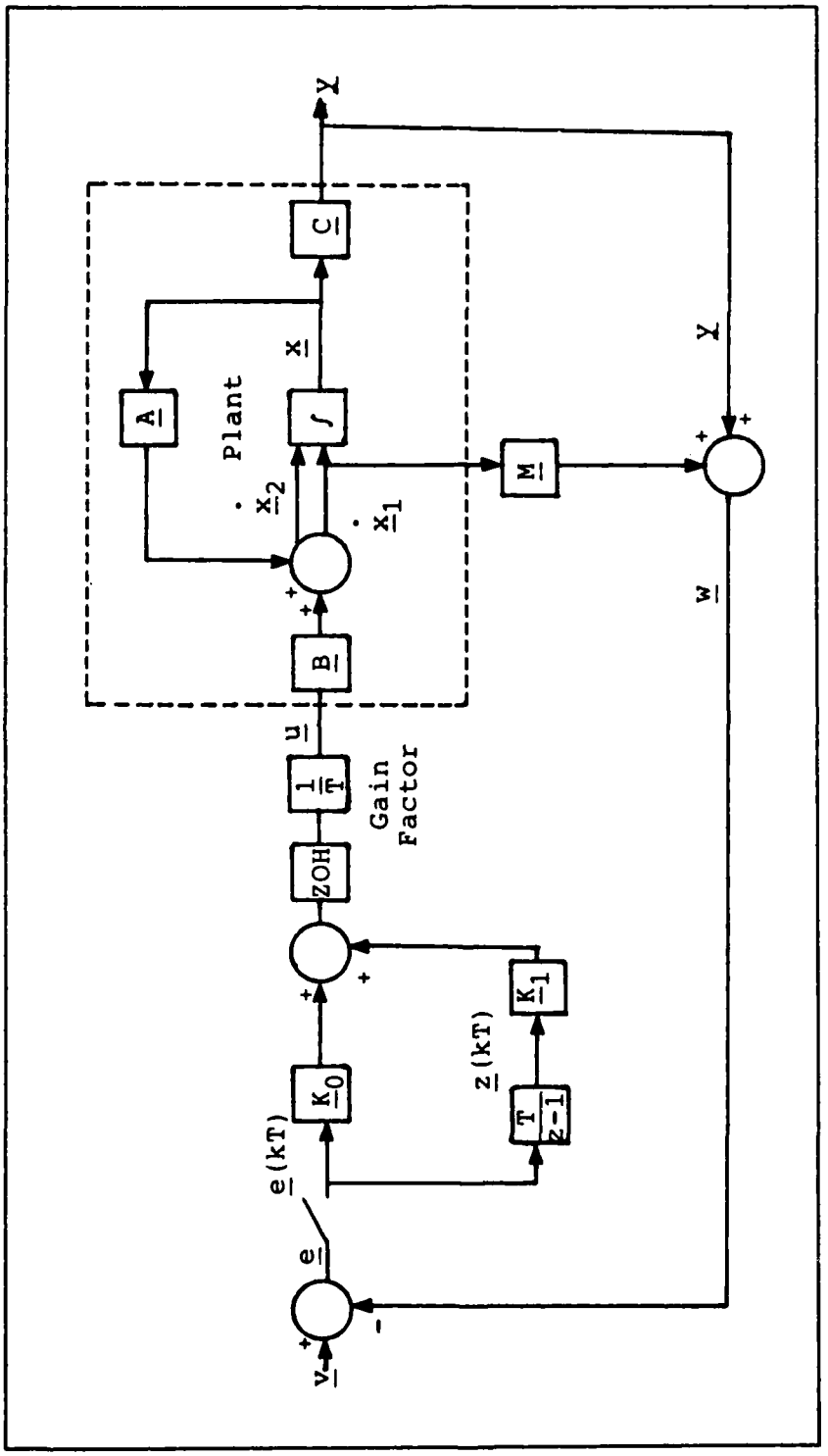

Figure A-2. System Block Diagram -- Discrete Case

$$\begin{bmatrix} \underline{0} \\ \hline \underline{B}_2 \end{bmatrix} \tag{A-7}$$

then

$$[\underline{CB}] = [\underline{C}_2\underline{B}_2] \tag{A-8}$$

$$[\underline{FB}] = [\underline{F}_2\underline{B}_2] \tag{A-9}$$

Regular Plant

For the system to be classified as "regular" the first Markov parameter $[\underline{CB}]$ must have full rank. If this is true the gain matricies can be found from

$$\underline{K}_0 = [\underline{CB}]^{-1}\underline{\Sigma} \tag{A-10}$$

and

$$\underline{K}_1 = \bar{\alpha}[\underline{CB}]^{-1}\underline{\Sigma} \tag{A-11}$$

where

$\bar{\alpha}$ is a constant which assigns the ratio of proportional to integral control

$\underline{\Sigma}$ is the diagonal weighting matrix

The diagonal weighting matrix, $\underline{\Sigma} = \text{diag}\{\sigma_1, \sigma_2, \ldots, \sigma_\ell\}$, is specified by the designer. Each σ_i $(i = 1,\ldots,\ell)$ determines the weighting of the effect of a particular error signal on each control input.

Irregular Plant

If the first Markov parameter [$\underline{CB}$] is rank deficient, then the plant is called "irregular". In this case, the $\underline{C}$ matrix must be replaced by

$$\underline{F} = [\underline{F}_1 \,|\, \underline{F}_2] \tag{A-12}$$

where

$$\underline{F}_1 = [\underline{C}_1 + \underline{MA}_{11}] \tag{A-13}$$

$$\underline{F}_2 = [\underline{C}_2 + \underline{MA}_{12}] \tag{A-14}$$

The matrix $\underline{M}$ in the above equations is a measurement matrix which is chosen such that the matrix [$\underline{FB}$] has full rank. The designer chooses the measurement matrix so that it is as sparse as possible, thus the smallest number of additional measurements are required. Reference 12 gives an approach for selecting the measurement matrix to achieve optimal decoupling. Once $\underline{M}$ is formed, $\underline{K}_0$ and $\underline{K}_1$ are computed by

$$\underline{K}_0 = [\underline{FB}]^{-1}\underline{\Sigma} \tag{A-15}$$

$$\underline{K}_1 = \bar{\alpha}[\underline{FB}]^{-1}\underline{\Sigma} \tag{A-16}$$

which are similar to Equations (A-10) and (A-11).

For irregular plants the error vector $\underline{e}$ is defined as

$$\underline{e} = \underline{v} - \underline{w} \tag{A-17}$$

where

$$\underline{w} = \underline{y} + \underline{M}\dot{\underline{x}}_1 \qquad \text{(A-18)}$$

For step inputs the values of the rates, $\dot{\underline{x}}_1$, become zero in the steady state because they represent kinematic variables.

Asymptotic Characteristics

As the gain factor of the system, g (or 1/T for the discrete case), approaches infinity, the system transfer function matrix G(s) assumes the asymptotic form

$$\underline{\Gamma}(\lambda) = \tilde{\underline{\Gamma}}(\lambda) + \hat{\underline{\Gamma}}(\lambda) \qquad \text{(A-19)}$$

where

$\tilde{\underline{\Gamma}}(\lambda)$ is the slow transfer function matrix

$\hat{\underline{\Gamma}}(\lambda)$ is the fast transfer function matrix

The roots of the asymptotic closed-loop transfer function may be grouped into three sets: $\underline{Z}_1$, $\underline{Z}_2$, and $\underline{Z}_3$. Table A-1 gives the equations for finding these asymptotic roots. Sets $\underline{Z}_1$ and $\underline{Z}_2$ correspond to the slow modes of the system, where the modes associated with the roots in $\underline{Z}_1$ become uncontrollable, and, for regular plants, the modes associated with the roots in $\underline{Z}_2$ become unobservable as the gain increases. Set $\underline{Z}_3$, the infinite roots, are associated with the fast modes of the system which become dominant as the gain increases.

The roots in set $\underline{Z}_2$ correspond to the transmission zeros of the system which are not altered by output feedback. Since infinite gain cannot be implemented, and is not

Table A-1

Asymptotic Equations for Zero-$\underline{B}_2$ Form

System represented by:

$$\begin{bmatrix} \dot{\underline{x}}_1 \\ \hline \dot{\underline{x}}_2 \end{bmatrix} = \left[\begin{array}{c|c} \hat{\underline{A}}_{11} & \hat{\underline{A}}_{12} \\ \hline \hat{\underline{A}}_{21} & \hat{\underline{A}}_{22} \end{array}\right] \begin{bmatrix} \underline{x}_1 \\ \hline \underline{x}_2 \end{bmatrix} + \begin{bmatrix} \underline{0} \\ \hline \hat{\underline{B}}_2 \end{bmatrix} \underline{u} \qquad \text{and} \qquad \underline{y} = \left[\hat{\underline{C}}_1 \mid \hat{\underline{C}}_2\right] \begin{bmatrix} \underline{x}_1 \\ \hline \underline{x}_2 \end{bmatrix}$$

	Continuous Case (s-plane)	Discrete Case (z-plane)
	Gain Factor = g	Gain Factor = 1/T
$\tilde{\underline{\Gamma}}(\lambda)$	$= \underline{C}_0(\lambda \underline{I}_n - \underline{A}_0)^{-1}\underline{B}_0$	$= \underline{C}_0(\lambda \underline{I}_n - \underline{A}_0)^{-1}\underline{B}_0$
$\hat{\underline{\Gamma}}(\lambda)$	$= (\lambda \underline{I}_m + g\hat{\underline{C}}_2\hat{\underline{B}}_2\underline{K}_0)^{-1} g\hat{\underline{C}}_2\hat{\underline{B}}_2\underline{K}_0$	$= (\lambda \underline{I}_m - \underline{I}_m + \hat{\underline{C}}_2\hat{\underline{B}}_2\underline{K}_0)^{-1}\hat{\underline{C}}_2\hat{\underline{B}}_2\underline{K}_0$
Finite Roots		
$\underline{Z}_1$	$= \{\lvert \lambda \underline{K}_0 + \underline{K}_1 \rvert = \underline{0}\}$	$= \{\lvert \lambda \underline{I}_m - \underline{I}_m + T\underline{K}_0^{-1}\underline{K}_1 \rvert = \underline{0}\}$
$\underline{Z}_2$	$= \{\lvert \lambda \underline{I}_{n-m} - \hat{\underline{A}}_{11} + \hat{\underline{A}}_{12}\hat{\underline{C}}_2^{-1}\hat{\underline{C}}_1 \rvert = \underline{0}\}$	$= \{\lvert \lambda \underline{I}_{n-m} - T\hat{\underline{A}}_{11} + \hat{\underline{A}}_{12}\hat{\underline{C}}_2^{-1}\hat{\underline{C}}_1 \rvert = \underline{0}\}$
Infinite Roots		
$\underline{Z}_3$	$= \{\lvert \lambda \underline{I}_m + g\hat{\underline{C}}_2\hat{\underline{B}}_2\underline{K}_0 \rvert = \underline{0}\}$	$= \{\lvert \lambda \underline{I}_m - \underline{I}_m + \hat{\underline{C}}_2\hat{\underline{B}}_2\underline{K}_0 \rvert = \underline{0}\}$

where

$$\underline{A}_0 = \left[\begin{array}{c|c} -\underline{K}_0^{-1}\underline{K}_1 & \underline{0} \\ \hline \hat{\underline{A}}_{12}\hat{\underline{C}}_2^{-1}\underline{K}_0^{-1}\underline{K}_1 & \hat{\underline{A}}_{11} - \hat{\underline{A}}_{12}\hat{\underline{C}}_2^{-1}\hat{\underline{C}}_1 \end{array}\right]$$

$$\underline{B}_0 = \begin{bmatrix} \underline{0} \\ \hline \hat{\underline{A}}_{12}\hat{\underline{C}}_2^{-1} \end{bmatrix}$$

Regular Design	Irregular Design
$\underline{C}_0 = \left[\underline{K}_0^{-1}\underline{K}_1 \mid \underline{0}\right]$	$\underline{C}_0 = \left[\hat{\underline{C}}_2\underline{F}_2^{-1}\underline{K}_0^{-1}\underline{K}_1 \mid \hat{\underline{C}}_1 - \hat{\underline{C}}_2\underline{F}_2^{-1}\underline{F}_1\right]$

desirable, the closed-loop roots of the system tend to migrate toward the transmission zeros. This may adversely affect the system stability if the location of these zeros is in the unstable region. Reference 11 gives a procedure for locating the transmission zeros of a system.

As the gain increases the system output responses become increasingly decoupled. The asymptotic closed-loop transfer function for the continuous case has the form

$$\underline{\Gamma}(\lambda) = \text{diag}\{ \frac{g\sigma_1}{\lambda+g\sigma_1}, \frac{g\sigma_2}{\lambda+g\sigma_2}, \ldots, \frac{g\sigma_\ell}{\lambda+g\sigma_\ell} \} \qquad \text{(A-20)}$$

For the discrete case the form is

$$\underline{\Gamma}(\lambda) = \text{diag}\{ \frac{\sigma_1}{\lambda-1+\sigma_1}, \frac{\sigma_2}{\lambda-1+\sigma_2}, \ldots, \frac{\sigma_\ell}{\lambda-1+\sigma_\ell} \} \qquad \text{(A-21)}$$

where the σ_i ($i = 1,\ldots,\ell$) are determined by the weighting matrix, $\underline{\Sigma}$.

The computer program MULTI is of great value in reducing the time required to achieve a satisfactory design. The MULTI User's Manual (8) describes the program and its operation.

Appendix B: Dimensionalized Derivatives

This appendix lists equations for the dimensionalized derivatives used in the aircraft models. These dimensionalized derivatives are inserted directly into the state space models of Equations (2-2) and (2-4). Reference 4 is the source of information for the equations. In the equations, $(\ )_b$ denotes that the coefficients are expressed in the body axis reference frame. The stability axis to body axis conversion equations begin with Equation (B-57).

Longitudinal Derivatives

$$X'_\theta = -g\cos\theta_T \tag{B-1}$$

$$X'_u = \frac{\bar{q}S}{mU}(C_{x_u})_b \tag{B-2}$$

$$X'_\alpha = \frac{\bar{q}S}{m}(C_{x_\alpha})_b \tag{B-3}$$

$$X'_q = \frac{\bar{q}Sc}{2mU}(C_{x_q})_b - U\alpha_T \tag{B-4}$$

$$Z'_\theta = -\frac{g}{U}\sin\theta_T \tag{B-5}$$

$$Z'_u = \frac{\bar{q}S}{mU^2}(C_{z_u})_b \tag{B-6}$$

$$Z'_\alpha = \frac{\bar{q}S}{mU}(C_{z_\alpha})_b \tag{B-7}$$

$$Z'_q = 1 + \frac{\bar{q}Sc}{2mU^2}(C_{z_q})_b \tag{B-8}$$

$$M'_\theta = \left[\frac{\bar{q}Sc^2}{2UI_y}(C_{m_{\dot{\alpha}}})_b\right] Z'_\theta \tag{B-9}$$

$$M'_u = \frac{\bar{q}Sc}{UI_y}(C_{m_u})_b + \left[\frac{\bar{q}Sc^2}{2UI_y}(C_{m_{\dot{\alpha}}})_b\right] Z'_u \tag{B-10}$$

$$M'_\alpha = \frac{\bar{q}Sc}{I_y}(C_{m_\alpha})_b + \left[\frac{\bar{q}Sc}{2UI_y}(C_{m_{\dot{\alpha}}})_b\right] Z'_\alpha \tag{B-11}$$

$$M'_q = \frac{\bar{q}Sc^2}{2UI_y}\left[(C_{m_q})_b + (C_{m_{\dot{\alpha}}})_b Z'_q\right] \tag{B-12}$$

Lateral Derivatives

$$Y'_\phi = \frac{g\cos\theta_T}{U} \tag{B-13}$$

$$Y'_\beta = \frac{\bar{q}S}{mU}(C_{Y_\beta})_b \tag{B-14}$$

$$Y'_p = \frac{\bar{q}Sb}{2mU^2}(C_{Y_p})_b + \alpha_T \tag{B-15}$$

$$Y'_r = \frac{\bar{q}Sb}{2mU^2}(C_{Y_r})_b - 1 \tag{B-16}$$

$$L'_\beta = \frac{\frac{\bar{q}Sb}{I_x}(C_{\ell_\beta})_b + \frac{I_{xz}}{I_x}\frac{\bar{q}Sb}{I_z}(C_{n_\beta})_b}{1 + \frac{(I_{xz})^2}{(I_x)(I_z)}} \tag{B-17}$$

$$L'_p = \frac{\frac{\bar{q}Sb^2}{2UI_x}(C_{\ell_p})_b + \frac{I_{xz}}{I_x}\frac{\bar{q}Sb^2}{2UI_z}(C_{n_p})_b}{1 + \frac{(I_{xz})^2}{(I_x)(I_z)}} \qquad \text{(B-18)}$$

$$L'_r = \frac{\frac{\bar{q}Sb^2}{2UI_x}(C_{\ell_r})_b + \frac{I_{xz}}{I_x}\frac{\bar{q}Sb^2}{2UI_z}(C_{n_r})_b}{1 + \frac{(I_{xz})^2}{(I_x)(I_z)}} \qquad \text{(B-19)}$$

$$N'_\beta = \frac{\frac{\bar{q}Sb}{I_z}(C_{n_\beta})_b + \frac{I_{xz}}{I_z}\frac{\bar{q}Sb}{I_x}(C_{\ell_\beta})_b}{1 + \frac{(I_{xz})^2}{(I_x)(I_z)}} \qquad \text{(B-20)}$$

$$N'_p = \frac{\frac{\bar{q}Sb^2}{2UI_z}(C_{n_p})_b + \frac{I_{xz}}{I_z}\frac{\bar{q}Sb^2}{2UI_x}(C_{\ell_p})_b}{1 + \frac{(I_{xz})^2}{(I_x)(I_z)}} \qquad \text{(B-21)}$$

$$N'_r = \frac{\frac{\bar{q}Sb^2}{2UI_z}(C_{n_r})_b + \frac{I_{xz}}{I_z}\frac{\bar{q}Sb^2}{2UI_x}(C_{\ell_r})_b}{1 + \frac{(I_{xz})^2}{(I_x)(I_z)}} \qquad \text{(B-22)}$$

Control Surface Derivatives -- Healthy Aircraft

$$X'_{\delta e_t} = \frac{\bar{q}S}{m} (C_{x_{\delta e}})_b \tag{B-23}$$

$$X'_{\delta f_t} = \frac{\bar{q}S}{m} (C_{x_{\delta f}})_b \tag{B-24}$$

$$Z'_{\delta e_t} = \frac{\bar{q}S}{mU} (C_{z_{\delta e}})_b \tag{B-25}$$

$$Z'_{\delta f_t} = \frac{\bar{q}S}{mU} (C_{z_{\delta f}})_b \tag{B-26}$$

$$M'_{\delta e_t} = \frac{\bar{q}Sc}{I_y} (C_{m_{\delta e}})_b + \left[\frac{\bar{q}Sc^2}{2UI_y} (C_{m_{\dot{\alpha}}})_b\right] Z'_{\delta e_t} \tag{B-27}$$

$$M'_{\delta f_t} = \frac{\bar{q}Sc}{I_y} (C_{m_{\delta f}})_b + \left[\frac{\bar{q}Sc^2}{2UI_y} (C_{m_{\dot{\alpha}}})_b\right] Z'_{\delta f_t} \tag{B-28}$$

$$M'_{\delta c} = \frac{\bar{q}Sc}{I_y} (C_{m_{\delta c}})_b \tag{B-29}$$

Note: Reference 1 is the source of information for $(C_{m_{\delta c}})_b$. The rigid data points (2:4-55 - 4-123) are averaged for canard deflections of 15 and 25 degrees and then flexiblized with altitude (2:9-17).

$$Y'_{\delta a} = \frac{\bar{q}S}{mU} \left[(C_{Y_{\delta DF}})_b + 0.25 (C_{Y_{\delta DT}})_b\right] \tag{B-30}$$

$$Y'_{\delta r} = \frac{\bar{q}S}{mU} (C_{Y_{\delta r}})_b \tag{B-31}$$

$$Y'_{\delta c} = \frac{\bar{q}S}{mU} (C_{Y_{\delta c}})_b \tag{B-32}$$

$$L'_{\delta a} = \frac{\frac{\bar{q}Sb}{I_x}(C_{\ell_{\delta a}})_b + \frac{I_{xz}}{I_x}\frac{\bar{q}Sb}{I_z}(C_{n_{\delta a}})_b}{1 + \frac{(I_{xz})^2}{(I_x)(I_z)}} \qquad \text{(B-33)}$$

where $(C_{\ell_{\delta a}})_b = (C_{\ell_{\delta DF}})_b + 0.25\,(C_{\ell_{\delta DT}})_b$

$(C_{n_{\delta a}})_b = (C_{n_{\delta DF}})_b + 0.25\,(C_{n_{\delta DT}})_b$

$$L'_{\delta r} = \frac{\frac{\bar{q}Sb}{I_x}(C_{\ell_{\delta r}})_b + \frac{I_{xz}}{I_x}\frac{\bar{q}Sb}{I_z}(C_{n_{\delta r}})_b}{1 + \frac{(I_{xz})^2}{(I_x)(I_z)}} \qquad \text{(B-34)}$$

$$L'_{\delta c} = \frac{\frac{\bar{q}Sb}{I_x}(C_{\ell_{\delta c}})_b + \frac{I_{xz}}{I_x}\frac{\bar{q}Sb}{I_z}(C_{n_{\delta c}})_b}{1 + \frac{(I_{xz})^2}{(I_x)(I_z)}} \qquad \text{(B-35)}$$

$$N'_{\delta a} = \frac{\frac{\bar{q}Sb}{I_z}(C_{n_{\delta a}})_b + \frac{I_{xz}}{I_z}\frac{\bar{q}Sb}{I_x}(C_{\ell_{\delta a}})_b}{1 + \frac{(I_{xz})^2}{(I_x)(I_z)}} \qquad \text{(B-36)}$$

where $(C_{n_{\delta a}})_b = (C_{n_{\delta DF}})_b + 0.25\,(C_{n_{\delta DT}})_b$

$(C_{\ell_{\delta a}})_b = (C_{\ell_{\delta DF}})_b + 0.25\,(C_{\ell_{\delta DT}})_b$

$$N'_{\delta r} = \frac{\frac{\bar{q}Sb}{I_z}(C_{n_{\delta r}})_b + \frac{I_{xz}}{I_z}\frac{\bar{q}Sb}{I_x}(C_{\ell_{\delta r}})_b}{1 + \frac{(I_{xz})^2}{(I_x)(I_z)}} \quad \text{(B-37)}$$

$$N'_{\delta c} = \frac{\frac{\bar{q}Sb}{I_z}(C_{n_{\delta c}})_b + \frac{I_{xz}}{I_z}\frac{\bar{q}Sb}{I_x}(C_{\ell_{\delta c}})_b}{1 + \frac{(I_{xz})^2}{(I_x)(I_z)}} \quad \text{(B-38)}$$

Control Surface Derivatives -- Failed Right Elevator

$$X'_{\delta e_\ell} = 0.5\,(X'_{\delta e_t}) \quad \text{(B-39)}$$

$$X'_{\delta f_r} = 0.5\,(X'_{\delta f_t}) \quad \text{(B-40)}$$

$$X'_{\delta f_\ell} = 0.5\,(X'_{\delta f_t}) \quad \text{(B-41)}$$

$$Z'_{\delta e_\ell} = 0.5\,(Z'_{\delta e_t}) \quad \text{(B-42)}$$

$$Z'_{\delta f_r} = 0.5\,(Z'_{\delta f_t}) \quad \text{(B-43)}$$

$$Z'_{\delta f_\ell} = 0.5\,(Z'_{\delta f_t}) \quad \text{(B-44)}$$

$$M'_{\delta e_\ell} = 0.5\,(M'_{\delta e_t}) \quad \text{(B-45)}$$

$$M'_{\delta f_r} = 0.5\,(M'_{\delta f_t}) \quad \text{(B-46)}$$

$$M'_{\delta f_\ell} = 0.5\ (M'_{\delta f_t}) \tag{B-47}$$

$$Y'_{\delta e_\ell} = -\ 0.5\ (0.25)\ \frac{\bar{q}S}{mU}\ (C_{y_{\delta DT}})_b \tag{B-48}$$

$$Y'_{\delta f_r} = 0.5\ \frac{\bar{q}S}{mU}\ (C_{y_{\delta DF}})_b \tag{B-49}$$

$$Y'_{\delta f_\ell} = -\ 0.5\ \frac{\bar{q}S}{mU}\ (C_{y_{\delta DF}})_b \tag{B-50}$$

$$L'_{\delta e_\ell} = -0.125\left[\frac{\frac{\bar{q}Sb}{I_x}(C_{\ell_{\delta DT}})_b + \frac{I_{xz}}{I_x}\frac{\bar{q}Sb}{I_z}(C_{n_{\delta DT}})_b}{1 + \frac{(I_{xz})^2}{(I_x)(I_z)}}\right] \tag{B-51}$$

$$L'_{\delta f_r} = 0.5\left[\frac{\frac{\bar{q}Sb}{I_x}(C_{\ell_{\delta DF}})_b + \frac{I_{xz}}{I_x}\frac{\bar{q}Sb}{I_z}(C_{n_{\delta DF}})_b}{1 + \frac{(I_{xz})^2}{(I_x)(I_z)}}\right] \tag{B-52}$$

$$L'_{\delta f_\ell} = -\ 0.5\left[\frac{\frac{\bar{q}Sb}{I_x}(C_{\ell_{\delta DF}})_b + \frac{I_{xz}}{I_x}\frac{\bar{q}Sb}{I_z}(C_{n_{\delta DF}})_b}{1 + \frac{(I_{xz})^2}{(I_x)(I_z)}}\right] \tag{B-53}$$

$$N'_{\delta e_\ell} = -0.125\left[\frac{\frac{\bar{q}Sb}{I_z}(C_{n_{\delta DT}})_b + \frac{I_{xz}}{I_z}\frac{\bar{q}Sb}{I_x}(C_{\ell_{\delta DT}})_b}{1 + \frac{(I_{xz})^2}{(I_x)(I_z)}}\right] \quad \text{(B-54)}$$

$$N'_{\delta f_r} = 0.5\left[\frac{\frac{\bar{q}Sb}{I_z}(C_{n_{\delta DF}})_b + \frac{I_{xz}}{I_z}\frac{\bar{q}Sb}{I_x}(C_{\ell_{\delta DF}})_b}{1 + \frac{(I_{xz})^2}{(I_x)(I_z)}}\right] \quad \text{(B-55)}$$

$$N'_{\delta f_\ell} = -0.5\left[\frac{\frac{\bar{q}Sb}{I_z}(C_{n_{\delta DF}})_b + \frac{I_{xz}}{I_z}\frac{\bar{q}Sb}{I_x}(C_{\ell_{\delta DF}})_b}{1 + \frac{(I_{xz})^2}{(I_x)(I_z)}}\right] \quad \text{(B-56)}$$

Stability to Body Axis Conversions

Note: In the following equations, a δ by itself indicates that the conversion is the same for all control surface derivatives.

$$(C_{x_u})_b = -(C_{D_u}+2C_D)\cos^2\alpha_T - (C_{L_\alpha}+C_D)\sin^2\alpha_T + (C_{D_\alpha}+C_{L_u}+C_L)\cos\alpha_T \sin\alpha_T \quad \text{(B-57)}$$

$$(C_{x_\alpha})_b = (C_L - C_{D_\alpha})\cos^2\alpha_T + (C_{L_u}+2C_L)\sin^2\alpha_T + (C_{L_\alpha} - C_{D_u} - C_D)\cos\alpha_T \sin\alpha_T \quad \text{(B-58)}$$

$$(C_{x_q})_b = C_{L_q} \sin\alpha_T \tag{B-59}$$

$$(C_{x_\delta})_b = -C_{D_\delta} \cos\alpha_T + C_{L_\delta} \sin\alpha_T \tag{B-60}$$

$$(C_{z_u})_b = (C_{D_\alpha} - C_L) \sin^2\alpha_T - (C_{L_u} + 2C_L) \cos^2\alpha_T + (C_{L_\alpha} - C_{D_u} - C_D) \cos\alpha_T \sin\alpha_T \tag{B-61}$$

$$(C_{z_\alpha})_b = -(C_{L_\alpha} + C_D) \cos^2\alpha_T - (C_{D_u} + 2C_D) \sin^2\alpha_T - (C_{L_u} + C_L + C_{D_\alpha}) \cos\alpha_T \sin\alpha_T \tag{B-62}$$

$$(C_{z_{\dot\alpha}})_b = -C_{L_{\dot\alpha}} \cos^2\alpha_T \tag{B-63}$$

$$(C_{z_q})_b = -C_{L_q} \cos\alpha_T \tag{B-64}$$

$$(C_{z_\delta})_b = -C_{L_\delta} \cos\alpha_T - C_{D_\delta} \sin\alpha_T \tag{B-65}$$

$$(C_{m_u})_b = (C_{m_u} + 2C_m) \cos\alpha_T - C_{m_\alpha} \sin\alpha_T \tag{B-66}$$

$$(C_{m_\alpha})_b = C_{m_\alpha} \cos\alpha_T + (C_{m_u} + 2C_m) \sin\alpha_T \tag{B-67}$$

$$(C_{m_{\dot\alpha}})_b = C_{m_{\dot\alpha}} \cos\alpha_T \tag{B-68}$$

$$(C_{m_q})_b = C_{m_q} \tag{B-69}$$

$$(C_{m_\delta})_b = C_{m_\delta} \tag{B-70}$$

$$(C_{y_\beta})_b = C_{y_\beta} \tag{B-71}$$

$$(C_{y_p})_b = C_{y_p} \cos\alpha_T - C_{y_r} \sin\alpha_T \tag{B-72}$$

$$(C_{y_r})_b = C_{y_r} \cos\alpha_T + C_{y_p} \sin\alpha_T \tag{B-73}$$

$$(C_{y_\delta})_b = C_{y_\delta} \tag{B-74}$$

$$(C_{\ell_\beta})_b = C_{\ell_\beta} \cos\alpha_T - C_{n_\beta} \sin\alpha_T \tag{B-75}$$

$$(C_{\ell_p})_b = C_{\ell_p} \cos^2\alpha_T + C_{n_r} \sin^2\alpha_T - (C_{\ell_r} + C_{n_p}) \sin\alpha_T \cos\alpha_T \tag{B-76}$$

$$(C_{\ell_r})_b = C_{\ell_r} \cos^2\alpha_T - C_{n_p} \sin^2\alpha_T + (C_{\ell_p} - C_{n_r}) \sin\alpha_T \cos\alpha_T \tag{B-77}$$

$$(C_{\ell_\delta})_b = C_{\ell_\delta} \cos\alpha_T - C_{n_\delta} \sin\alpha_T \tag{B-78}$$

$$(C_{n_\beta})_b = C_{n_\beta} \cos\alpha_T + C_{\ell_\beta} \sin\alpha_T \tag{B-79}$$

$$(C_{n_p})_b = C_{n_p} \cos^2\alpha_T - C_{\ell_r} \sin^2\alpha_T + (C_{\ell_p} - C_{n_r}) \sin\alpha_T \cos\alpha_T \tag{B-80}$$

$$(C_{n_r})_b = C_{n_r} \cos^2\alpha_T + C_{\ell_p} \sin^2\alpha_T + (C_{\ell_r} + C_{n_p}) \sin\alpha_T \cos\alpha_T \quad \text{(B-81)}$$

$$(C_{n_\delta})_b = C_{n_\delta} \cos\alpha_T + C_{\ell_\delta} \sin\alpha_T \quad \text{(B-82)}$$

Note: A question was raised late in the study about consistency of units in the longitudinal stability to body axis conversion equations that involve the terms C_{L_u}, C_{D_u}, and C_{m_u}. All of the body axis aerodynamic coefficients calculated with these equations should be dimensionless; however, the stabiltiy axis aerodynamic coefficients C_{L_u}, C_{D_u}, and C_{m_u} listed in Appendix C have units of per feet per second squared. These aerodynamic coefficients were taken from Reference 4 and are also available from Reference 1.

In order to make the units consistent in the body to stability axis conversion equations, C_{L_u}, C_{D_u}, and C_{m_u} should first be multiplied by the trim velocity before substitution into the conversion equations. Equations (B-57), (B-61), and (B-66) are particularly affected by the correction; however, the primed dimensional derivatives X'_u, Z'_u, and M'_u, calculated with Equations (B-2), (B-6), and (B-10), remain small in magnitude. The designs and simulations in this study are therefore essentially unaffected by the correction and are still valid.

The same error exists in several references and

computer programs used by the Flight Dynamics Laboratory; however, because the terms C_{L_u}, C_{D_u}, and C_{m_u} have small values, they are normally deleted from aircraft models (1).

Appendix C: Aerodynamic Data

This appendix contains all of the aerodynamic data used in the thesis. Reference 4 is the source of most of the data; however, the primed dimensional derivatives were checked with the equations in Appendix B. The thrust data is given in Table 2-1, and the derivative M'_{δ_C} is calculated with Equation (B-29).

The Tables in this appendix list aircraft aerodynamic coefficients in the stability axis, primed dimensional derivatives in the body axis, and MULTI data files for each flight condition considered in this study. The aerodynamic coefficients are entered into the equations of Appendix B to calculate the primed dimensional derivatives. The dimensional derivatives are entered directly into the aircraft models, given by Equations (2-40) and (2-41). The units for the derivatives are: radians for angles; radians per second for angular rates; feet per second for velocity; and g's for accelerations. MULTI data files are given for easy verification of design responses.

Table C-1 lists aircraft parameters that are common to all flight conditions.

Table C-1

Aircraft Parameters Common to All Flight Conditions

S	(wing reference area) = 300.0 ft^2
c	(wing mean aerodynamic cord) = 11.32 ft
b	(wing span) = 30.0 ft
W	(weight) = 21,018.0 lbs
m	(mass) = 652.73 slugs
I_x	(x-axis moment of inertia) = 10,033.4 ft^2
I_y	(y-axis moment of inertia) = 53,876.3 ft^2
I_z	(z-axis moment of inertia) = 61,278.4 ft^2
I_{xz}	(product of inertia) = 282.132 ft^2

Table C-2

Aerodynamic Coefficients in the Stability Axis

for 0.9 Mach at 20,000 Feet

$\bar{q}$ (dynamic pressure) = 552.11295 lbs/ft^2

V_T (trim velocity) = 933.23 ft/sec

α_T (trim angle of attack) = 0.03246 radians

C_L	= 0.126186	C_D	= 0.023766
$C_{L_u}(\frac{1}{ft/sec})$	= -0.000442	$C_{D_u}(\frac{1}{ft/sec})$	= 0.000160
$C_{L_\alpha}(\frac{1}{deg})$	= 0.094812	$C_{D_\alpha}(\frac{1}{deg})$	= 0.002636
$C_{L_{\dot{\alpha}}}(\frac{1}{radian})$	= -1.357762	---	
$C_{L_q}(\frac{1}{radian})$	= 3.161717	---	
$C_{L_{\delta e_t}}(\frac{1}{deg})$	= 0.009578	$C_{D_{\delta e_t}}(\frac{1}{deg})$	= 0.000173
$C_{L_{\delta f_t}}(\frac{1}{deg})$	= 0.015718	$C_{D_{\delta f_t}}(\frac{1}{deg})$	= 0.000351
C_m	= 0.0	$C_{y_\beta}(\frac{1}{deg})$	= -0.022052
$C_{m_u}(\frac{1}{ft/sec})$	= -0.000060	$C_{y_p}(\frac{1}{radian})$	= 0.057563
$C_{m_\alpha}(\frac{1}{deg})$	= 0.001938	$C_{y_r}(\frac{1}{radian})$	= 0.557635
$C_{m_{\dot{\alpha}}}(\frac{1}{radian})$	= -1.307597	$C_{y_{\delta DF}}(\frac{1}{deg})$	= -0.000088
$C_{m_q}(\frac{1}{radian})$	= -2.382199	$C_{y_{\delta DT}}(\frac{1}{deg})$	= 0.001708

Table C-2 (continued)

$C_{m_{\delta e_t}}(\frac{1}{deg}) = -0.012086$	$C_{y_{\delta r}}(\frac{1}{deg}) = 0.002377$
$C_{m_{\delta f_t}}(\frac{1}{deg}) = -0.003280$	---
$C_{m_{\delta c}}(\frac{1}{deg}) = -0.000495$	$C_{y_{\delta c}}(\frac{1}{deg}) = 0.001716$
$C_{\ell_\beta}(\frac{1}{deg}) = -0.001901$	$C_{n_\beta}(\frac{1}{deg}) = 0.001675$
$C_{\ell_p}(\frac{1}{radian}) = -0.351217$	$C_{n_p}(\frac{1}{radian}) = -0.005541$
$C_{\ell_r}(\frac{1}{radian}) = 0.021937$	$C_{n_r}(\frac{1}{radian}) = -0.279120$
$C_{\ell_{\delta DF}}(\frac{1}{deg}) = -0.001804$	$C_{n_{\delta DF}}(\frac{1}{deg}) = -0.000160$
$C_{\ell_{\delta DT}}(\frac{1}{deg}) = -0.000997$	$C_{n_{\delta DT}}(\frac{1}{deg}) = -0.001816$
$C_{\ell_{\delta r}}(\frac{1}{deg}) = 0.000331$	$C_{n_{\delta r}}(\frac{1}{deg}) = -0.279120$
$C_{\ell_{\delta c}}(\frac{1}{deg}) = 0.001256$	$C_{n_{\delta c}}(\frac{1}{deg}) = 0.000230$

Table C-3

Primed Dimensional Derivatives in the Body Axis

for 0.9 Mach at 20,000 Feet

$X'_{\theta} = -32.1830$	$Z'_{\theta} = -0.001120$	$M'_{\theta} = 0.000309$
$X'_{u} = -0.012075$	$Z'_{u} = -0.000022$	$M'_{u} = -0.000130$
$X'_{\alpha} = 38.2906$	$Z'_{\alpha} = -1.48446$	$M'_{\alpha} = 4.27171$
$X'_{q} = -30.1376$	$Z'_{q} = 0.994789$	$M'_{q} = -0.777221$
$X'_{\delta e_t} = 2.005930$	$Z'_{\delta e_t} = -0.149227$	$M'_{\delta e_t} = -24.0581$
$X'_{\delta f_t} = 2.31681$	$Z'_{\delta f_t} = -0.244924$	$M'_{\delta f_t} = -6.47269$
$X'_{\delta T} = 19.254$	---	$M'_{\delta c} = -0.9864$
$Y'_{\phi} = 0.034486$	---	---
$Y'_{\beta} = -0.343554$	$L'_{\beta} = -55.2526$	$N'_{\beta} = 7.2370$
$Y'_{p} = 0.032636$	$L'_{p} = -2.80004$	$N'_{p} = -0.023184$
$Y'_{r} = -0.997556$	$L'_{r} = 0.145674$	$N'_{r} = -0.362530$
$Y'_{\delta DF} = -0.001371$	$L'_{\delta DF} = -51.0502$	$N'_{\delta DF} = -1.25006$
$Y'_{\delta DT} = 0.026609$	$L'_{\delta DT} = -50.7290$	$N'_{\delta DT} = -5.13710$
$Y'_{\delta r} = 0.037032$	$L'_{\delta r} = 10.3955$	$N'_{\delta r} = -5.80890$
$Y'_{\delta c} = 0.026734$	$L'_{\delta c} = 5.53185$	$N'_{\delta c} = 5.89254$

Table C-4

Healthy Aircraft Data File for use with MULTI Option #9

for 0.9 Mach at 20,000 Feet

```
1
14 6 6
0 0 0 1 0 0 0 0 0 0 0 0 0 0
-32.1830 -.012075 38.2906 -30.1376 0 0 0 0 2.00593 2.31681 0 0 0 19.254
-.00112 -.000022 -1.48446 .994789 0 0 0 0 -.149227 -.244924 0 0 0 0
.000309 -.000130 4.27171 -.777221 0 0 0 0 -24.0581 -6.47269 0 0 -.9864 0
0 0 0 0 0 0 1 0 0 0 0 0 0 0
0 0 0 0 .034486 -.343554 .032636 -.997556 0 0 .0052813 .037032 .026734 0
0 0 0 0 0 -55.2526 -2.80004 .145674 0 0 -63.73245 10.3955 5.53185 0
0 0 0 0 0 7.237 -.023184 -.36253 0 0 -2.534335 -5.8089 5.89254 0
0 0 0 0 0 0 0 0 -20 0 0 0 0 0
0 0 0 0 0 0 0 0 0 -20 0 0 0 0
0 0 0 0 0 0 0 0 0 0 -20 0 0 0
0 0 0 0 0 0 0 0 0 0 0 -20 0 0
0 0 0 0 0 0 0 0 0 0 0 0 -20 0
0 0 0 0 0 0 0 0 0 0 0 0 0 -1
0 0 0 0 0 0
0 0 0 0 0 0
0 0 0 0 0 0
0 0 0 0 0 0
0 0 0 0 0 0
0 0 0 0 0 0
0 0 0 0 0 0
20 0 0 0 0 0
0 20 0 0 0 0
0 0 20 0 0 0
0 0 0 20 0 0
0 0 0 0 20 0
0 0 0 0 0 1
0 1 0 0 0 0 0 0 0 0 0 0 0 0
.0001339 .0005813 44.8737 -.1857 0 0 0 0 -6.09774 4.2943 0 0 -.4273 0
0 0 0 1 0 0 0 0 0 0 0 0 0 0
0 0 0 0 0 -6.8217 -.005034 -.08623 0 0 -.9449 -1.4433 3.3276 0
0 0 0 0 0 0 1 0 0 0 0 0 0 0
0 0 0 0 0 0 0 1 0 0 0 0 0 0
N
Y
1 1 1 1 1 1
-72
72
1
-72
72
1
-72
72
1
-72
72
1
-72
72
1
-1000
1000
1
N
```

Table C-5

Failed Aircraft Data File for use with MULTI Option #9

for 0.9 Mach at 20,000 Feet

```
1
14 6 6
0 0 0 1 0 0 0 0 0 0 0 0 0 0
-32.1830 -.012075 38.2906 -30.1376 0 0 0 0 1.002965 1.1584 1.1584 0 0 19.254
-.00112 -.000022 -1.48446 .994789 0 0 0 0 -.07461 -.1225 -.1225 0 0 0
.000309 -.000130 4.2717 -.777221 0 0 0 0 -12.0291 -3.2363 -3.2363 0 -.9864 0
0 0 0 0 0 0 1 0 0 0 0 0 0 0
0 0 0 0 .03449 -.3436 .03264 -.9976 -.003326 -.000686 .000686 .0370 .0267 0
0 0 0 0 0 -55.2526 -2.80004 .145674 6.3411 -25.5251 25.5251 10.3955 5.5319 0
0 0 0 0 0 7.237 -.023184 -.36253 .642138 -.62503 .62503 -5.8089 5.89254 0
0 0 0 0 0 0 0 0 -20 0 0 0 0 0
0 0 0 0 0 0 0 0 0 -20 0 0 0 0
0 0 0 0 0 0 0 0 0 0 -20 0 0 0
0 0 0 0 0 0 0 0 0 0 0 -20 0 0
0 0 0 0 0 0 0 0 0 0 0 0 -20 0
0 0 0 0 0 0 0 0 0 0 0 0 0 -1
0 0 0 0 0 0
0 0 0 0 0 0
0 0 0 0 0 0
0 0 0 0 0 0
0 0 0 0 0 0
0 0 0 0 0 0
0 0 0 0 0 0
20 0 0 0 0 0
0 20 0 0 0 0
0 0 20 0 0 0
0 0 0 20 0 0
0 0 0 0 20 0
0 0 0 0 0 1
0 1 0 0 0 0 0 0 0 0 0 0 0 0
.0001339 .0005813 44.8737 -.1857 0 0 0 0 -3.04887 2.14715 2.14715 0 -.4273 0
0 0 0 1 0 0 0 0 0 0 0 0 0 0
0 0 0 0 0 -6.8217 -.005034 -.08623 .1818 -.2906 .2906 -1.4433 3.3276 0
0 0 0 0 0 0 1 0 0 0 0 0 0 0
0 0 0 0 0 0 0 1 0 0 0 0 0 0
N
Y
1 1 1 1 1 1
-72
72
1
-72
72
1
-72
72
1
-72
72
1
-72
72
1
-72
72
1
-1000
1000
1
N
```

Table C-6

Aerodynamic Coefficients in the Stability Axis

for 0.6 Mach at 30,000 Feet

$\bar{q}$ (dynamic pressure) = 158.81 lbs/ft^2	
V_T (trim velocity) = 596.91 ft/sec	
α_T (trim angle of attack) = 0.08212 radians	
C_L = 0.439013	C_D = 0.044151
$C_{L_u}(\frac{1}{ft/sec})$ = 0.000158	$C_{D_u}(\frac{1}{ft/sec})$ = 0.000050
$C_{L_\alpha}(\frac{1}{deg})$ = 0.073559	$C_{D_\alpha}(\frac{1}{deg})$ = 0.008210
$C_{L_{\dot{\alpha}}}(\frac{1}{radian})$ = -1.029896	---
$C_{L_q}(\frac{1}{radian})$ = 2.437286	---
$C_{L_{\delta e_t}}(\frac{1}{deg})$ = 0.009473	$C_{D_{\delta e_t}}(\frac{1}{deg})$ = 0.000019
$C_{L_{\delta f_t}}(\frac{1}{deg})$ = 0.015850	$C_{D_{\delta f_t}}(\frac{1}{deg})$ = 0.001808
C_m = 0.0	$C_{y_\beta}(\frac{1}{deg})$ = -0.021995
$C_{m_u}(\frac{1}{ft/sec})$ = -0.000106	$C_{y_p}(\frac{1}{radian})$ = 0.132102
$C_{m_\alpha}(\frac{1}{deg})$ = 0.004356	$C_{y_r}(\frac{1}{radian})$ = 0.536904
$C_{m_{\dot{\alpha}}}(\frac{1}{radian})$ = -0.747194	$C_{y_{\delta DF}}(\frac{1}{deg})$ = 0.000051
$C_{m_q}(\frac{1}{radian})$ = -2.859448	$C_{y_{\delta DT}}(\frac{1}{deg})$ = 0.002055

Table C-6 (continued)

$C_{m_{\delta e_t}}(\frac{1}{deg}) = -0.010229$	$C_{y_{\delta r}}(\frac{1}{deg}) = 0.003021$
$C_{m_{\delta f_t}}(\frac{1}{deg}) = -0.000383$	---
$C_{m_{\delta c}}(\frac{1}{deg}) = -0.000463$	$C_{y_{\delta c}}(\frac{1}{deg}) = 0.001047$
$C_{\ell_\beta}(\frac{1}{deg}) = -0.002209$	$C_{n_\beta}(\frac{1}{deg}) = 0.001972$
$C_{\ell_p}(\frac{1}{radian}) = -0.243246$	$C_{n_p}(\frac{1}{radian}) = -0.013813$
$C_{\ell_r}(\frac{1}{radian}) = 0.071941$	$C_{n_r}(\frac{1}{radian}) = -0.484330$
$C_{\ell_{\delta DF}}(\frac{1}{deg}) = -0.002141$	$C_{n_{\delta DF}}(\frac{1}{deg}) = 0.000035$
$C_{\ell_{\delta DT}}(\frac{1}{deg}) = -0.001742$	$C_{n_{\delta DT}}(\frac{1}{deg}) = -0.000940$
$C_{\ell_{\delta r}}(\frac{1}{deg}) = 0.000364$	$C_{n_{\delta r}}(\frac{1}{deg}) = -0.001520$
$C_{\ell_{\delta c}}(\frac{1}{deg}) = 0.000138$	$C_{n_{\delta c}}(\frac{1}{deg}) = 0.001121$

Table C-7

Primed Dimensional Derivatives in the Body Axis

for 0.6 Mach at 30,000 Feet

$X'_\theta = -32.0915$	$Z'_\theta = -0.004425$	$M'_\theta = 0.000313$
$X'_u = -0.005142$	$Z'_u = -0.000109$	$M'_u = -0.000337$
$X'_\alpha = 23.0402$	$Z'_\alpha = -0.526422$	$M'_\alpha = 2.52708$
$X'_q = -48.8785$	$Z'_q = 0.997184$	$M'_q = -0.341902$
$X'_{\delta e_t} = 3.17035$	$Z'_{\delta e_t} = -0.066156$	$M'_{\delta e_t} = -5.86214$
$X'_{\delta f_t} = -2.09855$	$Z'_{\delta f_t} = -0.111711$	$M'_{\delta f_t} = -0.211773$
$X'_{\delta T} = 10.555$	---	$M'_{\delta c} = -0.2657$
$Y'_\phi = 0.05376$	---	---
$Y'_\beta = -0.154099$	$L'_\beta = -19.2246$	$N'_\beta = 2.29583$
$Y'_p = 0.082387$	$L'_p = -0.893601$	$N'_p = -0.000888$
$Y'_r = -0.998322$	$L'_r = 0.318845$	$N'_r = -0.278676$
$Y'_{\delta DF} = 0.000357$	$L'_{\delta DF} = -17.4468$	$N'_{\delta DF} = -0.268403$
$Y'_{\delta DT} = 0.014398$	$L'_{\delta DT} = -13.5832$	$N'_{\delta DT} = -1.50547$
$Y'_{\delta r} = 0.021165$	$L'_{\delta r} = 3.92325$	$N'_{\delta r} = -1.96651$
$Y'_{\delta c} = 0.007335$	$L'_{\delta c} = 0.414519$	$N'_{\delta c} = 1.51008$

Table C-8

Healthy Aircraft Data File for use with MULTI Option #9

for 0.6 Mach at 30,000 Feet

```
1
14 6 6
0 0 0 1 0 0 0 0 0 0 0 0 0 0
-32.0915 -.005142 23.0402 -48.8785 0 0 0 0 3.17035 -2.09855 0 0 10.555
-.004425 -.000109 -.526422 .0997184 0 0 0 0 -.066156 -.111711 0 0 0 0
.000313 -.000337 2.52708 -.341902 0 0 0 0 -5.86214 -.211773 0 0 -.2657 0
0 0 0 0 0 0 1 0 0 0 0 0 0 0
0 0 0 0 .05376 -.154099 .082387 -.998322 0 0 .0039565 .021165 .007335 0
0 0 0 0 0 -19.2246 -.893601 .318845 0 0 -20.8426 3.92325 .414519 0
0 0 0 0 0 2.29583 -.000888 -.278676 0 0 -.6447705 -1.96651 1.51008 0
0 0 0 0 0 0 0 0 -20 0 0 0 0 0
0 0 0 0 0 0 0 0 0 -20 0 0 0 0
0 0 0 0 0 0 0 0 0 0 -20 0 0 0
0 0 0 0 0 0 0 0 0 0 0 -20 0 0
0 0 0 0 0 0 0 0 0 0 0 0 -20 0
0 0 0 0 0 0 0 0 0 0 0 0 0 -1
0 0 0 0 0 0
0 0 0 0 0 0
0 0 0 0 0 0
0 0 0 0 0 0
0 0 0 0 0 0
0 0 0 0 0 0
0 0 0 0 0 0
0 0 0 0 0 0
20 0 0 0 0 0
0 20 0 0 0 0
0 0 20 0 0 0
0 0 0 20 0 0
0 0 0 0 20 0
0 0 0 0 0 1
0 1 0 0 0 0 0 0 0 0 0 0 0 0
.0001356 .001875 10.8534 -.09592 0 0 0 0 -1.3133 1.9791 0 0 -.1151 0
0 0 0 1 0 0 0 0 0 0 0 0 0 0
0 0 0 0 0 -1.862 .004608 -.08962 0 0 -.2060 -.4596 .7902 0
0 0 0 0 0 0 1 0 0 0 0 0 0 0
0 0 0 0 0 0 0 1 0 0 0 0 0 0
N
Y
1 1 1 1 1 1
-72
72
1
-72
72
1
-72
72
1
-72
72
1
-72
72
1
-1000
1000
1
N
```

Table C-9

Failed Aircraft Data File for use with MULTI Option #9

for 0.6 Mach at 30,000 Feet

```
1
14 6 6
0 0 0 1 0 0 0 0 0 0 0 0 0 0
-32.092 -.00514 23.040 -48.879 0 0 0 0 1.58518 -1.04928 -1.04928 0 0 10.555
-.00443 -.000109 -.52642 .099718 0 0 0 0 -.03308 -.05586 -.05586 0 0 0
.000313 -.000337 2.5271 -.34190 0 0 0 0 -2.9311 -.1059 -.1059 0 -.2657 0
0 0 0 0 0 0 1 0 0 0 0 0 0 0
0 0 0 0 .0538 -.1541 .0824 -.9983 -.00178 .0001785 -.0001785 .02117 .00734 0
0 0 0 0 0 -19.225 -.8936 .3188 1.6979 -8.7234 8.7234 3.9233 .41452 0
0 0 0 0 0 2.2958 -.000888 -.27868 .1882 -.1342 .1342 -1.9665 1.51008 0
0 0 0 0 0 0 0 0 -20 0 0 0 0 0
0 0 0 0 0 0 0 0 0 -20 0 0 0 0
0 0 0 0 0 0 0 0 0 0 -20 0 0 0
0 0 0 0 0 0 0 0 0 0 0 -20 0 0
0 0 0 0 0 0 0 0 0 0 0 0 -20 0
0 0 0 0 0 0 0 0 0 0 0 0 0 -1
0 0 0 0 0 0
0 0 0 0 0 0
0 0 0 0 0 0
0 0 0 0 0 0
0 0 0 0 0 0
0 0 0 0 0 0
0 0 0 0 0 0
0 0 0 0 0 0
20 0 0 0 0 0
0 20 0 0 0 0
0 0 20 0 0 0
0 0 0 20 0 0
0 0 0 0 20 0
0 0 0 0 0 1
0 1 0 0 0 0 0 0 0 0 0 0 0 0
.0001356 .001875 10.8534 -.09592 0 0 0 0 -.65665 .98955 .9855 0 -.1151 0
0 0 0 1 0 0 0 0 0 0 0 0 0 0
0 0 0 0 0 -1.862 .004608 -.08962 .04816 -.05483 .05483 -.4596 .7902 0
0 0 0 0 0 0 1 0 0 0 0 0 0 0
0 0 0 0 0 0 0 1 0 0 0 0 0 0
N
Y
1 1 1 1 1 1
-72
72
1
-72
72
1
-72
72
1
-72
72
1
-72
72
1
-1000
1000
1
N
```

Table C-10

Aerodynamic Coefficients in the Stability Axis

for 1.6 Mach at 30,000 Feet

$\bar{q}$ (dynamic pressure) = 1129.3126 lbs/ft^2	
V_T (trim velocity) = 1591.75 ft/sec	
α_T (trim angle of attack) = 0.02932 radians	
C_L = 0.060695	C_D = 0.046574
$C_{L_u}(\frac{1}{ft/sec})$ = 0.000027	$C_{D_u}(\frac{1}{ft/sec})$ = 0.000002
$C_{L_\alpha}(\frac{1}{deg})$ = 0.066129	$C_{D_\alpha}(\frac{1}{deg})$ = 0.001457
$C_{L_{\dot{\alpha}}}(\frac{1}{radian})$ = -2.974699	---
$C_{L_q}(\frac{1}{radian})$ = 3.458724	---
$C_{L_{\delta e_t}}(\frac{1}{deg})$ = 0.006180	$C_{D_{\delta e_t}}(\frac{1}{deg})$ = -0.000135
$C_{L_{\delta f_t}}(\frac{1}{deg})$ = 0.004004	$C_{D_{\delta f_t}}(\frac{1}{deg})$ = 0.000565
C_m = 0.0	$C_{y_\beta}(\frac{1}{deg})$ = -0.019192
$C_{m_u}(\frac{1}{ft/sec})$ = -0.000046	$C_{y_p}(\frac{1}{radian})$ = 0.026463
$C_{m_\alpha}(\frac{1}{deg})$ = -0.010705	$C_{y_r}(\frac{1}{radian})$ = 0.516864
$C_{m_{\dot{\alpha}}}(\frac{1}{radian})$ = 0.501981	$C_{y_{\delta DF}}(\frac{1}{deg})$ = 0.000362
$C_{m_q}(\frac{1}{radian})$ = -1.889366	$C_{y_{\delta DT}}(\frac{1}{deg})$ = 0.000281

Table C-10 (continued)

$C_{m_{\delta e_t}}(\frac{1}{deg}) = -0.008061$	$C_{y_{\delta r}}(\frac{1}{deg}) = 0.000552$
$C_{m_{\delta f_t}}(\frac{1}{deg}) = -0.001432$	---
$C_{m_{\delta c}}(\frac{1}{deg}) = 0.000050$	$C_{y_{\delta c}}(\frac{1}{deg}) = 0.001541$
$C_{\ell_\beta}(\frac{1}{deg}) = -0.001702$	$C_{n_\beta}(\frac{1}{deg}) = 0.00088$
$C_{\ell_p}(\frac{1}{radian}) = -0.257331$	$C_{n_p}(\frac{1}{radian}) = 0.004371$
$C_{\ell_r}(\frac{1}{radian}) = 0.018261$	$C_{n_r}(\frac{1}{radian}) = -0.246367$
$C_{\ell_{\delta DF}}(\frac{1}{deg}) = -0.000250$	$C_{n_{\delta DF}}(\frac{1}{deg}) = -0.000236$
$C_{\ell_{\delta DT}}(\frac{1}{deg}) = -0.000811$	$C_{n_{\delta DT}}(\frac{1}{deg}) = -0.000317$
$C_{\ell_{\delta r}}(\frac{1}{deg}) = 0.000077$	$C_{n_{\delta r}}(\frac{1}{deg}) = -0.000349$
$C_{\ell_{\delta c}}(\frac{1}{deg}) = 0.000232$	$C_{n_{\delta c}}(\frac{1}{deg}) = 0.000973$

Table C-11

Primed Dimensional Derivatives in the Body Axis

for 1.6 Mach at 30,000 Feet

$X'_\theta = -32.1861$	$Z'_\theta = -0.000593$	$M'_\theta = -0.000075$
$X'_u = -0.030046$	$Z'_u = -0.000002$	$M'_u = 0.000802$
$X'_\alpha = 45.1941$	$Z'_\alpha = -1.25100$	$M'_\alpha = -43.8012$
$X'_q = -46.5132$	$Z'_q = 0.995991$	$M'_q = -0.351737$
$X'_{\delta e_t} = 9.40431$	$Z'_{\delta e_t} = -0.115337$	$M'_{\delta e_t} = -32.8919$
$X'_{\delta f_t} = -13.3021$	$Z'_{\delta f_t} = -0.075084$	$M'_{\delta f_t} = -5.85004$
$X'_{\delta T} = 7.230$	---	$M'_{\delta c} = 0.2043$
$Y'_\phi = 0.02022$	---	---
$Y'_\beta = -0.358564$	$L'_\beta = -100.032$	$N'_\beta = 7.42422$
$Y'_p = 0.029374$	$L'_p = -2.46287$	$N'_p = -0.005040$
$Y'_r = -0.998410$	$L'_r = 0.160287$	$N'_r = -0.383316$
$Y'_{\delta DF} = 0.006763$	$L'_{\delta DF} = -14.1689$	$N'_{\delta DF} = -2.37673$
$Y'_{\delta DT} = 0.005250$	$L'_{\delta DT} = -46.6078$	$N'_{\delta DT} = -3.45190$
$Y'_{\delta r} = 0.010313$	$L'_{\delta r} = 4.96942$	$N'_{\delta r} = -3.27086$
$Y'_{\delta c} = 0.028790$	$L'_{\delta c} = 12.0662$	$N'_{\delta c} = 9.36290$

Table C-12

Healthy Aircraft Data File for use with MULTI Option #9

for 1.6 Mach at 30,000 Feet

```
1
14 6 6
0 0 0 1 0 0 0 0 0 0 0 0 0 0
-32.1861 -.030046 45.1941 -46.5132 0 0 0 0 9.40431 -13.3021 0 0 0 7.230
-.000593 -.000002 -1.251 .995991 0 0 0 0 -.115337 -.075084 0 0 0 0
-.000075 .000802 -43.8012 -.351737 0 0 0 0 -32.8919 -5.85004 0 0 .2043 0
0 0 0 0 0 0 1 0 0 0 0 0 0 0
0 0 0 0 .02022 -.358564 .029374 -.99841 0 0 .0080755 .010313 .02879 0
0 0 0 0 0 -100.032 -2.46287 .0160287 0 0 -25.82085 4.96942 12.0662 0
0 0 0 0 0 7.42422 -.00504 -.383316 0 0 -3.2397 -3.27086 9.3629 0
0 0 0 0 0 0 0 0 -20 0 0 0 0 0
0 0 0 0 0 0 0 0 0 -20 0 0 0 0
0 0 0 0 0 0 0 0 0 0 -20 0 0 0
0 0 0 0 0 0 0 0 0 0 0 -20 0 0
0 0 0 0 0 0 0 0 0 0 0 0 -20 0
0 0 0 0 0 0 0 0 0 0 0 0 0 -1
0 0 0 0 0 0
0 0 0 0 0 0
0 0 0 0 0 0
0 0 0 0 0 0
0 0 0 0 0 0
0 0 0 0 0 0
0 0 0 0 0 0
20 0 0 0 0 0
0 20 0 0 0 0
0 0 20 0 0 0
0 0 0 20 0 0
0 0 0 0 20 0
0 0 0 0 0 1
0 1 0 0 0 0 0 0 0 0 0 0 0 0
-.00003249 .0004463 42.865 .04579 0 0 0 0 -8.5483 1.1772 0 0 .08851 0
0 0 0 1 0 0 0 0 0 0 0 0 0 0
0 0 0 0 0 -14.5086 .0004118 -.08747 0 0 -1.004339 -.90723 5.4795 0
0 0 0 0 0 0 1 0 0 0 0 0 0 0
0 0 0 0 0 0 0 1 0 0 0 0 0 0
N
Y
1 1 1 1 1 1
-72
72
1
-72
72
1
-72
72
1
-72
72
1
-72
72
1
-1000
1000
1
N
```

Table C-13

Failed Aircraft Data File for use with MULTI Option #9

for 1.6 Mach at 30,000 Feet

```
1
14 6 6
0 0 0 1 0 0 0 0 0 0 0 0 0 0
-32.186 -.030046 45.1941 -46.5132 0 0 0 0 4.7022 -6.6511 -6.6511 0 0 7.230
-.000593 -.000002 -1.251 .995991 0 0 0 0 -.05767 -.03754 -.03754 0 0 0
-.000075 .000802 -43.8012 -.3517 0 0 0 0 -16.4460 -2.925 -2.925 0 .2043 0
0 0 0 0 0 0 1 0 0 0 0 0 0 0
0 0 0 0 .02022 -.35856 .02937 -.9984 -.000656 .00338 -.00338 .01031 .02879 0
0 0 0 0 0 -100.032 -2.4629 .0160287 5.826 -7.0845 7.0845 4.9694 12.0662 0
0 0 0 0 0 7.42422 -.00504 -.383316 .4315 -1.1884 1.1884 -3.27086 9.3629 0
0 0 0 0 0 0 0 0 -20 0 0 0 0 0
0 0 0 0 0 0 0 0 0 -20 0 0 0 0
0 0 0 0 0 0 0 0 0 0 -20 0 0 0
0 0 0 0 0 0 0 0 0 0 0 -20 0 0
0 0 0 0 0 0 0 0 0 0 0 0 -20 0
0 0 0 0 0 0 0 0 0 0 0 0 0 -1
0 0 0 0 0 0
0 0 0 0 0 0
0 0 0 0 0 0
0 0 0 0 0 0
0 0 0 0 0 0
0 0 0 0 0 0
0 0 0 0 0 0
0 0 0 0 0 0
20 0 0 0 0 0
0 20 0 0 0 0
0 0 20 0 0 0
0 0 0 20 0 0
0 0 0 0 20 0
0 0 0 0 0 1
0 1 0 0 0 0 0 0 0 0 0 0 0 0
-.00003249 .0004463 42.865 .04579 0 0 0 0 -4.2742 .5886 .5886 0 .08851 0
0 0 0 1 0 0 0 0 0 0 0 0 0 0
0 0 0 0 0 -14.5086 .0004118 -.08747 .1545 -.3477 .3477 -.90723 5.4795 0
0 0 0 0 0 0 1 0 0 0 0 0 0 0
0 0 0 0 0 0 0 1 0 0 0 0 0 0
N
Y
1 1 1 1 1 1
-72
72
1
-72
72
1
-72
72
1
-72
72
1
-72
72
1
-1000
1000
1
N
```

The aerodynamic coefficients for the previous three flight conditions appear in Reference 4 and were originally obtained from Reference 1; however, in both these references, landing approach data is given for 0.2 Mach at 30 feet with the flaperons completely deflected downward. The trim angle of attack α_T for this flight condition is 14.98 degrees. For the study in this thesis it is desirable to evaluate the aircraft's performance with the flaperons trimmed at zero degrees and at a higher speed, which yields a smaller α_T. A landing approach condition of 0.3 Mach at 30 feet is therefore chosen for this thesis.

It is assumed that the aircraft's equations of motion are linear for a small change in velocity; therefore, most of the aerodynamic coefficients for the 0.2 Mach flight condition are applicable to the 0.3 Mach flight condition. The lift coefficient C_L changes with the inverse of the dynamic pressure $\bar{q}$, and the drag coefficient C_D is decreased by $C_{D_{\delta f}}$ times the maximum flaperon deflection, because the new trim condition for the flaperons is at zero degrees.

The trim angle of attack is calculated from the lift and moment equations:

$$C_L = C_{L_0} + C_{L_\alpha}\alpha_T + C_{L_{\delta e}}\delta e_T \qquad \text{(C-1)}$$

$$C_m = C_{m_0} + C_{m_\alpha}\alpha_T + C_{m_{\delta e}}\delta e_T \qquad \text{(C-2)}$$

These equations are solved simultaneously for α_T yielding

$$\alpha_T = \frac{C_{L_{\delta e}} C_{m_0} + C_{m_{\delta e}} (C_L - C_{L_0})}{C_{m_{\delta e}} C_{L_\alpha} - C_{L_{\delta e}} C_{m_\alpha}} \qquad \text{(C-3)}$$

The lift and moment coefficients at the zero lift line (C_{L_0} and C_{m_0}) are not given in the either Reference 1 or 4. These values are calculated for the 0.2 Mach flight condition by solving Equations (C-1) and (C-2) with the known angle of attack and trim elevator deflection. Although C_{L_0} and C_{m_0} do not change much for a small change in velocity, it is assumed that these values change by the same ratio as the change in C_L. The assumption gives a "worst case" trim angle of attack for the new flight condition.

The primed dimensional derivatives are calculated using the computer program CAT (Conversion And Transformation) which implements the equations of Appendix B (4:276-294).

Table C-14

Aerodynamic Coefficients in the Stability Axis

for 0.3 Mach at 30 Feet

$\bar{q}$ (dynamic pressure) = 133.163 lbs/ft^2

V_T (trim velocity) = 334.9 ft/sec

α_T (trim angle of attack) = 0.14484 radians

C_L	= 0.526120	C_D	= 0.167204
$C_{L_u}(\frac{1}{ft/sec})$	= -0.000178	$C_{D_u}(\frac{1}{ft/sec})$	= 0.000063
$C_{L_\alpha}(\frac{1}{deg})$	= 0.053031	$C_{D_\alpha}(\frac{1}{deg})$	= 0.027636
$C_{L_{\dot{\alpha}}}(\frac{1}{radian})$	= -0.775892	---	
$C_{L_q}(\frac{1}{radian})$	= 1.428590	---	
$C_{L_{\delta e_t}}(\frac{1}{deg})$	= 0.010306	$C_{D_{\delta e_t}}(\frac{1}{deg})$	= 0.002519
$C_{L_{\delta f_t}}(\frac{1}{deg})$	= 0.004004	$C_{D_{\delta f_t}}(\frac{1}{deg})$	= 0.002519
C_m	= 0.0	$C_{y_\beta}(\frac{1}{deg})$	= -0.020613
$C_{m_u}(\frac{1}{ft/sec})$	= 0.000032	$C_{y_p}(\frac{1}{radian})$	= 0.214209
$C_{m_\alpha}(\frac{1}{deg})$	= 0.001755	$C_{y_r}(\frac{1}{radian})$	= 0.640146
$C_{m_{\dot{\alpha}}}(\frac{1}{radian})$	= 0.017115	$C_{y_{\delta DF}}(\frac{1}{deg})$	= 0.001493
$C_{m_q}(\frac{1}{radian})$	= -6.716320	$C_{y_{\delta DT}}(\frac{1}{deg})$	= 0.003154

Table C-14 (continued)

$C_{m_{\delta e_t}}(\frac{1}{deg}) = -0.010622$	$C_{Y_{\delta r}}(\frac{1}{deg}) = 0.003103$
$C_{m_{\delta f_t}}(\frac{1}{deg}) = 0.001000$	---
$C_{m_{\delta c}}(\frac{1}{deg}) = -.0195035$	$C_{Y_{\delta c}}(\frac{1}{deg}) = 0.000893$
$C_{\ell_\beta}(\frac{1}{deg}) = -0.003015$	$C_{n_\beta}(\frac{1}{deg}) = 0.002824$
$C_{\ell_p}(\frac{1}{radian}) = -0.201582$	$C_{n_p}(\frac{1}{radian}) = -0.065499$
$C_{\ell_r}(\frac{1}{radian}) = 0.224680$	$C_{n_r}(\frac{1}{radian}) = -0.509547$
$C_{\ell_{\delta DF}}(\frac{1}{deg}) = -0.001373$	$C_{n_{\delta DF}}(\frac{1}{deg}) = -0.000566$
$C_{\ell_{\delta DT}}(\frac{1}{deg}) = -0.001658$	$C_{n_{\delta DT}}(\frac{1}{deg}) = -0.000769$
$C_{\ell_{\delta r}}(\frac{1}{deg}) = 0.000033$	$C_{n_{\delta r}}(\frac{1}{deg}) = -0.001716$
$C_{\ell_{\delta c}}(\frac{1}{deg}) = 0.000074$	$C_{n_{\delta c}}(\frac{1}{deg}) = 0.000665$

Table C-15

Primed Dimensional Derivatives in the Body Axis

for 0.3 Mach at 30 Feet

$X'_\theta = -31.8627$	$Z'_\theta = -0.013880$	$M'_\theta = -0.000033$
$X'_u = -0.016994$	$Z'_u = -0.000326$	$M'_u = -0.000364$
$X'_\alpha = -36.9184$	$Z'_\alpha = -0.629959$	$M'_\alpha = 0.833706$
$X'_q = -48.3011$	$Z'_q = 0.995634$	$M'_q = -0.950374$
$X'_{\delta e_t} = -3.52376$	$Z'_{\delta e_t} = -0.110589$	$M'_{\delta e_t} = -5.10864$
$X'_{\delta f_t} = -8.00387$	$Z'_{\delta f_t} = -0.090118$	$M'_{\delta f_t} = 0.48071$
$X'_{\delta T} = 22.291$	---	$M'_{\delta c} = -0.16371$
$Y'_\phi = 0.095141$	---	---
$Y'_\beta = -0.215833$	$L'_\beta = -23.1367$	$N'_\beta = 2.53712$
$Y'_p = 0.141584$	$L'_p = -1.23522$	$N'_p = -0.027433$
$Y'_r = -0.994562$	$L'_r = 1.40799$	$N'_r = -0.414331$
$Y'_{\delta DF} = 0.015633$	$L'_{\delta DF} = -8.76403$	$N'_{\delta DF} = -0.890051$
$Y'_{\delta DT} = 0.033025$	$L'_{\delta DT} = -10.5014$	$N'_{\delta DT} = -1.16925$
$Y'_{\delta r} = 0.032491$	$L'_{\delta r} = 1.86570$	$N'_{\delta r} = -1.88884$
$Y'_{\delta c} = 0.009350$	$L'_{\delta c} = -0.13479$	$N'_{\delta c} = 0.748726$

Table C-16

Healthy Aircraft Data File for use with MULTI Option #9

for 0.3 Mach at 30 Feet

```
1
14 6 6
0 0 0 1 0 0 0 0 0 0 0 0 0 0
-32.8627 -.01699 -36.9184 -48.3011 0 0 0 0 -3.5238 -8.0039 0 0 0 22.291
-.01388 -.000326 -.62996 .995634 0 0 0 0 -.110589 -.090118 0 0 0 0
-.0000333 -.000364 .83371 -.950374 0 0 0 0 -5.10864 .480707 0 0 -.1637 0
0 0 0 0 0 0 1 0 0 0 0 0 0 0
0 0 0 0 .095141 -.215833 .145841 -.994562 0 0 .023889 .032491 .0093504 0
0 0 0 0 0 -23.1367 -1.23522 1.40799 0 0 -11.38938 1.86570 -.13479 0
0 0 0 0 0 2.537 -.027433 -.41433 0 0 -1.182364 -1.8888 .748726 0
0 0 0 0 0 0 0 0 -20 0 0 0 0 0
0 0 0 0 0 0 0 0 0 -20 0 0 0 0
0 0 0 0 0 0 0 0 0 0 -20 0 0 0
0 0 0 0 0 0 0 0 0 0 0 -20 0 0
0 0 0 0 0 0 0 0 0 0 0 0 -20 0
0 0 0 0 0 0 0 0 0 0 0 0 0 -1
0 0 0 0 0 0
0 0 0 0 0 0
0 0 0 0 0 0
0 0 0 0 0 0
0 0 0 0 0 0
0 0 0 0 0 0
0 0 0 0 0 0
20 0 0 0 0 0
0 20 0 0 0 0
0 0 20 0 0 0
0 0 0 20 0 0
0 0 0 0 20 0
0 0 0 0 0 1
0 1 0 0 0 0 0 0 0 0 0 0 0 0
-.000014 .0032362 6.91315 -.3663 0 0 0 0 -1.06302 1.4553 0 0 -.0709 0
0 0 0 1 0 0 0 0 0 0 0 0 0 0
0 0 0 0 0 -1.1456 -.001706 -.12294 0 0 -.2638 -.48038 .42162 0
0 0 0 0 0 0 1 0 0 0 0 0 0 0
0 0 0 0 0 0 0 1 0 0 0 0 0 0
N
Y
1 1 1 1 1 1
-72
72
1
-72
72
1
-72
72
1
-72
72
1
-72
72
1
-1000
1000
1
N
```

Table C-17

Failed Aircraft Data File for use with MULTI Option #9

for 0.3 Mach at 30 Feet

```
1
14 6 6
0 0 0 1 0 0 0 0 0 0 0 0 0 0
-32.8627 -.01699 -36.9184 -48.301 0 0 0 0 -1.7619 -4.0019 -4.0019 0 0 22.291
-.01388 -.000326 -.62996 .99563 0 0 0 0 -.05529 -.045059 -.045059 0 0 0
-.0000333 -.000364 .83371 -.950374 0 0 0 0 -2.5543 .24035 .24035 0 -.16371 0
0 0 0 0 0 0 1 0 0 0 0 0 0 0
0 0 0 0 .09514 -.2158 .14584 -.995 -.004128 .007816 -.007816 .03249 .00935 0
0 0 0 0 0 -23.1367 -1.23522 1.40799 1.3127 -4.382 4.382 1.866 -.13479 0
0 0 0 0 0 2.537 -.027433 -.41433 .14616 -.44503 .44503 -1.8888 .748726 0
0 0 0 0 0 0 0 0 -20 0 0 0 0 0
0 0 0 0 0 0 0 0 0 -20 0 0 0 0
0 0 0 0 0 0 0 0 0 0 -20 0 0 0
0 0 0 0 0 0 0 0 0 0 0 -20 0 0
0 0 0 0 0 0 0 0 0 0 0 0 -20 0
0 0 0 0 0 0 0 0 0 0 0 0 0 -1
0 0 0 0 0 0
0 0 0 0 0 0
0 0 0 0 0 0
0 0 0 0 0 0
0 0 0 0 0 0
0 0 0 0 0 0
0 0 0 0 0 0
0 0 0 0 0 0
20 0 0 0 0 0
0 20 0 0 0 0
0 0 20 0 0 0
0 0 0 20 0 0
0 0 0 0 20 0
0 0 0 0 0 1
0 1 0 0 0 0 0 0 0 0 0 0 0 0
-.000014 .0032362 6.91315 -.3663 0 0 0 0 -.53151 .57277 .57277 0 -.070922 0
0 0 0 1 0 0 0 0 0 0 0 0 0 0
0 0 0 0 0 -1.1456 -.001706 -.12294 .020385 -.111503 .111503 -.48038 .42162 0
0 0 0 0 0 0 1 0 0 0 0 0 0 0
0 0 0 0 0 0 0 1 0 0 0 0 0 0
N
Y
1 1 1 1 1 1
-72
72
1
-72
72
1
-72
72
1
-72
72
1
-72
72
1
-1000
1000
1
N
```

AD-A151 908 MULTIVARIABLE CONTROL LAW DESIGN FOR THE AFTI/F-16 WITH A FAILED CONTROL SURFACE(U) AIR FORCE INST OF TECH WRIGHT-PATTERSON AFB OH SCHOOL OF ENGI.. R A ESLINGER

UNCLASSIFIED DEC 84 AFIT/GE/ENG/84D-28 F/G 1/2 NL

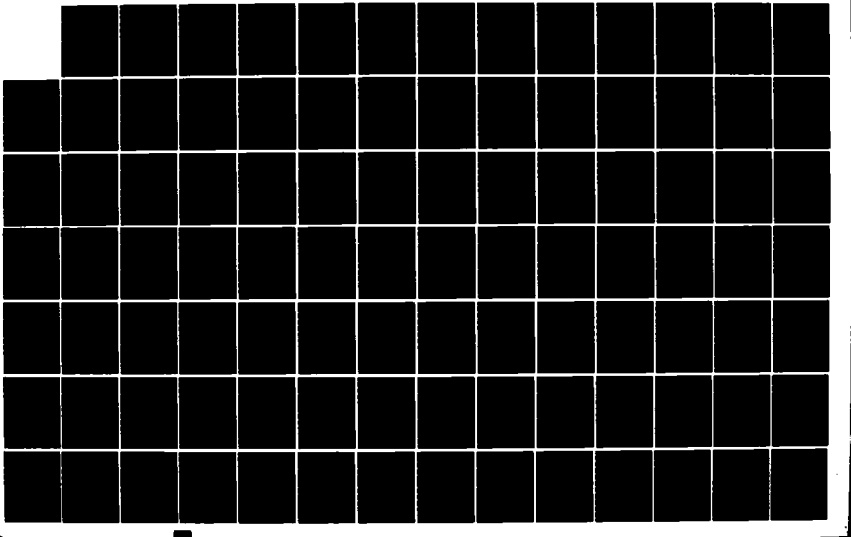

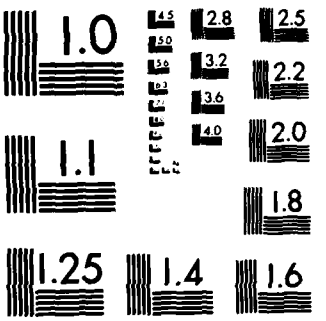

Appendix D: Continued Design Responses

Chapter II presents the simulation response plots for the transonic flight condition (0.9 Mach at 20,000 feet). This appendix gives the response plots for the other three flight conditions considered in this thesis, which are subsonic flight (0.6 Mach at 30,000 feet), supersonic flight (1.6 Mach at 30,000 feet), and landing approach (0.3 Mach at 30 feet). The order of presentation is similar to that of Chapter II.

Subsonic Flight (0.6 Mach at 30,000 Feet)

The subsonic flight condition is chosen to demonstrate maneuverabiltiy at a cruising speed for the aircraft. The dynamic pressure is relatively low because of the high altitude; therefore, the control surfaces are less effective at this flight condition than at the transonic flight condition.

G-Command Maneuver. Tables D-1 and D-2 list the design parameters for the g-command maneuver for the healthy and failed right elevator models. As shown in the tables, the same design parameters, $\bar{\alpha}$, $\underline{\Sigma}$, and ε, are used for both aircraft models.

Figures D-1 through D-7 show the simulation responses for the g-command maneuver. For this maneuver the healthy aircraft longitudinal responses change very little when the right horizontal tail fails. Also, the healthy aircraft

lateral responses are zero and are very small with the failed model. For these reasons Figures D-1 through D-3 give simulation responses for both the healthy and failed aircraft models.

The maximum normal acceleration command of 3.1g is limited by the flaperon deflection. For the failure case, the left elevator deflects approximately twice the amount required when both tail halves are working. The flaperon deflection is slightly asymmetric for the failure case in order to compensate for the rolling moment created by the left elevator deflection. The rudder and canard compensate for the adverse yaw caused by a difference in drag between the left and right halves of the aircraft.

Table D-1

G-Command: Healthy Model, 0.6 Mach at 30,000 Feet

Sampling Time: T = 0.02 second

$\bar{\alpha} = 1.2$

$\epsilon = 1.0$

$\Sigma = \text{diag}\{ 2.0, 0.04, 1.0, 1.0, 1.0, 1.0\}$

$$\underline{K}_0 = \begin{bmatrix} 0.0 & -0.3565E-04 & -0.8330E-01 & -0.5402E-02 & 0.5400E-04 & 0.5158E-02 \\ -0.3473E-14 & 0.9869E-03 & -0.5527E-01 & 0.3198E-02 & -0.3198E-04 & -0.3054E-02 \\ 0.0 & 0.0 & 0.0 & 0.1806E-01 & -0.9219E-02 & -0.3528E-01 \\ 0.0 & 0.0 & 0.0 & 0.8364E-01 & 0.2127E-02 & -0.1756E+00 \\ 0.0 & 0.0 & 0.0 & 0.1166E+00 & -0.1166E-02 & -0.1114E+00 \\ 0.1895E+01 & 0.4139E-02 & 0.2806E+00 & 0.4517E-01 & -0.4516E-03 & -0.4313E-01 \end{bmatrix}$$

$$\underline{K}_1 = \begin{bmatrix} 0.0 & -0.4278E-04 & -0.9996E-01 & -0.6482E-02 & 0.6480E-04 & 0.6189E-02 \\ -0.4167E-14 & 0.1184E-02 & -0.6633E-01 & 0.3838E-02 & -0.3837E-04 & -0.3665E-02 \\ 0.0 & 0.0 & 0.0 & 0.2168E-01 & -0.1106E-01 & -0.4233E-01 \\ 0.0 & 0.0 & 0.0 & 0.1004E+00 & 0.2553E-02 & -0.2108E+00 \\ 0.0 & 0.0 & 0.0 & 0.1400E+00 & -0.1399E-02 & -0.1336E+00 \\ 0.2274E+01 & 0.4966E-02 & 0.3367E+00 & 0.5420E-01 & -0.5419E-03 & -0.5175E-01 \end{bmatrix}$$

Input Ramp Time: 0.4 second

Command Vector:

$u = 0.0$

$A_{n_p} = 3.1$ g (step)

$q = 0.1672$ radian/second (step)

$A_{y_p} = 0.0$

$p = 0.0$

$r = 0.0$

Table D-2

G-Command: Failed Model, 0.6 Mach at 30,000 Feet

Sampling Time: T = 0.02 second

$\bar{\alpha} = 1.2$

$\epsilon = 1.0$

$\Sigma = \text{diag}\{ 2.0, 0.04, 1.0, 1.0, 1.0, 1.0\}$

$$\underline{K}_0 = \begin{bmatrix} 0.4482E-14 & -0.7129E-04 & -0.1665E+00 & -0.1081E-01 & 0.1129E-03 & 0.1033E-01 \\ -0.2244E-14 & 0.9786E-03 & -0.7458E-01 & 0.2420E-01 & -0.1137E-01 & -0.4531E-01 \\ -0.3025E-14 & 0.9952E-03 & -0.3599E-01 & -0.1779E-01 & 0.1131E-01 & 0.3920E-01 \\ -0.7669E-16 & -0.5852E-05 & -0.1367E-01 & 0.8571E-01 & 0.6232E-03 & -0.1806E+00 \\ -0.4928E-15 & -0.2051E-06 & -0.4791E-03 & 0.1167E+00 & -0.1218E-02 & -0.1115E+00 \\ 0.1895E+01 & 0.4138E-02 & 0.2804E+00 & 0.4520E-01 & -0.4718E-03 & -0.4319E-01 \end{bmatrix}$$

$$\underline{K}_1 = \begin{bmatrix} 0.5379E-14 & -0.8554E-04 & -0.1999E+00 & -0.1297E-01 & 0.1354E-03 & 0.1240E-01 \\ -0.2693E-14 & 0.1174E-02 & -0.8950E-01 & 0.2903E-01 & -0.1365E-01 & -0.5437E-01 \\ -0.3630E-14 & 0.1194E-02 & -0.4319E-01 & -0.2135E-01 & 0.1357E-01 & 0.4703E-01 \\ -0.9202E-16 & -0.7022E-05 & -0.1641E-01 & 0.1029E+00 & 0.7479E-03 & -0.2167E+00 \\ -0.5913E-15 & -0.2461E-06 & -0.5749E-03 & 0.1400E+00 & -0.1462E-02 & -0.1338E+00 \\ 0.2274E+01 & 0.4966E-02 & 0.3365E+00 & 0.5424E-01 & -0.5662E-03 & -0.5183E-01 \end{bmatrix}$$

Input Ramp Time: 0.4 second

Command Vector:

$u = 0.0$

$A_{n_p} = 3.1$ g (step)

$q = 0.1672$ radian/second (step)

$A_{y_p} = 0.0$

$p = 0.0$

$r = 0.0$

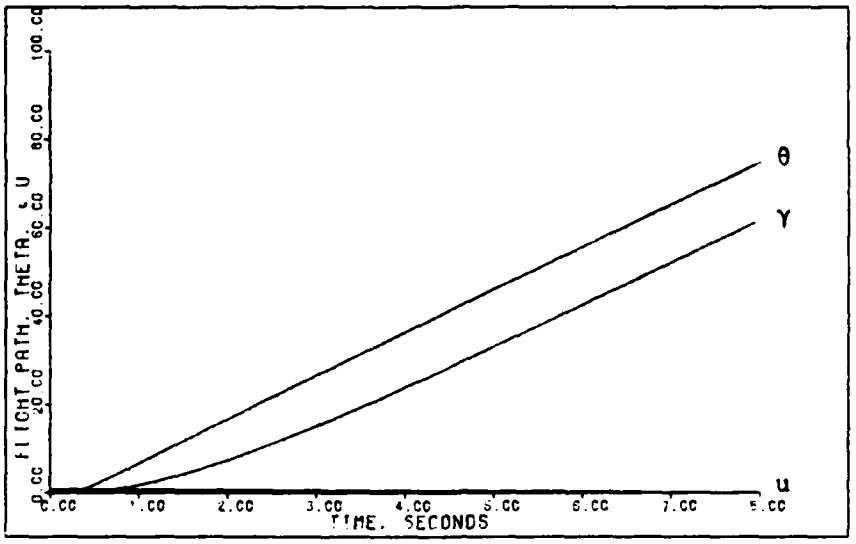

Figure D-1: 0.6M Healthy/Failed G-Command -- Flight Path Angle, Pitch Angle, and Forward Velocity

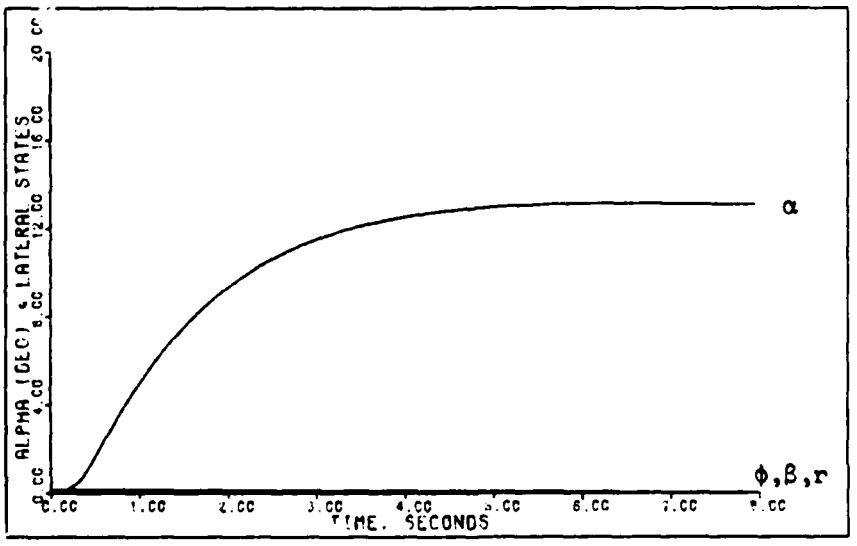

Figure D-2: 0.6M Healthy/Failed G-Command -- Angle of Attack, Roll Angle, Sideslip Angle, and Yaw Rate

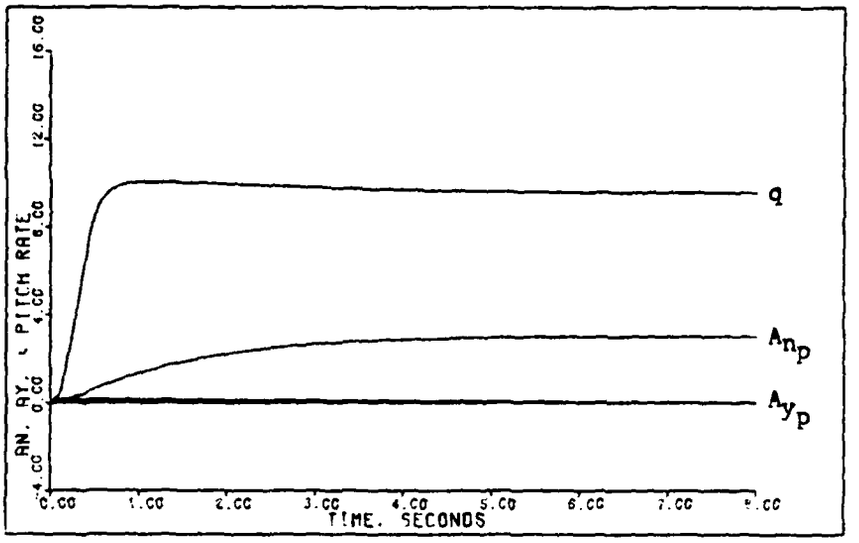

Figure D-3: 0.6M Healthy/Failed G-Command -- Pitch Rate, Normal Acceleration, and Lateral Acceleration

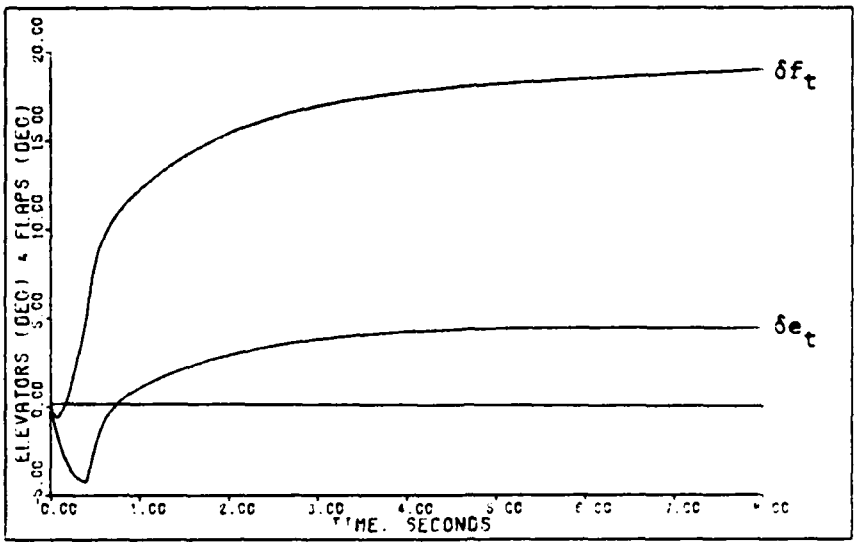

Figure D-4: 0.6M Healthy G-Command -- Elevator and Flap Deflections

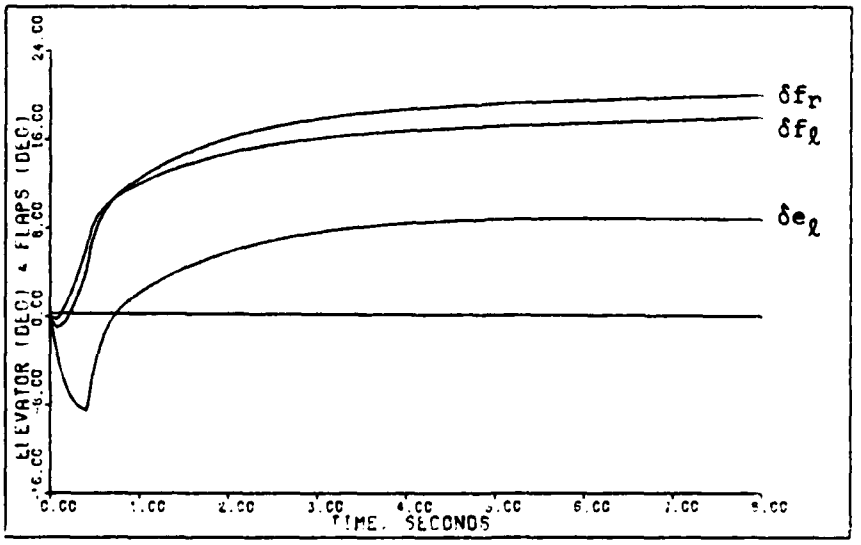

Figure D-5: 0.6M Failed G-Command -- Left Elevator and Flaperon Deflections

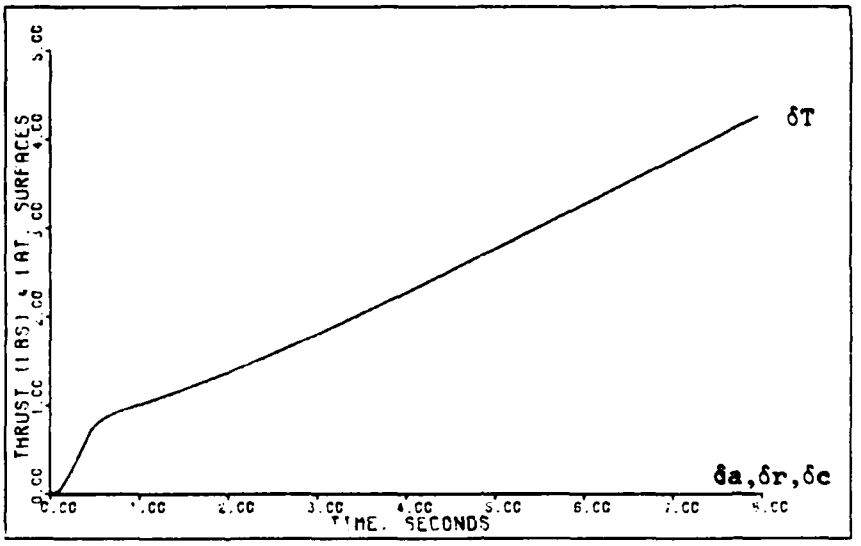

Figure D-6: 0.6M Healthy G-Command -- Aileron, Rudder, and Canard Deflections and Thrust

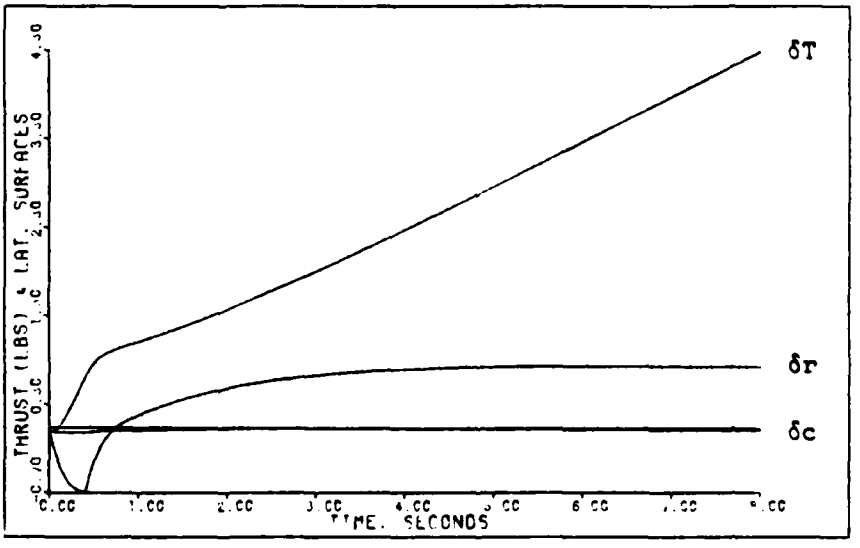

Figure D-7: 0.6M Failed G-Command -- Rudder and Canard Deflections and Thrust

Pitch Pointing Maneuver. Tables D-3 and D-4 give the design parameters for the pitch pointing maneuver. As with the g-command maneuver the design parameters $\bar{\alpha}$, $\underline{\Sigma}$, and ε are the same for the healthy and failed models.

The simulation responses for the pitch pointing maneuver are given in Figures D-8 through D-14. The maximum pointing angle commanded is limited by the flaperon deflection. For the same reasons discussed in the g-command maneuver section, Figures D-8 through D-10 give simulation responses for both the healthy and failed aircraft models. For the failure case the left elevator must deflect approximately twice the angle of the healthy elevator deflection. Also, for the failure model, the flaperons deflect asymmetrically to counter the roll induced by the failed right horizontal tail, and the rudder and canard deflect to compensate for adverse yaw.

Table D-3

Pitch Pointing: Healthy Model, 0.6 Mach at 30,000 Feet

Sampling Time: T = 0.02 second

$\bar{\alpha} = 2.0$

$\epsilon = 1.0$

$\underline{\Sigma} = \text{diag}\{ 2.0, 1.5, 1.0, 1.0, 1.0, 1.0 \}$

$$\underline{K}_0 = \begin{bmatrix} 0.0 & -0.1337E-02 & -0.8330E-01 & -0.5402E-02 & 0.5400E-04 & 0.5158E-02 \\ -0.3473E-14 & 0.3701E-01 & -0.5527E-01 & 0.3198E-02 & -0.3198E-04 & -0.3054E-02 \\ 0.0 & 0.0 & 0.0 & 0.1806E-01 & -0.9219E-02 & -0.3528E-01 \\ 0.0 & 0.0 & 0.0 & 0.8364E-01 & 0.2127E-02 & -0.1756E+00 \\ 0.0 & 0.0 & 0.0 & 0.1166E+00 & -0.1166E-02 & -0.1114E+00 \\ 0.1895E+01 & 0.1552E+00 & 0.2806E+00 & 0.4517E-01 & -0.4516E-03 & -0.4313E-01 \end{bmatrix}$$

$$\underline{K}_1 = \begin{bmatrix} 0.0 & -0.2674E-02 & -0.1666E+00 & -0.1080E-01 & 0.1080E-03 & 0.1032E-01 \\ -0.6946E-14 & 0.7402E-01 & -0.1105E+00 & 0.6397E-02 & -0.6395E-04 & -0.6108E-02 \\ 0.0 & 0.0 & 0.0 & 0.3613E-01 & -0.1844E-01 & -0.7055E-01 \\ 0.0 & 0.0 & 0.0 & 0.1673E+00 & 0.4254E-02 & -0.3513E+00 \\ 0.0 & 0.0 & 0.0 & 0.2333E+00 & -0.2332E-02 & -0.2227E+00 \\ 0.3790E+01 & 0.3104E+00 & 0.5612E+00 & 0.9034E-01 & -0.9031E-03 & -0.8625E-01 \end{bmatrix}$$

Input Ramp Time: 0.2 second

Command Vector:

$u = 0.0$

$A_{n_p} = 0.0$

$q = 0.05934$ radian/second (1 second pulse)

$A_{y_p} = 0.0$

$p = 0.0$

$r = 0.0$

Table D-4

Pitch Pointing: Failed Model, 0.6 Mach at 30,000 Feet

Sampling Time: T = 0.02 second

$\bar{\alpha} = 2.0$

$\epsilon = 1.0$

$\underline{\Sigma} = \text{diag}\{ 2.0, 1.5, 1.0, 1.0, 1.0, 1.0 \}$

$$\underline{K}_0 = \begin{bmatrix} 0.4482E-14 & -0.2673E-02 & -0.1665E+00 & -0.1081E-01 & 0.1129E-03 & 0.1033E-01 \\ -0.2244E-14 & 0.3670E-01 & -0.7458E-01 & 0.2420E-01 & -0.1137E-01 & -0.4531E-01 \\ -0.3025E-14 & 0.3732E-01 & -0.3599E-01 & -0.1779E-01 & 0.1131E-01 & 0.3920E-01 \\ -0.7669E-16 & -0.2194E-03 & -0.1367E-01 & 0.8571E-01 & 0.6232E-03 & -0.1806E+00 \\ -0.4928E-15 & -0.7690E-05 & -0.4791E-03 & 0.1167E+00 & -0.1218E-02 & -0.1115E+00 \\ 0.1895E+01 & 0.1552E+00 & 0.2804E+00 & 0.4520E-01 & -0.4718E-03 & -0.4319E-01 \end{bmatrix}$$

$$\underline{K}_1 = \begin{bmatrix} 0.8965E-14 & -0.5346E-02 & -0.3331E+00 & -0.2162E-01 & 0.2257E-03 & 0.2066E-01 \\ -0.4488E-14 & 0.7340E-01 & -0.1492E+00 & 0.4839E-01 & -0.2275E-01 & -0.9062E-01 \\ -0.6051E-14 & 0.7464E-01 & -0.7199E-01 & -0.3559E-01 & 0.2262E-01 & 0.7839E-01 \\ -0.1534E-15 & -0.4389E-03 & -0.2734E-01 & 0.1714E+00 & 0.1246E-02 & -0.3612E+00 \\ -0.9855E-15 & -0.1538E-04 & -0.9582E-03 & 0.2334E+00 & -0.2437E-02 & -0.2231E+00 \\ 0.3790E+01 & 0.3104E+00 & 0.5608E+00 & 0.9039E-01 & -0.9436E-03 & -0.8639E-01 \end{bmatrix}$$

Input Ramp Time: 0.2 second

Command Vector:

$u = 0.0$

$A_{n_p} = 0.0$

$q = 0.05934$ radian/second (1 second pulse)

$A_{y_p} = 0.0$

$p = 0.0$

$r = 0.0$

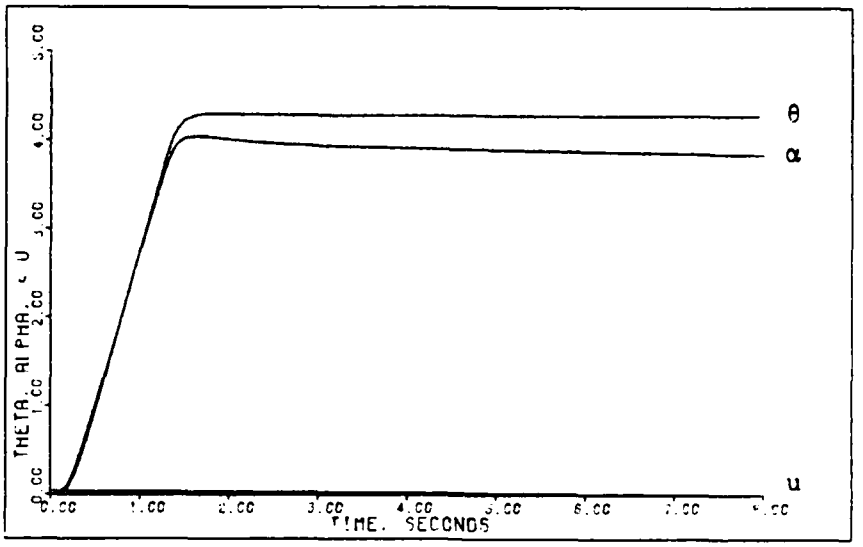

Figure D-8: 0.6M Healthy/Failed Pitch Pointing -- Pitch Angle, Angle of Attack, and Forward Velocity

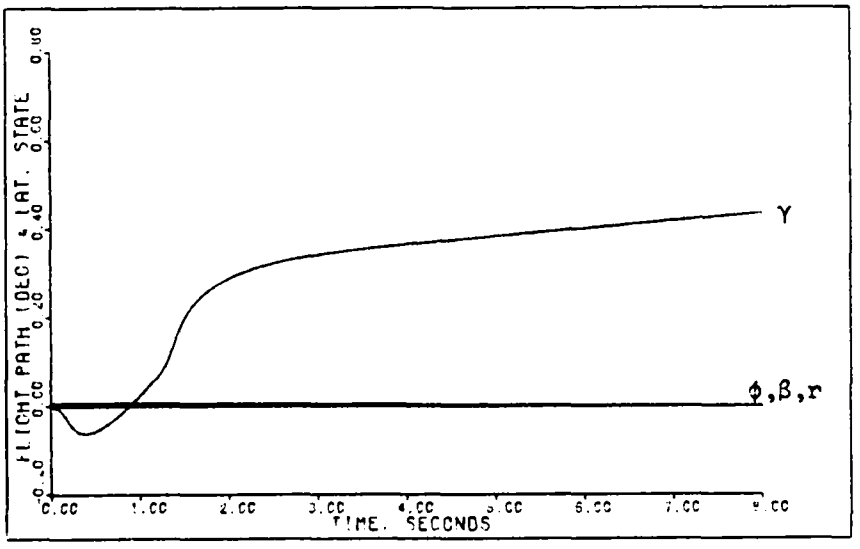

Figure D-9: 0.6M Healthy/Failed Pitch Pointing -- Flight Path Angle, Roll Angle, Sideslip Angle, and Yaw Rate

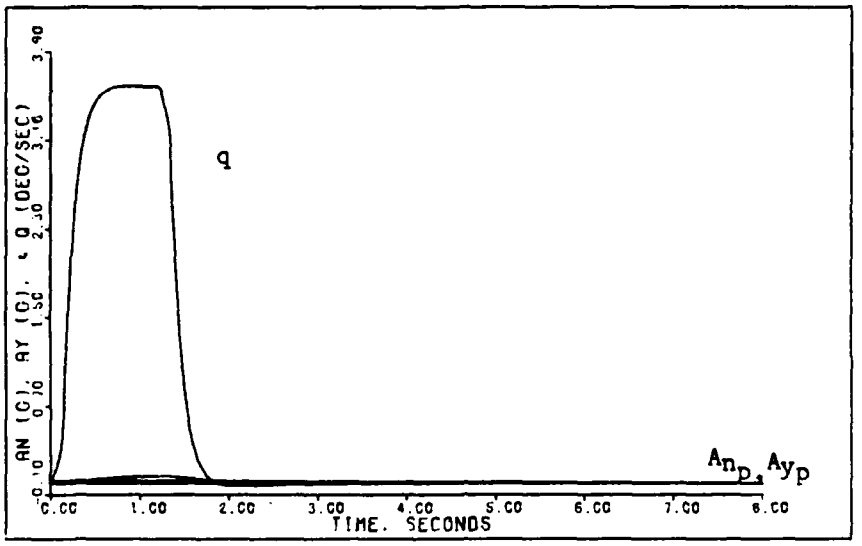

Figure D-10: 0.6M Healthy/Failed Pitch Pointing -- Normal Acceleration and Lateral Acceleration

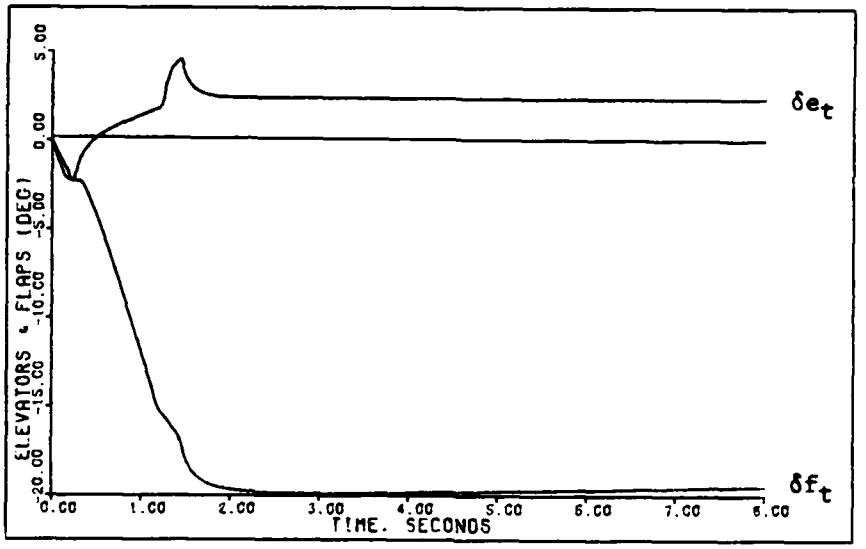

Figure D-11: 0.6M Healthy Pitch Pointing -- Elevator and Flap Deflections

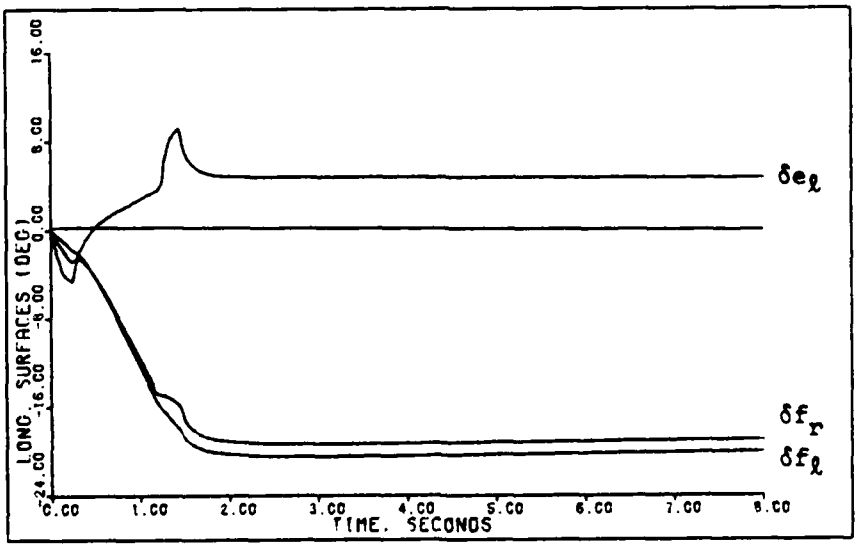

Figure D-12: 0.6M Failed Pitch Pointing -- Left Elevator and Flaperon Deflections

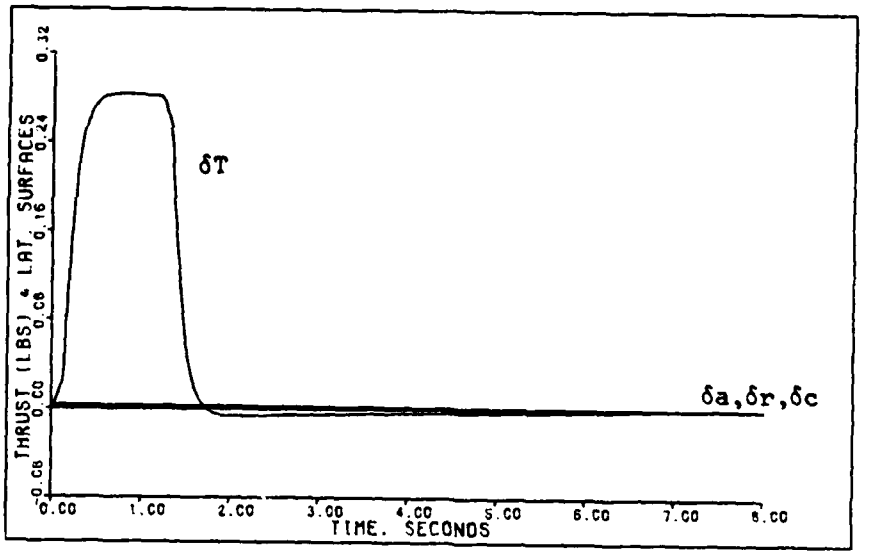

Figure D-13: 0.6M Healthy Pitch Pointing -- Aileron, Rudder, and Canard Deflections and Thrust

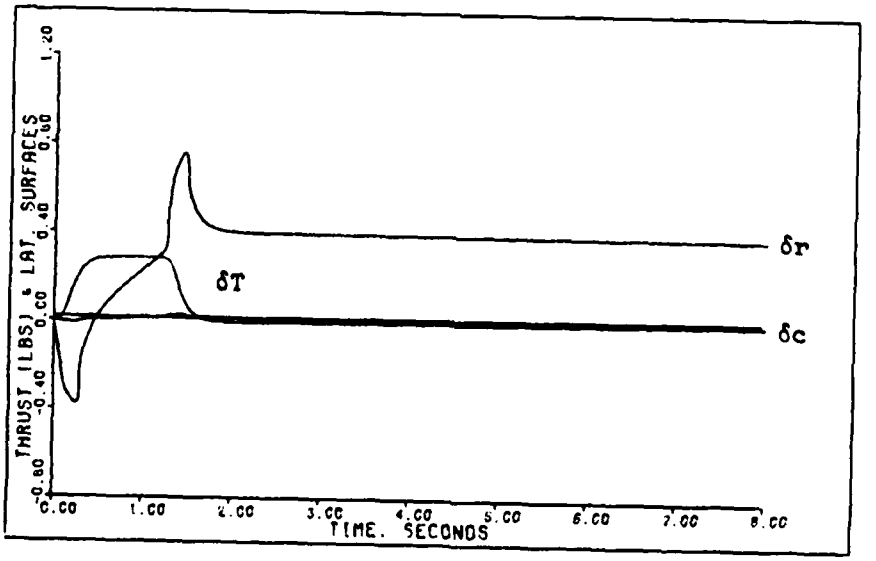

Figure D-14: 0.6M Failed Pitch Pointing -- Rudder and Canard Deflections and Thrust

Longitudinal Translation Maneuver. Tables D-5 and D-6 give the design parameters for the longitudinal translation maneuver. Once again the design parameters $\bar{\alpha}$, $\underline{\Sigma}$, and ϵ are the same for the healthy and failed models.

The simulation responses for the longitudinal translation maneuver are given in Figures D-15 through D-21. As discussed in the g-command maneuver section Figures D-15 through D-17 give simulation responses for both the healthy and failed aircraft models. The maximum longitudinal translation command of 0.5g for one second, which yields a normal velocity of approximately 22.5 feet/second, is limited by the flaperon deflection.

As is usually the case with longitudinal maneuvers, the failure model requires that the left elevator must deflect approximately twice the angle of the healthy elevator deflection. Also, for the failure model, the flaperons deflect asymmetrically to counter the roll induced by the failed right horizontal tail, and the rudder and canard deflect to compensate for adverse yaw.

Table D-5

Longitudinal Translation: Healthy Model,
0.6 Mach at 30,000 Feet

Sampling Time: T = 0.02 second

$\bar{\alpha} = 3.5$

$\epsilon = 1.0$

$\underline{\Sigma} = \text{diag}\{\ 2.0,\ 1.0,\ 0.8,\ 1.0,\ 1.0,\ 1.0\ \}$

$$\underline{K}_0 = \begin{bmatrix} 0.0 & -0.8913E-03 & -0.6664E-01 & -0.5402E-02 & 0.5400E-04 & 0.5158E-02 \\ -0.3473E-15 & 0.2467E-01 & -0.4422E-01 & 0.3198E-02 & -0.3198E-04 & -0.3054E-02 \\ 0.0 & 0.0 & 0.0 & 0.1806E-01 & -0.9219E-02 & -0.3528E-01 \\ 0.0 & 0.0 & 0.0 & 0.8364E-01 & 0.2127E-02 & -0.1756E+00 \\ 0.0 & 0.0 & 0.0 & 0.1166E+00 & -0.1166E-02 & -0.1114E+00 \\ 0.1895E+00 & 0.1035E+00 & 0.2245E+00 & 0.4517E-01 & -0.4516E-03 & -0.4313E-01 \end{bmatrix}$$

$$\underline{K}_1 = \begin{bmatrix} 0.0 & -0.3120E-02 & -0.2332E+00 & -0.1891E-01 & 0.1890E-03 & 0.1805E-01 \\ -0.1215E-14 & 0.8635E-01 & -0.1548E+00 & 0.1119E-01 & -0.1119E-03 & -0.1069E-01 \\ 0.0 & 0.0 & 0.0 & 0.6322E-01 & -0.3226E-01 & -0.1235E+00 \\ 0.0 & 0.0 & 0.0 & 0.2927E+00 & 0.7445E-02 & -0.6148E+00 \\ 0.0 & 0.0 & 0.0 & 0.4082E+00 & -0.4081E-02 & -0.3898E+00 \\ 0.6632E+00 & 0.3621E+00 & 0.7857E+00 & 0.1581E+00 & -0.1580E-02 & -0.1509E+00 \end{bmatrix}$$

Input Ramp Time: 0.2 second

Command Vector:

$u = 0.0$

$A_{n_p} = 0.5$ g (1 second pulse)

$q = 0.0$

$A_{y_p} = 0.0$

$p = 0.0$

$r = 0.0$

Table D-6

Longitudinal Translation: Failed Model,
0.6 Mach at 30,000 Feet

Sampling Time: T = 0.02 second

$\bar{\alpha} = 3.5$

$\epsilon = 1.0$

$\underline{\Sigma} = \text{diag}\{ 2.0, 1.0, 0.8, 1.0, 1.0, 1.0 \}$

$$\underline{K}_0 = \begin{bmatrix} 0.4482E-15 & -0.1782E-02 & -0.1332E+00 & -0.1081E-01 & 0.1129E-03 & 0.1033E-01 \\ -0.2244E-15 & 0.2447E-01 & -0.5967E-01 & 0.2420E-01 & -0.1137E-01 & -0.4531E-01 \\ -0.3025E-15 & 0.2488E-01 & -0.2879E-01 & -0.1779E-01 & 0.1131E-01 & 0.3920E-01 \\ -0.7669E-17 & -0.1463E-03 & -0.1094E-01 & 0.8571E-01 & 0.6232E-03 & -0.1806E+00 \\ -0.4928E-16 & -0.5127E-05 & -0.3833E-03 & 0.1167E+00 & -0.1218E-02 & -0.1115E+00 \\ 0.1895E+00 & 0.1035E+00 & 0.2243E+00 & 0.4520E-01 & -0.4718E-03 & -0.4319E-01 \end{bmatrix}$$

$$\underline{K}_1 = \begin{bmatrix} 0.1569E-14 & -0.6238E-02 & -0.4663E+00 & -0.3784E-01 & 0.3950E-03 & 0.3616E-01 \\ -0.7854E-15 & 0.8563E-01 & -0.2088E+00 & 0.8468E-01 & -0.3981E-01 & -0.1586E+00 \\ -0.1059E-14 & 0.8708E-01 & -0.1008E+00 & -0.6228E-01 & 0.3958E-01 & 0.1372E+00 \\ -0.2684E-16 & -0.5120E-03 & -0.3828E-01 & 0.3000E+00 & 0.2181E-02 & -0.6321E+00 \\ -0.1725E-15 & -0.1794E-04 & -0.1342E-02 & 0.4085E+00 & -0.4264E-02 & -0.3904E+00 \\ 0.6632E+00 & 0.3621E+00 & 0.7851E+00 & 0.1582E+00 & -0.1651E-02 & -0.1512E+00 \end{bmatrix}$$

Input Ramp Time: 0.2 second

Command Vector:

$u = 0.0$

$A_{n_p} = 0.5$ g (1 second pulse)

$q = 0.0$

$A_{y_p} = 0.0$

$p = 0.0$

$r = 0.0$

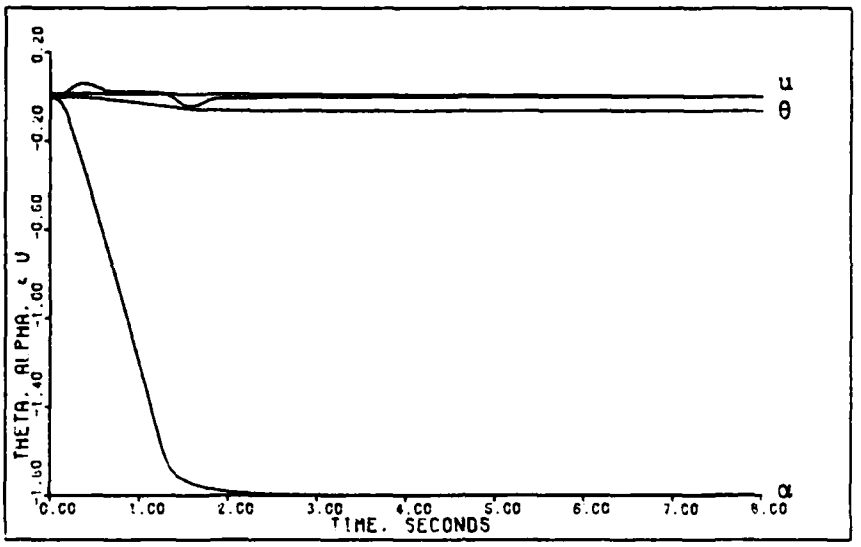

Figure D-15: 0.6M Healthy/Failed Longitudinal Translation -- Pitch Angle, Angle of Attack, and Forward Velocity

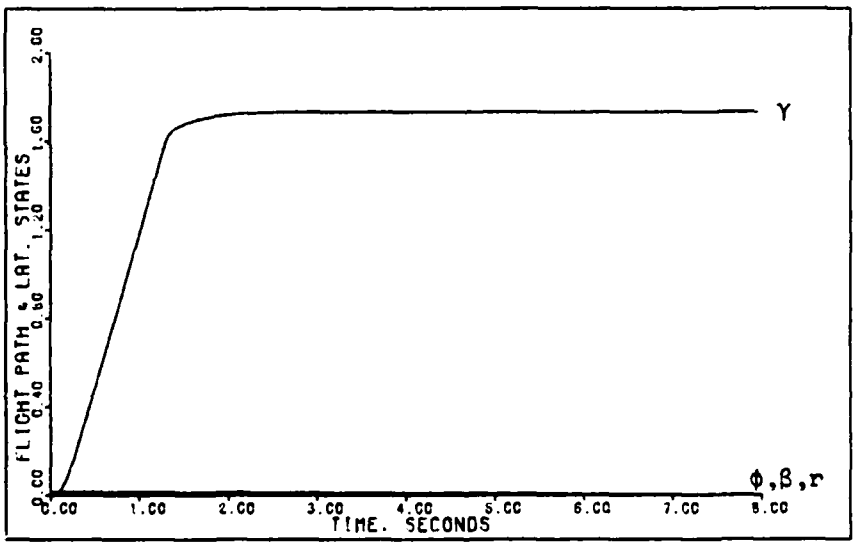

Figure D-16: 0.6M Healthy/Failed Longitudinal Translation -- Flight Path Angle, Roll Angle, Sideslip Angle, and Yaw Rate

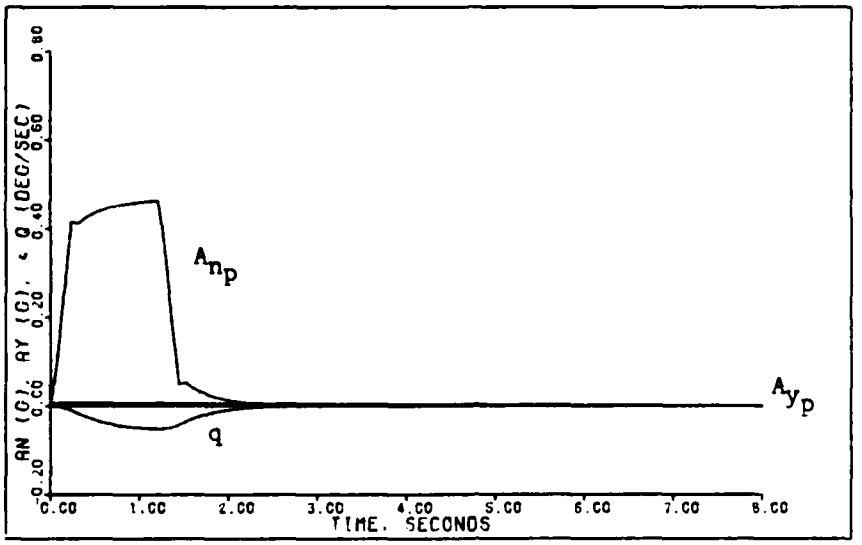

Figure D-17: 0.6M Healthy/Failed Longitudinal Translation -- Pitch Rate, Normal Acceleration, and Lateral Acceleration

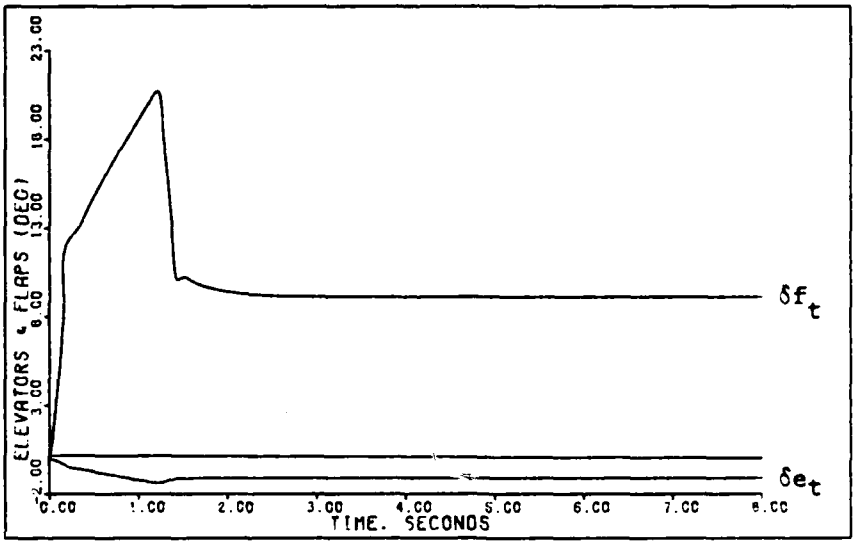

Figure D-18: 0.6M Healthy Longitudinal Translation -- Elevator and Flap Deflections

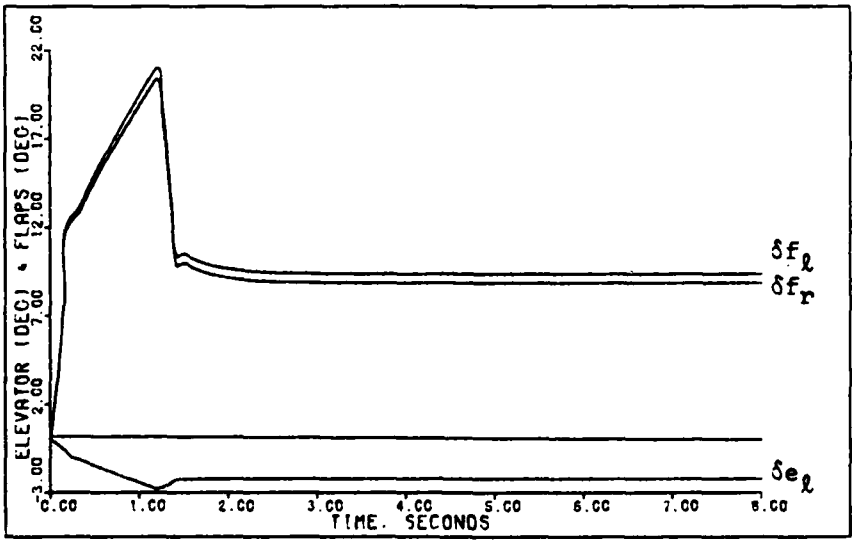

Figure D-19: 0.6M Failed Longitudinal Translation -- Left Elevator and Flaperon Deflections

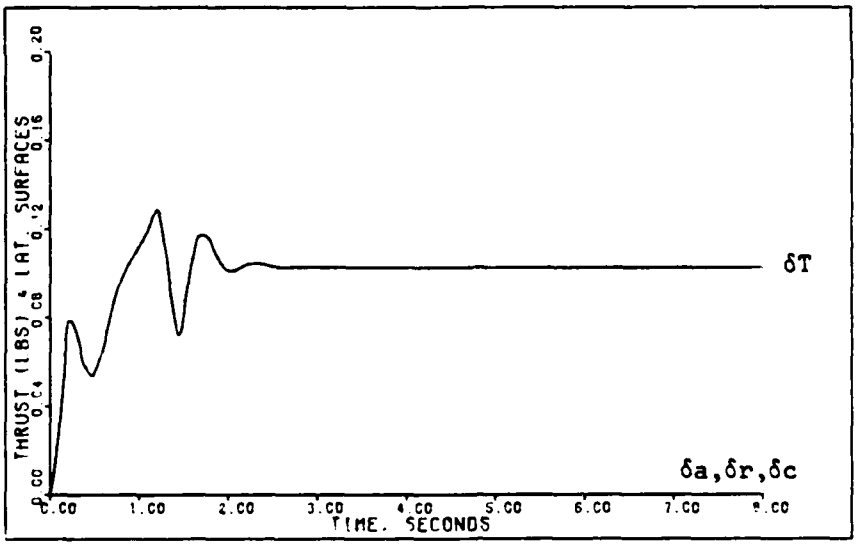

Figure D-20: 0.6M Healthy Longitudinal Translation -- Aileron, Rudder, and Canard Deflections and Thrust

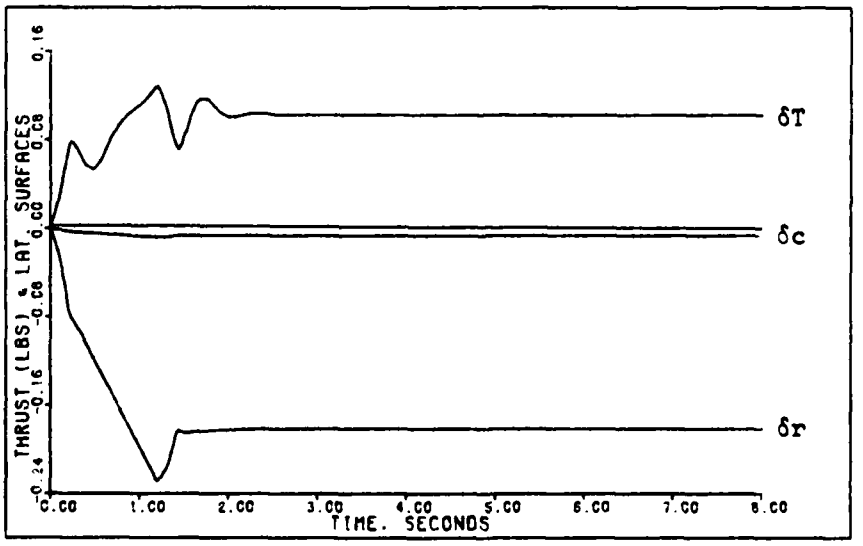

Figure D-21: 0.6M Failed Longitudinal Translation -- Rudder and Canard Deflections and Thrust

Roll About Velocity Vector Maneuver. As discussed in Chapter IV the roll maneuver requires some modification to the healthy and failure models. Tables D-7 and D-8, give the design parameters $\bar{\alpha}$, Σ, and ϵ for the roll maneuver. The parameters are the same for the healthy and failed models.

The simulation responses for the roll maneuver are given in Figures D-22 through D-28. For this maneuver the longitudinal responses are very small for both the healthy and failure models. Also, the healthy aircraft lateral responses change very little when the right horizontal tail fails. For these reasons Figures D-22 through D-24 give simulation responses for both the healthy and failed aircraft models.

The roll rate commanded is limited to 200 degrees per second for three seconds in order to avoid generating too large a sideslip angle.

The aileron deflection for the healthy aircraft is less than the flaperon deflections for the failure case because the aileron deflection includes a contribution from the horizontal tail. When the right horizontal tail fails the flaperons must deflect more to achieve the commanded roll rate. The rudder and canard deflections are unaffected by the failure of the right horizontal tail.

Table D-7

Roll About Velocity Vector: Healthy Model,
0.6 Mach at 30,000 Feet

Sampling Time: T = 0.02 second

$\bar{\alpha} = 2.0$

$\epsilon = 1.0$

$\underline{\Sigma} = \text{diag}\{\ 2.0,\ 1.0,\ 0.8,\ 0.25,\ 0.18,\ 0.3\ \}$

$$\underline{K}_0 = \begin{bmatrix} 0.0 & -0.8913E-03 & -0.6664E-01 & -0.1350E-02 & 0.9721E-05 & 0.1547E-02 \\ -0.3473E-14 & 0.2467E-01 & -0.4422E-01 & 0.7996E-03 & -0.5756E-05 & -0.9161E-03 \\ 0.0 & 0.0 & 0.0 & 0.4516E-02 & -0.1659E-02 & -0.1058E-01 \\ 0.0 & 0.0 & 0.0 & 0.2091E-01 & 0.3829E-03 & -0.5269E-01 \\ 0.0 & 0.0 & 0.0 & 0.2916E-01 & -0.2099E-03 & -0.3341E-01 \\ 0.1895E+01 & 0.1035E+00 & 0.2245E+00 & 0.1129E-01 & -0.8128E-04 & -0.1294E-01 \end{bmatrix}$$

$$\underline{K}_1 = \begin{bmatrix} 0.0 & -0.1783E-02 & -0.1333E+00 & -0.2701E-02 & 0.1944E-04 & 0.3095E-02 \\ -0.6946E-14 & 0.4935E-01 & -0.8844E-01 & 0.1599E-02 & -0.1151E-04 & -0.1832E-02 \\ 0.0 & 0.0 & 0.0 & 0.9031E-02 & -0.3319E-02 & -0.2117E-01 \\ 0.0 & 0.0 & 0.0 & 0.4182E-01 & 0.7658E-03 & -0.1054E+00 \\ 0.0 & 0.0 & 0.0 & 0.5831E-01 & -0.4198E-03 & -0.6681E-01 \\ 0.3790E+01 & 0.2069E+00 & 0.4489E+00 & 0.2258E-01 & -0.1626E-03 & -0.2588E-01 \end{bmatrix}$$

Input Ramp Time: 0.3 second

Command Vector:

$u = 0.0$

$A_{n_p} = 0.0$

$q = 0.0$

$A_{y_p} = 0.0$

$p = 3.491$ radians/second (3 second pulse)

$r\text{-}\alpha_T = 0.0$

Table D-8

Roll About Velocity Vector: Failed Model,
0.6 Mach at 30,000 Feet

Sampling Time: T = 0.02 second

$\bar{\alpha} = 2.0$

$\epsilon = 1.0$

$\Sigma = \text{diag}\{ 2.0, 1.0, 0.8, 0.25, 0.18, 0.3 \}$

$$\underline{K}_0 = \begin{bmatrix} 0.4482E-14 & -0.1782E-02 & -0.1332E+00 & -0.2703E-02 & 0.2031E-04 & 0.3099E-02 \\ -0.2244E-14 & 0.2447E-01 & -0.5967E-01 & 0.6049E-02 & -0.2047E-02 & -0.1359E-01 \\ -0.3025E-14 & 0.2488E-01 & -0.2879E-01 & -0.4449E-02 & 0.2035E-02 & 0.1176E-01 \\ -0.7669E-16 & -0.1463E-03 & -0.1094E-01 & 0.2143E-01 & 0.1122E-03 & -0.5418E-01 \\ -0.4928E-15 & -0.5127E-05 & -0.3833E-03 & 0.2918E-01 & -0.2193E-03 & -0.3346E-01 \\ 0.1895E+01 & 0.1035E+00 & 0.2243E+00 & 0.1130E-01 & -0.8493E-04 & -0.1296E-01 \end{bmatrix}$$

$$\underline{K}_1 = \begin{bmatrix} 0.8965E-14 & -0.3564E-02 & -0.2665E+00 & -0.5405E-02 & 0.4063E-04 & 0.6199E-02 \\ -0.4488E-14 & 0.4893E-01 & -0.1193E+00 & 0.1210E-01 & -0.4095E-02 & -0.2719E-01 \\ -0.6051E-14 & 0.4976E-01 & -0.5759E-01 & -0.8897E-02 & 0.4071E-02 & 0.2352E-01 \\ -0.1534E-15 & -0.2926E-03 & -0.2188E-01 & 0.4286E-01 & 0.2244E-03 & -0.1084E+00 \\ -0.9855E-15 & -0.1025E-04 & -0.7666E-03 & 0.5835E-01 & -0.4386E-03 & -0.6692E-01 \\ 0.3790E+01 & 0.2069E+00 & 0.4487E+00 & 0.2260E-01 & -0.1699E-03 & -0.2592E-01 \end{bmatrix}$$

Input Ramp Time: 0.3 second

Command Vector:

$u = 0.0$

$A_{n_p} = 0.0$

$q = 0.0$

$A_{y_p} = 0.0$

$p = 3.491$ radians/second (3 second pulse)

$r-\alpha_T = 0.0$

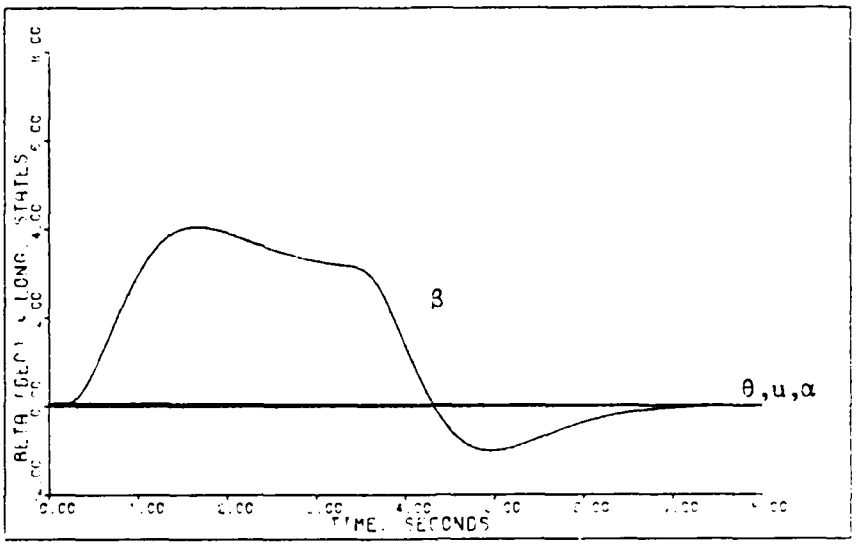

Figure D-22: 0.6M Healthy/Failed Roll -- Sideslip Angle, Pitch Angle, Angle of Attack, and Forward Velocity

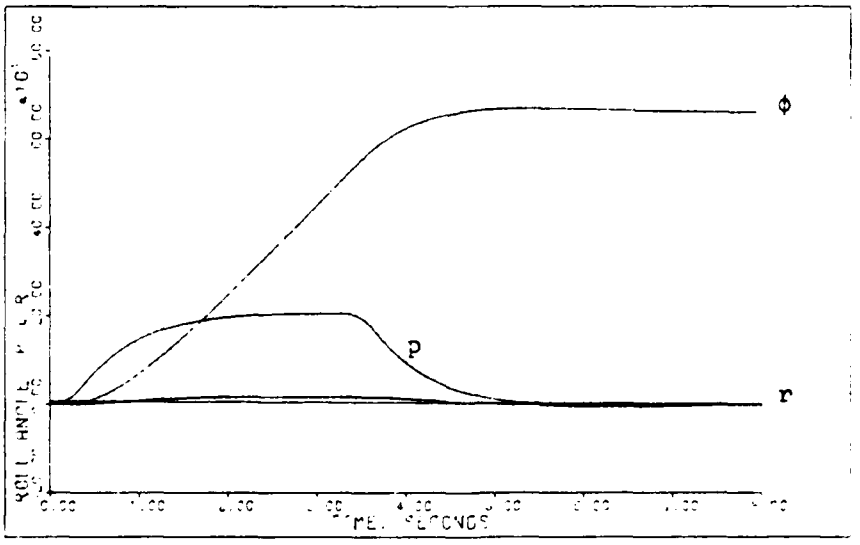

Figure D-23: 0.6M Healthy/Failed Roll -- Roll Angle, Roll Rate, and Yaw Rate

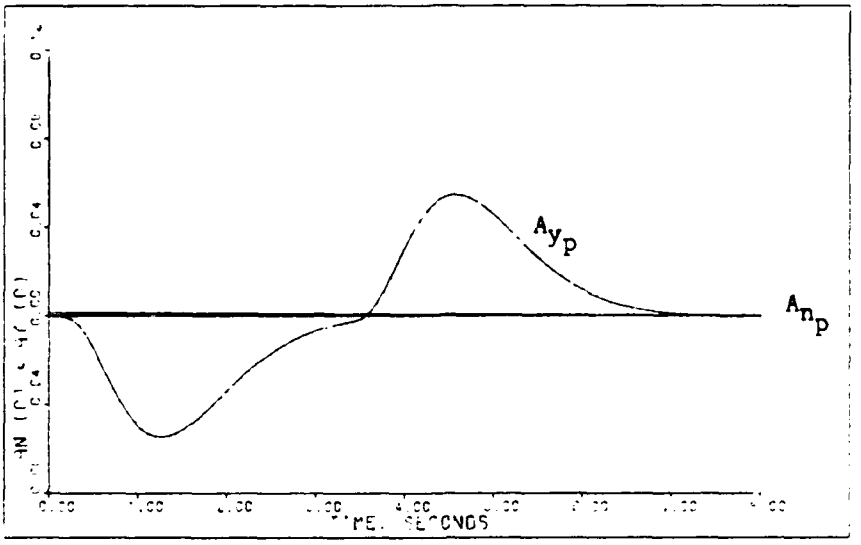

Figure D-24: 0.6M Healthy/Failed Roll -- Normal Acceleration and Lateral Acceleration

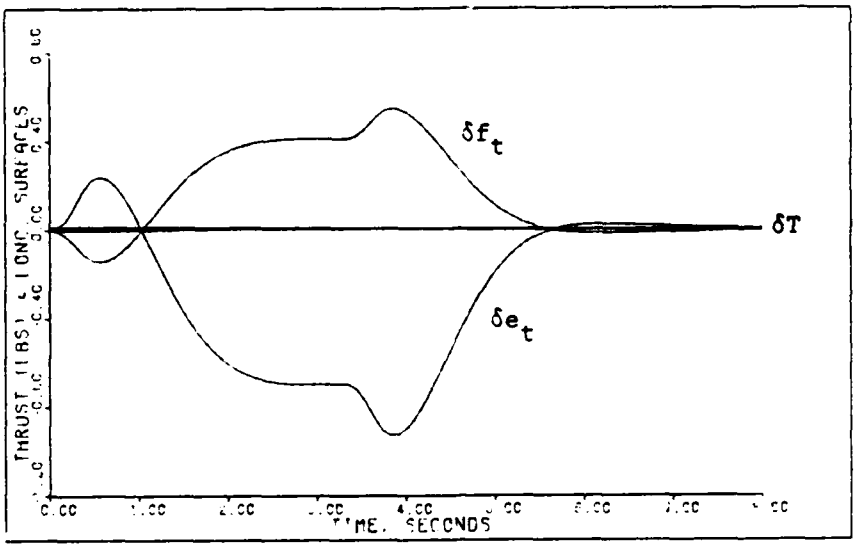

Figure D-25: 0.6M Healthy Roll -- Elevator and Flap Deflections and Thrust

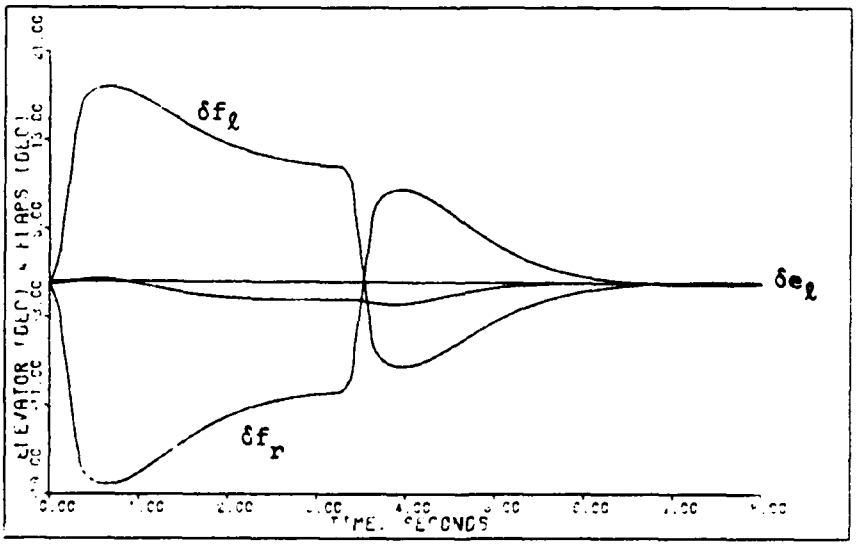

Figure D-26: 0.6M Failed Roll -- Left Elevator and Flaperon Deflections

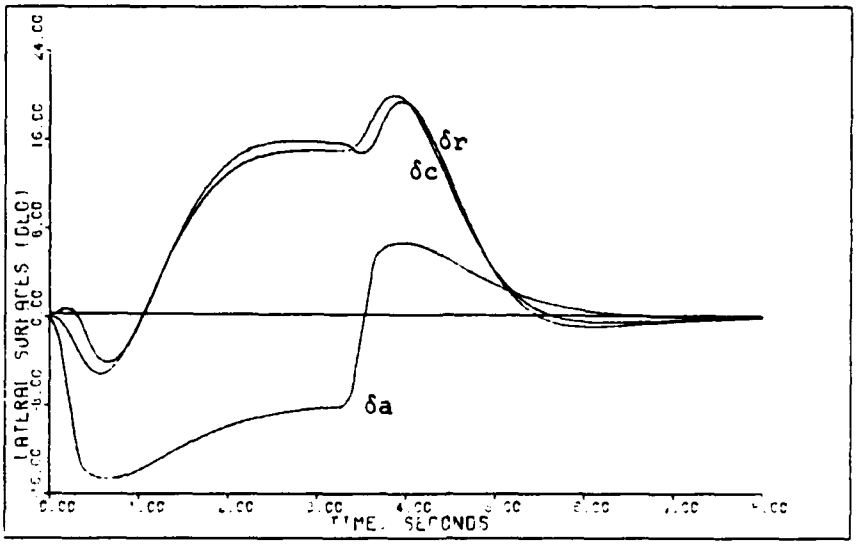

Figure D-27: 0.6M Healthy Roll -- Aileron, Rudder, and Canard Deflections

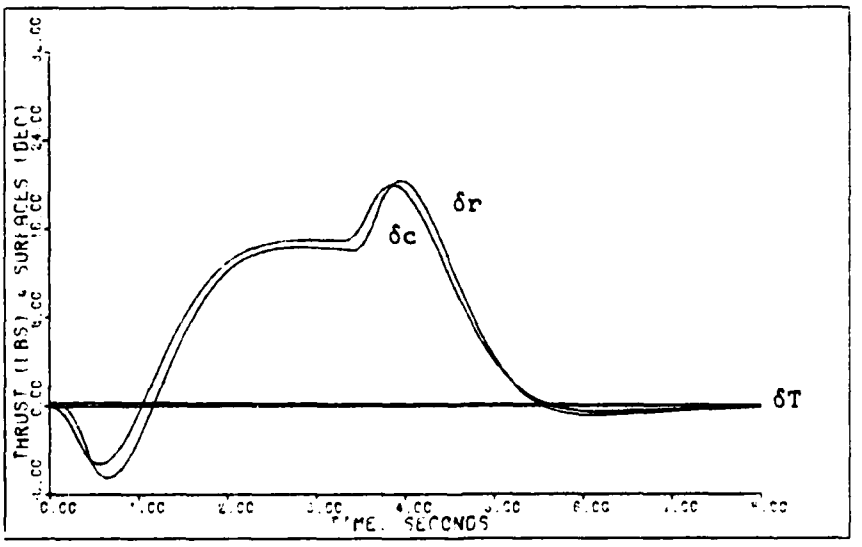

Figure D-28: 0.6M Failed Roll -- Rudder and Canard Deflections and Thrust

Sideforce (Flat Turn) Maneuver. Tables D-9 and D-10 give the design parameters for both the healthy and failed cases of the sideforce maneuver. The same parameters are used for both cases.

Figures D-29 through D-35 present the simulation responses for a 0.2g sideforce command. The maximum value commanded is limited by the canard deflection. As with the roll maneuver Figures D-29 through D-31 give simulation responses for both the healthy and failed models.

For this maneuver the horizontal tail is mainly used to counter the longitudinal pitching moment produced by the canard deflection although it also contributes to roll control for the healthy aircraft case. When the right horizontal tail fails the left horizontal tail deflects approximately twice the deflection of the healthy elevators. The flaperons deflect slightly asymmetrically to compensate for the roll created by the failed right horizontal tail. The rudder and canard deflections change only slightly for the failure case.

Table D-9

Sideforce Maneuver: Healthy Model,
0.6 Mach at 30,000 Feet

Sampling Time: T = 0.02 second

$\bar{\alpha} = 1.2$

$\varepsilon = 1.0$

$\underline{\Sigma} = \text{diag}\{\ 2.0,\ 0.04,\ 1.0,\ 1.0,\ 1.0,\ 1.0\}$

$$\underline{K}_0 = \begin{bmatrix} 0.0 & -0.3565E-04 & -0.8330E-01 & -0.5402E-02 & 0.5400E-04 & 0.5158E-02 \\ -0.3473E-14 & 0.9869E-03 & -0.5527E-01 & 0.3198E-02 & -0.3198E-04 & -0.3054E-02 \\ 0.0 & 0.0 & 0.0 & 0.1806E-01 & -0.9219E-02 & -0.3528E-01 \\ 0.0 & 0.0 & 0.0 & 0.8364E-01 & 0.2127E-02 & -0.1756E+00 \\ 0.0 & 0.0 & 0.0 & 0.1166E+00 & -0.1166E-02 & -0.1114E+00 \\ 0.1895E+01 & 0.4139E-02 & 0.2806E+00 & 0.4517E-01 & -0.4516E-03 & -0.4313E-01 \end{bmatrix}$$

$$\underline{K}_1 = \begin{bmatrix} 0.0 & -0.4278E-04 & -0.9996E-01 & -0.6482E-02 & 0.6480E-04 & 0.6189E-02 \\ -0.4167E-14 & 0.1184E-02 & -0.6633E-01 & 0.3838E-02 & -0.3837E-04 & -0.3665E-02 \\ 0.0 & 0.0 & 0.0 & 0.2168E-01 & -0.1106E-01 & -0.4233E-01 \\ 0.0 & 0.0 & 0.0 & 0.1004E+00 & 0.2553E-02 & -0.2108E+00 \\ 0.0 & 0.0 & 0.0 & 0.1400E+00 & -0.1399E-02 & -0.1336E+00 \\ 0.2274E+01 & 0.4966E-02 & 0.3367E+00 & 0.5420E-01 & -0.5419E-03 & -0.5175E-01 \end{bmatrix}$$

Input Ramp Time: 0.5 second

Command Vector:

$u = 0.0$

$A_{n_p} = 0.0$

$q = 0.0$

$A_{y_p} = 0.2$ g (step)

$p = 0.0$

$r = 0.01079$ radian/second (step)

Table D-10

Sideforce Maneuver: Failed Model,
0.6 Mach at 30,000 Feet

Sampling Time: T = 0.02 second

$\bar{\alpha} = 1.2$

$\varepsilon = 1.0$

$\Sigma = \text{diag}\{ 2.0, 0.04, 1.0, 1.0, 1.0, 1.0\}$

$$\underline{K}_0 = \begin{bmatrix} 0.4482E-14 & -0.7129E-04 & -0.1665E+00 & -0.1081E-01 & 0.1129E-03 & 0.1033E-01 \\ -0.2244E-14 & 0.9786E-03 & -0.7458E-01 & 0.2420E-01 & -0.1137E-01 & -0.4531E-01 \\ -0.3025E-14 & 0.9952E-03 & -0.3599E-01 & -0.1779E-01 & 0.1131E-01 & 0.3920E-01 \\ -0.7669E-16 & -0.5852E-05 & -0.1367E-01 & 0.8571E-01 & 0.6232E-03 & -0.1806E+00 \\ -0.4928E-15 & -0.2051E-06 & -0.4791E-03 & 0.1167E+00 & -0.1218E-02 & -0.1115E+00 \\ 0.1895E+01 & 0.4138E-02 & 0.2804E+00 & 0.4520E-01 & -0.4718E-03 & -0.4319E-01 \end{bmatrix}$$

$$\underline{K}_1 = \begin{bmatrix} 0.5379E-14 & -0.8554E-04 & -0.1999E+00 & -0.1297E-01 & 0.1354E-03 & 0.1240E-01 \\ -0.2693E-14 & 0.1174E-02 & -0.8950E-01 & 0.2903E-01 & -0.1365E-01 & -0.5437E-01 \\ -0.3630E-14 & 0.1194E-02 & -0.4319E-01 & -0.2135E-01 & 0.1357E-01 & 0.4703E-01 \\ -0.9202E-16 & -0.7022E-05 & -0.1641E-01 & 0.1029E+00 & 0.7479E-03 & -0.2167E+00 \\ -0.5913E-15 & -0.2461E-06 & -0.5749E-03 & 0.1400E+00 & -0.1462E-02 & -0.1338E+00 \\ 0.2274E+01 & 0.4966E-02 & 0.3365E+00 & 0.5424E-01 & -0.5662E-03 & -0.5183E-01 \end{bmatrix}$$

Input Ramp Time: 0.5 second

Command Vector:

$u = 0.0$

$A_{n_p} = 0.0$

$q = 0.0$

$A_{y_p} = 0.2$ g (step)

$p = 0.0$

$r = 0.01079$ radian/second (step)

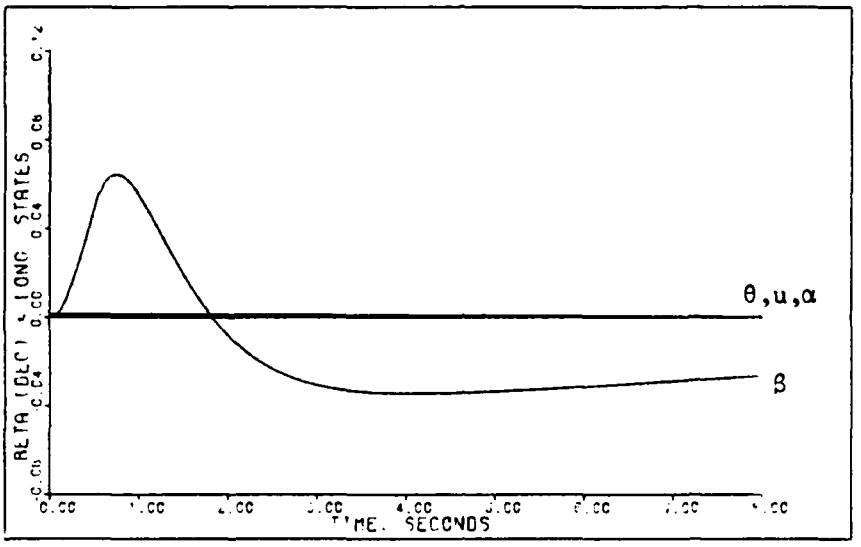

Figure D-29: 0.6M Healthy/Failed Sideforce -- Sideslip Angle, Pitch Angle, Angle of Attack, and Forward Velocity

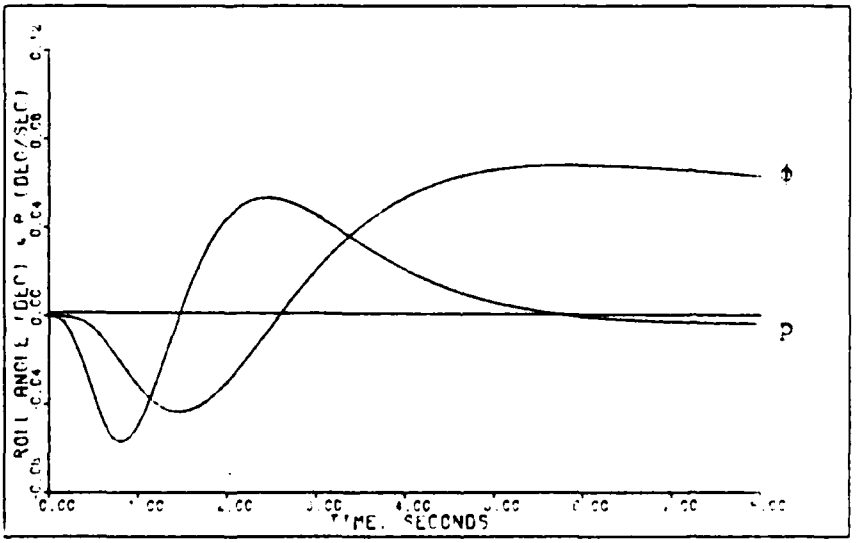

Figure D-30: 0.6M Healthy/Failed Sideforce -- Roll Angle and Roll Rate

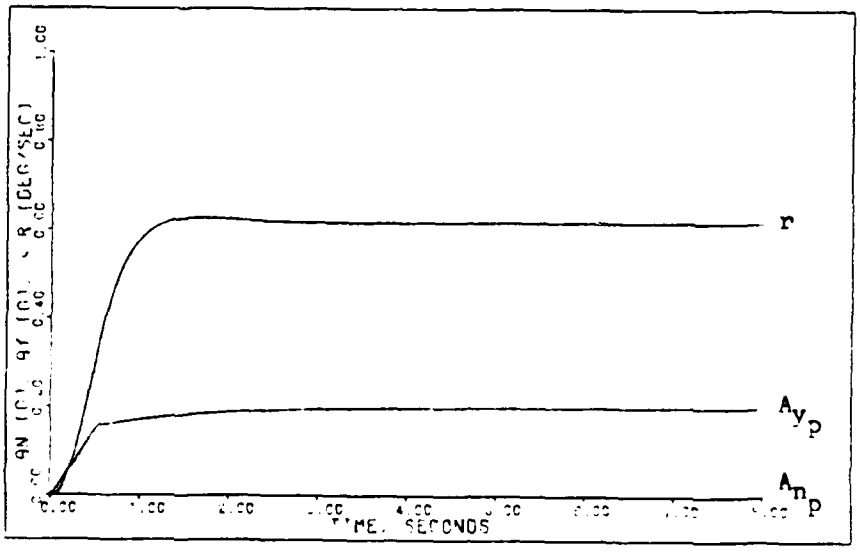

Figure D-31: 0.6M Healthy/Failed Sideforce -- Normal Acceleration, Lateral Acceleration, and Yaw Rate

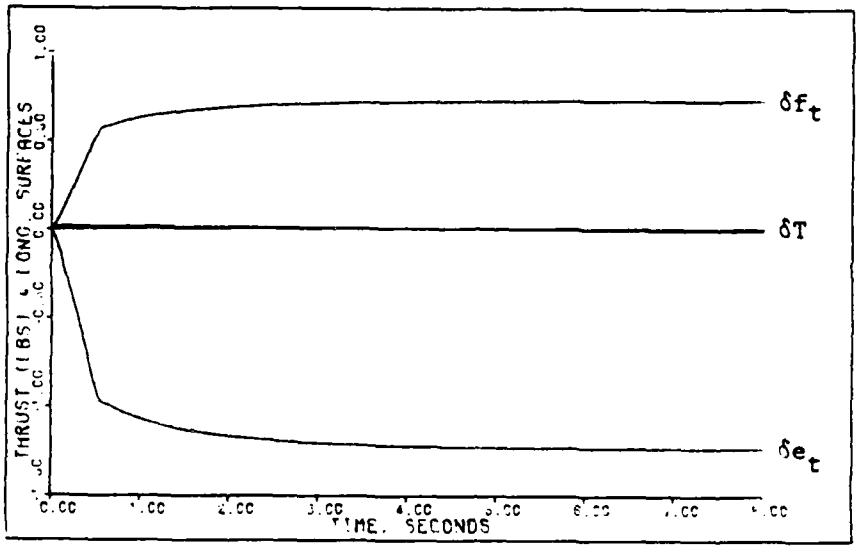

Figure D-32: 0.6M Healthy Sideforce -- Elevator and Flap Deflections and Thrust

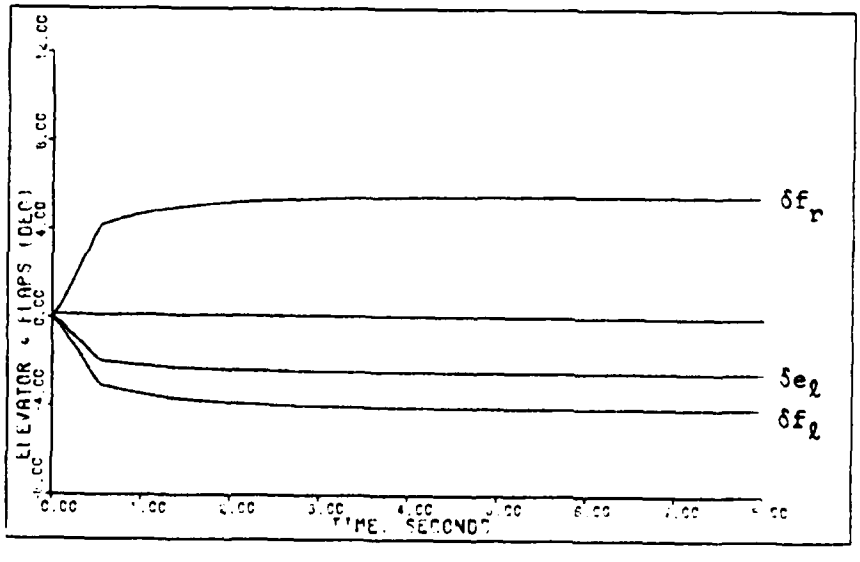

Figure D-33: 0.6M Failed Sideforce -- Left Elevator and Flaperon Deflections

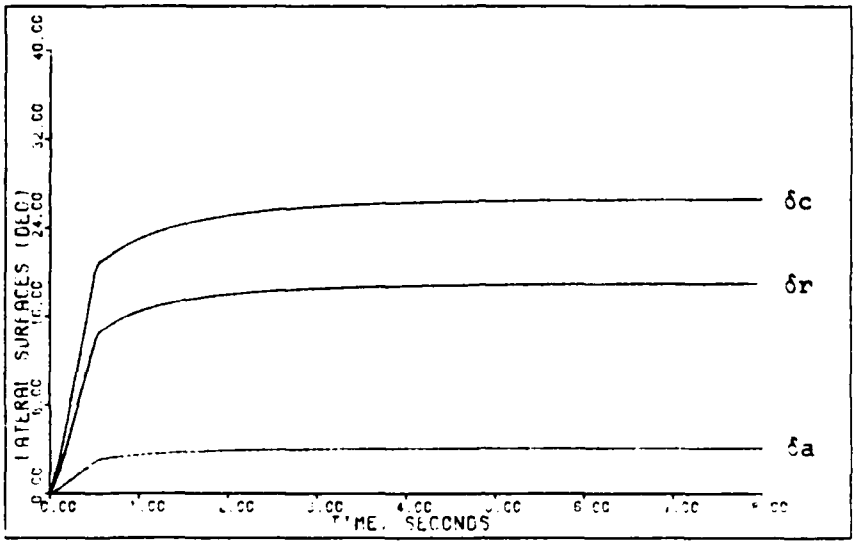

Figure D-34: 0.6M Healthy Sideforce -- Aileron, Rudder, and Canard Deflections

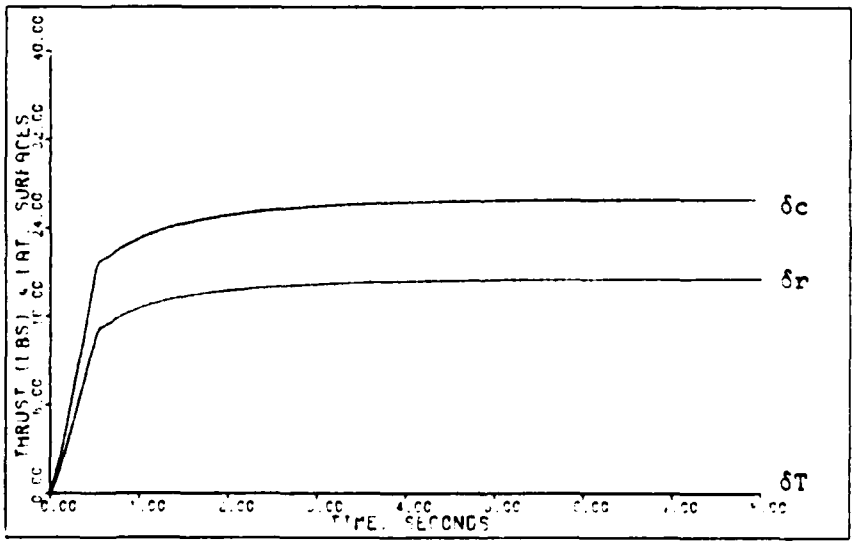

Figure D-35: 0.6M Failed Sideforce -- Rudder and Canard Deflections and Thrust

Yaw Pointing Maneuver. The design parameters for the yaw pointing maneuver are given in Tables D-11 and D-12 for both the healthy and failed models. The parameters are the same for both cases.

Figures D-36 through D-42 present the simulation responses for a four degree yaw pointing command. The maximum angle commanded for this maneuver is limited by the ability to hold the roll angle to a small value. As with the roll maneuver Figures D-36 through D-38 give simulation responses for both the healthy and failed aircraft models.

For the yaw pointing maneuver the horizontal tail is used for both pitch and roll control. When the right horizontal tail fails the flaperons take over the roll control and deflect asymmetrically to counter the rolling moment of the left horizontal tail, which deflects for pitch control. The rudder and canard responses are not affected much by the failure for this maneuver.

Table D-11

Yaw Pointing: Healthy Model, 0.6 Mach at 30,000 Feet

Sampling Time: T = 0.02 second

$\bar{\alpha} = 4.0$

$\varepsilon = 1.0$

$\underline{\Sigma} = \text{diag}\{ 2.0, 0.04, 1.0, 0.7, 2.5, 1.5\}$

$$\underline{K}_0 = \begin{bmatrix} 0.0 & -0.3565E-04 & -0.8330E-01 & -0.3781E-02 & 0.1350E-03 & 0.7736E-02 \\ -0.3473E-14 & 0.9869E-03 & -0.5527E-01 & 0.2239E-02 & -0.7994E-04 & -0.4581E-02 \\ 0.0 & 0.0 & 0.0 & 0.1264E-01 & -0.2305E-01 & -0.5292E-01 \\ 0.0 & 0.0 & 0.0 & 0.5855E-01 & 0.5318E-02 & -0.2635E+00 \\ 0.0 & 0.0 & 0.0 & 0.8164E-01 & -0.2915E-02 & -0.1670E+00 \\ 0.1895E+01 & 0.4139E-02 & 0.2806E+00 & 0.3162E-01 & -0.1129E-02 & -0.6469E-01 \end{bmatrix}$$

$$\underline{K}_1 = \begin{bmatrix} 0.0 & -0.1426E-03 & -0.3332E+00 & -0.1512E-01 & 0.5400E-03 & 0.3095E-01 \\ -0.1389E-13 & 0.3948E-02 & -0.2211E+00 & 0.8956E-02 & -0.3198E-03 & -0.1832E-01 \\ 0.0 & 0.0 & 0.0 & 0.5058E-01 & -0.9219E-01 & -0.2117E+00 \\ 0.0 & 0.0 & 0.0 & 0.2342E+00 & 0.2127E-01 & -0.1054E+01 \\ 0.0 & 0.0 & 0.0 & 0.3266E+00 & -0.1166E-01 & -0.6681E+00 \\ 0.7579E+01 & 0.1655E-01 & 0.1122E+01 & 0.1265E+00 & -0.4516E-02 & -0.2588E+00 \end{bmatrix}$$

Input Ramp Time: 0.2 second

Command Vector:

$u = 0.0$

$A_{n_p} = 0.0$

$q = 0.0$

$A_{y_p} = 0.0$

$p = 0.0$

$r = -0.06981$ radian/second (1 second pulse)

Table D-12

Yaw Pointing: Failed Model, 0.6 Mach at 30,000 Feet

Sampling Time: T = 0.02 second

$\bar{\alpha} = 4.0$

$\epsilon = 1.0$

$\underline{\Sigma} = \text{diag}\{ 2.0, 0.04, 1.0, 0.7, 2.5, 1.5 \}$

$$\underline{K}_0 = \begin{bmatrix} 0.4482E-14 & -0.7129E-04 & -0.1665E+00 & -0.7567E-02 & 0.2821E-03 & 0.1550E-01 \\ -0.2244E-14 & 0.9786E-03 & -0.7458E-01 & 0.1694E-01 & -0.2844E-01 & -0.6797E-01 \\ -0.3025E-14 & 0.9952E-03 & -0.3599E-01 & -0.1246E-01 & 0.2827E-01 & 0.5879E-01 \\ -0.7669E-16 & -0.5852E-05 & -0.1367E-01 & 0.6000E-01 & 0.1558E-02 & -0.2709E+00 \\ -0.4928E-15 & -0.2051E-06 & -0.4791E-03 & 0.8169E-01 & -0.3046E-02 & -0.1673E+00 \\ 0.1895E+01 & 0.4138E-02 & 0.2804E+00 & 0.3164E-01 & -0.1180E-02 & -0.6479E-01 \end{bmatrix}$$

$$\underline{K}_1 = \begin{bmatrix} 0.1793E-13 & -0.2851E-03 & -0.6662E+00 & -0.3027E-01 & 0.1129E-02 & 0.6199E-01 \\ -0.8976E-14 & 0.3915E-02 & -0.2983E+00 & 0.6775E-01 & -0.1137E+00 & -0.2719E+00 \\ -0.1210E-13 & 0.3981E-02 & -0.1440E+00 & -0.4983E-01 & 0.1131E+00 & 0.2342E+00 \\ -0.3067E-15 & -0.2341E-04 & -0.5469E-01 & 0.2400E+00 & 0.6232E-02 & -0.1084E+01 \\ -0.1971E-14 & -0.8203E-06 & -0.1916E-02 & 0.3268E+00 & -0.1218E-01 & -0.6692E+00 \\ 0.7579E+01 & 0.1655E-01 & 0.1122E+01 & 0.1265E+00 & -0.4718E-02 & -0.2592E+00 \end{bmatrix}$$

Input Ramp Time: 0.2 second

Command Vector:

$u = 0.0$

$A_{n_p} = 0.0$

$q = 0.0$

$A_{y_p} = 0.0$

$p = 0.0$

$r = -0.06981$ radian/second (1 second pulse)

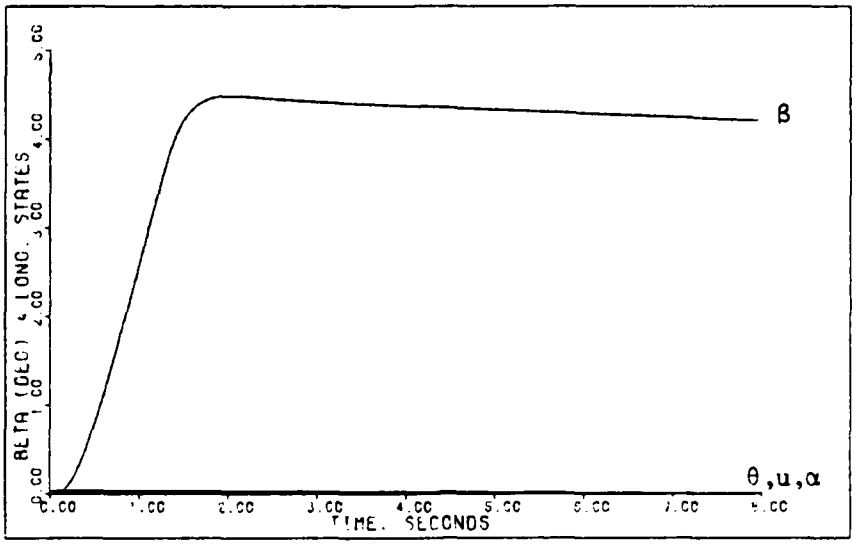

Figure D-36: 0.6M Healthy/Failed Yaw Pointing -- Sideslip Angle, Pitch Angle, Angle of Attack, and Forward Velocity

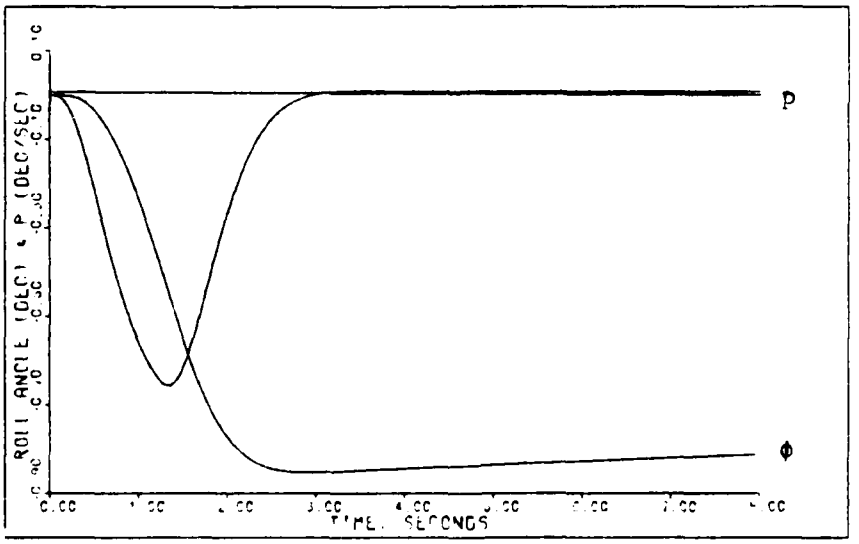

Figure D-37: 0.6M Healthy/Failed Yaw Pointing -- Roll Angle and Roll Rate

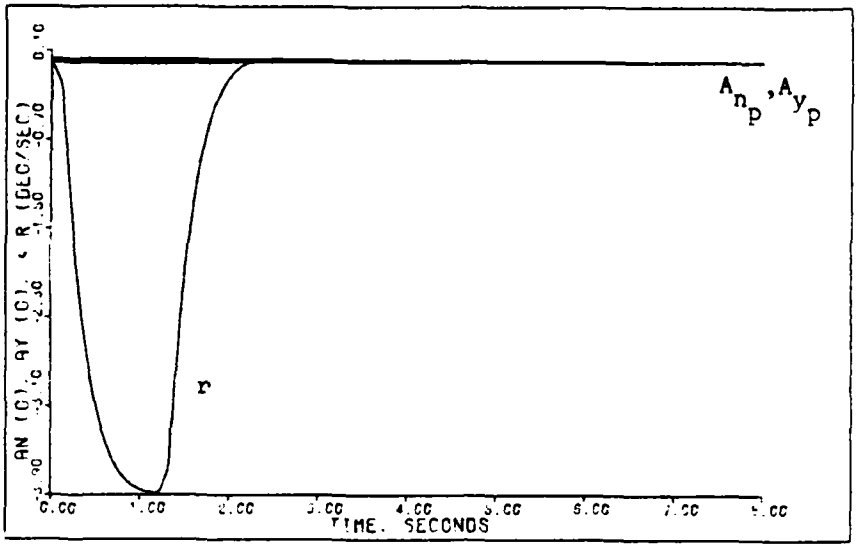

Figure D-38: 0.6M Healthy/Failed Yaw Pointing -- Normal Acceleration, Lateral Acceleration, and Yaw Rate

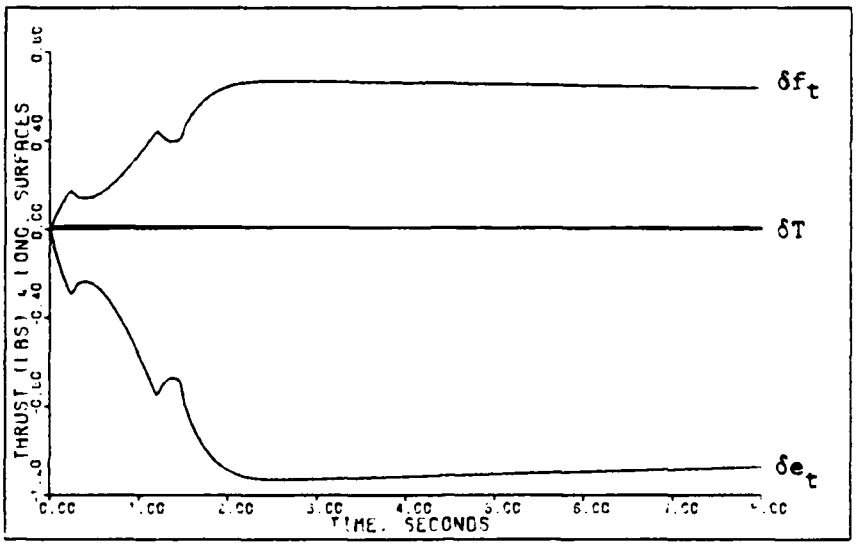

Figure D-39: 0.6M Healthy Yaw Pointing -- Elevator and Flap Deflections and Thrust

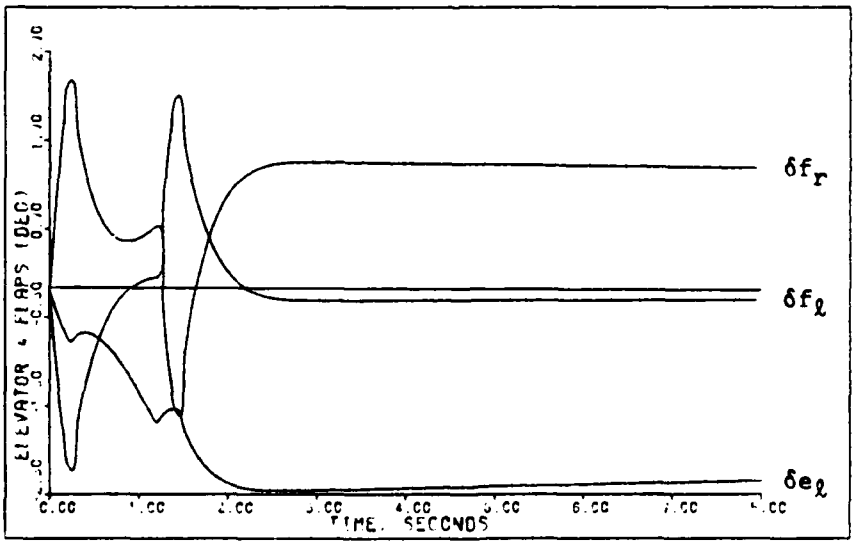

Figure D-40: 0.6M Failed Yaw Pointing -- Left Elevator and Flaperon Deflections

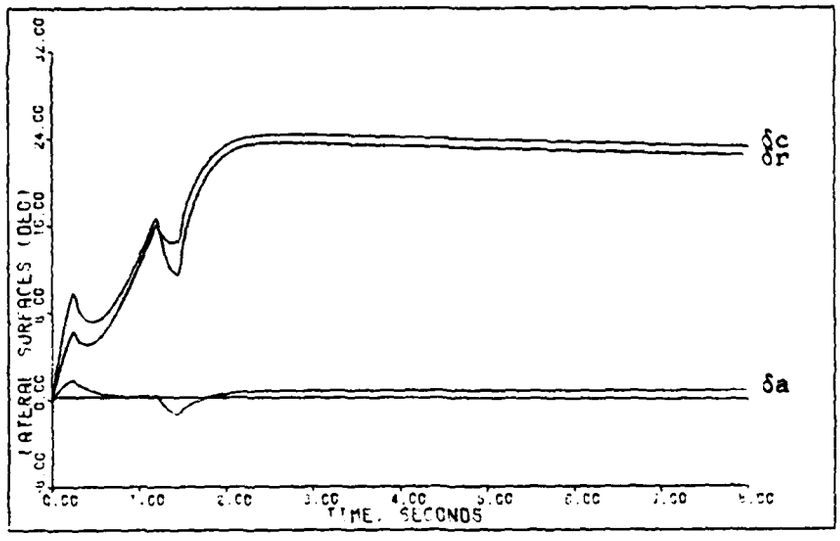

Figure D-41: 0.6M Healthy Yaw Pointing -- Aileron, Rudder, and Canard Deflections

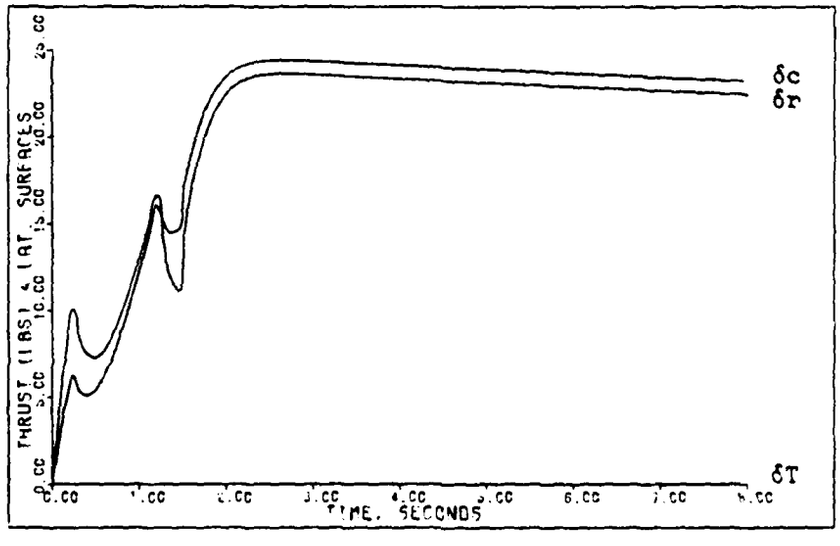

Figure D-42: 0.6M Failed Yaw Pointing -- Rudder and Canard Deflections and Thrust

Lateral Translation Maneuver. Tables D-13 and D-14 give the design parameters for the lateral translation maneuver. As indicated in the tables the same design parameters are used for both the healthy and failed aircraft models.

The simulation responses for a 0.17g lateral acceleration command, which corresponds to a steady-state lateral velocity value of 8.2 feet/second, are given in Figures D-43 through D-49. The maximum lateral acceleration commanded for this maneuver is limited by the canard deflection. As explained for the roll maneuver, Figures D-43 through D-45 give simulation responses for both the healthy and failed aircraft models.

For the lateral translation maneuver the horizontal tail is used mainly as an elevator to counter the small pitch moment generated by the canard deflection. When the right horizontal tail fails the left horizontal tail deflects to approximately twice the elevator deflection of the healthy aircraft simulation, and the flaperons deflect asymmetrically to counter the rolling moment of the left horizontal tail. The rudder and canard responses are not affected much by the failure for this maneuver.

Table D-13

Lateral Translation: Healthy Model,
0.6 Mach at 30,000 Feet

Sampling Time: T = 0.02 second

$\bar{\alpha} = 2.0$

$\epsilon = 1.0$

$\underline{\Sigma} = diag\{ 2.0,\ 0.04,\ 1.0,\ 3.0,\ 0.7,\ 0.7\}$

$$\underline{K}_0 = \begin{bmatrix} 0.0 & -0.3565E-04 & -0.8330E-01 & -0.1621E-01 & 0.3780E-04 & 0.3610E-02 \\ -0.3473E-14 & 0.9869E-03 & -0.5527E-01 & 0.9595E-02 & -0.2238E-04 & -0.2138E-02 \\ 0.0 & 0.0 & 0.0 & 0.5419E-01 & -0.6453E-02 & -0.2469E-01 \\ 0.0 & 0.0 & 0.0 & 0.2509E+00 & 0.1489E-02 & -0.1230E+00 \\ 0.0 & 0.0 & 0.0 & 0.3499E+00 & -0.8162E-03 & -0.7795E-01 \\ 0.1895E+01 & 0.4139E-02 & 0.2806E+00 & 0.1355E+00 & -0.3161E-03 & -0.3019E-01 \end{bmatrix}$$

$$\underline{K}_1 = \begin{bmatrix} 0.0 & -0.7130E-04 & -0.1666E+00 & -0.3241E-01 & 0.7561E-04 & 0.7221E-02 \\ -0.6946E-14 & 0.1974E-02 & -0.1105E+00 & 0.1919E-01 & -0.4477E-04 & -0.4275E-02 \\ 0.0 & 0.0 & 0.0 & 0.1084E+00 & -0.1291E-01 & -0.4939E-01 \\ 0.0 & 0.0 & 0.0 & 0.5018E+00 & 0.2978E-02 & -0.2459E+00 \\ 0.0 & 0.0 & 0.0 & 0.6998E+00 & -0.1632E-02 & -0.1559E+00 \\ 0.3790E+01 & 0.8277E-02 & 0.5612E+00 & 0.2710E+00 & -0.6322E-03 & -0.6038E-01 \end{bmatrix}$$

Input Ramp Time: 0.5 second

Command Vector:

$u = 0.0$

$A_{n_p} = 0.0$

$q = 0.0$

$A_{y_p} = 0.17\ g$ (1 second pulse)

$p = 0.0$

$r = 0.0$

Table D-14

Lateral Translation: Failed Model,
0.6 Mach at 30,000 Feet

Sampling Time: T = 0.02 second

$\bar{\alpha} = 2.0$

$\epsilon = 1.0$

$\underline{\Sigma} = \text{diag}\{ 2.0,\ 0.04,\ 1.0,\ 3.0,\ 0.7,\ 0.7 \}$

$$\underline{K}_0 = \begin{bmatrix} 0.4482E-14 & -0.7129E-04 & -0.1665E+00 & -0.3243E-01 & 0.7900E-04 & 0.7232E-02 \\ -0.2244E-14 & 0.9786E-03 & -0.7458E-01 & 0.7259E-01 & -0.7962E-02 & -0.3172E-01 \\ -0.3025E-14 & 0.9952E-03 & -0.3599E-01 & -0.5338E-01 & 0.7915E-02 & 0.2744E-01 \\ -0.7669E-16 & -0.5852E-05 & -0.1367E-01 & 0.2571E+00 & 0.4363E-03 & -0.1264E+00 \\ -0.4928E-15 & -0.2051E-06 & -0.4791E-03 & 0.3501E+00 & -0.8528E-03 & -0.7807E-01 \\ 0.1895E+01 & 0.4138E-02 & 0.2804E+00 & 0.1356E+00 & -0.3303E-03 & -0.3023E-01 \end{bmatrix}$$

$$\underline{K}_1 = \begin{bmatrix} 0.8965E-14 & -0.1426E-03 & -0.3331E+00 & -0.6486E-01 & 0.1580E-03 & 0.1446E-01 \\ -0.4488E-14 & 0.1957E-02 & -0.1492E+00 & 0.1452E+00 & -0.1592E-01 & -0.6344E-01 \\ -0.6051E-14 & 0.1990E-02 & -0.7199E-01 & -0.1068E+00 & 0.1583E-01 & 0.5487E-01 \\ -0.1534E-15 & -0.1170E-04 & -0.2734E-01 & 0.5143E+00 & 0.8725E-03 & -0.2528E+00 \\ -0.9855E-15 & -0.4101E-06 & -0.9582E-03 & 0.7002E+00 & -0.1706E-02 & -0.1561E+00 \\ 0.3790E+01 & 0.8277E-02 & 0.5608E+00 & 0.2712E+00 & -0.6605E-03 & -0.6047E-01 \end{bmatrix}$$

Input Ramp Time: 0.5 second

Command Vector:

$u = 0.0$

$A_{n_p} = 0.0$

$q = 0.0$

$A_{y_p} = 0.17$ g (1 second pulse)

$p = 0.0$

$r = 0.0$

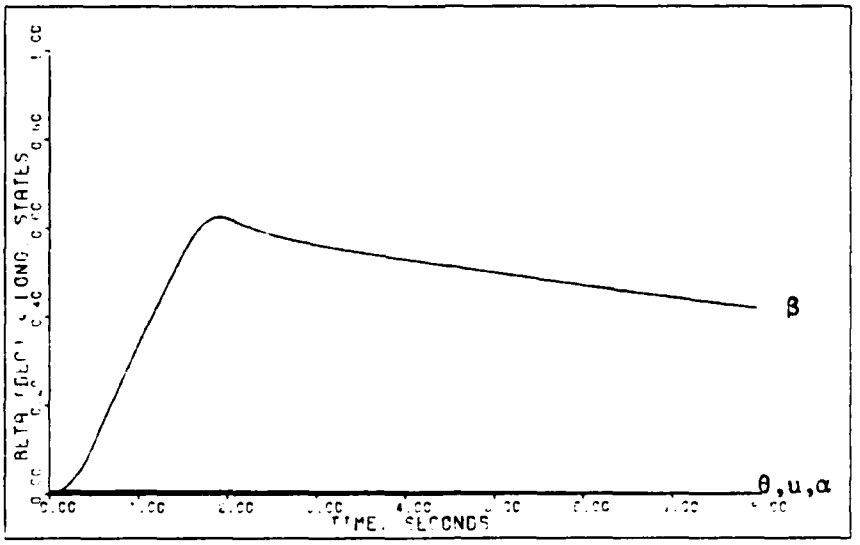

Figure D-43: 0.6M Healthy/Failed Lateral Translation -- Sideslip Angle, Pitch Angle, Angle of Attack, and Forward Velocity

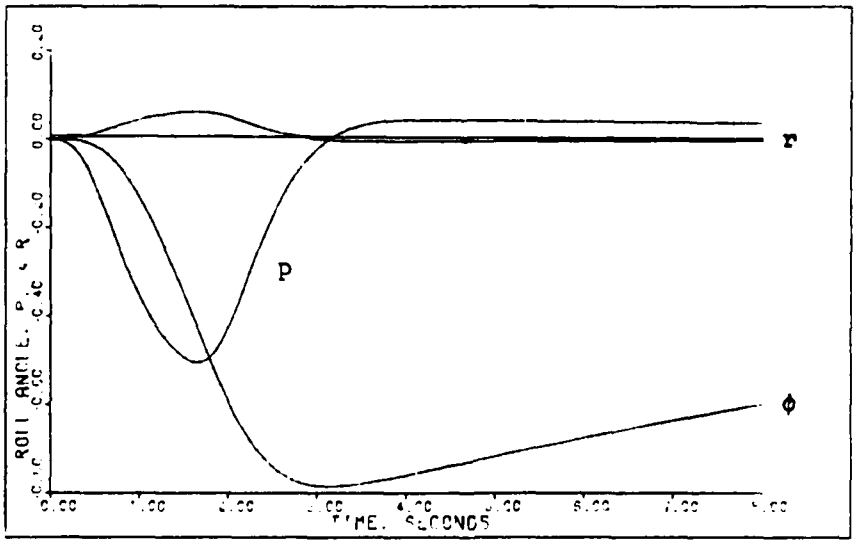

Figure D-44: 0.6M Healthy/Failed Lateral Translation -- Roll Angle, Roll Rate, and Yaw Rate

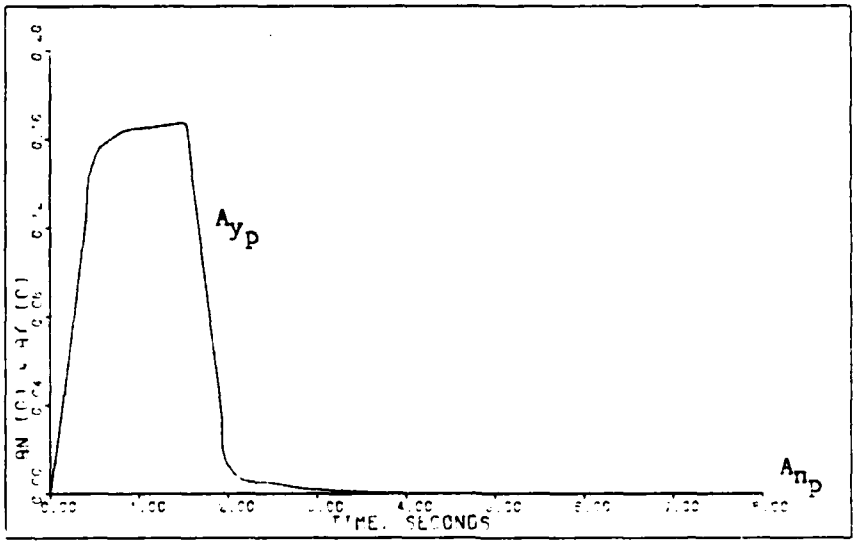

Figure D-45: 0.6M Healthy/Failed Lateral Translation -- Normal Acceleration and Lateral Acceleration

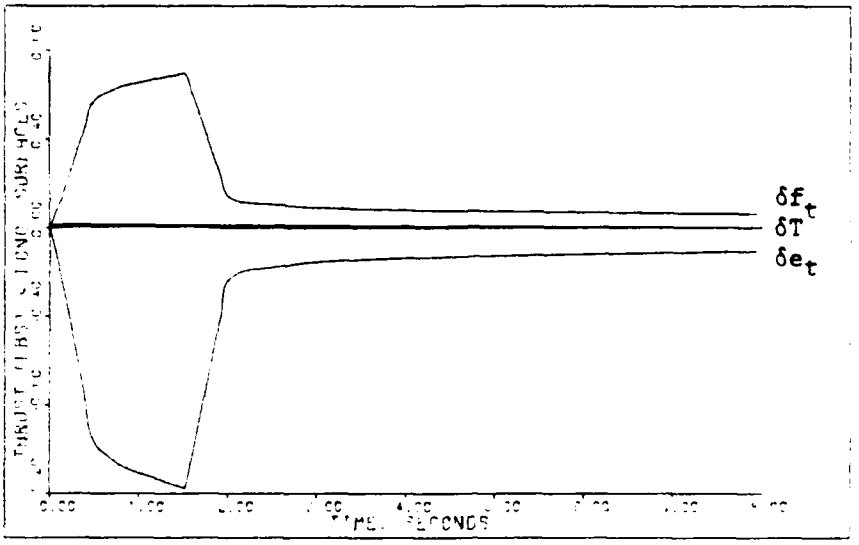

Figure D-46: 0.6M Healthy Lateral Translation -- Elevator and Flap Deflections and Thrust

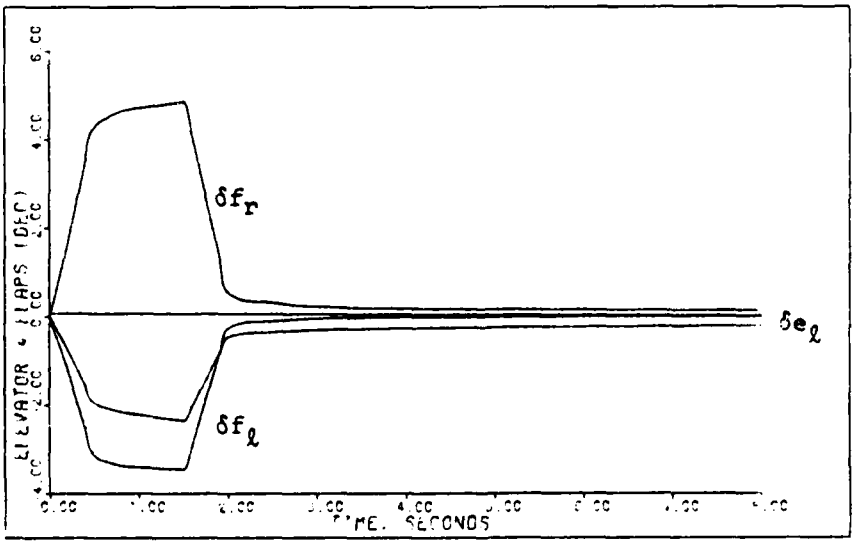

Figure D-47: 0.6M Failed Lateral Translation -- Left Elevator and Flaperon Deflections

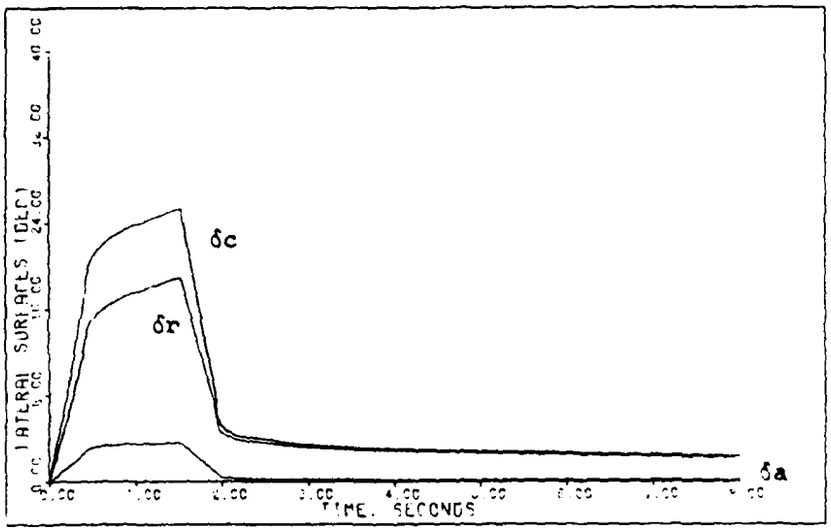

Figure D-48: 0.6M Healthy Lateral Translation -- Aileron, Rudder, and Canard Deflections

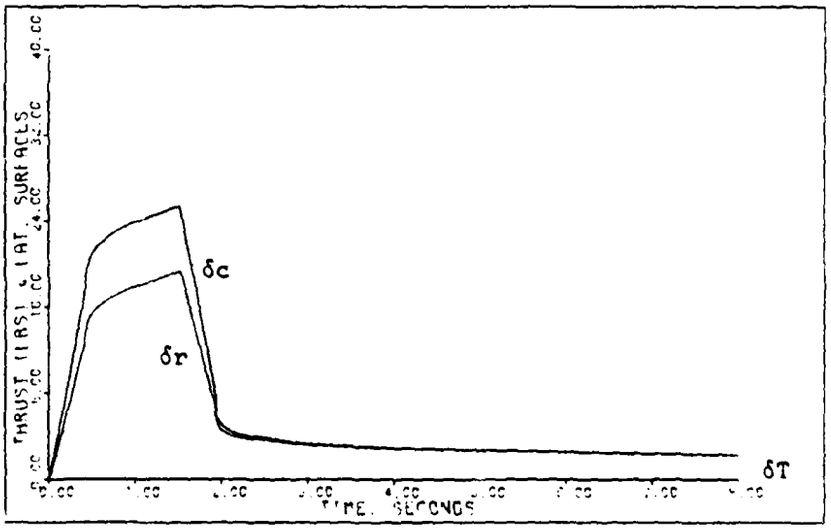

Figure D-49: 0.6M Failed Lateral Translation -- Rudder and Canard Deflections and Thrust

Supersonic Flight (1.6 Mach at 30,000 Feet)

The supersonic flight condition is chosen to demonstrate maneuverabiltiy of the aircraft at high speed. The dynamic pressure has a large value at this flight condition because of the high velocity; therefore, designs are fairly easy for the healthy aircraft model because the control surfaces are very effective in maneuvering the aircraft. Designs for the failed right horizontal tail model are slightly more difficult because the horizontal tail makes a large contribution to roll control. When the right horizontal tail fails, the flaperons are required to take over complete roll control which may lead to large flaperon deflections.

G-Command Maneuver. Tables D-15 and D-16 list the design parameters for the g-command maneuver for the healthy and failed right elevator models. As shown in the tables, the same design parameters are used for both aircraft models.

Figures D-50 through D-56 show the simulation responses for the g-command maneuver. For the same reasons given for the longitudinal maneuvers of the subsonic flight condition, Figures D-50 through D-52 give simulation responses for both the healthy and failed aircraft models.

The maximum normal acceleration command of 8.5 g is limited by the ability to hold the angle of attack to a relatively low value. For the failure case, the left elevator deflects approximately twice the amount required

when both tail halves are operational. The flaperon deflection is asymmetric for the failure case in order to compensate for the rolling moment created by the left elevator deflection. The rudder and canard compensate for the adverse yaw caused by a difference in drag between the left and right halves of the aircraft.

Table D-15

G-Command: Healthy Model, 1.6 Mach at 30,000 Feet

Sampling Time: T = 0.02 second

$\bar{\alpha} = 3.5$

$\epsilon = 1.0$

$\underline{\Sigma} = \text{diag}\{ 2.0, 0.021, 1.8, 1.0, 1.0, 1.0\}$

$$\underline{K}_0 = \begin{bmatrix} 0.0 & -0.6923E-04 & -0.1194E-01 & 0.1530E-03 & -0.2106E-05 & -0.1730E-03 \\ 0.0 & 0.3892E-03 & -0.8671E-01 & -0.2351E-03 & 0.3235E-05 & 0.2657E-03 \\ 0.0 & 0.0 & 0.0 & 0.1531E-01 & -0.6716E-02 & -0.2720E-01 \\ 0.0 & 0.0 & 0.0 & 0.3609E-01 & 0.5947E-02 & -0.9215E-01 \\ 0.0 & 0.0 & 0.0 & 0.1791E-01 & -0.2464E-03 & -0.2024E-01 \\ 0.2766E+01 & 0.1612E-01 & -0.2880E+01 & -0.1263E-01 & 0.1738E-03 & 0.1428E-01 \end{bmatrix}$$

$$\underline{K}_1 = \begin{bmatrix} 0.0 & -0.2423E-03 & -0.4179E-01 & 0.5356E-03 & -0.7370E-05 & -0.6055E-03 \\ 0.0 & 0.1362E-02 & -0.3035E+00 & -0.8228E-03 & 0.1132E-04 & 0.9301E-03 \\ 0.0 & 0.0 & 0.0 & 0.5360E-01 & -0.2351E-01 & -0.9518E-01 \\ 0.0 & 0.0 & 0.0 & 0.1263E+00 & 0.2081E-01 & -0.3225E+00 \\ 0.0 & 0.0 & 0.0 & 0.6268E-01 & -0.8624E-03 & -0.7085E-01 \\ 0.9682E+01 & 0.5643E-01 & -0.1008E+02 & -0.4421E-01 & 0.6083E-03 & 0.4998E-01 \end{bmatrix}$$

Input Ramp Time: 0.4 second

Command Vector:

$u = 0.0$

$A_{n_p} = 8.5$ g (step)

$q = 0.1719$ radian/second (step)

$A_{y_p} = 0.0$

$p = 0.0$

$r = 0.0$

Table D-16

G-Command: Failed Model, 1.6 Mach at 30,000 Feet

Sampling Time: T = 0.02 second

$\bar{\alpha} = 3.5$

$\varepsilon = 1.0$

$\underline{\Sigma} = \text{diag}\{2.0,\ 0.021,\ 1.8,\ 1.0,\ 1.0,\ 1.0\}$

$$\underline{K}_0 = \begin{bmatrix} -0.5389E-16 & -0.1384E-03 & -0.2388E-01 & 0.3020E-03 & -0.2454E-05 & -0.3388E-03 \\ 0.0 & 0.3403E-03 & -0.9515E-01 & 0.2601E-01 & -0.1146E-01 & -0.4627E-01 \\ -0.4012E-15 & 0.4381E-03 & -0.7828E-01 & -0.2647E-01 & 0.1146E-01 & 0.4679E-01 \\ 0.2597E-15 & 0.2030E-04 & 0.3502E-02 & 0.3156E-01 & 0.7917E-02 & -0.8413E-01 \\ 0.6572E-16 & 0.1059E-05 & 0.1827E-03 & 0.1767E-01 & -0.1436E-03 & -0.1982E-01 \\ 0.2766E+01 & 0.1612E-01 & -0.2880E+01 & -0.1246E-01 & 0.1013E-03 & 0.1398E-01 \end{bmatrix}$$

$$\underline{K}_1 = \begin{bmatrix} -0.1886E-15 & -0.4845E-03 & -0.8357E-01 & 0.1057E-02 & -0.8588E-05 & -0.1186E-02 \\ 0.0 & 0.1191E-02 & -0.3330E+00 & 0.9103E-01 & -0.4011E-01 & -0.1619E+00 \\ -0.1404E-14 & 0.1533E-02 & -0.2740E+00 & -0.9265E-01 & 0.4012E-01 & 0.1638E+00 \\ 0.9089E-15 & 0.7106E-04 & 0.1226E-01 & 0.1104E+00 & 0.2771E-01 & -0.2944E+00 \\ 0.2300E-15 & 0.3707E-05 & 0.6394E-03 & 0.6185E-01 & -0.5025E-03 & -0.6938E-01 \\ 0.9682E+01 & 0.5643E-01 & -0.1008E+02 & -0.4363E-01 & 0.3544E-03 & 0.4894E-01 \end{bmatrix}$$

Input Ramp Time: 0.4 second

Command Vector:

$u = 0.0$

$A_{n_p} = 8.5$ g (step)

$q = 0.1719$ radian/second (step)

$A_{y_p} = 0.0$

$p = 0.0$

$r = 0.0$

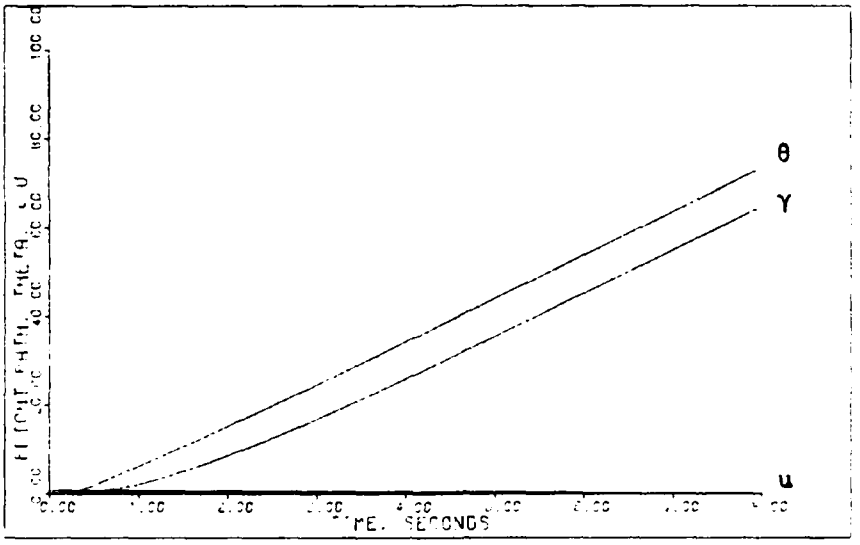

Figure D-50: 1.6M Healthy/Failed G-Command -- Flight Path Angle, Pitch Angle, and Forward Velocity

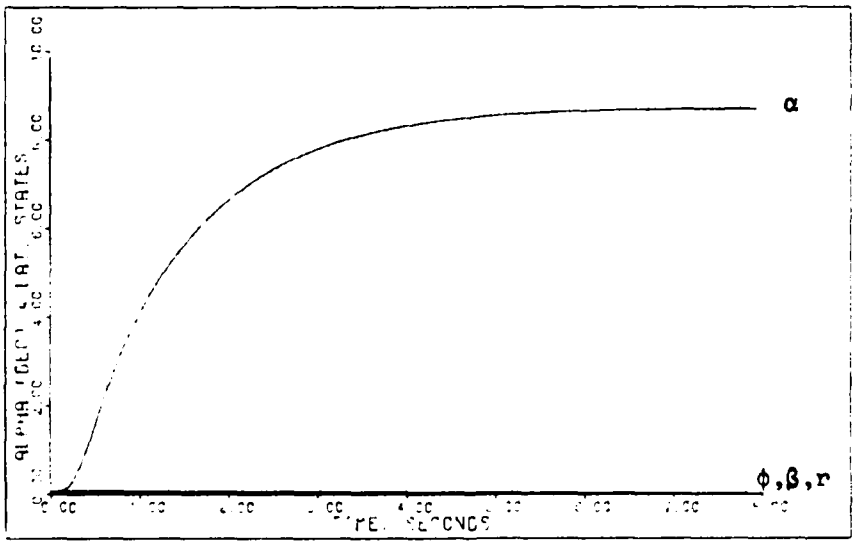

Figure D-51: 1.6M Healthy/Failed G-Command -- Angle of Attack, Roll Angle, Sideslip Angle, and Yaw Rate

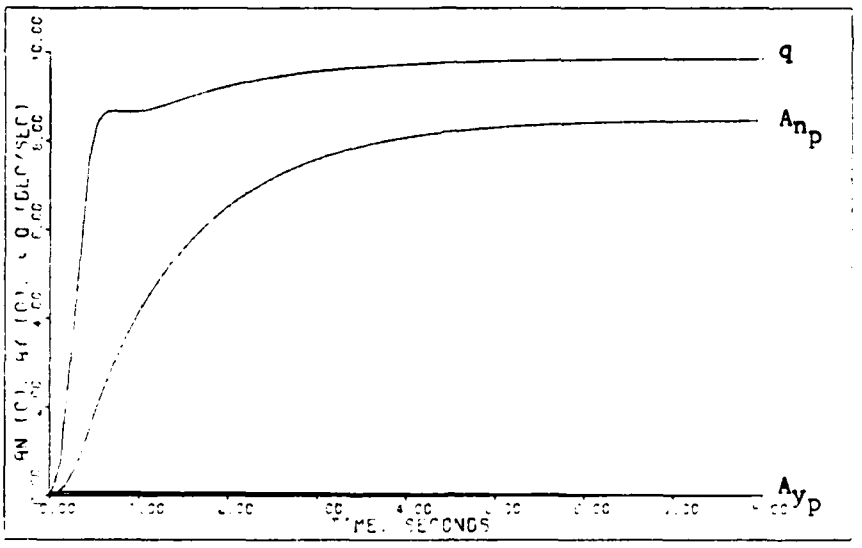

Figure D-52: 1.6M Healthy/Failed G-Command -- Pitch Rate, Normal Acceleration, and Lateral Acceleration

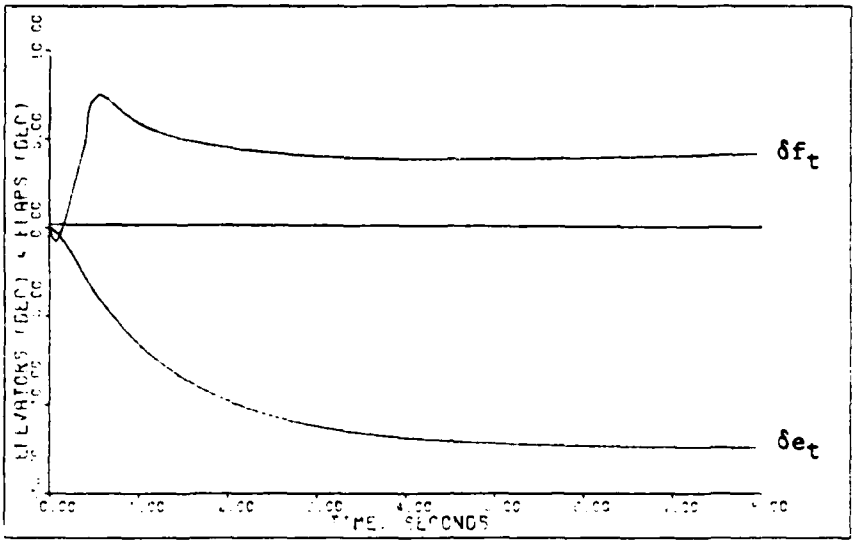

Figure D-53: 1.6M Healthy G-Command -- Elevator and Flap Deflections

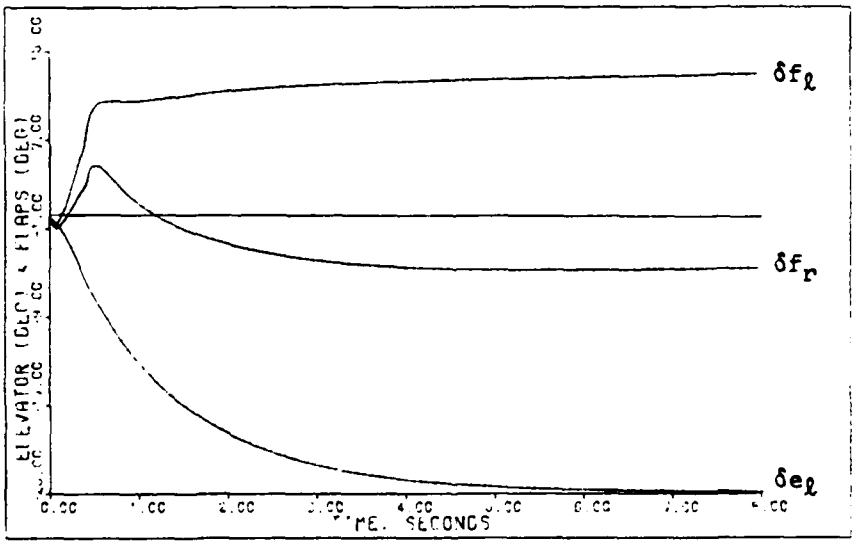

Figure D-54: 1.6M Failed G-Command -- Left Elevator and Flaperon Deflections

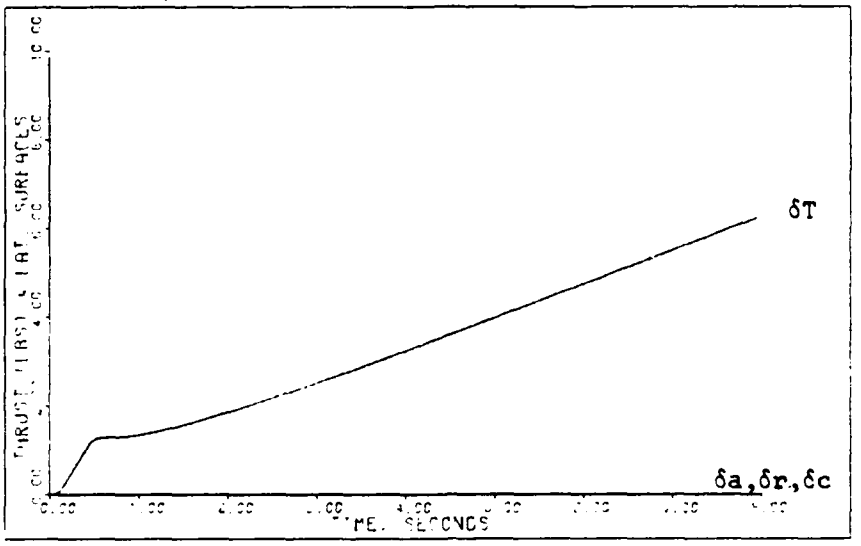

Figure D-55: 1.6M Healthy G-Command -- Aileron, Rudder, and Canard Deflections and Thrust

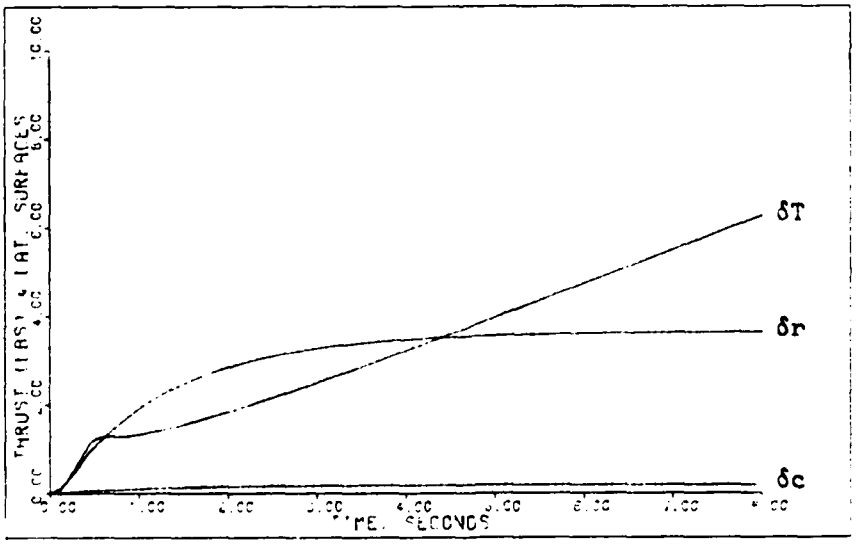

Figure D-56: 1.6M Failed G-Command -- Rudder and Canard Deflections and Thrust

Pitch Pointing Maneuver. Tables D-17 and D-18 give the design parameters for the pitch pointing maneuver. Unlike the designs presented up to this point, the design parameters are not the same for the healthy and failed models. The parameters are changed for the failure case in order to avoid overshooting the maximum flaperon deflection. Acceptable responses for the failure case are achieved without lowering the commanded pitch pointing angle.

The simulation responses for the pitch pointing maneuver with the healthy aircraft model are given in Figures D-57 through D-61. Figures D-62 through D-66 give the responses for the failure model. The maximum pointing angle commanded is limited by the flaperon deflection in both cases. For the failure model, the flaperons deflect asymmetrically to counter the roll induced by the left horizontal tail deflection, and the rudder and canard deflect to compensate for adverse yaw.

As shown in Figures D-61 and D-66 the thrust response is negative, which is not realistic. The negative response is due to commanding large inputs to a perturbation model. For the perturbation model a small flaperon deflection actually decreases drag. For large flaperon deflections the drag should increase, but the model still indicates a decrease in drag. This decrease in drag is manifested by an increase in forward velocity. The thrust is therefore negative to maintain zero change in velocity. Although a negative thrust is disturbing, it does not affect any of the

other aircraft responses and serves only to hold velocity constant.

Table D-17

Pitch Pointing: Healthy Model, 1.6 Mach at 30,000 Feet

Sampling Time: T = 0.02 second

$\bar{\alpha} = 4.5$

$\varepsilon = 1.0$

$\underline{\Sigma} = \text{diag}\{ 2.0, 1.5, 2.5, 1.0, 1.0, 1.0 \}$

$$\underline{K}_0 = \begin{bmatrix} 0.0 & -0.4945E-02 & -0.1658E-01 & 0.1530E-03 & -0.2106E-05 & -0.1730E-03 \\ 0.0 & 0.2780E-01 & -0.1204E+00 & -0.2351E-03 & 0.3235E-05 & 0.2657E-03 \\ 0.0 & 0.0 & 0.0 & 0.1531E-01 & -0.6716E-02 & -0.2720E-01 \\ 0.0 & 0.0 & 0.0 & 0.3609E-01 & 0.5947E-02 & -0.9215E-01 \\ 0.0 & 0.0 & 0.0 & 0.1791E-01 & -0.2464E-03 & -0.2024E-01 \\ 0.2766E+01 & 0.1152E+01 & -0.4000E+01 & -0.1263E-01 & 0.1738E-03 & 0.1428E-01 \end{bmatrix}$$

$$\underline{K}_1 = \begin{bmatrix} 0.0 & -0.2225E-01 & -0.7463E-01 & 0.6887E-03 & -0.9476E-05 & -0.7785E-03 \\ 0.0 & 0.1251E+00 & -0.5419E+00 & -0.1058E-02 & 0.1456E-04 & 0.1196E-02 \\ 0.0 & 0.0 & 0.0 & 0.6892E-01 & -0.3022E-01 & -0.1224E+00 \\ 0.0 & 0.0 & 0.0 & 0.1624E+00 & 0.2676E-01 & -0.4147E+00 \\ 0.0 & 0.0 & 0.0 & 0.8058E-01 & -0.1109E-02 & -0.9109E-01 \\ 0.1245E+02 & 0.5183E+01 & -0.1800E+02 & -0.5684E-01 & 0.7821E-03 & 0.6426E-01 \end{bmatrix}$$

Input Ramp Time: 0.2 second

Command Vector:

$u = 0.0$

$A_{n_p} = 0.0$

$q = 0.01745$ radian/second (1 second pulse)

$A_{y_p} = 0.0$

$p = 0.0$

$r = 0.0$

Table D-18

Pitch Pointing: Failed Model, 1.6 Mach at 30,000 Feet

Sampling Time: T = 0.02 second

$\bar{\alpha} = 3.5$

$\varepsilon = 1.0$

$\underline{\Sigma} = \text{diag}\{ 2.0, 1.5, 1.9, 1.0, 1.0, 1.0 \}$

$$\underline{K}_0 = \begin{bmatrix} -0.5389E-16 & -0.9888E-02 & -0.2520E-01 & 0.3020E-03 & -0.2454E-05 & -0.3388E-03 \\ 0.0 & 0.2431E-01 & -0.1004E+00 & 0.2601E-01 & -0.1146E-01 & -0.4627E-01 \\ -0.4012E-15 & 0.3129E-01 & -0.8263E-01 & -0.2647E-01 & 0.1146E-01 & 0.4679E-01 \\ 0.2597E-15 & 0.1450E-02 & 0.3696E-02 & 0.3156E-01 & 0.7917E-02 & -0.8413E-01 \\ 0.6572E-16 & 0.7565E-04 & 0.1928E-03 & 0.1767E-01 & -0.1436E-03 & -0.1982E-01 \\ 0.2766E+01 & 0.1152E+01 & -0.3040E+01 & -0.1246E-01 & 0.1013E-03 & 0.1398E-01 \end{bmatrix}$$

$$\underline{K}_1 = \begin{bmatrix} -0.1886E-15 & -0.3461E-01 & -0.8822E-01 & 0.1057E-02 & -0.8588E-05 & -0.1186E-02 \\ 0.0 & 0.8508E-01 & -0.3515E+00 & 0.9103E-01 & -0.4011E-01 & -0.1619E+00 \\ -0.1404E-14 & 0.1095E+00 & -0.2892E+00 & -0.9265E-01 & 0.4012E-01 & 0.1638E+00 \\ 0.9089E-15 & 0.5076E-02 & 0.1294E-01 & 0.1104E+00 & 0.2771E-01 & -0.2944E+00 \\ 0.2300E-15 & 0.2648E-03 & 0.6749E-03 & 0.6185E-01 & -0.5025E-03 & -0.6938E-01 \\ 0.9682E+01 & 0.4031E+01 & -0.1064E+02 & -0.4363E-01 & 0.3544E-03 & 0.4894E-01 \end{bmatrix}$$

Input Ramp Time: 0.2 second

Command Vector:

$u = 0.0$

$A_{n_p} = 0.0$

$q = 0.01745$ radian/second (1 second pulse)

$A_{y_p} = 0.0$

$p = 0.0$

$r = 0.0$

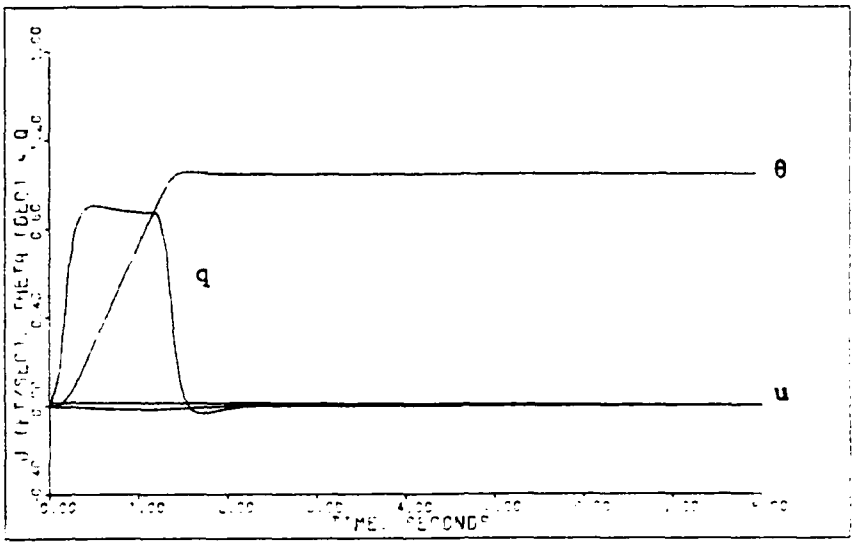

Figure D-57: 1.6M Healthy Pitch Pointing -- Pitch Angle, Pitch Rate, and Forward Velocity

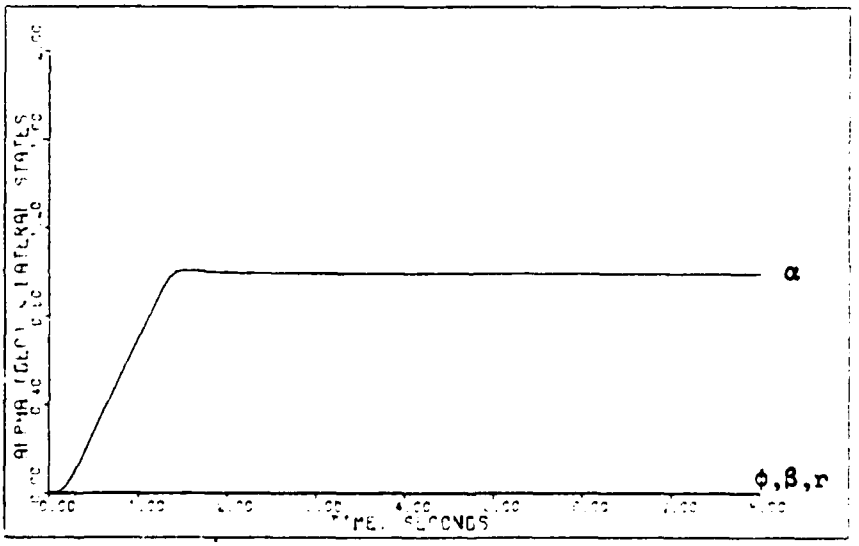

Figure D-58: 1.6M Healthy Pitch Pointing -- Angle of Attack, Roll Angle, Sideslip Angle, and Yaw Rate

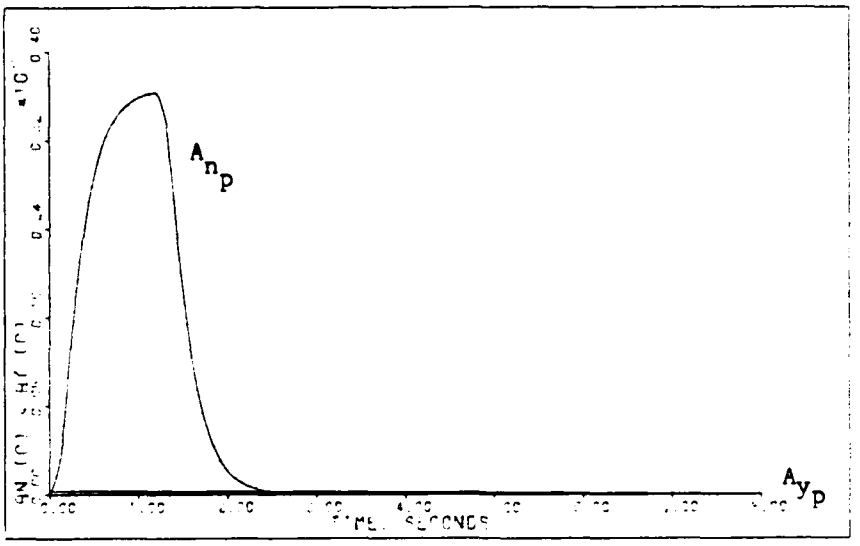

Figure D-59: 1.6M Healthy Pitch Pointing -- Normal Acceleration and Lateral Acceleration

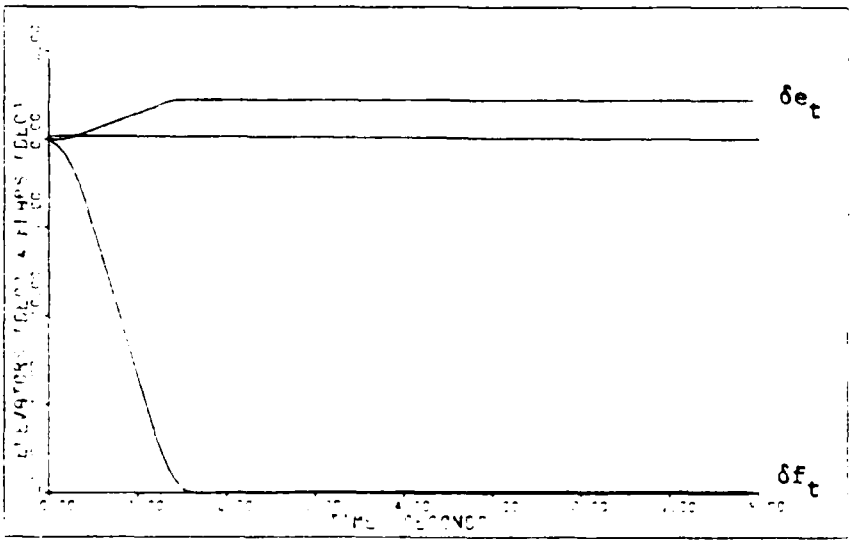

Figure D-60: 1.6M Healthy Pitch Pointing -- Elevator and Flap Deflections

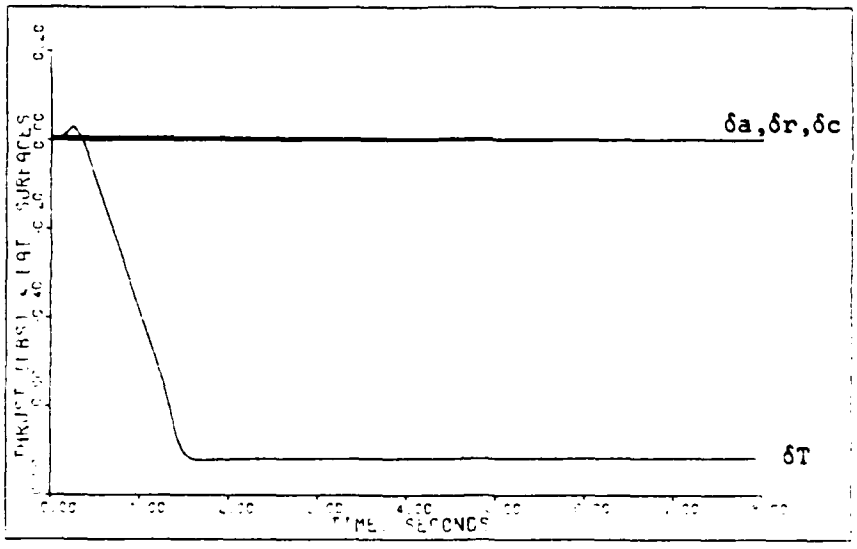

Figure D-61: 1.6M Healthy Pitch Pointing -- Aileron, Rudder, and Canard Deflections and Thrust

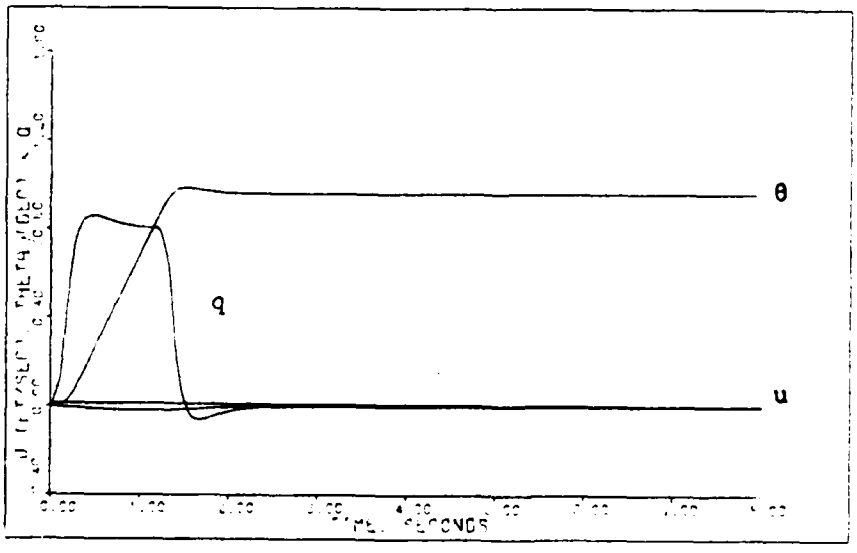

Figure D-62: 1.6M Failed Pitch Pointing -- Pitch Angle, Pitch Rate, and Forward Velocity

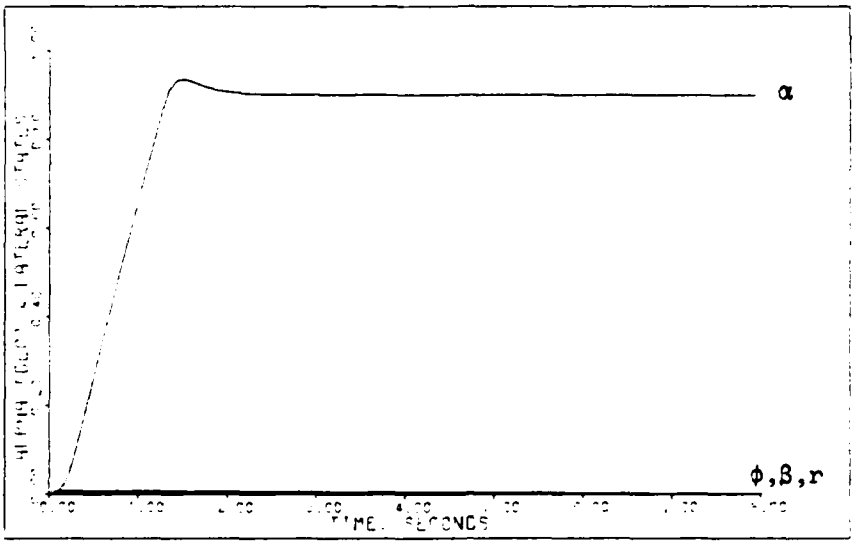

Figure D-63: 1.6M Failed Pitch Pointing -- Angle of Attack, Roll Angle, Sideslip Angle, and Yaw Rate

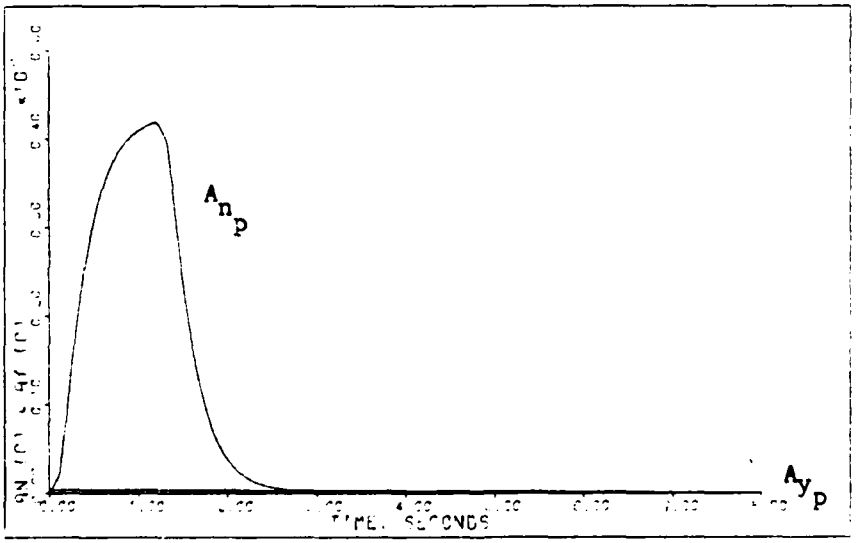

Figure D-64: 1.6M Failed Pitch Pointing -- Normal Acceleration and Lateral Acceleration

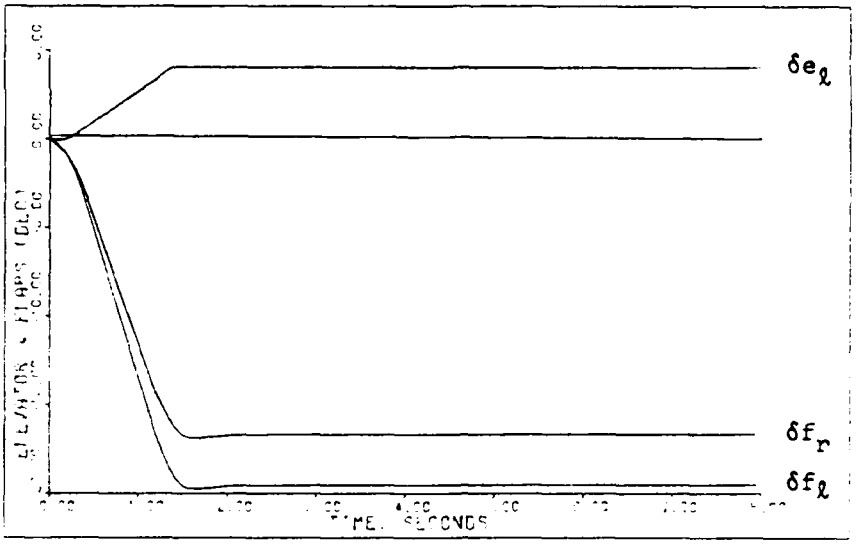

Figure D-65: 1.6M Failed Pitch Pointing -- Left Elevator and Flaperon Deflections

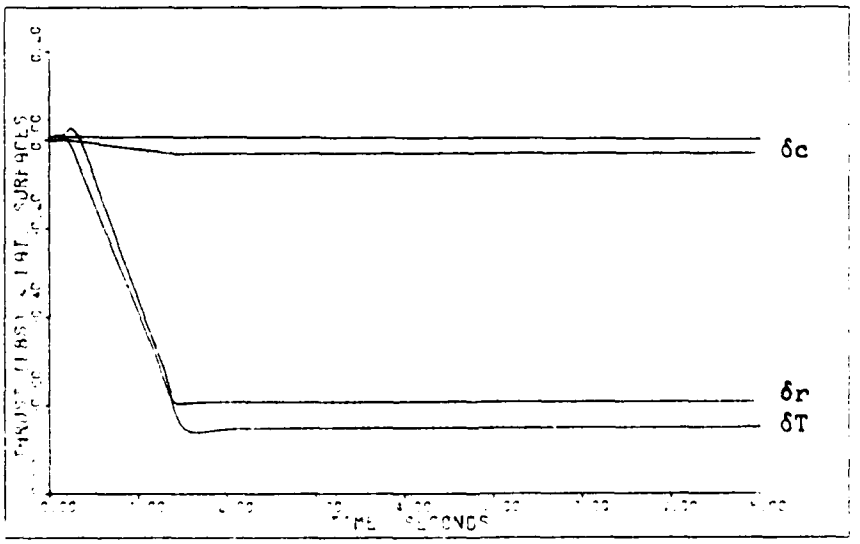

Figure D-66: 1.6M Failed Pitch Pointing -- Rudder and Canard Deflections and Thrust

Longitudinal Translation Maneuver. Tables D-19 and D-20 give the design parameters for the longitudinal translation maneuver. Although the design parameters are the same for the healthy and failed models, the commanded normal acceleration is reduced for the failed case in order not to overshoot the maximum flaperon deflection. A change in the design parameters for the failure case leads to unacceptable simulation responses.

The simulation responses for the healthy model longitudinal translation maneuver are given in Figures D-67 through D-71. The responses for the failure model are given in Figures D-72 through D-76. For the failure model, the flaperons deflect asymmetrically to counter the roll induced by the failed right horizontal tail, and the rudder and canard deflect to compensate for adverse yaw.

Table D-19

Longitudinal Translation: Healthy Model,
1.6 Mach at 30,000 Feet

Sampling Time: T = 0.02 second

$\bar{\alpha} = 3.5$

$\epsilon = 1.0$

$\underline{\Sigma} = \text{diag}\{\ 2.0,\ 1.0,\ 3.0,\ 1.0,\ 1.0,\ 1.0\ \}$

$$\underline{K}_0 = \begin{bmatrix} 0.0 & -0.3297E-02 & -0.1990E-01 & 0.1530E-03 & -0.2106E-05 & -0.1730E-03 \\ 0.0 & 0.1854E-01 & -0.1445E+00 & -0.2351E-03 & 0.3235E-05 & 0.2657E-03 \\ 0.0 & 0.0 & 0.0 & 0.1531E-01 & -0.6716E-02 & -0.2720E-01 \\ 0.0 & 0.0 & 0.0 & 0.3609E-01 & 0.5947E-02 & -0.9215E-01 \\ 0.0 & 0.0 & 0.0 & 0.1791E-01 & -0.2464E-03 & -0.2024E-01 \\ 0.2766E+01 & 0.7678E+00 & -0.4800E+01 & -0.1263E-01 & 0.1738E-03 & 0.1428E-01 \end{bmatrix}$$

$$\underline{K}_1 = \begin{bmatrix} 0.0 & -0.1154E-01 & -0.6965E-01 & 0.5356E-03 & -0.7370E-05 & -0.6055E-03 \\ 0.0 & 0.6487E-01 & -0.5058E+00 & -0.8228E-03 & 0.1132E-04 & 0.9301E-03 \\ 0.0 & 0.0 & 0.0 & 0.5360E-01 & -0.2351E-01 & -0.9518E-01 \\ 0.0 & 0.0 & 0.0 & 0.1263E+00 & 0.2081E-01 & -0.3225E+00 \\ 0.0 & 0.0 & 0.0 & 0.6268E-01 & -0.8624E-03 & -0.7085E-01 \\ 0.9682E+01 & 0.2687E+01 & -0.1680E+02 & -0.4421E-01 & 0.6083E-03 & 0.4998E-01 \end{bmatrix}$$

Input Ramp Time: 0.3 second

Command Vector:

$u = 0.0$

$A_{n_p} = 0.5$ g (1 second pulse)

$q = 0.0$

$A_{y_p} = 0.0$

$p = 0.0$

$r = 0.0$

Table D-20

Longitudinal Translation: Failed Model,
1.6 Mach at 30,000 Feet

Sampling Time: T = 0.02 second

$\bar{\alpha} = 3.5$

$\epsilon = 1.0$

$\underline{\Sigma} = \text{diag}\{ 2.0, 1.0, 3.0, 1.0, 1.0, 1.0 \}$

$$\underline{K}_0 = \begin{bmatrix} -0.5389E-16 & -0.6592E-02 & -0.3980E-01 & 0.3020E-03 & -0.2454E-05 & -0.3388E-03 \\ 0.0 & 0.1621E-01 & -0.1586E+00 & 0.2601E-01 & -0.1146E-01 & -0.4627E-01 \\ -0.4012E-15 & 0.2086E-01 & -0.1305E+00 & -0.2647E-01 & 0.1146E-01 & 0.4679E-01 \\ 0.2597E-15 & 0.9668E-03 & 0.5836E-02 & 0.3156E-01 & 0.7917E-02 & -0.8413E-01 \\ 0.6572E-16 & 0.5044E-04 & 0.3045E-03 & 0.1767E-01 & -0.1436E-03 & -0.1982E-01 \\ 0.2766E+01 & 0.7678E+00 & -0.4800E+01 & -0.1246E-01 & 0.1013E-03 & 0.1398E-01 \end{bmatrix}$$

$$\underline{K}_1 = \begin{bmatrix} -0.1886E-15 & -0.2307E-01 & -0.1393E+00 & 0.1057E-02 & -0.8588E-05 & -0.1186E-02 \\ 0.0 & 0.5672E-01 & -0.5550E+00 & 0.9103E-01 & -0.4011E-01 & -0.1619E+00 \\ -0.1404E-14 & 0.7302E-01 & -0.4566E+00 & -0.9265E-01 & 0.4012E-01 & 0.1638E+00 \\ .9089E-15 & 0.3384E-02 & 0.2043E-01 & 0.1104E+00 & 0.2771E-01 & -0.2944E+00 \\ 0.2300E-15 & 0.1765E-03 & 0.1066E-02 & 0.6185E-01 & -0.5025E-03 & -0.6938E-01 \\ 0.9682E+01 & 0.2687E+01 & -0.1680E+02 & -0.4363E-01 & 0.3544E-03 & 0.4894E-01 \end{bmatrix}$$

Input Ramp Time: 0.3 second

Command Vector:

$u = 0.0$

$A_{n_p} = 0.45$ g (1 second pulse)

$q = 0.0$

$A_{y_p} = 0.0$

$p = 0.0$

$r = 0.0$

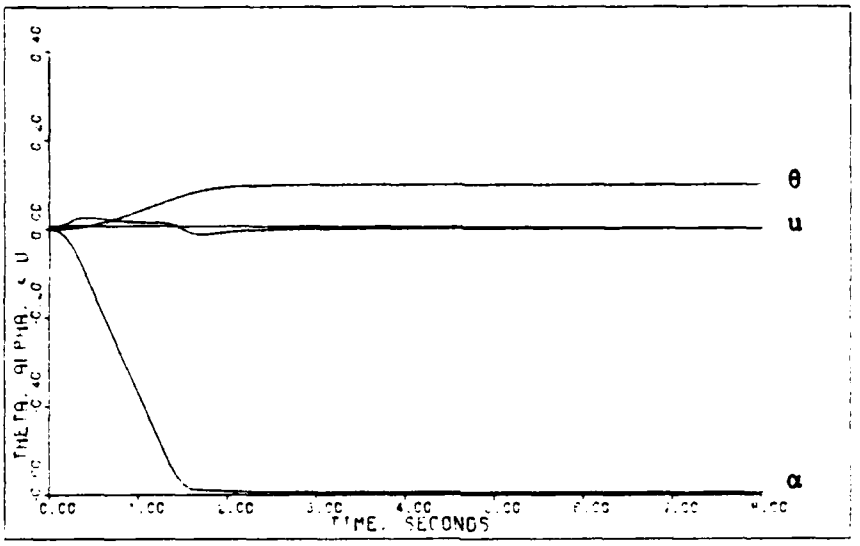

Figure D-67: 1.6M Healthy Longitudinal Translation -- Pitch Angle, Angle of Attack, and Forward Velocity

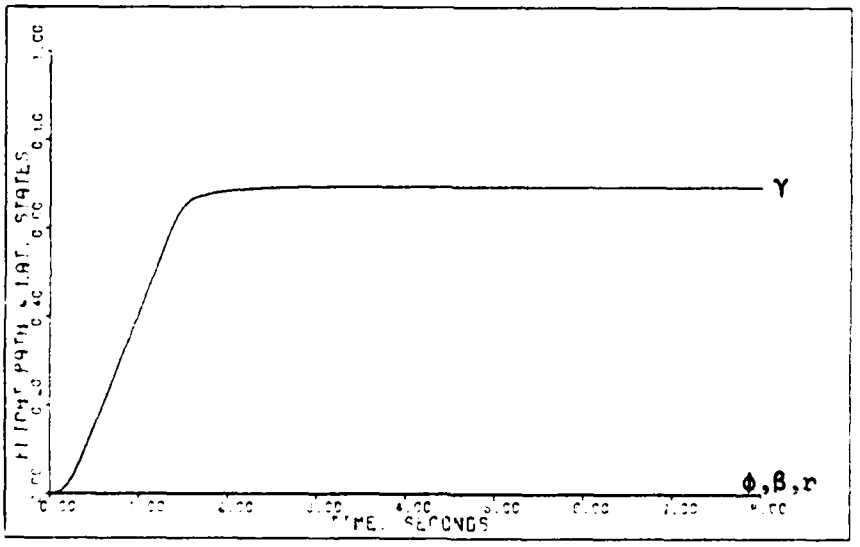

Figure D-68: 1.6M Healthy Longitudinal Translation -- Flight Path Angle, Roll Rate, Sideslip Angle, and Yaw Rate

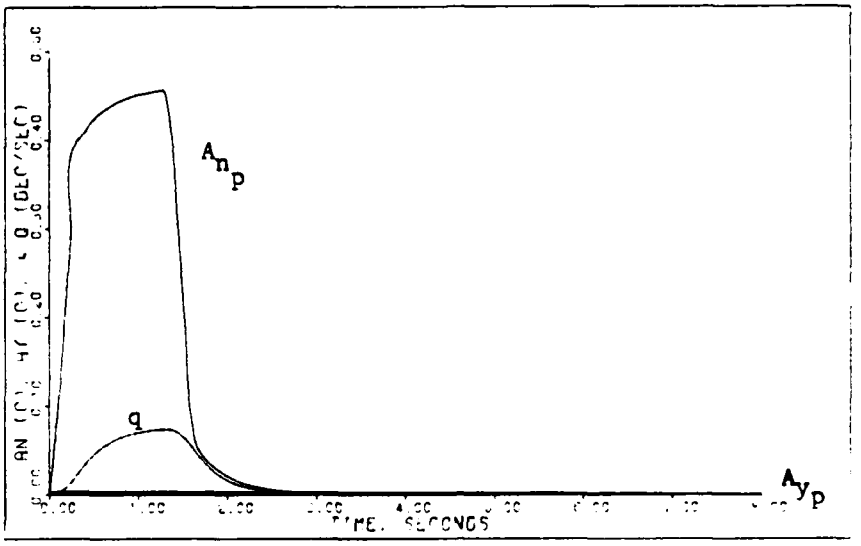

Figure D-69: 1.6M Healthy Longitudinal Translation -- Normal Acceleration, Lateral Acceleration, and Pitch Rate

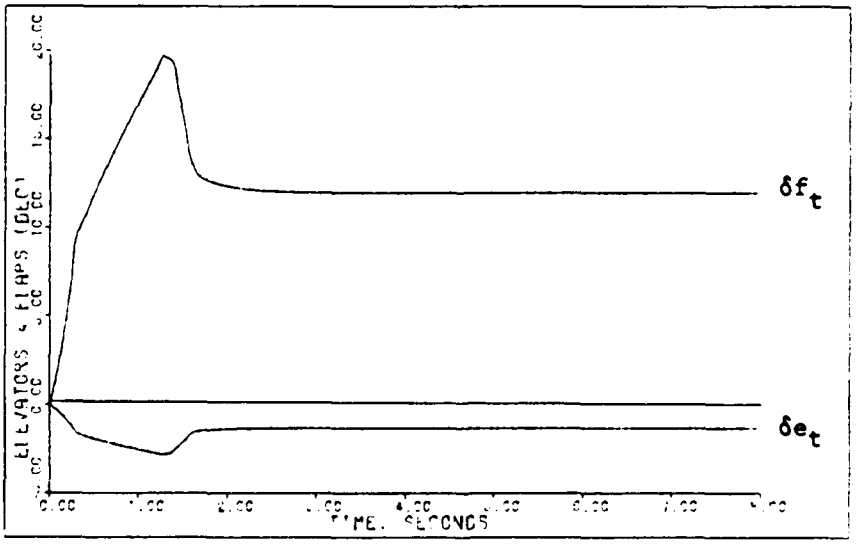

Figure D-70: 1.6M Healthy Longitudinal Translation -- Elevator and Flap Deflections

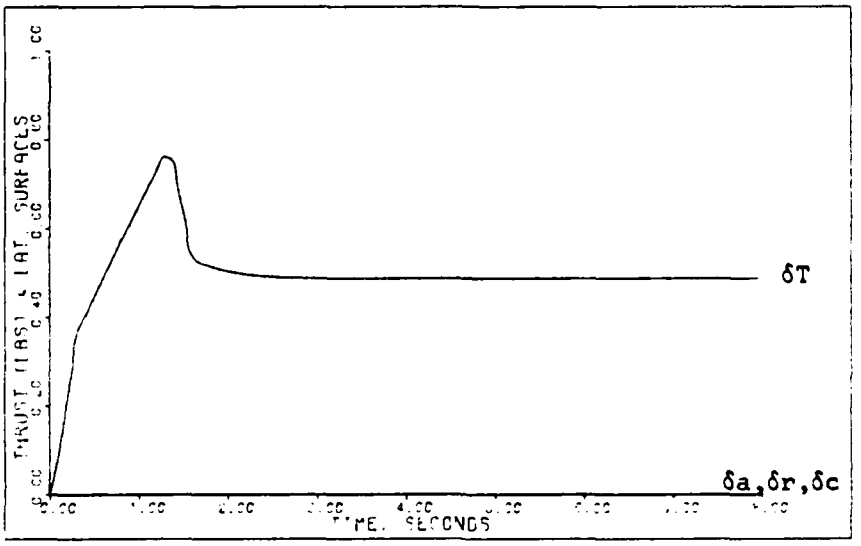

Figure D-71: 1.6M Healthy Longitudinal Translation -- Aileron, Rudder, and Canard Deflections and Thrust

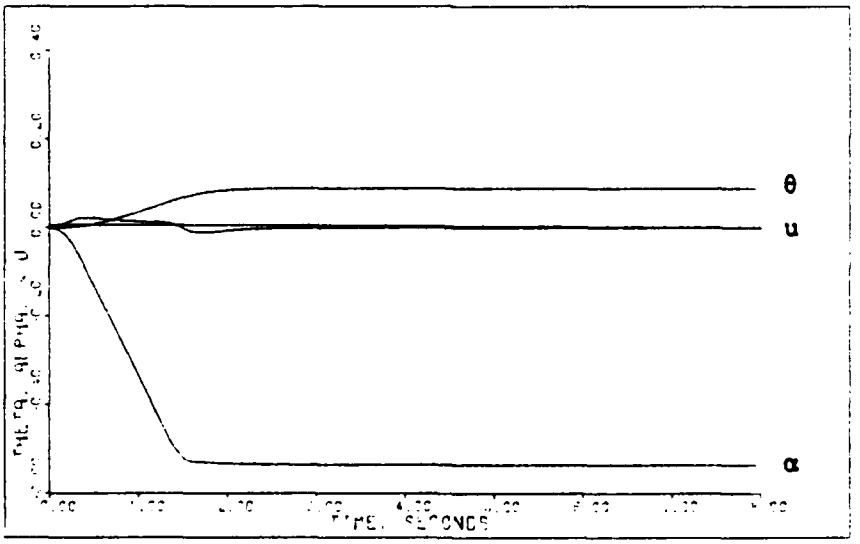

Figure D-72: 1.6M Failed Longitudinal Translation -- Pitch Angle, Angle of Attack, and Forward Velocity

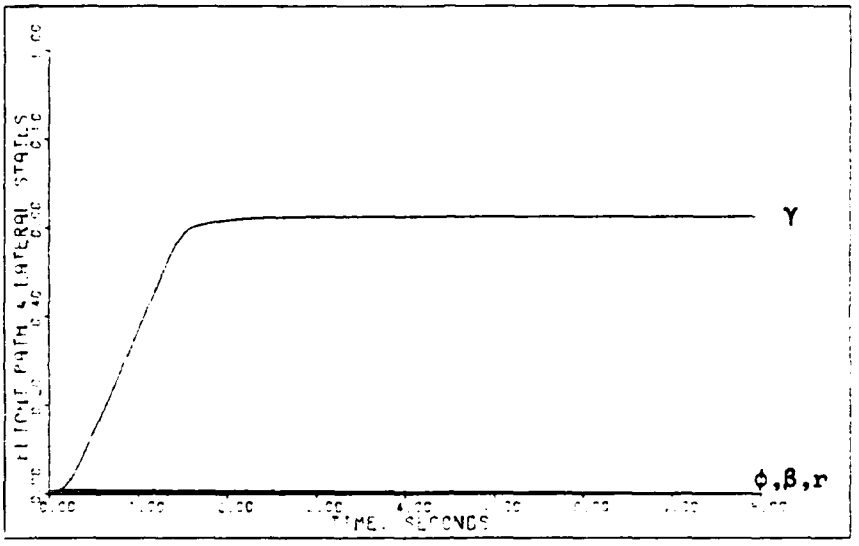

Figure D-73: 1.6M Failed Longitudinal Translation -- Flight Path Angle, Roll Angle, Sideslip Angle, and Yaw Rate

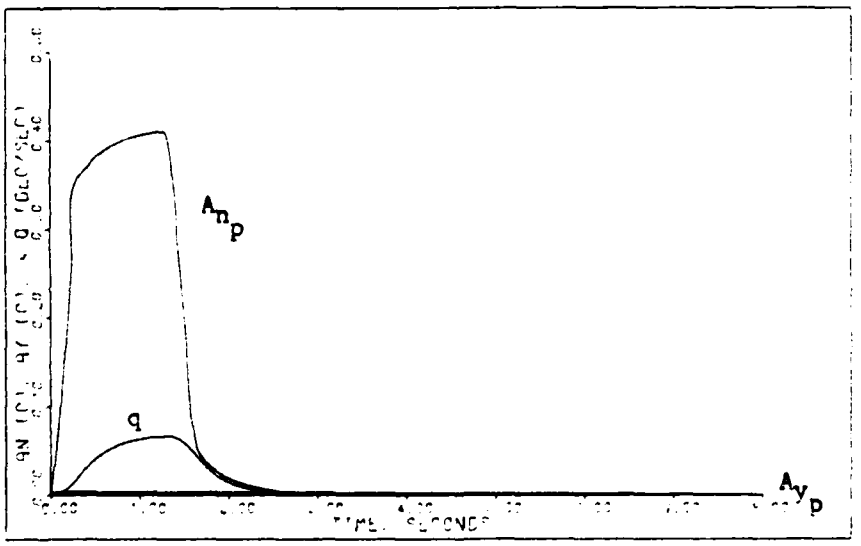

Figure D-74: 1.6M Failed Longitudinal Translation -- Normal Acceleration, Lateral Acceleration, and Pitch Rate

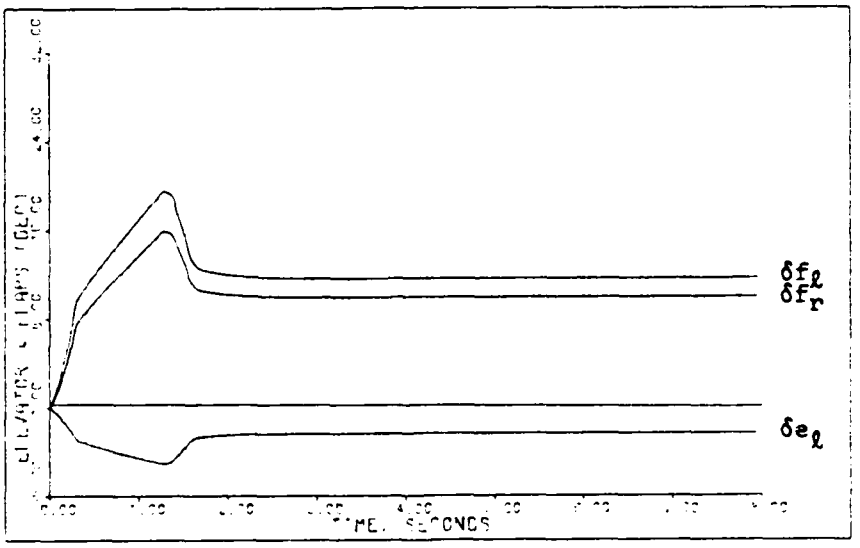

Figure D-75: 1.6M Failed Longitudinal Translation -- Left Elevator and Flaperon Deflections

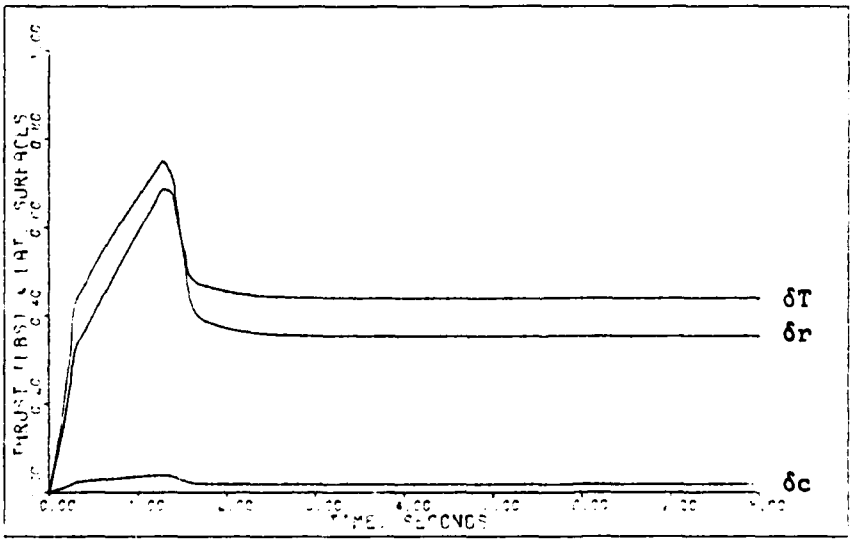

Figure D-76: 1.6M Failed Longitudinal Translation -- Rudder and Canard Deflections and Thrust

Roll About Velocity Vector Maneuver. As discussed in Chapter IV the roll maneuver requires some modification to the healthy and failure models. Tables D-21 and D-22, give the design parameters for the roll maneuver. The parameters are the same for the healthy and failed models; however, the roll rate commanded for the failure case is lowered from that of the healthy model in order not to overshoot the flaperon deflection limit.

The simulation responses for the healthy model roll maneuver are given in Figures D-77 through D-81, and the responses for the failed model are given in Figures D-82 through D-86. For the right horizontal tail case the flaperons deflect to achieve the commanded roll rate.

Table D-21

Roll About Velocity Vector: Healthy Model,
1.6 Mach at 30,000 Feet

Sampling Time: T = 0.02 second

$\bar{\alpha} = 1.0$

$\varepsilon = 1.0$

$\underline{\Sigma}$ = diag 2.0, 0.021, 1.8, 1.0, 1.0, 1.0

$$\underline{K}_0 = \begin{bmatrix} 0.0 & -0.6923E-04 & -0.1194E-01 & 0.1530E-03 & -0.2106E-05 & -0.1730E-03 \\ 0.0 & 0.3892E-03 & -0.8671E-01 & -0.2351E-03 & 0.3235E-05 & 0.2657E-03 \\ 0.0 & 0.0 & 0.0 & 0.1531E-01 & -0.6716E-02 & -0.2720E-01 \\ 0.0 & 0.0 & 0.0 & 0.3609E-01 & 0.5947E-02 & -0.9215E-01 \\ 0.0 & 0.0 & 0.0 & 0.1791E-01 & -0.2464E-03 & -0.2024E-01 \\ 0.2766E+01 & 0.1612E-01 & -0.2880E+01 & -0.1263E-01 & 0.1738E-03 & 0.1428E-01 \end{bmatrix}$$

$\underline{K}_1 = \underline{K}_0$

Input Ramp Time: 0.3 second

Command Vector:

$u = 0.0$

$A_{n_p} = 0.0$

$q = 0.0$

$A_{y_p} = 0.0$

$p = 3.491$ radians/second (3 second pulse)

$r-\alpha_T = 0.0$

Table D-22

Roll About Velocity Vector: Failed Model,
1.6 Mach at 30,000 Feet

Sampling Time: T = 0.02 second

$\bar{\alpha} = 1.0$

$\varepsilon = 1.0$

$\underline{\Sigma} = \text{diag}\{ 2.0, 0.021, 1.8, 1.0, 1.0, 1.0\}$

$$\underline{K}_0 = \begin{bmatrix} -0.5389E-16 & -0.1384E-03 & -0.2388E-01 & 0.3020E-03 & -0.2454E-05 & -0.3388E-03 \\ 0.0 & 0.3403E-03 & -0.9515E-01 & 0.2601E-01 & -0.1146E-01 & -0.4627E-01 \\ -0.4012E-15 & 0.4381E-03 & -0.7828E-01 & -0.2647E-01 & 0.1146E-01 & 0.4679E-01 \\ 0.2597E-15 & 0.2039E-04 & 0.3502E-02 & 0.3156E-01 & 0.7917E-02 & -0.8413E-01 \\ 0.6572E-16 & 0.1059E-05 & 0.1827E-03 & 0.1767E-01 & -0.1436E-03 & -0.1982E-01 \\ 0.2766E+01 & 0.1612E-01 & -0.2880E+01 & -0.1246E-01 & 0.1013E-03 & 0.1398E-01 \end{bmatrix}$$

$\underline{K}_1 = \underline{K}_0$

Input Ramp Time: 0.3 second

Command Vector:

$u = 0.0$

$A_{n_p} = 0.0$

$q = 0.0$

$A_{y_p} = 0.0$

$p = 2.182$ radians/second (3 second pulse)

$r - \alpha_T = 0.0$

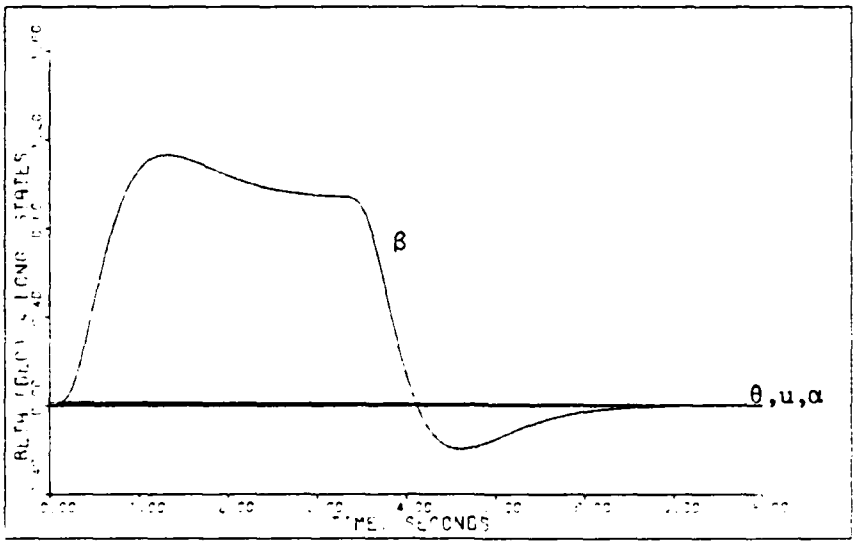

Figure D-77: 1.6M Healthy Roll -- Sideslip Angle, Pitch Angle, Angle of Attack, and Forward Velocity

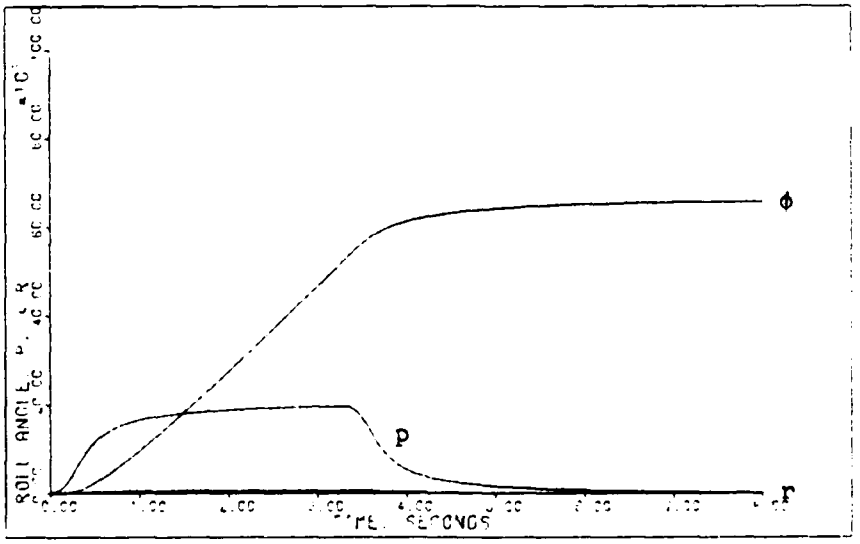

Figure D-78: 1.6M Healthy Roll -- Roll Angle, Roll Rate, and Yaw Rate

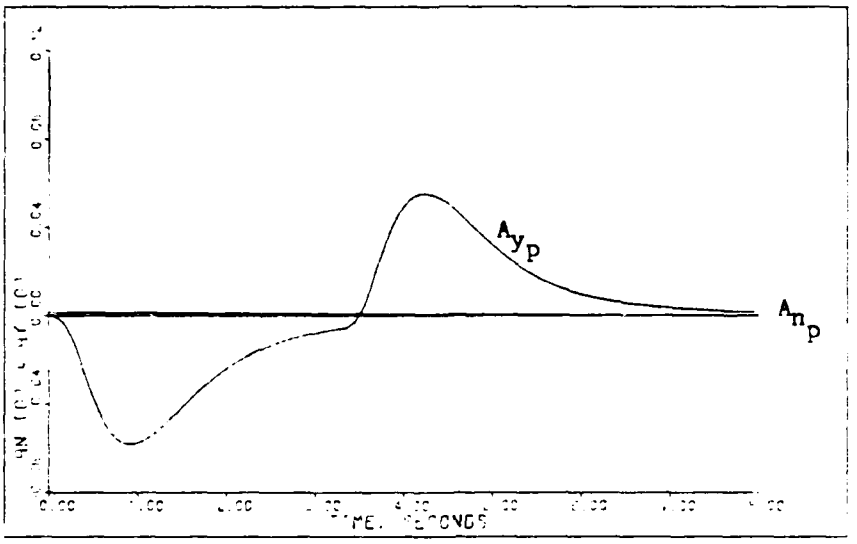

Figure D-79: 1.6M Healthy Roll -- Normal Acceleration and Lateral Acceleration

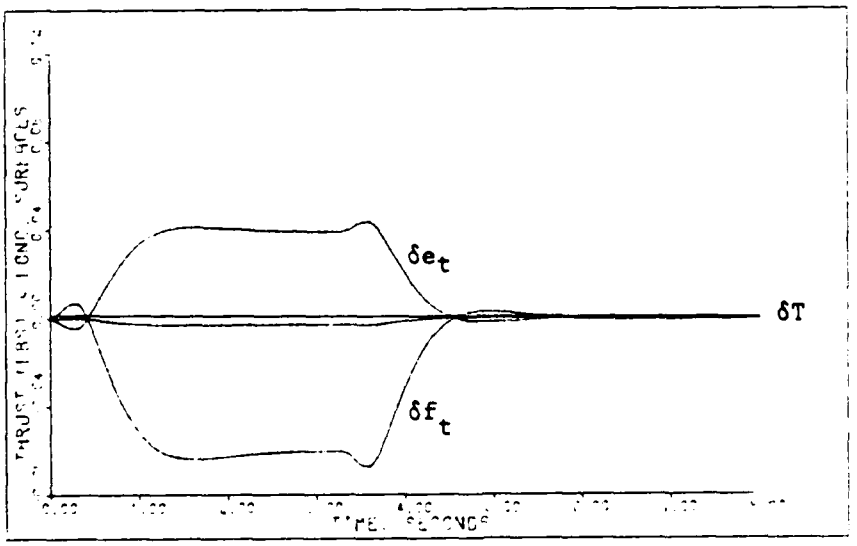

Figure D-80: 1.6M Healthy Roll -- Elevator and Flap Deflections, and Thrust

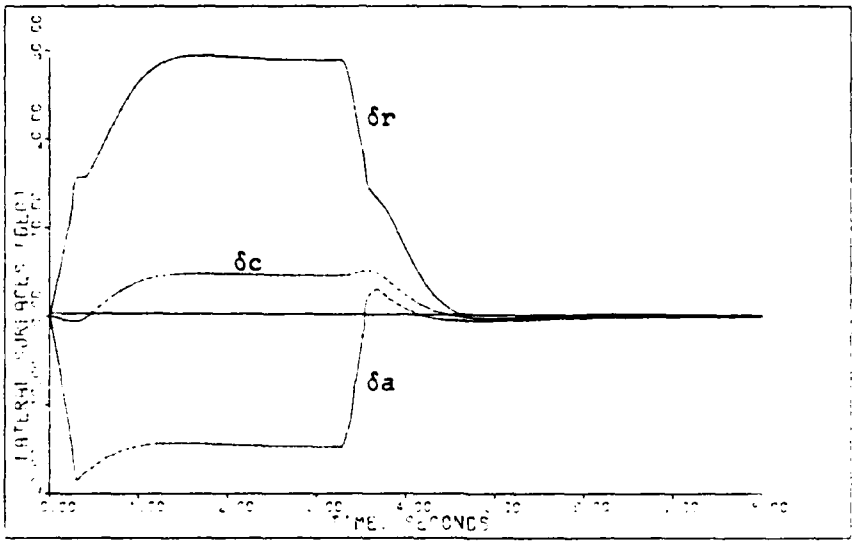

Figure D-81: 1.6M Healthy Roll -- Aileron, Rudder, and Canard Deflections

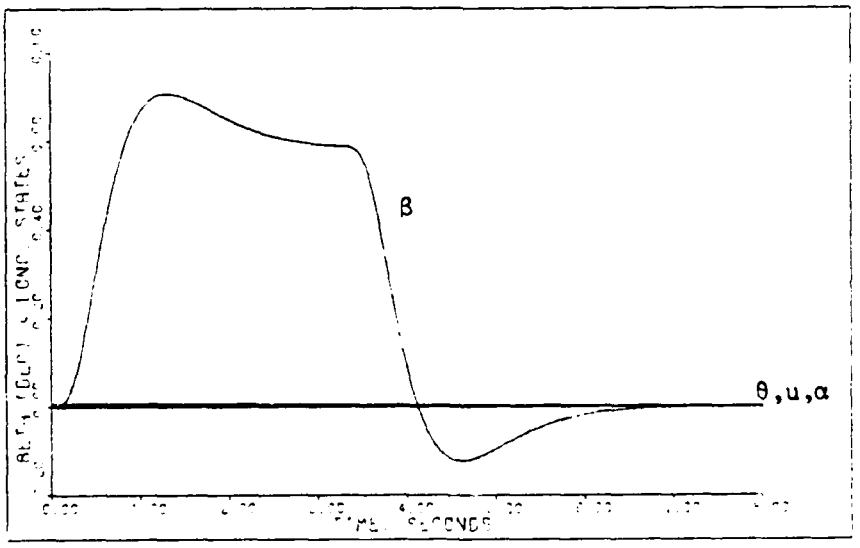

Figure D-82: 1.6M Failed Roll -- Sideslip Angle, Pitch Angle, Angle of Attack, and Forward Velocity

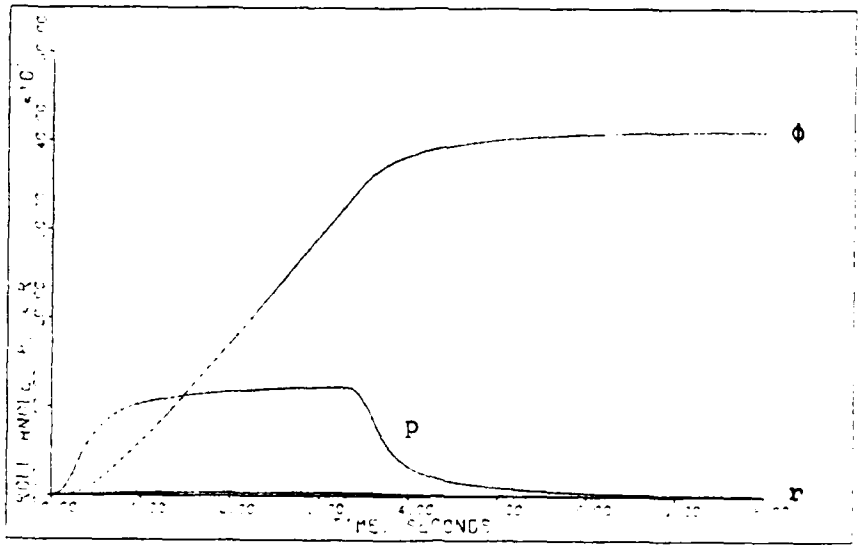

Figure D-83: 1.6M Failed Roll -- Roll Angle, Roll Rate, and Yaw Rate

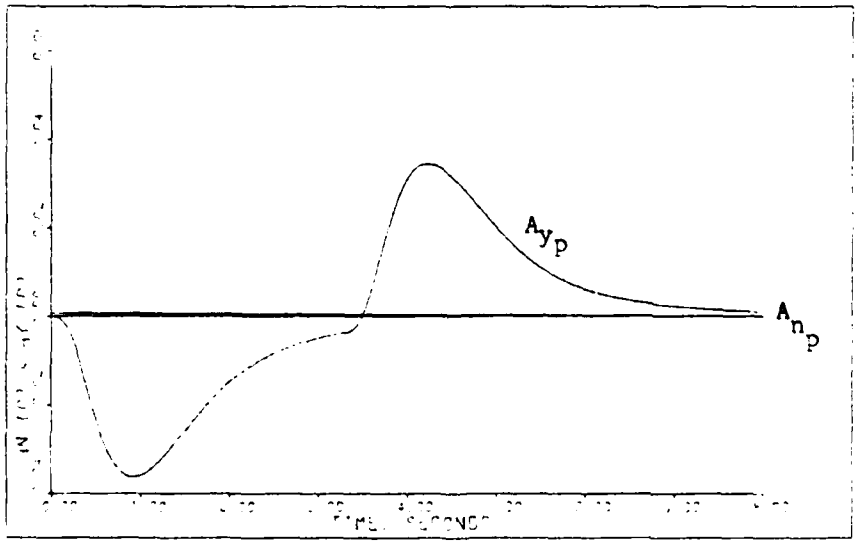

Figure D-84: 1.6M Failed Roll -- Normal Acceleration and Lateral Acceleration

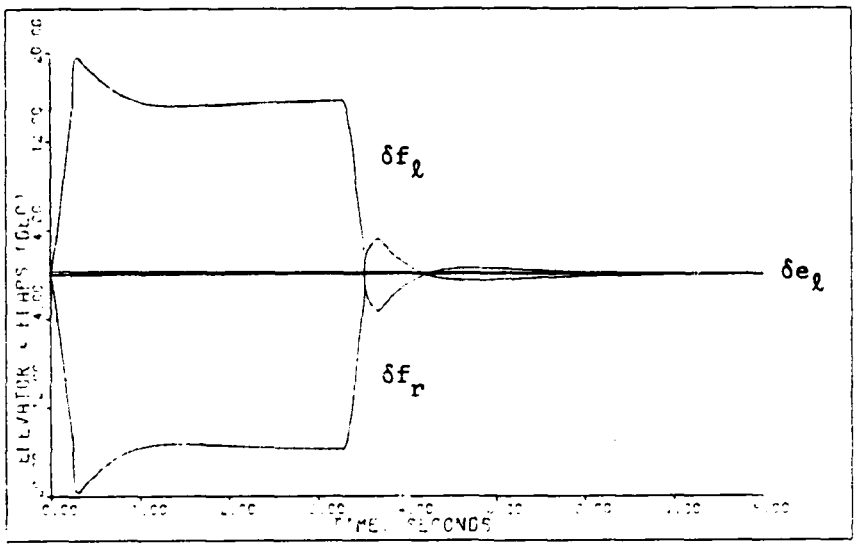

Figure D-85: 1.6M Failed Roll -- Left Elevator and Flaperon Deflections and Thrust

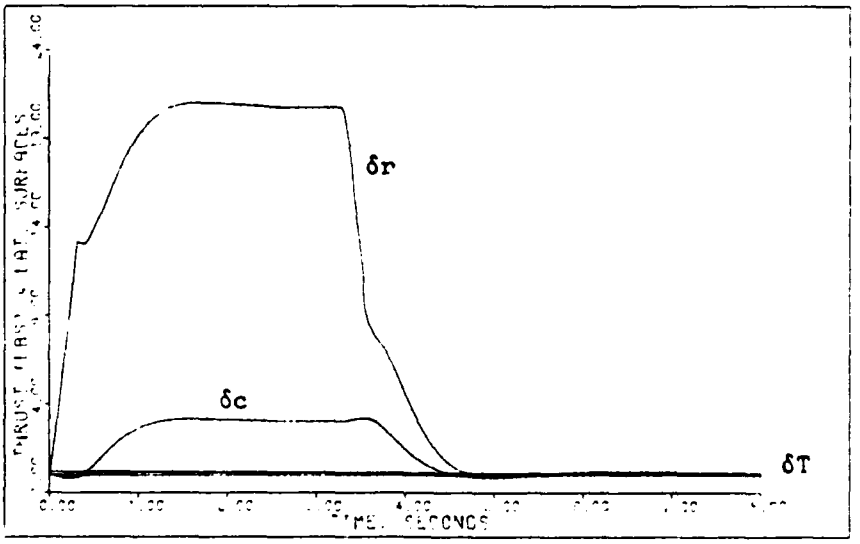

Figure D-86: 1.6M Failed Roll -- Rudder and Canard Deflections

Sideforce (Flat Turn) Maneuver. Tables D-23 and D-24 give the design parameters for both the healthy and failed cases of the sideforce maneuver. The same parameters are used for both cases.

Figures D-87 through D-93 present the simulation responses for a 0.6 g sideforce command. The maximum value commanded is limited by the rudder deflection. For this maneuver the longitudinal responses are very small for both the healthy and failure models. Also, the healthy aircraft lateral responses change very little when the right horizontal tail fails. for these reasons Figures D-87 through D-89 give simulation responses for both the healthy and failed aircraft models.

For this maneuver the horizontal tail is mainly used to counter the longitudinal pitching moment produced by the canard deflection although it also contributes to roll control for the healthy aircraft case. When the right horizontal tail fails the left horizontal tail deflects approximately twice the deflection of the healthy elevators. The flaperons deflect slightly asymmetrically to compensate for the roll created by the failed right horizontal tail. The rudder and canard deflections change only slightly for the failure case. For the same reasons given in the discussion of the supersonic pitch pointing maneuver, a negative thrust is generated. The negative thrust does not affect any of the other aircraft responses and is included in the model only to hold forward velocity constant.

Table D-23

Sideforce Maneuver: Healthy Model,
1.6 Mach at 30,000 Feet

Sampling Time: T = 0.02 second

$\bar{\alpha} = 3.5$

$\varepsilon = 1.0$

$\Sigma = \text{diag}\{ 2.0, 0.021, 1.8, 1.0, 1.0, 1.0 \}$

$$\underline{K}_0 = \begin{bmatrix} 0.0 & -0.6923E-04 & -0.1194E-01 & 0.1530E-03 & -0.2106E-05 & -0.1730E-03 \\ 0.0 & 0.3892E-03 & -0.8671E-01 & -0.2351E-03 & 0.3235E-05 & 0.2657E-03 \\ 0.0 & 0.0 & 0.0 & 0.1531E-01 & -0.6716E-02 & -0.2720E-01 \\ 0.0 & 0.0 & 0.0 & 0.3609E-01 & 0.5947E-02 & -0.9215E-01 \\ 0.0 & 0.0 & 0.0 & 0.1791E-01 & -0.2464E-03 & -0.2024E-01 \\ 0.2766E+01 & 0.1612E-01 & -0.2880E+01 & -0.1263E-01 & 0.1738E-03 & 0.1428E-01 \end{bmatrix}$$

$$\underline{K}_1 = \begin{bmatrix} 0.0 & -0.2423E-03 & -0.4179E-01 & 0.5356E-03 & -0.7370E-05 & -0.6055E-03 \\ 0.0 & 0.1362E-02 & -0.3035E+00 & -0.8228E-03 & 0.1132E-04 & 0.9301E-03 \\ 0.0 & 0.0 & 0.0 & 0.5360E-01 & -0.2351E-01 & -0.9518E-01 \\ 0.0 & 0.0 & 0.0 & 0.1263E+00 & 0.2081E-01 & -0.3225E+00 \\ 0.0 & 0.0 & 0.0 & 0.6268E-01 & -0.8624E-03 & -0.7085E-01 \\ 0.9682E+01 & 0.5643E-01 & -0.1008E+02 & -0.4421E-01 & 0.6083E-03 & 0.4998E-01 \end{bmatrix}$$

Input Ramp Time: 0.5 second

Command Vector:

$u = 0.0$

$A_{n_p} = 0.0$

$q = 0.0$

$A_{y_p} = 0.6$ g (step)

$p = 0.0$

$r = 0.01214$ radian/second (step)

Table D-24

Sideforce Maneuver: Failed Model,
1.6 Mach at 30,000 Feet

Sampling Time: T = 0.02 second

$\bar{\alpha} = 3.5$

$\varepsilon = 1.0$

$\Sigma = \text{diag}\{ 2.0,\ 0.021,\ 1.8,\ 1.0,\ 1.0,\ 1.0\}$

$$\underline{K}_0 = \begin{bmatrix} -0.5389E-16 & -0.1384E-03 & -0.2388E-01 & 0.3020E-03 & -0.2454E-05 & -0.3388E-03 \\ 0.0 & 0.3403E-03 & -0.9515E-01 & 0.2601E-01 & -0.1146E-01 & -0.4627E-01 \\ -0.4012E-15 & 0.4381E-03 & -0.7828E-01 & -0.2647E-01 & 0.1146E-01 & 0.4679E-01 \\ 0.2597E-15 & 0.2030E-04 & 0.3502E-02 & 0.3156E-01 & 0.7917E-02 & -0.8413E-01 \\ 0.6572E-16 & 0.1059E-05 & 0.1827E-03 & 0.1767E-01 & -0.1436E-03 & -0.1982E-01 \\ 0.2766E+01 & 0.1612E-01 & -0.2880E+01 & -0.1246E-01 & 0.1013E-03 & 0.1398E-01 \end{bmatrix}$$

$$\underline{K}_1 = \begin{bmatrix} -0.1886E-15 & -0.4845E-03 & -0.8357E-01 & 0.1057E-02 & -0.8588E-05 & -0.1186E-02 \\ 0.0 & 0.1191E-02 & -0.3330E+00 & 0.9103E-01 & -0.4011E-01 & -0.1619E+00 \\ -0.1404E-14 & 0.1533E-02 & -0.2740E+00 & -0.9265E-01 & 0.4012E-01 & 0.1638E+00 \\ 0.9089E-15 & 0.7106E-04 & 0.1226E-01 & 0.1104E+00 & 0.2771E-01 & -0.2944E+00 \\ 0.2300E-15 & 0.3707E-05 & 0.6394E-03 & 0.6185E-01 & -0.5025E-03 & -0.6938E-01 \\ 0.9682E+01 & 0.5643E-01 & -0.1008E+02 & -0.4363E-01 & 0.3544E-03 & 0.4894E-01 \end{bmatrix}$$

Input Ramp Time: 0.5 second

Command Vector:

$u = 0.0$

$A_{n_p} = 0.0$

$q = 0.0$

$A_{y_p} = 0.6$ g (step)

$p = 0.0$

$r = 0.01214$ radian/second (step)

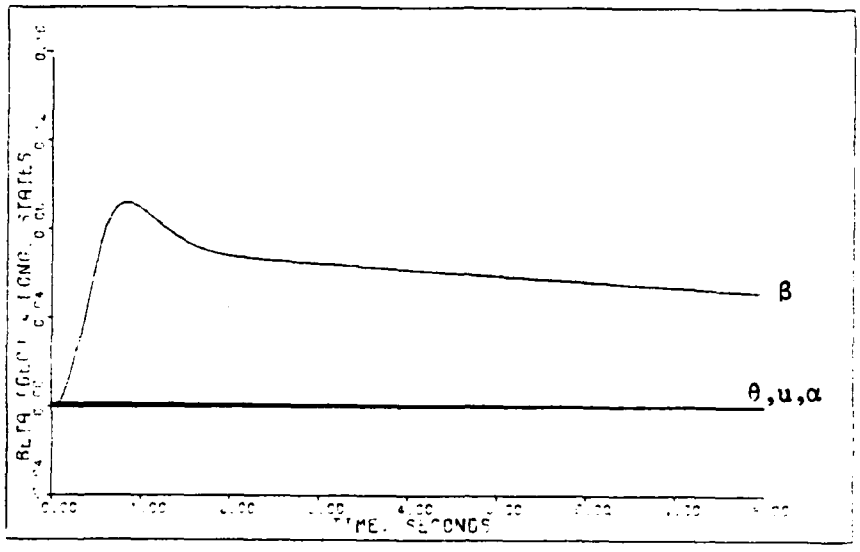

Figure D-87: 1.6M Healthy/Failed Sideforce -- Sideslip Angle, Pitch Angle, Angle of Attack, and Forward Velocity

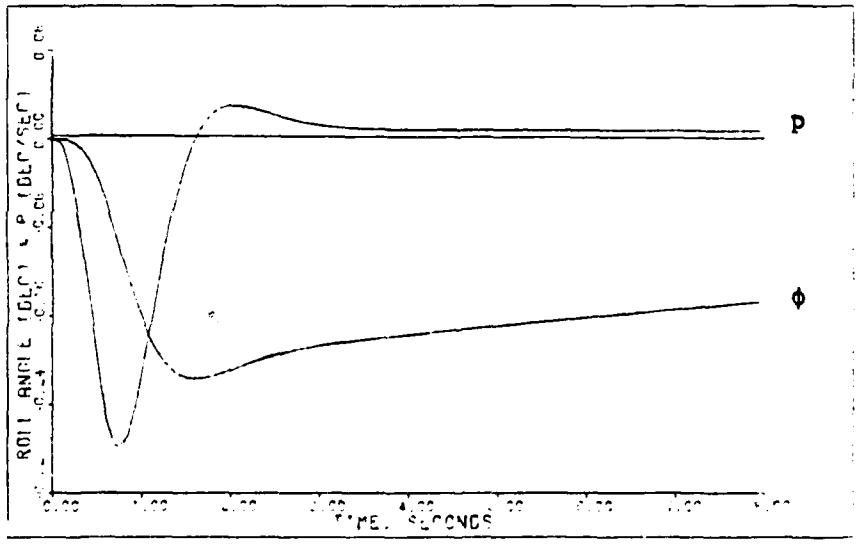

Figure D-88: 1.6M Healthy/Failed Sideforce -- Roll Angle and Roll Rate

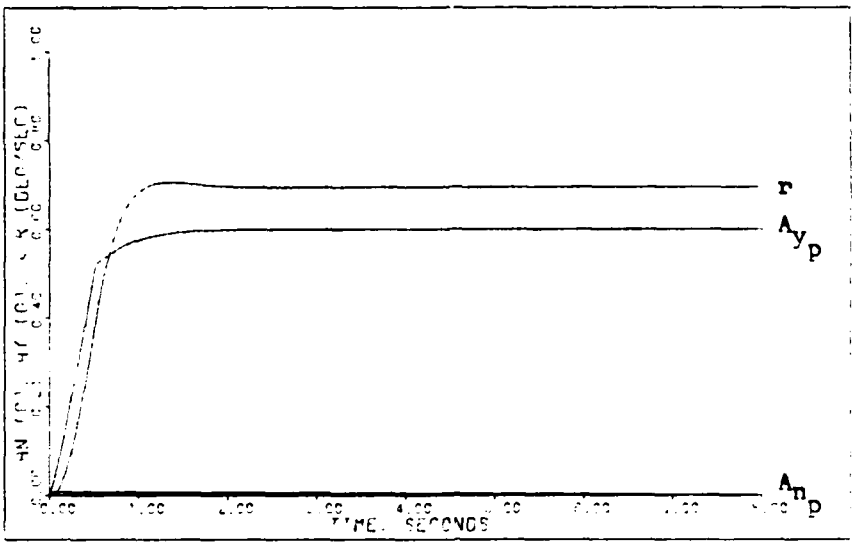

Figure D-89: 1.6M Healthy/Failed Sideforce -- Normal Acceleration, Lateral Acceleration, and Yaw Rate

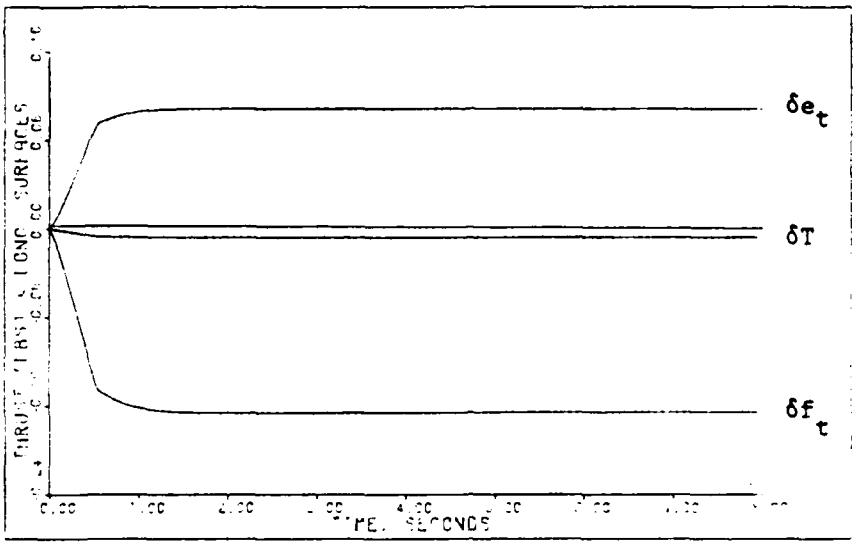

Figure D-90: 1.6M Healthy Sideforce -- Elevator and Flap Deflections and Thrust

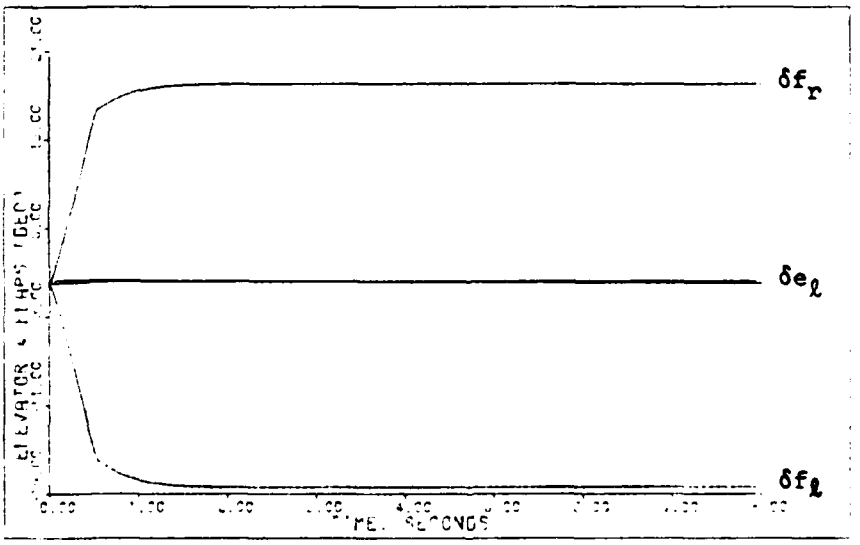

Figure D-91: 1.6M Failed Sideforce -- Left Elevator and Flaperon Deflections

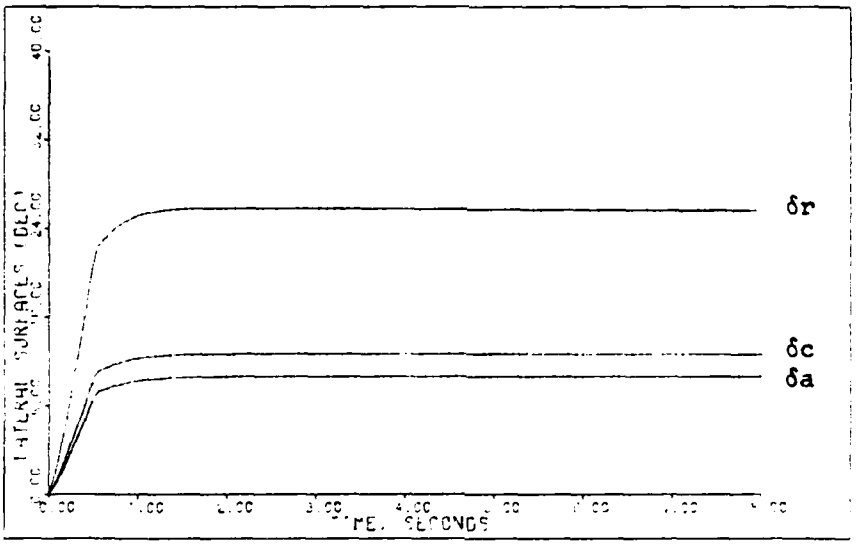

Figure D-92: 1.6M Healthy Sideforce -- Aileron, Rudder, and Canard Deflections

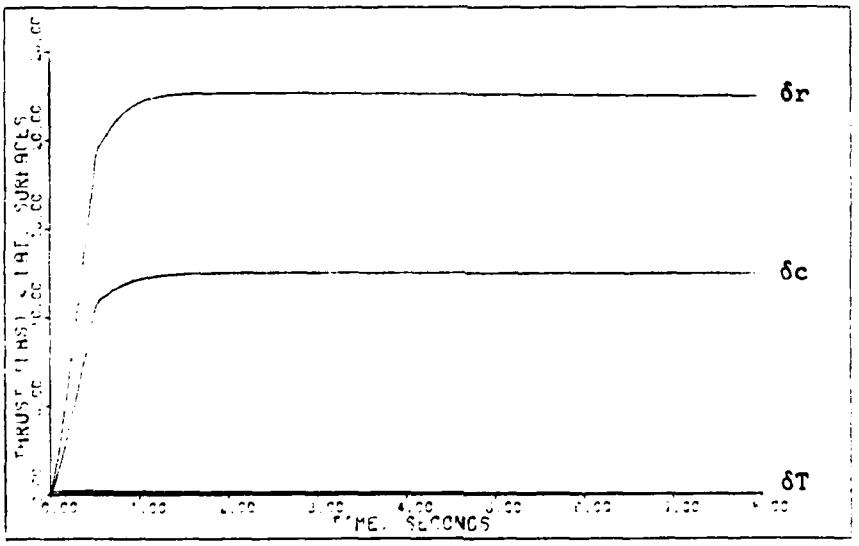

Figure D-93: 1.6M Failed Sideforce -- Rudder and Canard Deflections and Thrust

Yaw Pointing Maneuver. The design parameters for the yaw pointing maneuver are given in Tables D-25 and D-26 for both the healthy and failed models. The parameters are the same for both cases.

Figures D-94 through D-100 present the simulation responses for a one degree yaw pointing command. The maximum angle commanded for this maneuver is limited by the ability to hold the roll angle to a small value. As with the sideforce maneuver Figures D-94 through D-96 give simulation responses for both the healthy and failed aircraft models.

For the yaw pointing maneuver the horizontal tail is used mainly for roll control. When the right horizontal tail fails the flaperons take over the roll control. The rudder and canard responses are not affected much by the failure for this maneuver. As explained in the discussion of the supersonic pitch pointing maneuver, the negative thrust does not affect the simulation responses of interest.

Table D-25

Yaw Pointing: Healthy Model, 1.6 Mach at 30,000 Feet

Sampling Time: T = 0.02 second

$\bar{\alpha} = 5.5$

$\varepsilon = 1.0$

$\underline{\Sigma} = \text{diag}\{ 2.0, 0.021, 1.8, 1.0, 2.0, 3.1\}$

$$\underline{K}_0 = \begin{bmatrix} 0.0 & -0.6923E-04 & -0.1194E-01 & 0.1530E-03 & -0.4212E-05 & -0.5363E-03 \\ 0.0 & 0.3892E-03 & -0.8671E-01 & -0.2351E-03 & 0.6470E-05 & 0.8238E-03 \\ 0.0 & 0.0 & 0.0 & 0.1531E-01 & -0.1343E-01 & -0.8430E-01 \\ 0.0 & 0.0 & 0.0 & 0.3609E-01 & 0.1189E-01 & -0.2857E+00 \\ 0.0 & 0.0 & 0.0 & 0.1791E-01 & -0.4928E-03 & -0.6275E-01 \\ 0.2766E+01 & 0.1612E-01 & -0.2880E+01 & -0.1263E-01 & 0.3476E-03 & 0.4427E-01 \end{bmatrix}$$

$$\underline{K}_1 = \begin{bmatrix} 0.0 & -0.3808E-03 & -0.6567E-01 & 0.8417E-03 & -0.2316E-04 & -0.2950E-02 \\ 0.0 & 0.2141E-02 & -0.4769E+00 & -0.1293E-02 & 0.3558E-04 & 0.4531E-02 \\ 0.0 & 0.0 & 0.0 & 0.8423E-01 & -0.7388E-01 & -0.4637E+00 \\ 0.0 & 0.0 & 0.0 & 0.1985E+00 & 0.6542E-01 & -0.1571E+01 \\ 0.0 & 0.0 & 0.0 & 0.9849E-01 & -0.2710E-02 & -0.3451E+00 \\ 0.1521E+02 & 0.8868E-01 & -0.1584E+02 & -0.6948E-01 & 0.1912E-02 & 0.2435E+00 \end{bmatrix}$$

Input Ramp Time: 0.2 second

Command Vector:

$u = 0.0$

$A_{n_p} = 0.0$

$q = 0.0$

$A_{y_p} = 0.0$

$p = 0.0$

$r = -0.01745$ radian/second (1 second pulse)

Table D-26

Yaw Pointing: Failed Model, 1.6 Mach at 30,000 Feet

Sampling Time: T = 0.02 second

$\bar{\alpha} = 5.5$

$\epsilon = 1.0$

$\underline{\Sigma} = \text{diag}\{ 2.0, 0.021, 1.8, 1.0, 2.0, 3.1\}$

$$\underline{K}_0 = \begin{bmatrix} -0.2964E-15 & -0.7614E-03 & -0.1313E+00 & 0.1661E-02 & -0.2699E-04 & -0.5777E-02 \\ 0.0 & 0.1872E-02 & -0.5233E+00 & 0.1430E+00 & -0.1261E+00 & -0.7888E+00 \\ -0.2207E-14 & 0.2410E-02 & -0.4305E+00 & -0.1456E+00 & 0.1261E+00 & 0.7977E+00 \\ 0.1428E-14 & 0.1117E-03 & 0.1926E-01 & 0.1736E+00 & 0.8709E-01 & -0.1434E+01 \\ 0.3615E-15 & 0.5825E-05 & 0.1005E-02 & 0.9719E-01 & -0.1579E-02 & -0.3380E+00 \\ 0.1521E+02 & 0.8868E-01 & -0.1584E+02 & -0.6856E-01 & 0.1114E-02 & 0.2384E+00 \end{bmatrix}$$

$$\underline{K}_1 = \begin{bmatrix} -0.5389E-16 & -0.1384E-03 & -0.2388E-01 & 0.3020E-03 & -0.4908E-05 & -0.1050E-02 \\ 0.0 & 0.3403E-03 & -0.9515E-01 & 0.2601E-01 & -0.2292E-01 & -0.1434E+00 \\ -0.4012E-15 & 0.4381E-03 & -0.7828E-01 & -0.2647E-01 & 0.2293E-01 & 0.1450E+00 \\ 0.2597E-15 & 0.2030E-04 & 0.3502E-02 & 0.3156E-01 & 0.1583E-01 & -0.2608E+00 \\ 0.6572E-16 & 0.1059E-05 & 0.1827E-03 & 0.1767E-01 & -0.2871E-03 & -0.6145E-01 \\ 0.2766E+01 & 0.1612E-01 & -0.2880E+01 & -0.1246E-01 & 0.2025E-03 & 0.4335E-01 \end{bmatrix}$$

Input Ramp Time: 0.2 second

Command Vector:

$u = 0.0$

$A_{n_p} = 0.0$

$q = 0.0$

$A_{y_p} = 0.0$

$p = 0.0$

$r = -0.01745$ radian/second (1 second pulse)

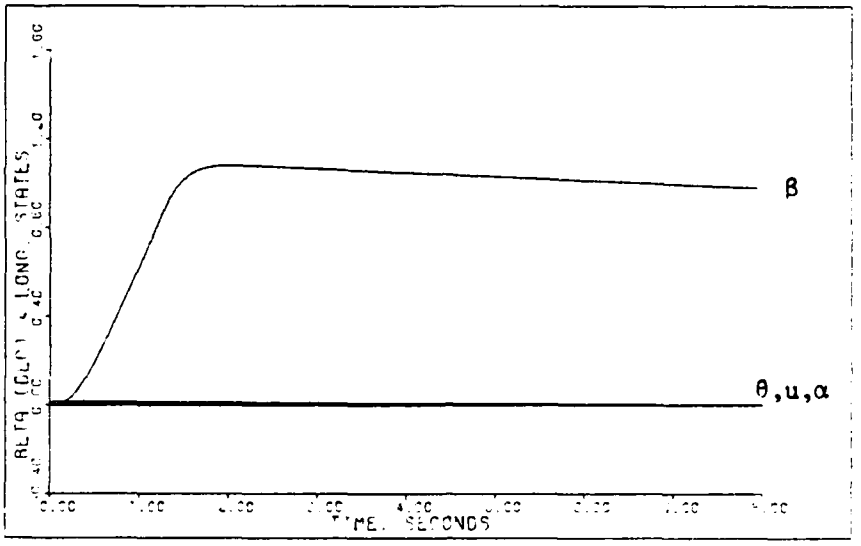

Figure D-94: 1.6M Healthy/Failed Yaw Pointing -- Sideslip Angle, Pitch Angle, Angle of Attack, and Forward Velocity

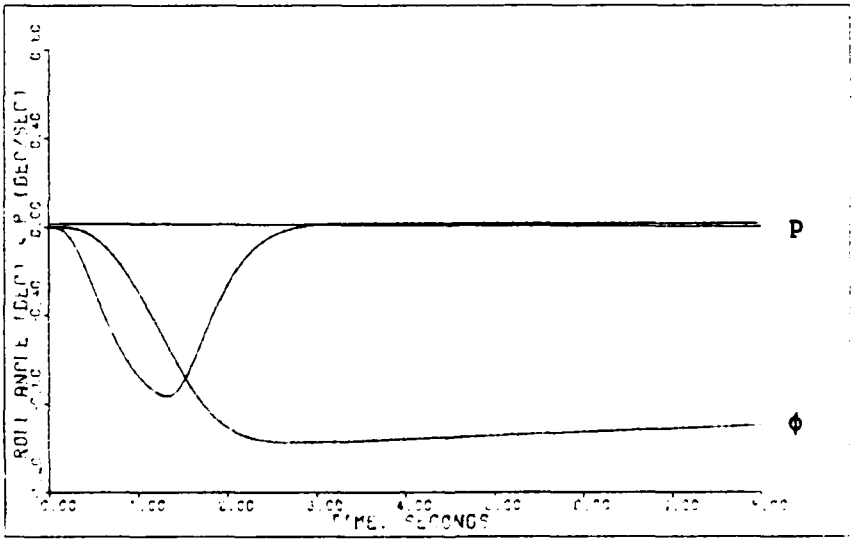

Figure D-95: 1.6M Healthy/Failed Yaw Pointing -- Roll Angle and Roll Rate

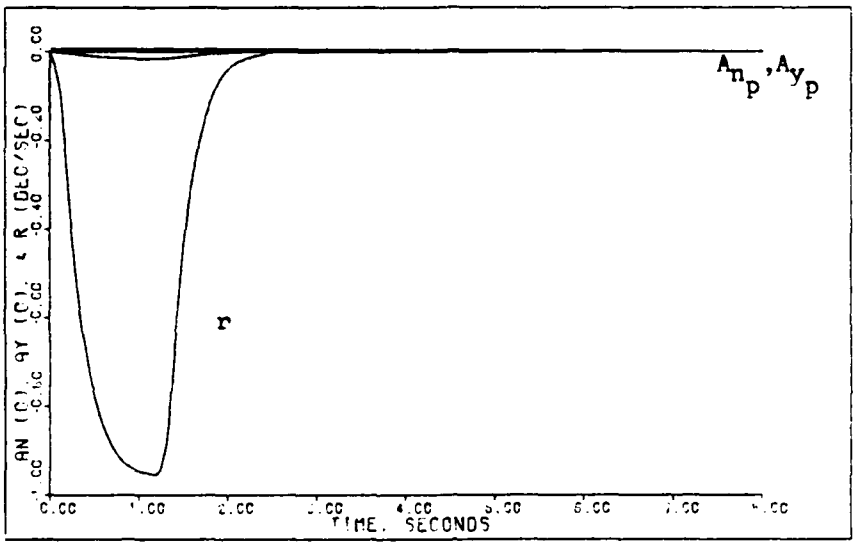

Figure D-96: 1.6M Healthy/Failed Yaw Pointing -- Normal Acceleration, Lateral Acceleration, and Yaw Rate

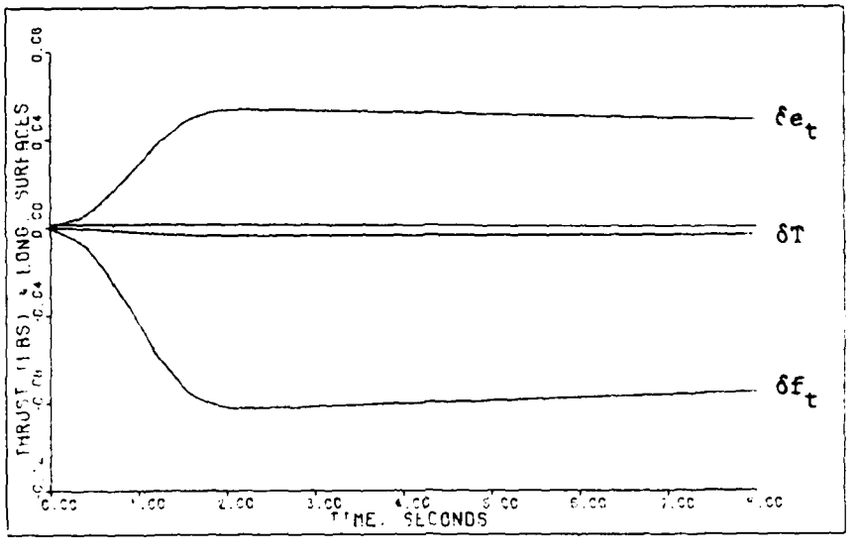

Figure D-97: 1.6M Healthy Yaw Pointing -- Elevator and Flap Deflections and Thrust

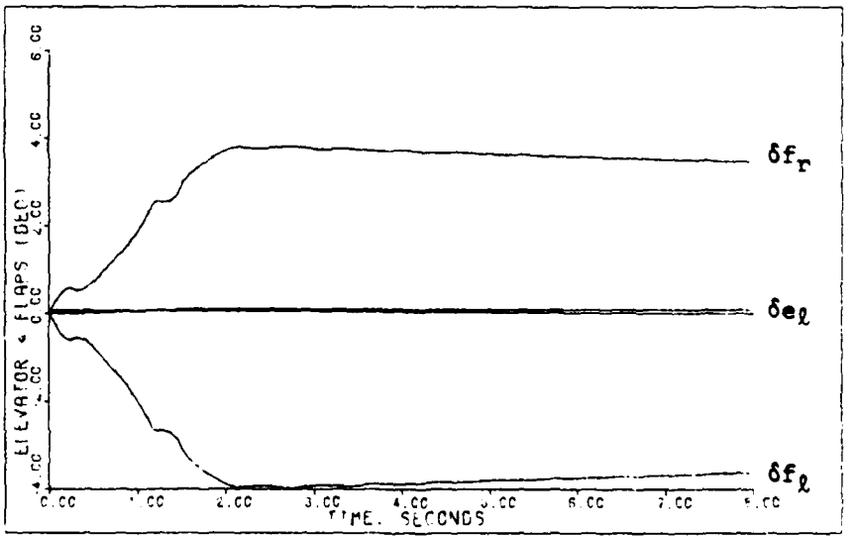

Figure D-98: 1.6M Failed Yaw Pointing -- Left Elevator and Flaperon Deflections

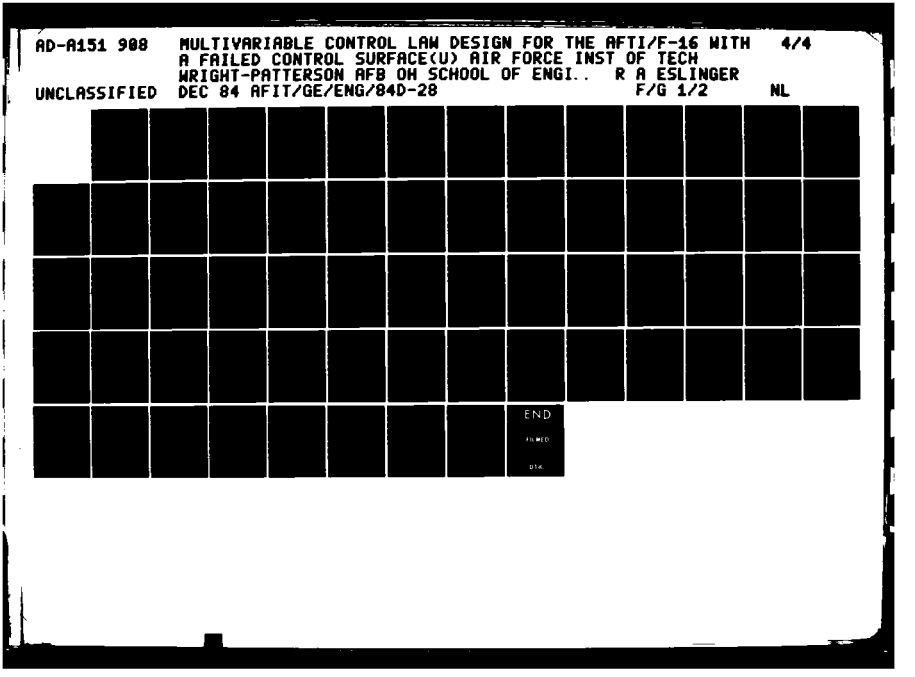
AD-A151 908 MULTIVARIABLE CONTROL LAW DESIGN FOR THE AFTI/F-16 WITH 4/4
A FAILED CONTROL SURFACE(U) AIR FORCE INST OF TECH
WRIGHT-PATTERSON AFB OH SCHOOL OF ENGI.. R A ESLINGER
UNCLASSIFIED DEC 84 AFIT/GE/ENG/84D-28 F/G 1/2 NL
END
FILMED
DTIC

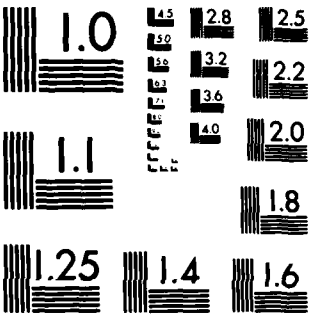

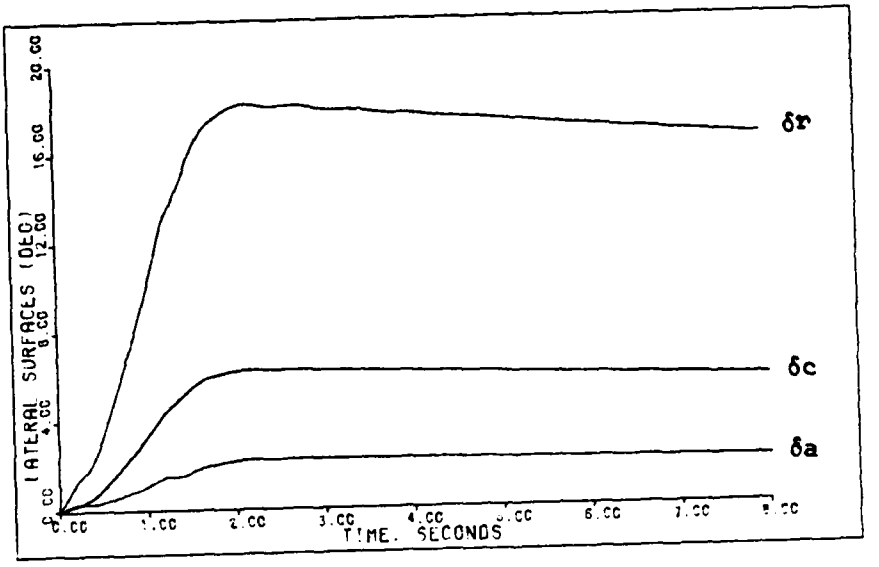

Figure D-99: 1.6M Healthy Yaw Pointing -- Aileron, Rudder, and Canard Deflections

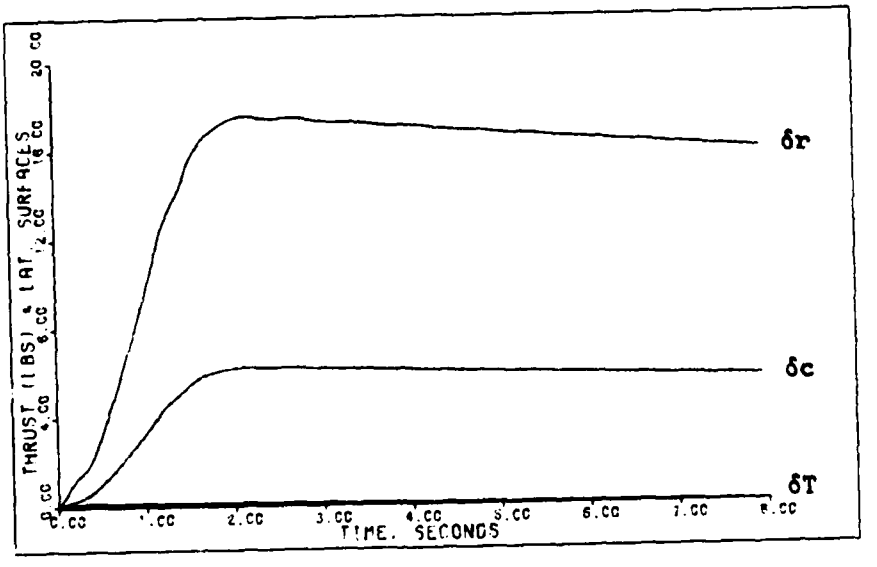

Figure D-100: 1.6M Failed Yaw Pointing -- Rudder and Canard Deflections and Thrust

Lateral Translation Maneuver. Tables D-27 and D-28 give the design parameters for the lateral translation maneuver. As indicated in the tables the same design parameters are used for both the healthy and failed aircraft models.

The simulation responses for a 0.45 g lateral acceleration command, which corresponds to a steady-state lateral velocity value of 21.7 feet/second, are given in Figures D-101 through D-107. The maximum lateral acceleration commanded for this maneuver is limited by the rudder deflection. As explained for the sideforce maneuver, Figures D-101 through D-103 give simulation responses for both the healthy and failed aircraft models.

For the lateral translation maneuver the horizontal tail is used mainly for roll control. When the right horizontal tail fails the flaperons take over complete roll control The rudder and canard responses are not affected much by the failure for this maneuver.

Table D-27

Lateral Translation: Healthy Model,
1.6 Mach at 30,000 Feet

Sampling Time: T = 0.02 second

$\bar{\alpha} = 3.5$

$\varepsilon = 1.0$

$\underline{\Sigma} = \text{diag}\{ 2.0, 0.021, 1.8, 0.9, 1.8, 2.9 \}$

$$\underline{K}_0 = \begin{bmatrix} 0.0 & -0.6923E-04 & -0.1194E-01 & 0.1377E-03 & -0.3790E-05 & -0.5017E-03 \\ 0.0 & 0.3892E-03 & -0.8671E-01 & -0.2116E-03 & 0.5823E-05 & 0.7707E-03 \\ 0.0 & 0.0 & 0.0 & 0.1378E-01 & -0.1209E-01 & -0.7887E-01 \\ 0.0 & 0.0 & 0.0 & 0.3248E-01 & 0.1070E-01 & -0.2672E+00 \\ 0.0 & 0.0 & 0.0 & 0.1612E-01 & -0.4435E-03 & -0.5870E-01 \\ 0.2766E+01 & 0.1612E-01 & -0.2880E+01 & -0.1137E-01 & 0.3129E-03 & 0.4141E-01 \end{bmatrix}$$

$$\underline{K}_1 = \begin{bmatrix} 0.0 & -0.2423E-03 & -0.4179E-01 & 0.4821E-03 & -0.1327E-04 & -0.1756E-02 \\ 0.0 & 0.1362E-02 & -0.3035E+00 & -0.7406E-03 & 0.2038E-04 & 0.2697E-02 \\ 0.0 & 0.0 & 0.0 & 0.4824E-01 & -0.4231E-01 & -0.2760E+00 \\ 0.0 & 0.0 & 0.0 & 0.1137E+00 & 0.3747E-01 & -0.9354E+00 \\ 0.0 & 0.0 & 0.0 & 0.5641E-01 & -0.1552E-02 & -0.2055E+00 \\ 0.9682E+01 & 0.5643E-01 & -0.1008E+02 & -0.3979E-01 & 0.1095E-02 & 0.1449E+00 \end{bmatrix}$$

Input Ramp Time: 0.5 second

Command Vector:

$u = 0.0$

$A_{n_p} = 0.0$

$q = 0.0$

$A_{y_p} = 0.45$ g (1 second pulse)

$p = 0.0$

$r = 0.0$

Table D-28

Lateral Translation: Failed Model,
1.6 Mach at 30,000 Feet

Sampling Time: T = 0.02 second

$\bar{\alpha} = 3.5$

$\epsilon = 1.0$

$\underline{\Sigma} = \text{diag}\{\ 2.0,\ 0.021,\ 1.8,\ 0.9,\ 1.8,\ 2.9\ \}$

$$\underline{K}_0 = \begin{bmatrix} -0.5389E-16 & -0.1384E-03 & -0.2388E-01 & 0.2718E-03 & -0.4417E-05 & -0.9826E-03 \\ 0.0 & 0.3403E-03 & -0.9515E-01 & 0.2341E-01 & -0.2063E-01 & -0.1342E+00 \\ -0.4012E-15 & 0.4381E-03 & -0.7828E-01 & -0.2383E-01 & 0.2063E-01 & 0.1357E+00 \\ 0.2597E-15 & 0.2030E-04 & 0.3502E-02 & 0.2840E-01 & 0.1425E-01 & -0.2440E+00 \\ 0.6572E-16 & 0.1059E-05 & 0.1827E-03 & 0.1590E-01 & -0.2584E-03 & -0.5749E-01 \\ 0.2766E+01 & 0.1612E-01 & -0.2880E+01 & -0.1122E-01 & 0.1823E-03 & 0.4055E-01 \end{bmatrix}$$

$$\underline{K}_1 = \begin{bmatrix} -0.1886E-15 & -0.4845E-03 & -0.8357E-01 & 0.9514E-03 & -0.1546E-04 & -0.3439E-02 \\ 0.0 & 0.1191E-02 & -0.3330E+00 & 0.8193E-01 & -0.7220E-01 & -0.4696E+00 \\ -0.1404E-14 & 0.1533E-02 & -0.2740E+00 & -0.8339E-01 & 0.7222E-01 & 0.4749E+00 \\ 0.9089E-15 & 0.7106E-04 & 0.1226E-01 & 0.9940E-01 & 0.4988E-01 & -0.8539E+00 \\ 0.2300E-15 & 0.3707E-05 & 0.6394E-03 & 0.5566E-01 & -0.9045E-03 & -0.2012E+00 \\ 0.9682E+01 & 0.5643E-01 & -0.1008E+02 & -0.3926E-01 & 0.6380E-03 & 0.1419E+00 \end{bmatrix}$$

Input Ramp Time: 0.5 second

Command Vector:

$u = 0.0$

$A_{n_p} = 0.0$

$q = 0.0$

$A_{y_p} = 0.45$ g (1 second pulse)

$p = 0.0$

$r = 0.0$

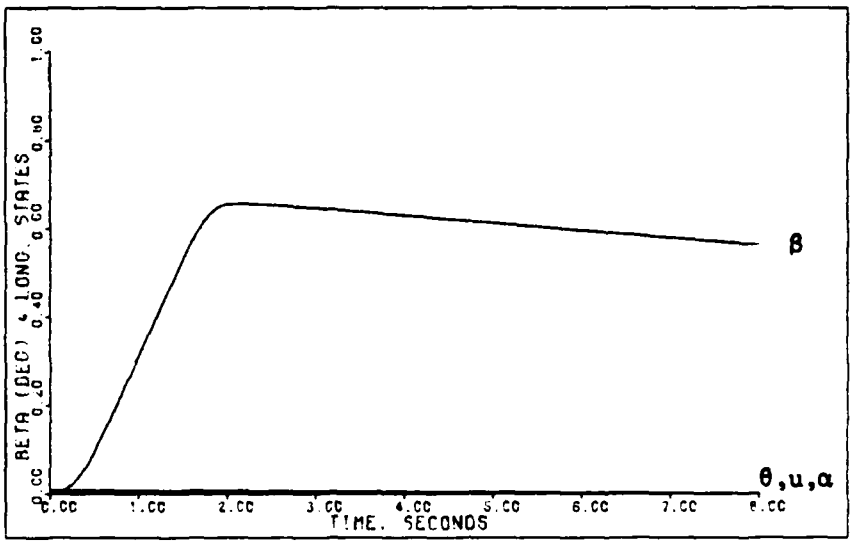

Figure D-101: 1.6M Healthy/Failed Lateral Translation -- Sideslip Angle, Pitch Angle, Angle of Attack, and Forward Velocity

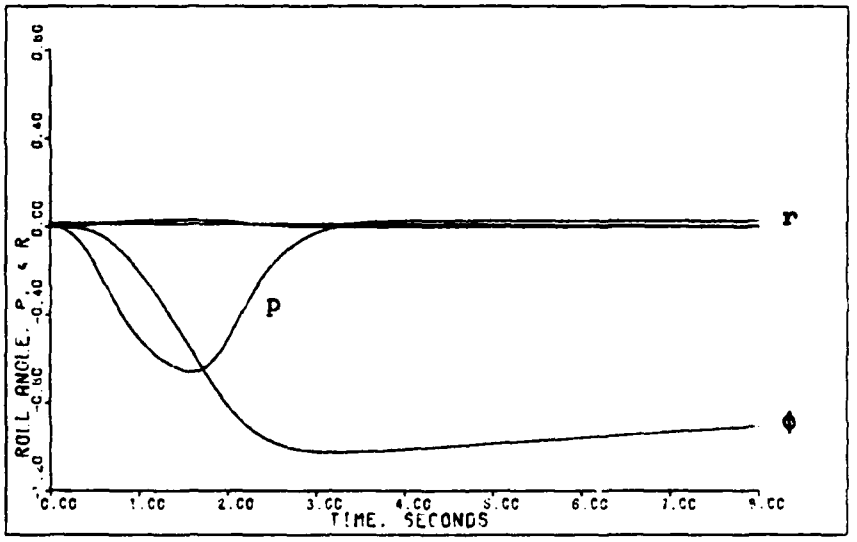

Figure D-102: 1.6M Healthy/Failed Lateral Translation -- Roll Angle, Roll Rate, and Yaw Rate

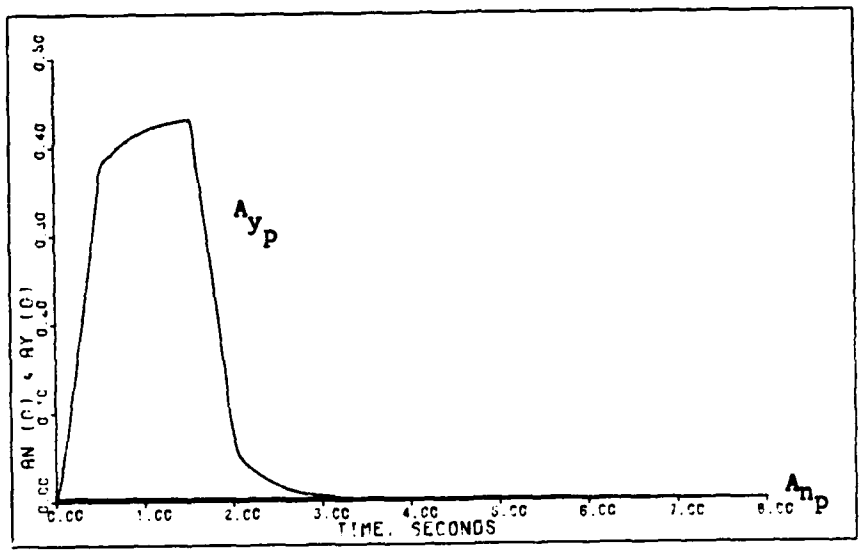

Figure D-103: 1.6M Healthy/Failed Lateral Translation -- Normal Acceleration and Lateral Acceleration

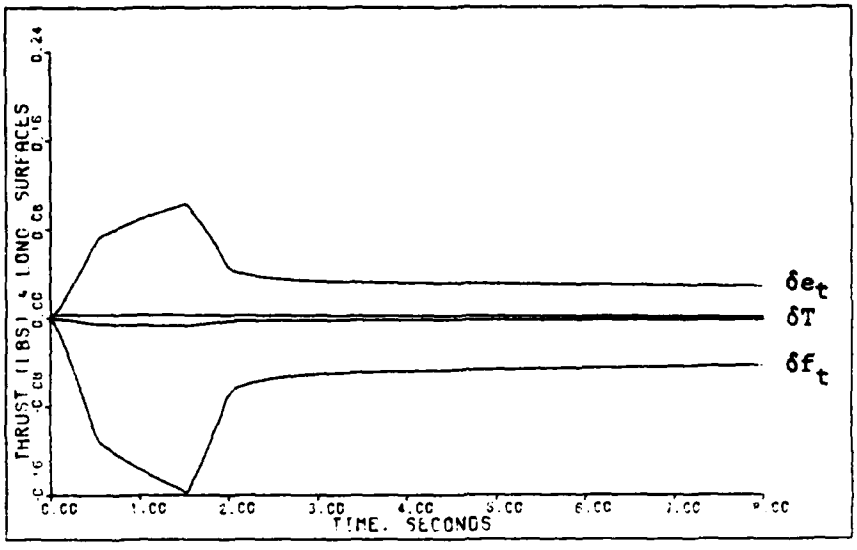

Figure D-104: 1.6M Healthy Lateral Translation -- Elevator and Flap Deflections and Thrust

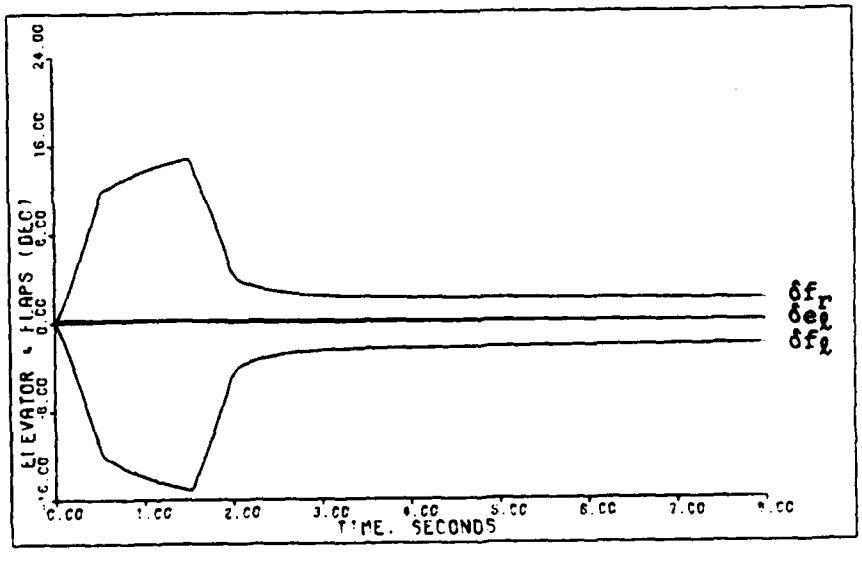

Figure D-105: 1.6M Failed Lateral Translation -- Left Elevator and Flaperon Deflections

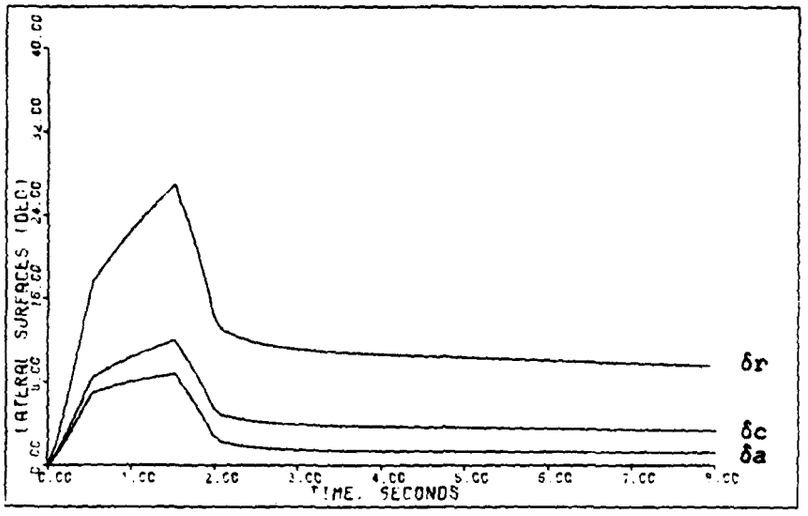

Figure D-106: 1.6M Healthy Lateral Translation -- Aileron, Rudder, and Canard Deflections

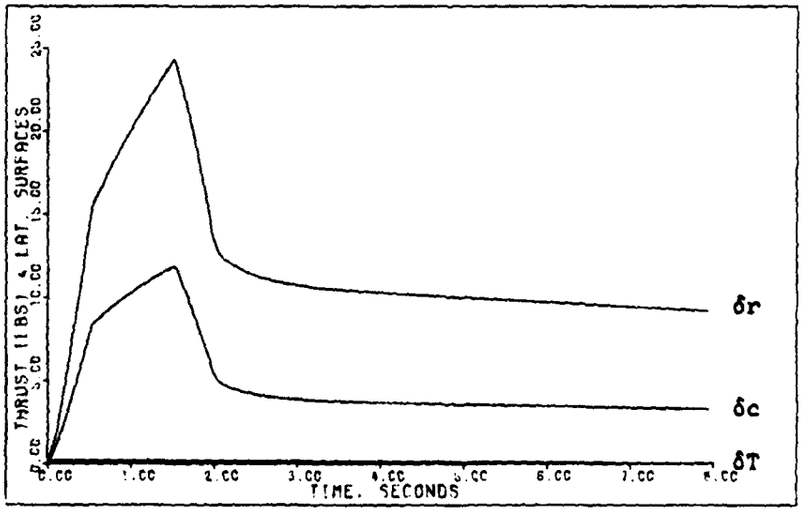

Figure D-107: 1.6M Failed Lateral Translation -- Rudder and Canard Deflections and Thrust

Landing Approach (0.3 Mach at 30 Feet)

The landing approach flight condition is chosen to demonstrate the aircraft's maneuverabiltiy at a low speed and low altitude. Designs at this flight condition are difficult due to the low dynamic pressure and high trim angle of attack. In reality the AFTI/F-16 lands with the flaperons deflected fully downward, and the design of control laws requires much information from pilots "flying" in simulators. Because this thesis is concerned with evaluating maximum performance at various flight conditions within the flight envelope, designs are attempted with the flaperons trimmed at zero degrees, and pilot interfacing is postponed for future research.

G-Command Maneuver. Tables D-29 and D-30 list the design parameters for the g-command maneuver for the healthy and failed right elevator models. As shown in the tables, the same design parameters are used for both aircraft models.

Figures D-108 through D-114 show the simulation responses for the g-command maneuver. For this maneuver the healthy aircraft longitudinal responses change very little when the right horizontal tail fails. Also, the healthy aircraft lateral responses are zero and are very small with the failed model. For these reasons Figures D-108 through D-110 give simulation responses for both the healthy and failed aircraft models.

The maximum normal acceleration command of 0.3 g is

limited by the flaperon deflection. For the failure case, the left elevator deflects approximately twice the amount required when both tail halves are working. The flaperon deflection is slightly asymmetric for the failure case in order to compensate for the rolling moment created by the left elevator deflection. The rudder and canard compensate for the adverse yaw caused by a difference in drag between the left and right halves of the aircraft.

Table D-29

G-Command: Healthy Model, 0.3 Mach at 30 Feet

Sampling Time: T = 0.02 second

$\bar{\alpha} = 1.0$

$\epsilon = 1.0$

$\underline{\Sigma} = \text{diag}\{ 2.0, 1.0, 1.0, 1.0, 1.0, 1.0 \}$

$$\underline{K}_0 = \begin{bmatrix} 0.0 & 0.4500E-02 & -0.1072E+00 & -0.6165E-02 & -0.7253E-04 & 0.6201E-02 \\ 0.0 & 0.4782E-01 & -0.9951E-01 & 0.7566E-02 & 0.8900E-04 & -0.7609E-02 \\ 0.0 & 0.0 & 0.0 & 0.1034E-01 & -0.1581E-01 & -0.2613E-01 \\ 0.0 & 0.0 & 0.0 & 0.7860E-01 & 0.1089E-01 & -0.1751E+00 \\ 0.0 & 0.0 & 0.0 & 0.2146E+00 & 0.2525E-02 & -0.2158E+00 \\ 0.8972E+00 & 0.3577E+00 & -0.1054E+01 & 0.3484E-01 & 0.4098E-03 & -0.3504E-01 \end{bmatrix}$$

$\underline{K}_1 = \underline{K}_0$

Input Ramp Time: 0.4 second

Command Vector:

$u = 0.0$

$A_{n_p} = 0.3$ g (step)

$q = 0.02884$ radian/second (step)

$A_{y_p} = 0.0$

$p = 0.0$

$r = 0.0$

Table D-30

G-Command: Failed Model, 0.3 Mach at 30 Feet

Sampling Time: T = 0.02 second

$\bar{\alpha} = 1.0$

$\varepsilon = 1.0$

$\underline{\Sigma} = \text{diag}\{\ 2.0,\ 1.0,\ 1.0,\ 1.0,\ 1.0,\ 1.0\}$

$$\underline{K}_0 = \begin{bmatrix} -0.4171E-16 & 0.8964E-02 & -0.2136E+00 & -0.1236E-01 & -0.1721E-04 & 0.1256E-01 \\ 0.0 & 0.4924E-01 & -0.1333E+00 & 0.1921E-01 & -0.2071E-01 & -0.4001E-01 \\ 0.0 & 0.4645E-01 & -0.6682E-01 & -0.4041E-02 & 0.2073E-01 & 0.2459E-01 \\ 0.1275E-15 & 0.2867E-03 & -0.6833E-02 & 0.7887E-01 & 0.9883E-02 & -0.1764E+00 \\ 0.6509E-15 & 0.6306E-03 & -0.1503E-01 & 0.2152E+00 & 0.2996E-03 & -0.2186E+00 \\ 0.8972E+00 & 0.3578E+00 & -0.1056E+01 & 0.3493E-01 & 0.4863E-04 & -0.3549E-01 \end{bmatrix}$$

$\underline{K}_1 = \underline{K}_0$

Input Ramp Time: 0.4 second

Command Vector:

u = 0.0

A_{n_p} = 0.3 g (step)

q = 0.02884 radian/second (step)

A_{y_p} = 0.0

p = 0.0

r = 0.0

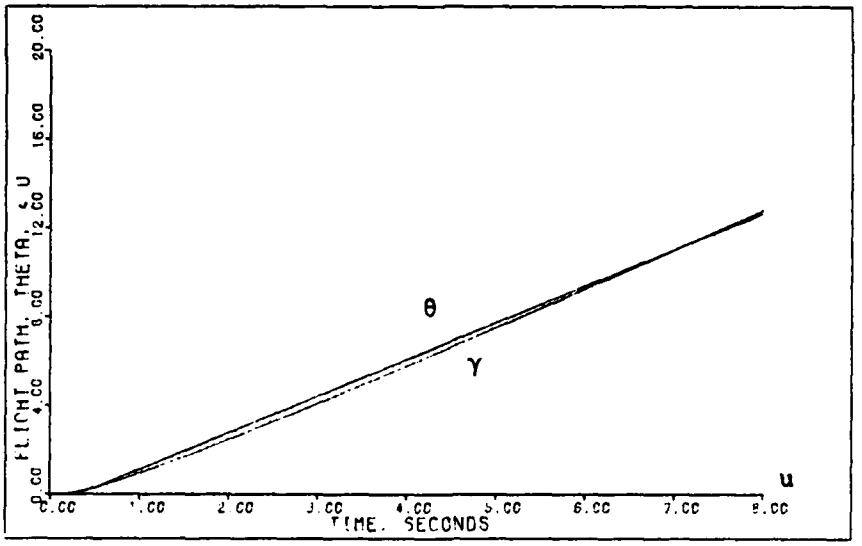

Figure D-108: 0.3M Healthy/Failed G-Command -- Flight Path Angle, Pitch Angle, and Forward Velocity

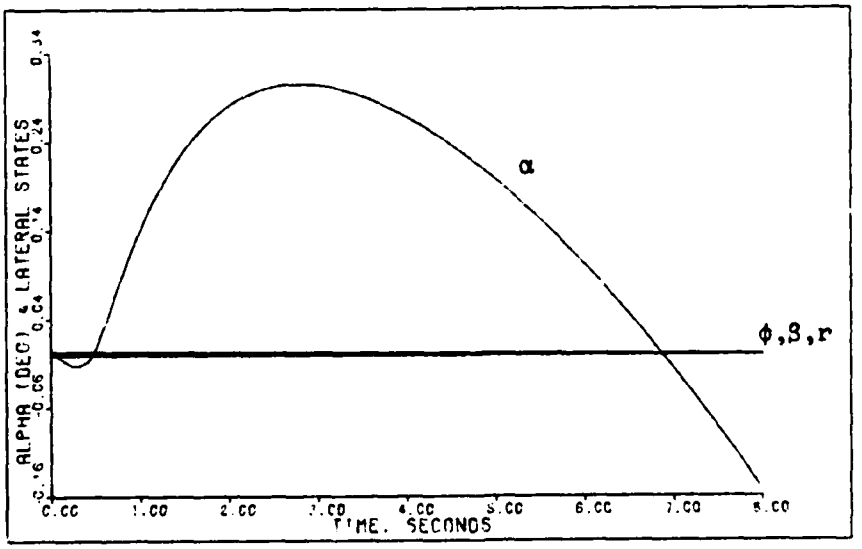

Figure D-109: 0.3M Healthy/Failed G-Command -- Angle of Attack, Roll Angle, Sideslip Angle, and Yaw Rate

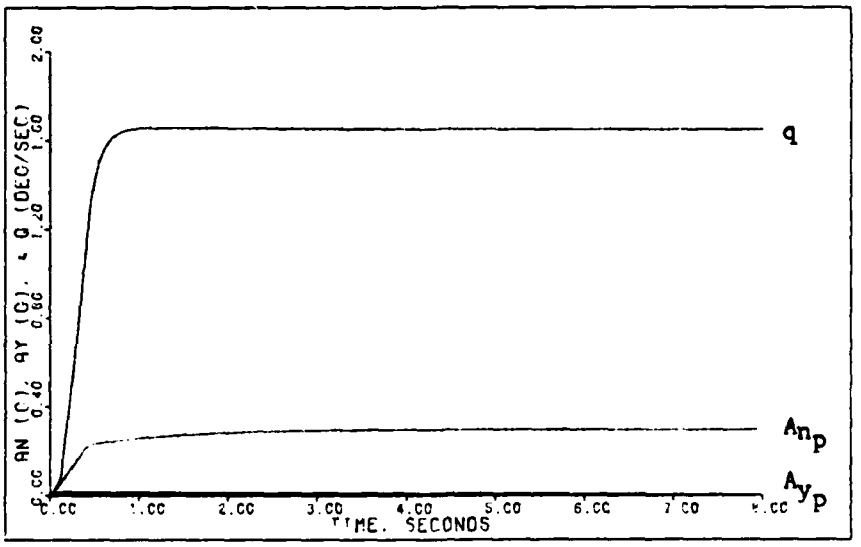

Figure D-110: 0.3M Healthy/Failed G-Command -- Pitch Rate, Normal Acceleration, and Lateral Acceleration

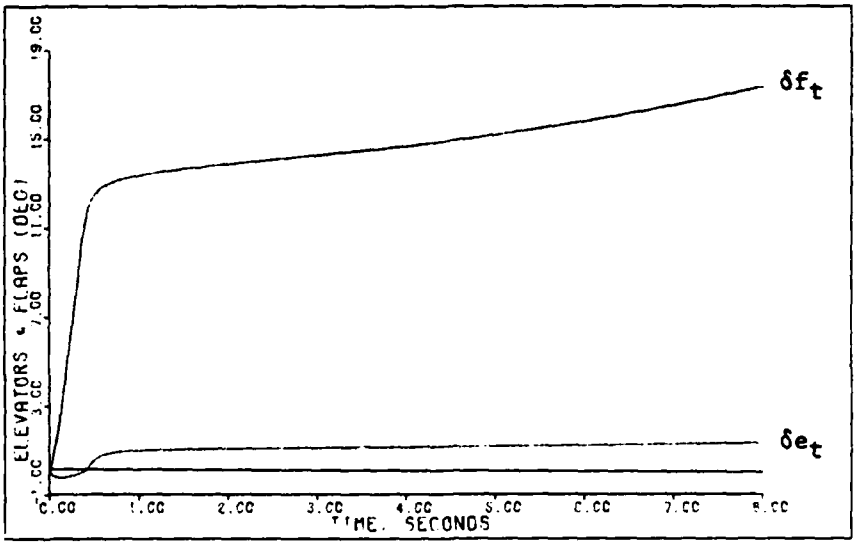

Figure D-111: 0.3M Healthy G-Command -- Elevator and Flap Deflections

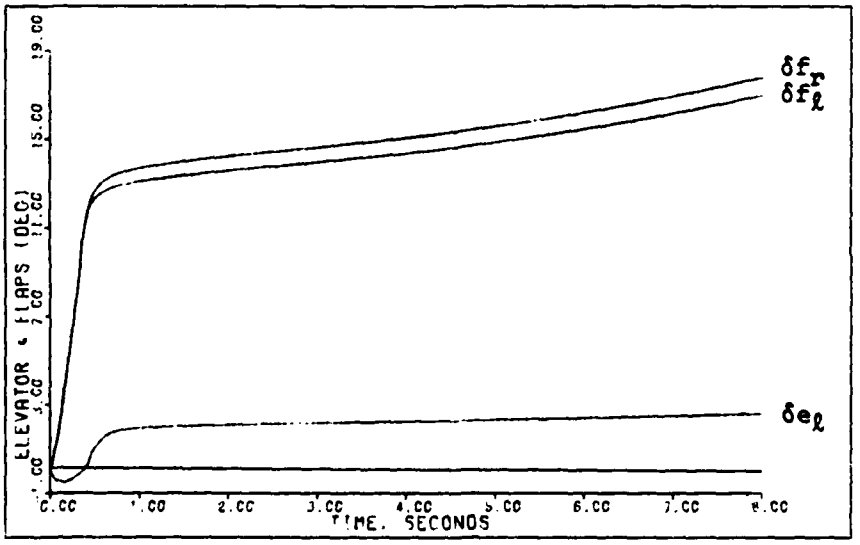

Figure D-112: 0.3M Failed G-Command -- Left Elevator and Flaperon Deflections

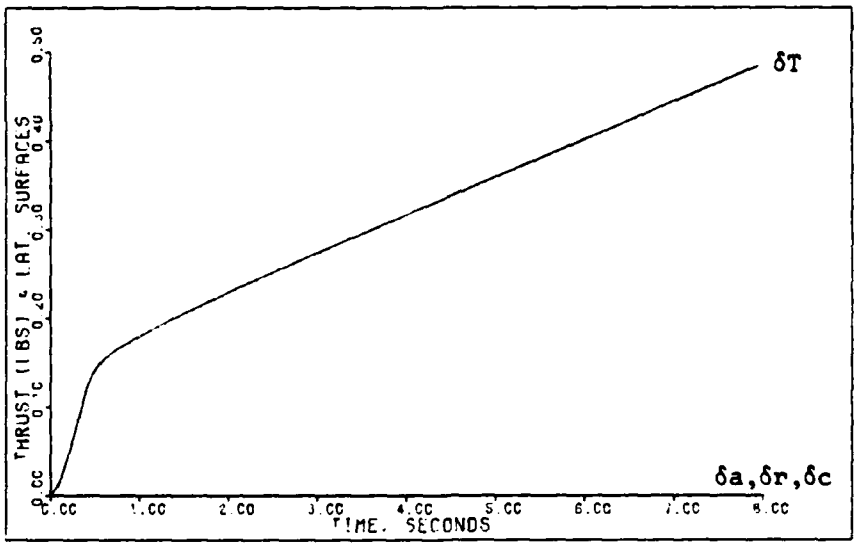

Figure D-113: 0.3M Healthy G-Command -- Aileron, Rudder, and Canard Deflections and Thrust

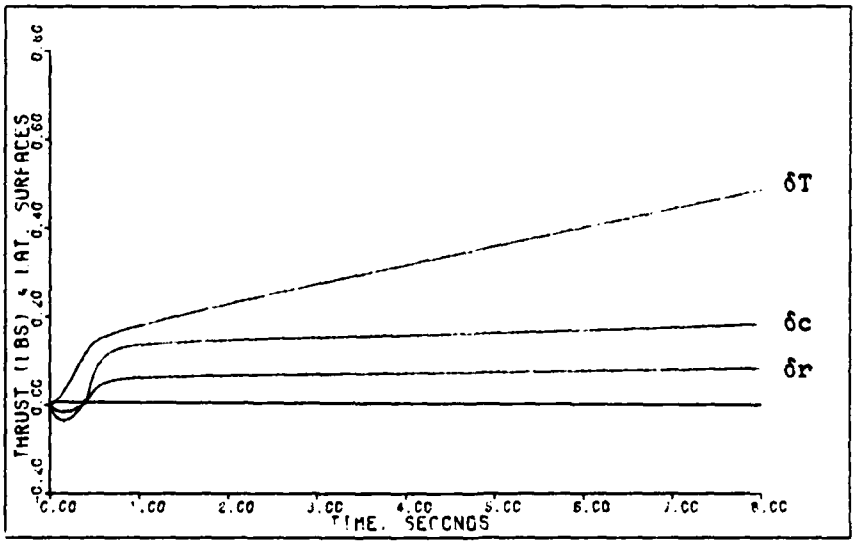

Figure D-114: 0.3M Failed G-Command -- Rudder and Canard Deflections and Thrust

Pitch Pointing Maneuver. Tables D-31 and D-32 give the design parameters for the pitch pointing maneuver. As with the g-command maneuver the design parameters are the same for the healthy and failed models.

The simulation responses for the pitch pointing maneuver are given in Figures D-115 through D-121. The maximum pointing angle commanded (3.5 degrees) is limited by the flaperon deflection. For the same reasons discussed in the g-command maneuver section, Figures D-115 through D-117 give simulation responses for both the healthy and failed aircraft models. For the failure case the left elevator must deflect approximately twice the angle of the healthy elevator deflection. Also, for the failure model, the flaperons deflect asymmetrically to counter the roll induced by the failed right horizontal tail, and the rudder and canard deflect to compensate for adverse yaw.

Table D-31

Pitch Pointing: Healthy Model, 0.3 Mach at 30 Feet

Sampling Time: T = 0.02 second

$\bar{\alpha} = 2.0$

$\varepsilon = 1.0$

$\underline{\Sigma} = \text{diag}\{\ 2.0,\ 2.0,\ 1.2,\ 1.0,\ 1.0,\ 1.0\ \}$

$$\underline{K}_0 = \begin{bmatrix} 0.0 & 0.9000E-02 & -0.1287E+00 & -0.6165E-02 & -0.7253E-04 & 0.6201E-02 \\ 0.0 & 0.9565E-01 & -0.1194E+00 & 0.7566E-02 & 0.8900E-04 & -0.7609E-02 \\ 0.0 & 0.0 & 0.0 & 0.1034E-01 & -0.1581E-01 & -0.2613E-01 \\ 0.0 & 0.0 & 0.0 & 0.7860E-01 & 0.1089E-01 & -0.1751E+00 \\ 0.0 & 0.0 & 0.0 & 0.2146E+00 & 0.2525E-02 & -0.2158E+00 \\ 0.8972E+00 & 0.7153E+00 & -0.1264E+01 & 0.3484E-01 & 0.4098E-03 & -0.3504E-01 \end{bmatrix}$$

$$\underline{K}_1 = \begin{bmatrix} 0.0 & 0.1800E-01 & -0.2574E+00 & -0.1233E-01 & -0.1451E-03 & 0.1240E-01 \\ 0.0 & 0.1913E+00 & -0.2388E+00 & 0.1513E-01 & 0.1780E-03 & -0.1522E-01 \\ 0.0 & 0.0 & 0.0 & 0.2067E-01 & -0.3161E-01 & -0.5225E-01 \\ 0.0 & 0.0 & 0.0 & 0.1572E+00 & 0.2179E-01 & -0.3502E+00 \\ 0.0 & 0.0 & 0.0 & 0.4292E+00 & 0.5049E-02 & -0.4317E+00 \\ 0.1794E+01 & 0.1431E+01 & -0.2529E+01 & 0.6968E-01 & 0.8196E-03 & -0.7007E-01 \end{bmatrix}$$

Input Ramp Time: 0.3 second

Command Vector:

$u = 0.0$

$A_{n_p} = 0.0$

$q = 0.04363$ radian/second (1 second pulse)

$A_{y_p} = 0.0$

$p = 0.0$

$r = 0.0$

Table D-32

Pitch Pointing: Failed Model, 0.3 Mach at 30 Feet

Sampling Time: T = 0.02 second

$\bar{\alpha} = 2.0$

$\epsilon = 1.0$

$\underline{\Sigma} = \text{diag}\{2.0, 2.0, 1.2, 1.0, 1.0, 1.0\}$

$$\underline{K}_0 = \begin{bmatrix} -0.4171E-16 & 0.1793E-01 & -0.2563E+00 & -0.1236E-01 & -0.1721E-04 & 0.1256E-01 \\ 0.0 & 0.9848E-01 & -0.1599E+00 & 0.1921E-01 & -0.2071E-01 & -0.4001E-01 \\ 0.0 & 0.9290E-01 & -0.8019E-01 & -0.4041E-02 & 0.2073E-01 & 0.2459E-01 \\ 0.1275E-15 & 0.5775E-03 & -0.8199E-02 & 0.7887E-01 & 0.9883E-02 & -0.1764E+00 \\ 0.6509E-15 & 0.1261E-02 & -0.1803E-01 & 0.2152E+00 & 0.2996E-03 & -0.2186E+00 \\ 0.8972E+00 & 0.7155E+00 & -0.1267E+01 & 0.3493E-01 & 0.4863E-04 & -0.3549E-01 \end{bmatrix}$$

$$\underline{K}_1 = \begin{bmatrix} -0.8343E-16 & 0.3586E-01 & -0.5127E+00 & -0.2473E-01 & -0.3442E-04 & 0.2512E-01 \\ 0.0 & 0.1970E+00 & -0.3198E+00 & 0.3843E-01 & -0.4143E-01 & -0.8001E-01 \\ 0.0 & 0.1858E+00 & -0.1604E+00 & -0.8083E-02 & 0.4147E-01 & 0.4918E-01 \\ 0.2551E-15 & 0.1147E-02 & -0.1640E-01 & 0.1577E+00 & 0.1977E-01 & -0.3527E+00 \\ 0.1302E-14 & 0.2522E-02 & -0.3607E-01 & 0.4305E+00 & 0.5991E-03 & -0.4372E+00 \\ 0.1794E+01 & 0.1431E+01 & -0.2535E+01 & 0.6986E-01 & 0.9725E-04 & -0.7098E-01 \end{bmatrix}$$

Input Ramp Time: 0.3 second

Command Vector:

$u = 0.0$

$A_{n_p} = 0.0$

$q = 0.04363$ radian/second (1 second pulse)

$A_{y_p} = 0.0$

$p = 0.0$

$r = 0.0$

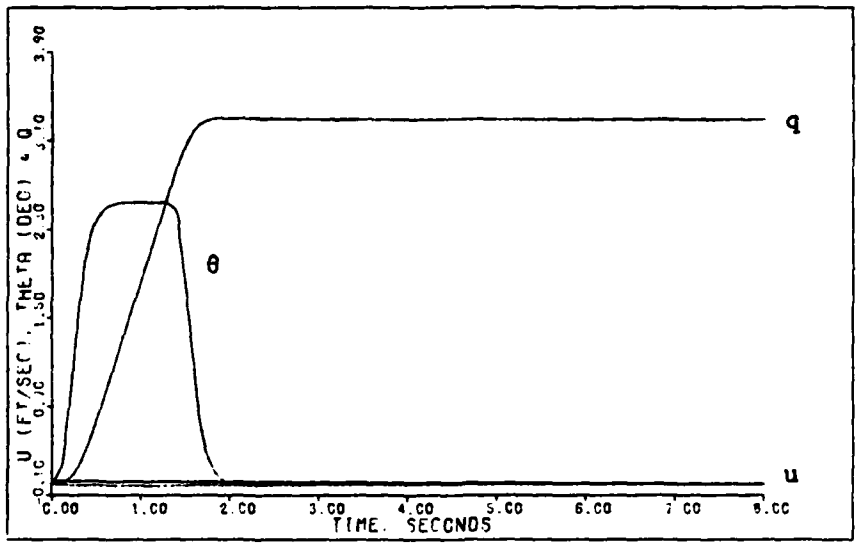

Figure D-115: 0.3M Healthy/Failed Pitch Pointing -- Pitch Angle, Pitch Rate, and Forward Velocity

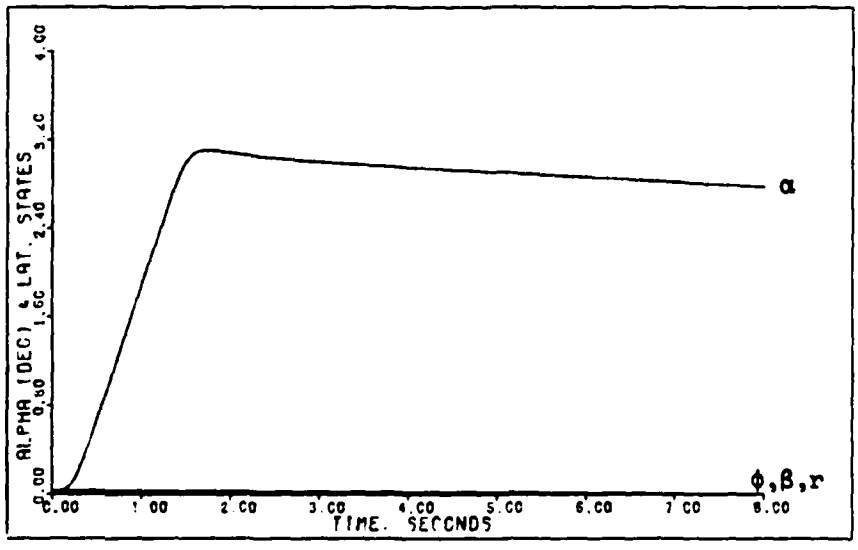

Figure D-116: 0.3M Healthy/Failed Pitch Pointing -- Angle of Attack, Roll Angle, Sideslip Angle, and Yaw Rate

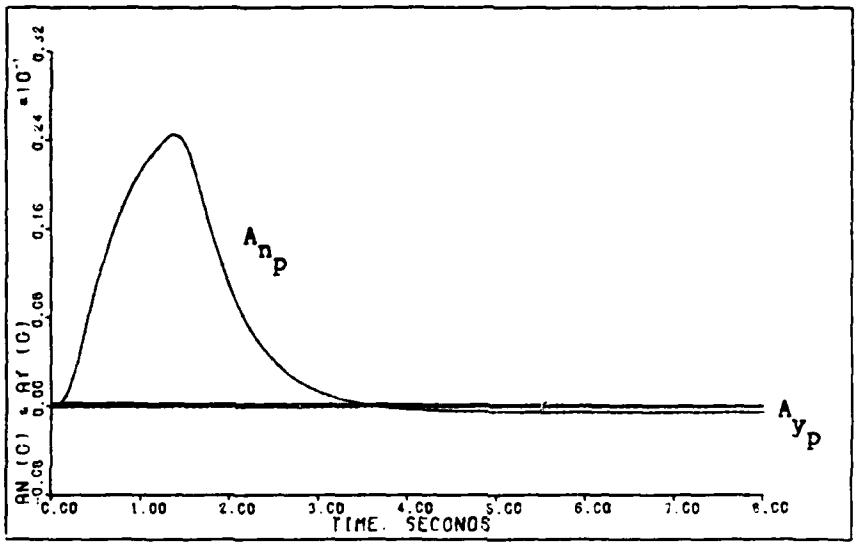

Figure D-117: 0.3M Healthy/Failed Pitch Pointing -- Normal Acceleration and Lateral Acceleration

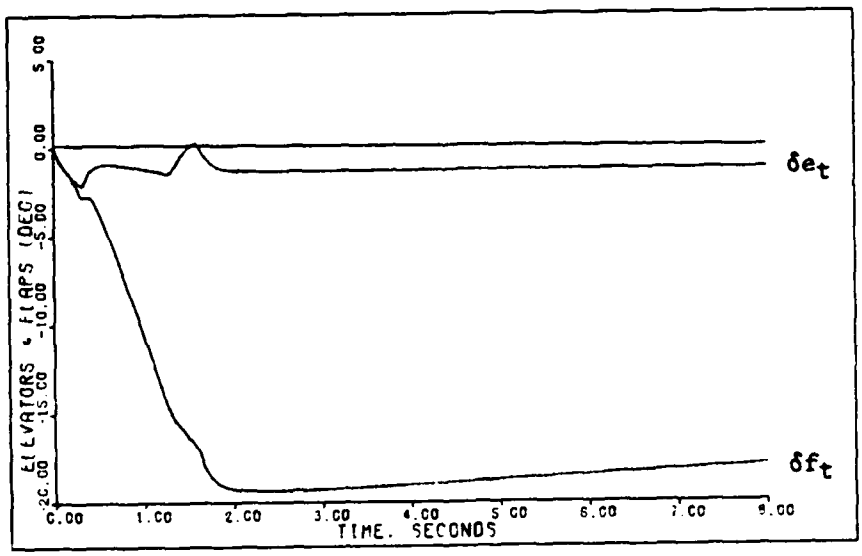

Figure D-118: 0.3M Healthy Pitch Pointing -- Elevator and Flap Deflections

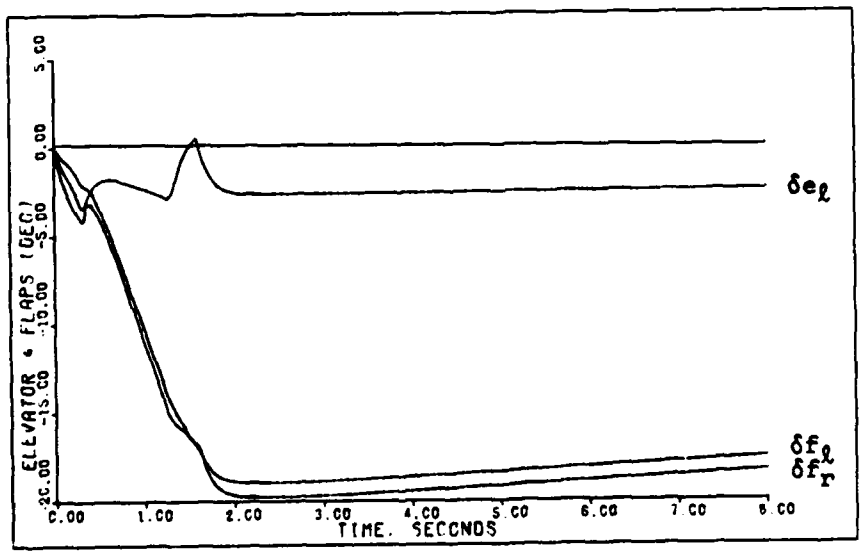

Figure D-119: 0.3M Failed Pitch Pointing -- Left Elevator and Flaperon Deflections

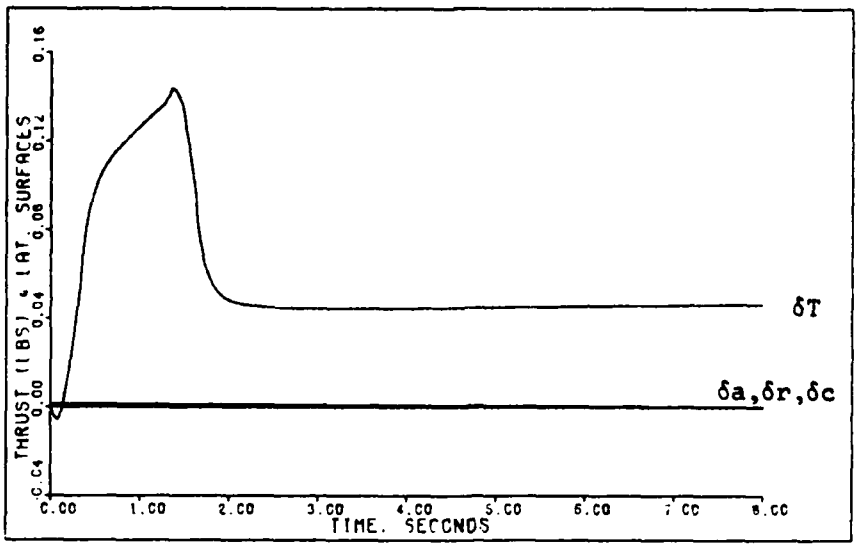

Figure D-120: 0.3M Healthy Pitch Pointing -- Aileron, Rudder, and Canard Deflections and Thrust

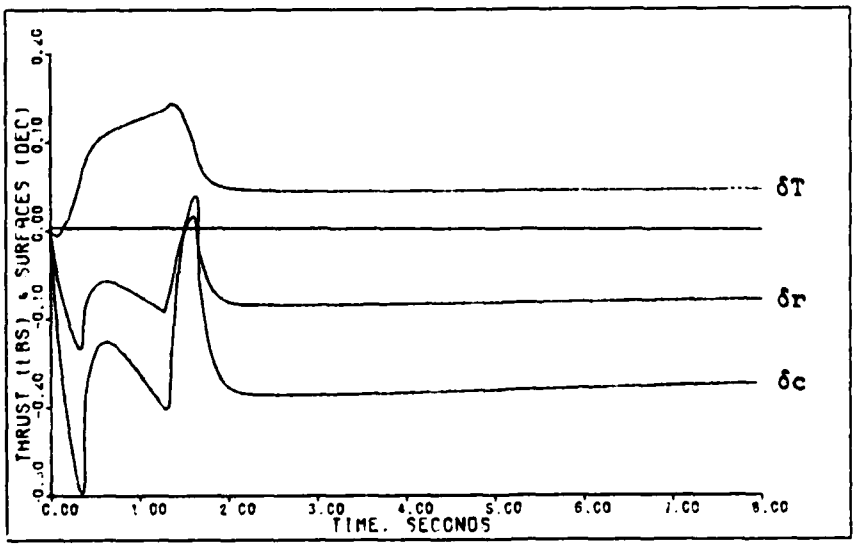

Figure D-121: 0.3M Failed Pitch Pointing -- Rudder and Canard Deflections and Thrust

Longitudinal Translation Maneuver. Tables D-33 and D-34 give the design parameters for the longitudinal translation maneuver. Once again the design parameters are the same for the healthy and failed models.

The simulation responses for the longitudinal translation maneuver are given in Figures D-122 through D-128. As discussed in the g-command maneuver section Figures D-122 through D-124 give simulation responses for both the healthy and failed aircraft models. The maximum longitudinal translation command of 0.2 g for one second, which yields a normal velocity of approximately 9.0 feet/second, is limited by the flaperon deflection.

As is usually the case with longitudinal maneuvers, the failure model requires that the left elevator must deflect approximately twice the angle of the healthy elevator deflection. Also, for the failure model, the flaperons deflect asymmetrically to counter the roll induced by the failed right horizontal tail, and the rudder and canard deflect to compensate for adverse yaw.

Table D-33

Longitudinal Translation: Healthy Model,
0.3 Mach at 30 Feet

Sampling Time: T = 0.02 second

$\bar{\alpha} = 2.0$

$\varepsilon = 1.0$

$\underline{\Sigma} = \text{diag}\{ 2.0, 3.0, 1.0, 1.0, 1.0, 1.0 \}$

$$\underline{K}_0 = \begin{bmatrix} 0.0 & 0.1350E-01 & -0.1072E+00 & -0.6165E-02 & -0.7253E-04 & 0.6201E-02 \\ 0.0 & 0.1435E+00 & -0.9951E-01 & 0.7566E-02 & 0.8900E-04 & -0.7609E-02 \\ 0.0 & 0.0 & 0.0 & 0.1034E-01 & -0.1581E-01 & -0.2613E-01 \\ 0.0 & 0.0 & 0.0 & 0.7860E-01 & 0.1089E-01 & -0.1751E+00 \\ 0.0 & 0.0 & 0.0 & 0.2146E+00 & 0.2525E-02 & -0.2158E+00 \\ 0.8972E+00 & 0.1073E+01 & -0.1054E+01 & 0.3484E-01 & 0.4098E-03 & -0.3504E-01 \end{bmatrix}$$

$$\underline{K}_1 = \begin{bmatrix} 0.0 & 0.2700E-01 & -0.2145E+00 & -0.1233E-01 & -0.1451E-03 & 0.1240E-01 \\ 0.0 & 0.2869E+00 & -0.1990E+00 & 0.1513E-01 & 0.1780E-03 & -0.1522E-01 \\ 0.0 & 0.0 & 0.0 & 0.2067E-01 & -0.3161E-01 & -0.5225E-01 \\ 0.0 & 0.0 & 0.0 & 0.1572E+00 & 0.2179E-01 & -0.3502E+00 \\ 0.0 & 0.0 & 0.0 & 0.4292E+00 & 0.5049E-02 & -0.4317E+00 \\ 0.1794E+01 & 0.2146E+01 & -0.2146E+01 & 0.6968E-01 & 0.8196E-03 & -0.7007E-01 \end{bmatrix}$$

Input Ramp Time: 0.4 second

Command Vector:

$u = 0.0$

$A_{n_p} = 0.2$ g (1 second pulse)

$q = 0.0$

$A_{y_p} = 0.0$

$p = 0.0$

$r = 0.0$

Table D-34

Longitudinal Translation: Failed Model,
0.3 Mach at 30 Feet

Sampling Time: T = 0.02 second

$\bar{\alpha} = 2.0$

$\epsilon = 1.0$

$\underline{\Sigma} = \text{diag}\{\ 2.0,\ 3.0,\ 1.0,\ 1.0,\ 1.0,\ 1.0\ \}$

$$\underline{K}_0 = \begin{bmatrix} -0.4171E-16 & 0.2689E-01 & -0.2136E+00 & -0.1236E-01 & -0.1721E-04 & 0.1256E-01 \\ 0.0 & 0.1477E+00 & -0.1333E+00 & 0.1921E-01 & -0.2071E-01 & -0.4001E-01 \\ 0.0 & 0.1394E+00 & -0.6682E-01 & -0.4041E-02 & 0.2073E-01 & 0.2459E-01 \\ 0.1275E-15 & 0.8602E-03 & -0.6833E-02 & 0.7887E-01 & 0.9883E-02 & -0.1764E+00 \\ 0.6509E-15 & 0.1892E-02 & -0.1503E-01 & 0.2152E+00 & 0.2996E-03 & -0.2186E+00 \\ 0.8972E+00 & 0.1073E+01 & -0.1056E+01 & 0.3493E-01 & 0.4863E-04 & -0.3549E-01 \end{bmatrix}$$

$$\underline{K}_1 = \begin{bmatrix} -0.8343E-16 & 0.5378E-01 & -0.4272E+00 & -0.2473E-01 & -0.3442E-04 & 0.2512E-01 \\ 0.0 & 0.2954E+00 & -0.2665E+00 & 0.3843E-01 & -0.4143E-01 & -0.8001E-01 \\ 0.0 & 0.2787E+00 & -0.1336E+00 & -0.8083E-02 & 0.4147E-01 & 0.4918E-01 \\ 0.2551E-15 & 0.1720E-02 & -0.1367E-01 & 0.1577E+00 & 0.1977E-01 & -0.3527E+00 \\ 0.1302E-14 & 0.3784E-02 & -0.3005E-01 & 0.4305E+00 & 0.5991E-03 & -0.4372E+00 \\ 0.1794E+01 & 0.2147E+01 & -0.2112E+01 & 0.6986E-01 & 0.9725E-04 & -0.7098E-01 \end{bmatrix}$$

Input Ramp Time: 0.4 second

Command Vector:

$u = 0.0$

$A_{n_p} = 0.2$ g (1 second pulse)

$q = 0.0$

$A_{y_p} = 0.0$

$p = 0.0$

$r = 0.0$

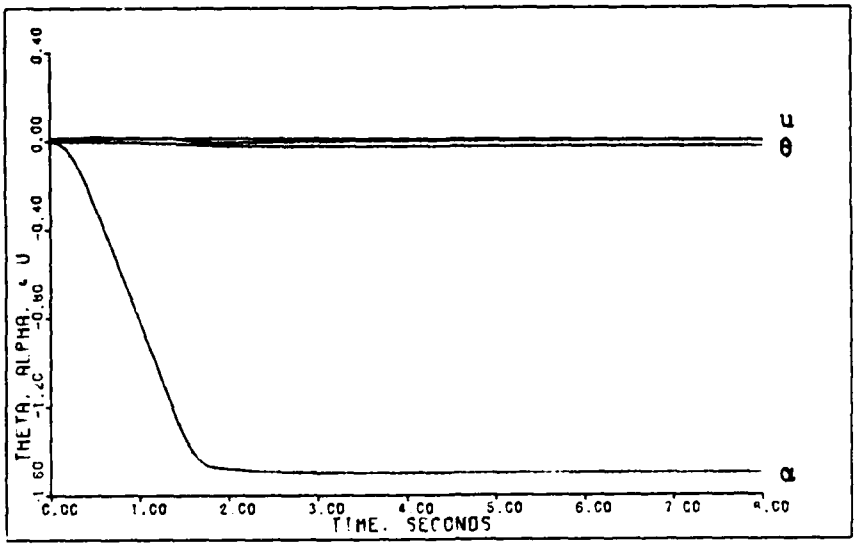

Figure D-122: 0.3M Healthy/Failed Longitudinal Translation -- Pitch Angle, Angle of Attack, and Forward Velocity

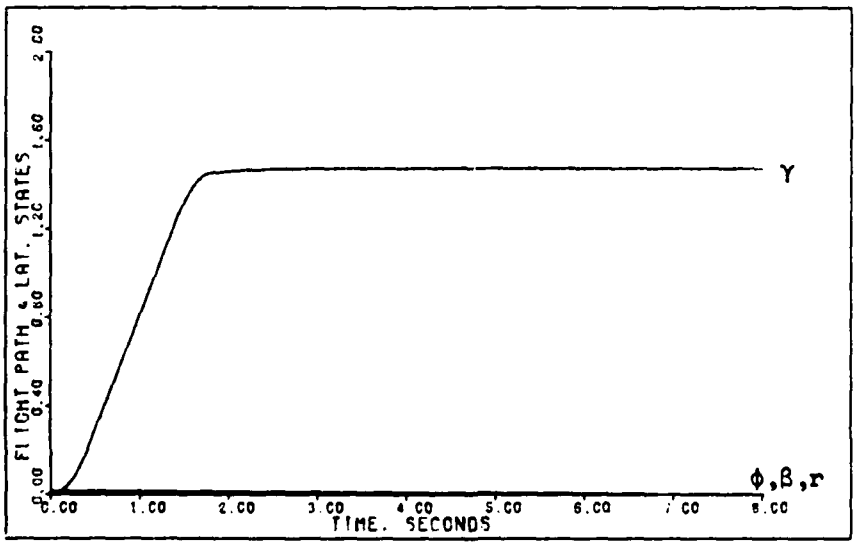

Figure D-123: 0.3M Healthy/Failed Longitudinal Translation -- Flight Path Angle, Roll Angle, Sideslip Angle, and Yaw Rate

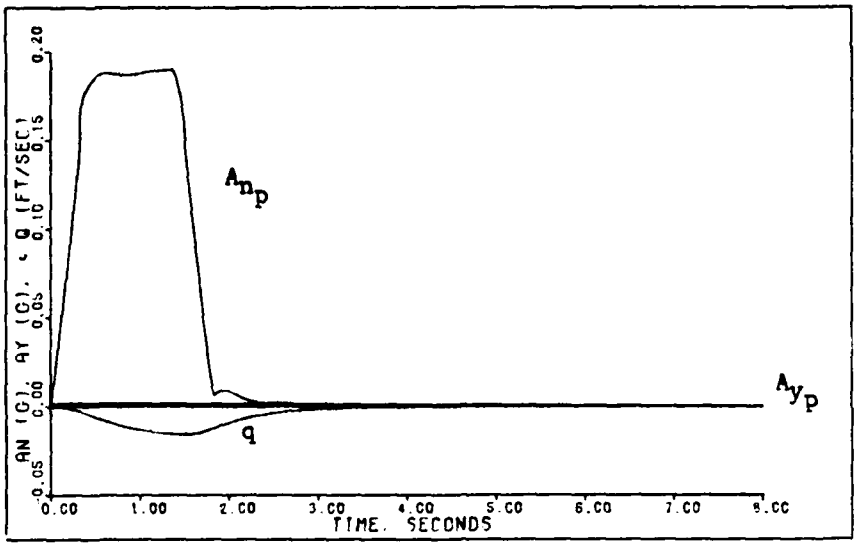

Figure D-124: 0.3M Healthy/Failed Longitudinal Translation -- Pitch Rate, Normal Acceleration, and Lateral Acceleration

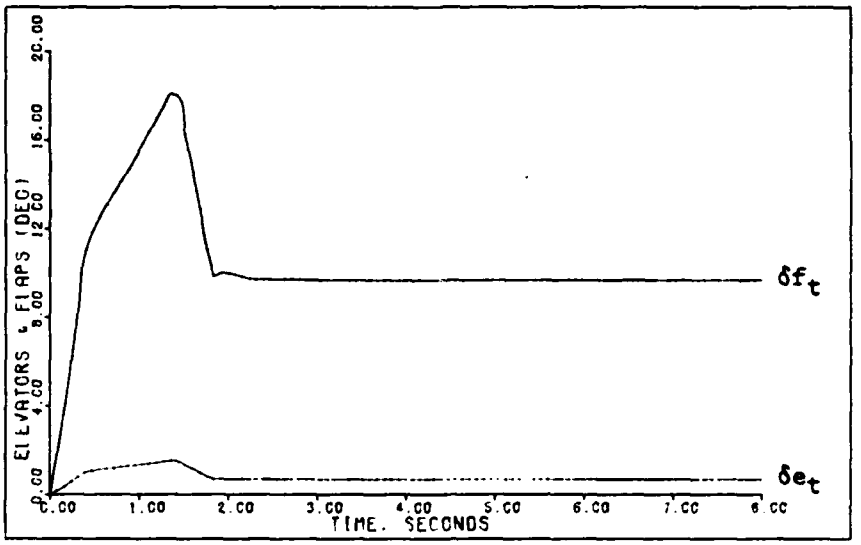

Figure D-125: 0.3M Healthy Longitudinal Translation -- Elevator and Flap Deflections

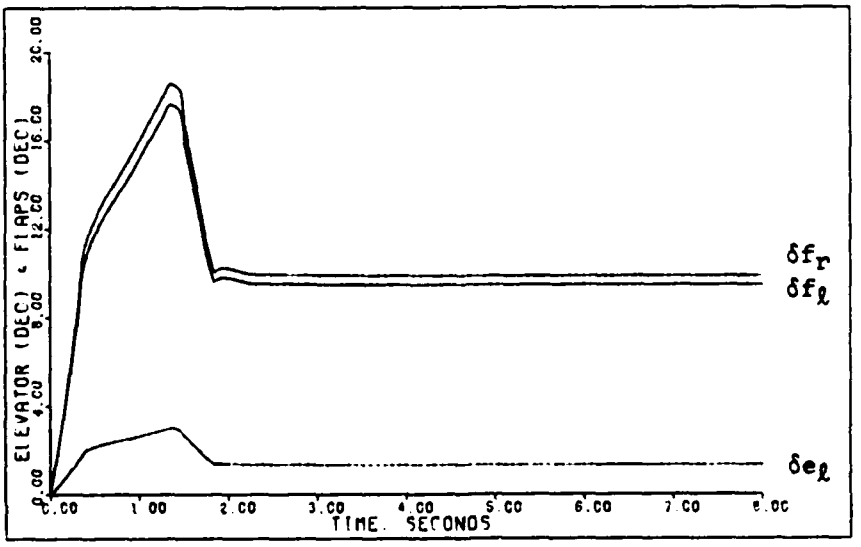

Figure D-126: 0.3M Failed Longitudinal Translation -- Left Elevator and Flaperon Deflections

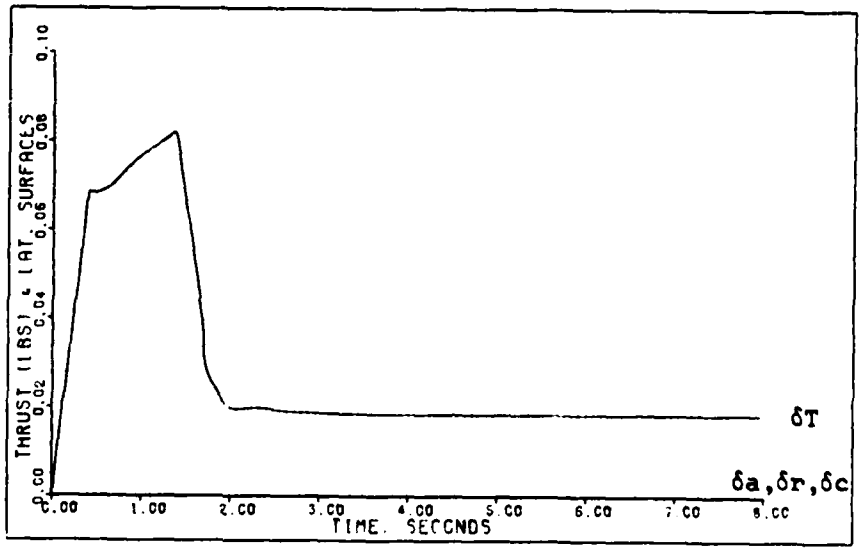

Figure D-127: 0.3M Healthy Longitudinal Translation -- Aileron, Rudder, and Canard Deflections and Thrust

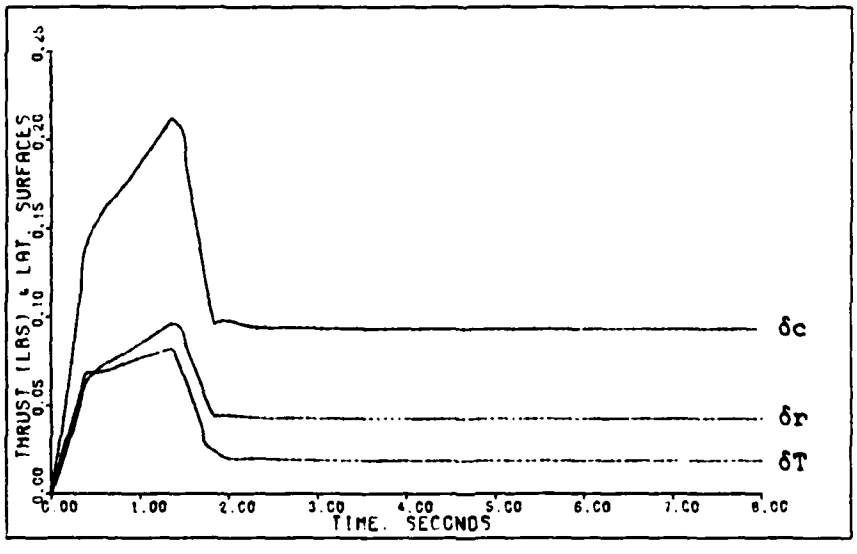

Figure D-128: 0.3M Failed Longitudinal Translation -- Rudder and Canard Deflections and Thrust

Roll About Velocity Vector Maneuver. As discussed in Chapter IV the roll maneuver requires some modification to the healthy and failure models. Tables D-35 and D-36, give the design parameters for the roll maneuver. The parameters are the same for the healthy and failed models; however, the roll rate commanded for the failure case is lowered from that of the healthy model in order not to overshoot the flaperon deflection limit.

The simulation responses for the healthy model roll maneuver are given in Figures D-129 through D-133, and the responses for the failed model are given in Figures D-134 through D-138. For the right horizontal tail case the flaperons deflect to achieve the commanded roll rate.

Table D-35

Roll About Velocity Vector: Healthy Model,
0.3 Mach at 30 Feet

Sampling Time: T = 0.02 second

$\bar{\alpha} = 2.5$

$\epsilon = 1.0$

$\underline{\Sigma} = \text{diag}\{ 2.0, 1.0, 1.0, 1.7, 2.0, 3.3 \}$

$$\underline{K}_0 = \begin{bmatrix} 0.0 & 0.4500E-02 & -0.1072E+00 & -0.1048E-01 & -0.1451E-03 & 0.2046E-01 \\ 0.0 & 0.4782E-01 & -0.9951E-01 & 0.1286E-01 & 0.1780E-03 & -0.2511E-01 \\ 0.0 & 0.0 & 0.0 & 0.1757E-01 & -0.3161E-01 & -0.8622E-01 \\ 0.0 & 0.0 & 0.0 & 0.1336E+00 & 0.2179E-01 & -0.5778E+00 \\ 0.0 & 0.0 & 0.0 & 0.3648E+00 & 0.5049E-02 & -0.7122E+00 \\ 0.8972E+00 & 0.3577E+00 & -0.1054E+01 & 0.5922E-01 & 0.8196E-03 & -0.1156E+00 \end{bmatrix}$$

$$\underline{K}_1 = \begin{bmatrix} 0.0 & 0.1125E-01 & -0.2681E+00 & -0.2620E-01 & -0.3626E-03 & 0.5115E-01 \\ 0.0 & 0.1196E+00 & -0.2488E+00 & 0.3215E-01 & 0.4450E-03 & -0.6277E-01 \\ 0.0 & 0.0 & 0.0 & 0.4393E-01 & -0.7903E-01 & -0.2155E+00 \\ 0.0 & 0.0 & 0.0 & 0.3341E+00 & 0.5447E-01 & -0.1444E+01 \\ 0.0 & 0.0 & 0.0 & 0.9121E+00 & 0.1262E-01 & -0.1781E+01 \\ 0.2243E+01 & 0.8942E+00 & -0.2634E+01 & 0.1481E+00 & 0.2049E-02 & -0.2890E+00 \end{bmatrix}$$

Input Ramp Time: 0.3 second

Command Vector:

$u = 0.0$

$A_{n_p} = 0.0$

$q = 0.0$

$A_{y_p} = 0.0$

$p = 1.222$ radians/second (3 second pulse)

$r-\alpha_T = 0.0$

Table D-36

Roll About Velocity Vector: Failed Model,
0.3 Mach at 30 Feet

Sampling Time: T = 0.02 second

$\bar{\alpha} = 2.5$

$\varepsilon = 1.0$

$\underline{\Sigma} = \text{diag}\{ 2.0, 1.0, 1.0, 1.7, 2.0, 3.3 \}$

$$\underline{K}_0 = \begin{bmatrix} -0.4171E-16 & 0.8964E-02 & -0.2136E+00 & -0.2102E-01 & -0.3442E-04 & 0.4145E-01 \\ 0.0 & 0.4924E-01 & -0.1333E+00 & 0.3266E-01 & -0.4143E-01 & -0.1320E+00 \\ 0.0 & 0.4645E-01 & -0.6682E-01 & -0.6870E-02 & 0.4147E-01 & 0.8115E-01 \\ 0.1275E-15 & 0.2867E-03 & -0.6833E-02 & 0.1341E+00 & 0.1977E-01 & -0.5820E+00 \\ 0.6509E-15 & 0.6306E-03 & -0.1503E-01 & 0.3658E+00 & 0.5991E-03 & -0.7215E+00 \\ 0.8972E+00 & 0.3578E+00 & -0.1056E+01 & 0.5938E-01 & 0.9725E-04 & -0.1171E+00 \end{bmatrix}$$

$$\underline{K}_1 = \begin{bmatrix} -0.1043E-15 & 0.2241E-01 & -0.5340E+00 & -0.5255E-01 & -0.8606E-04 & 0.1036E+00 \\ 0.0 & 0.1231E+00 & -0.3332E+00 & 0.8166E-01 & -0.1036E+00 & -0.3300E+00 \\ 0.0 & 0.1161E+00 & -0.1671E+00 & -0.1718E-01 & 0.1037E+00 & 0.2029E+00 \\ 0.3188E-15 & 0.7168E-03 & -0.1708E-01 & 0.3352E+00 & 0.4941E-01 & -0.1455E+01 \\ 0.1627E-14 & 0.1576E-02 & -0.3757E-01 & 0.9146E+00 & 0.1498E-02 & -0.1804E+01 \\ 0.2243E+01 & 0.8944E+00 & -0.2640E+01 & 0.1485E+00 & 0.2431E-03 & -0.2928E+00 \end{bmatrix}$$

Input Ramp Time: 0.3 second

Command Vector:

$u = 0.0$

$A_{n_p} = 0.0$

$q = 0.0$

$A_{y_p} = 0.0$

$p = 1.047$ radians/second (3 second pulse)

$r\text{-}\alpha_T = 0.0$

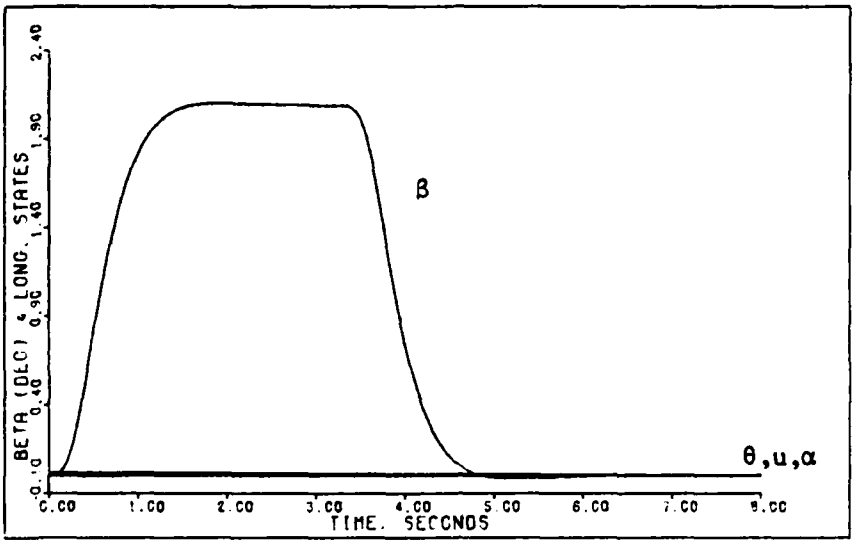

Figure D-129: 0.3M Healthy Roll -- Sideslip Angle, Pitch Angle, Angle of Attack, and Forward Velocity

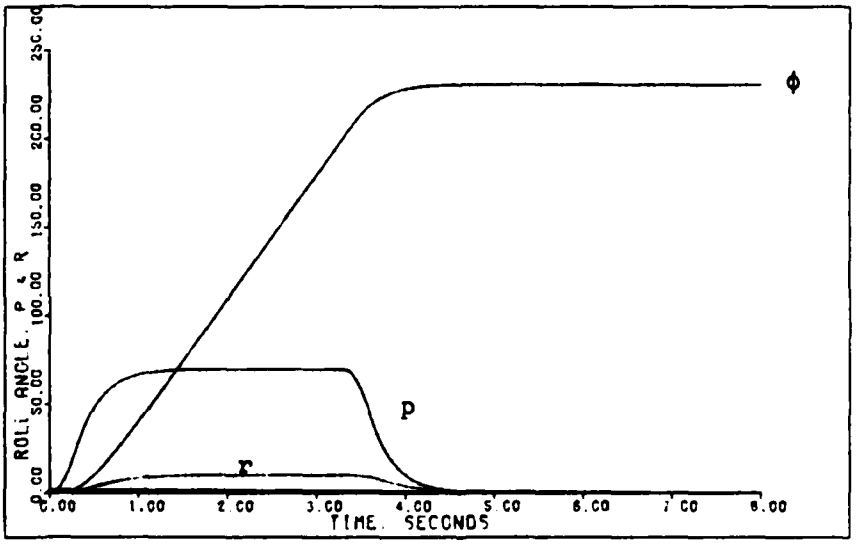

Figure D-130: 0.3M Healthy Roll -- Roll Angle, Roll Rate, and Yaw Rate

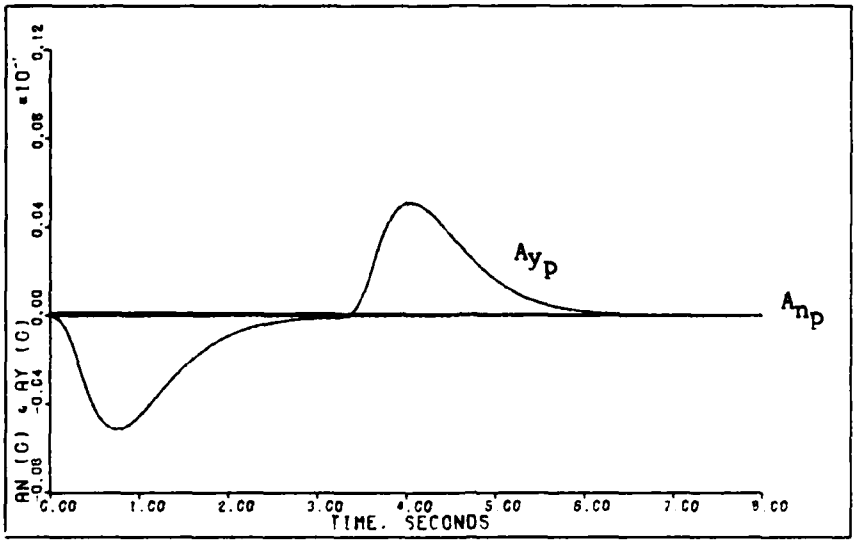

Figure D-131: 0.3M Healthy Roll -- Normal Acceleration and Lateral Acceleration

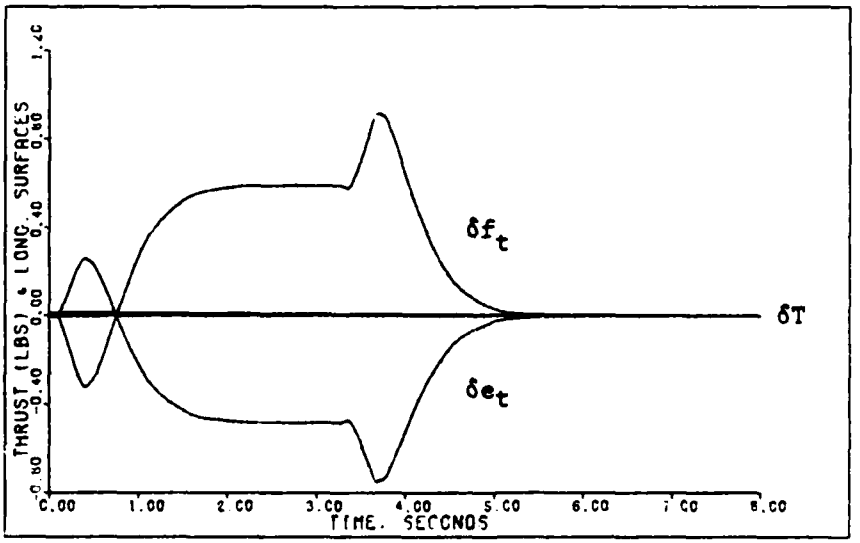

Figure D-132: 0.3M Healthy Roll -- Elevator and Flap Deflections, and Thrust

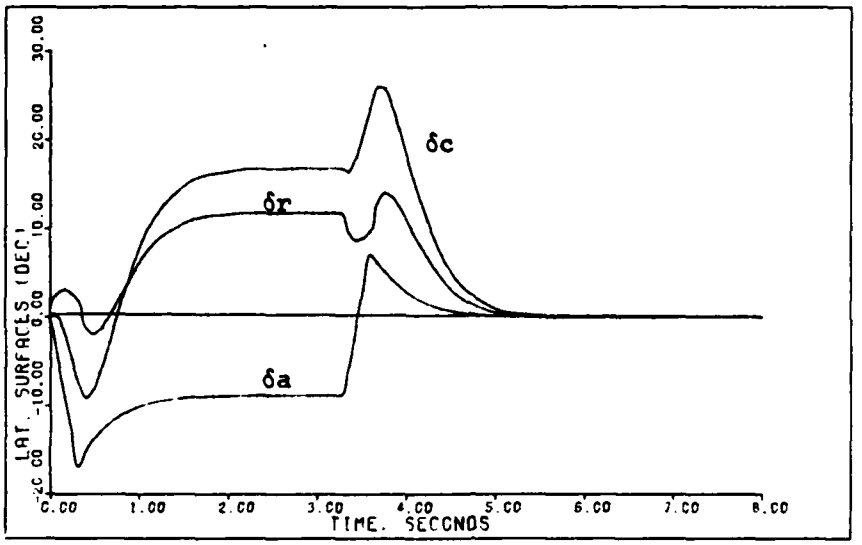

Figure D-133: 0.3M Healthy Roll -- Aileron, Rudder, and Canard Deflections

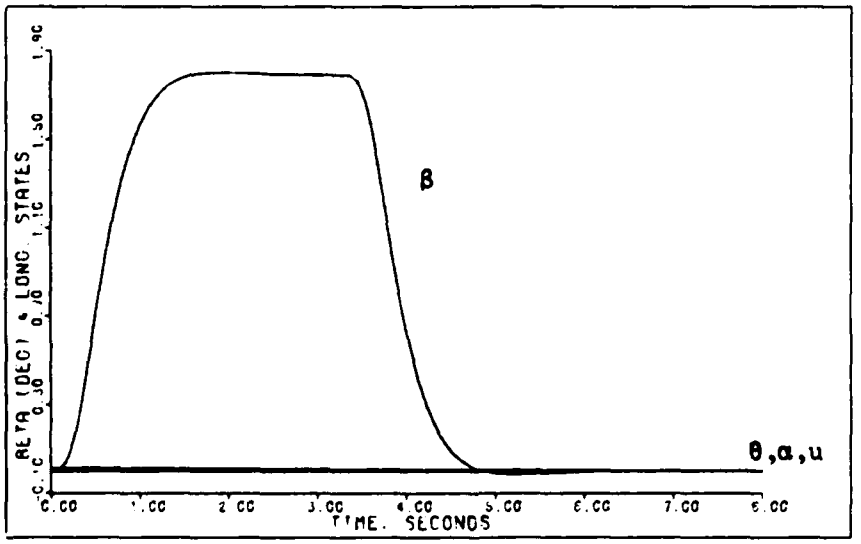

Figure D-134: 0.3M Failed Roll -- Sideslip Angle, Pitch Angle, Angle of Attack, and Forward Velocity

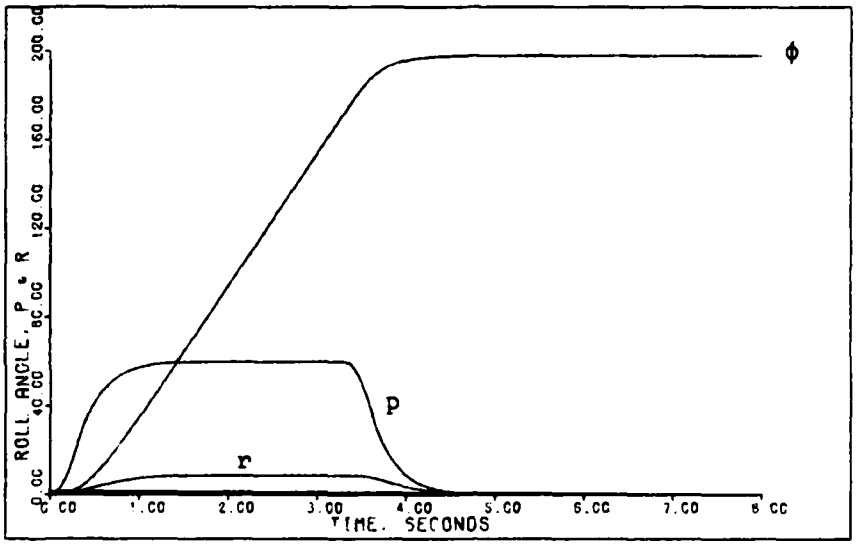

Figure D-135: 0.3M Failed Roll -- Roll Angle, Roll Rate, and Yaw Rate

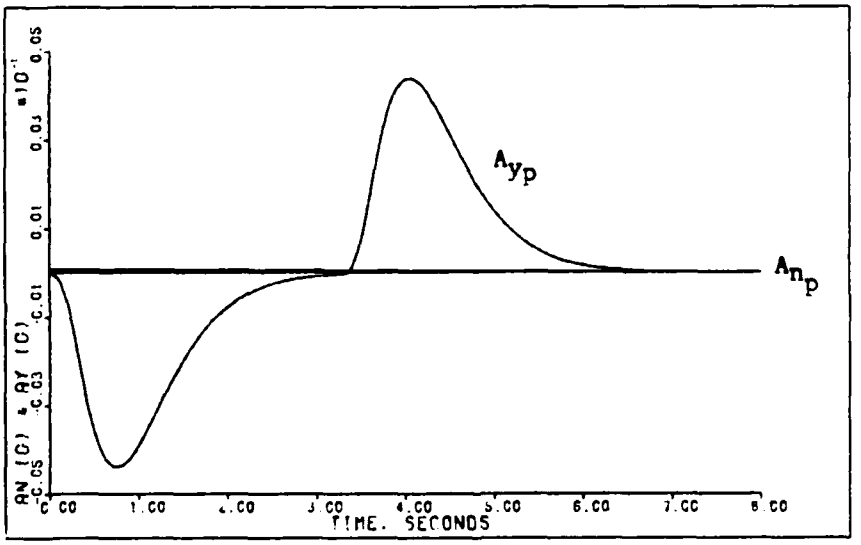

Figure D-136: 0.3M Failed Roll -- Normal Acceleration and Lateral Acceleration

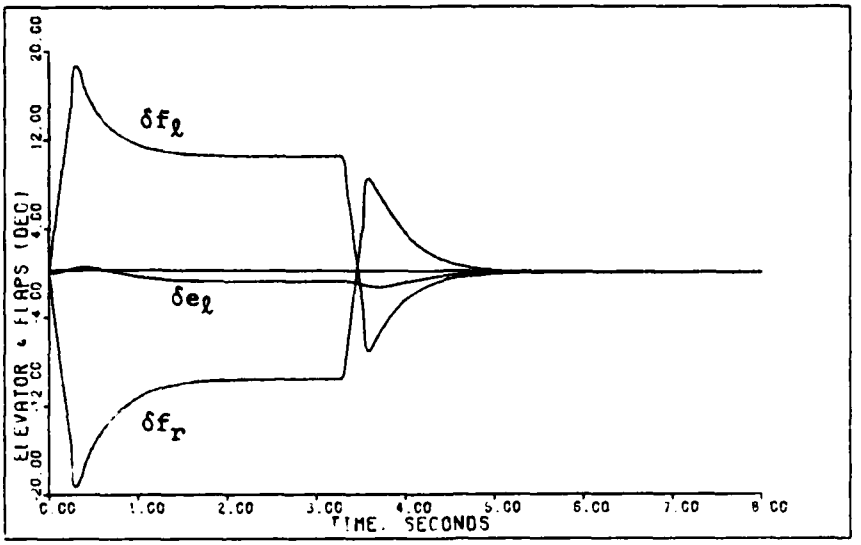

Figure D-137: 0.3M Failed Roll -- Left Elevator and Flaperon Deflections

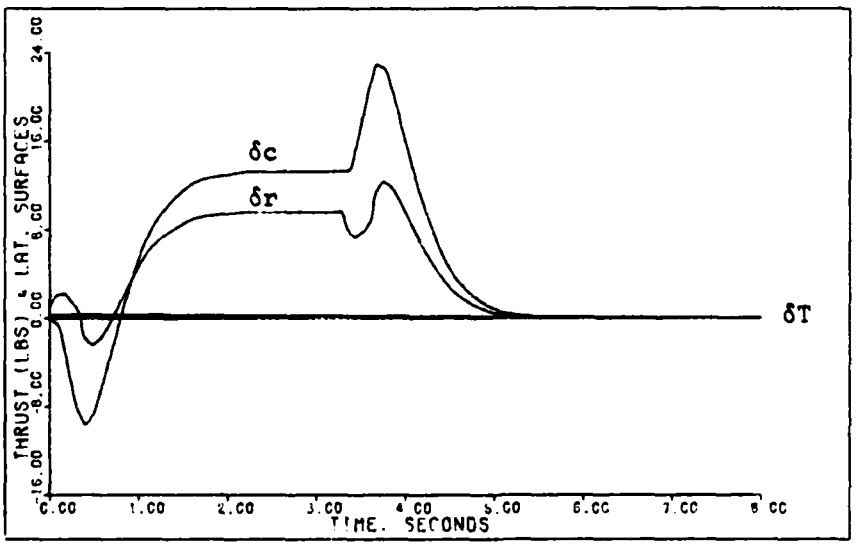

Figure D-138: 0.3M Failed Roll -- Rudder and Canard Deflections and Thrust

Sideforce (Flat Turn) Maneuver. Tables D-37 and D-38 give the design parameters for both the healthy and failed cases of the sideforce maneuver. The same parameters are used for both cases.

Figures D-139 through D-145 present the simulation responses for a 0.1 g sideforce command. The maximum value commanded is limited by the canard deflection. For this maneuver the longitudinal responses are very small for both the healthy and failure models. Also, the healthy aircraft lateral responses change very little when the right horizontal tail fails. For these reasons Figures D-139 through D-141 give simulation responses for both the healthy and failed aircraft models.

For this maneuver the horizontal tail is mainly used to counter the longitudinal pitching moment produced by the canard deflection although it also contributes to roll control for the healthy aircraft case. When the right horizontal tail fails the left horizontal tail deflects approximately twice the deflection of the healthy elevators. The flaperons deflect asymmetrically to compensate for the roll created by the failed right horizontal tail. The rudder and canard deflections change only slightly for the failure case.

Table D-37

Sideforce Maneuver: Healthy Model,
0.3 Mach at 30 Feet

Sampling Time: T = 0.02 second

$\bar{\alpha} = 1.0$

$\epsilon = 1.0$

$\underline{\Sigma} = \text{diag}\{\ 2.0,\ 1.0,\ 1.0,\ 1.0,\ 1.0,\ 1.0\ \}$

$$\underline{K}_0 = \begin{bmatrix} 0.0 & 0.4500E\text{-}02 & -0.1072E{+}00 & -0.6165E\text{-}02 & -0.7253E\text{-}04 & 0.6201E\text{-}02 \\ 0.0 & 0.4782E\text{-}01 & -0.9951E\text{-}01 & 0.7566E\text{-}02 & 0.8900E\text{-}04 & -0.7609E\text{-}02 \\ 0.0 & 0.0 & 0.0 & 0.1034E\text{-}01 & -0.1581E\text{-}01 & -0.2613E\text{-}01 \\ 0.0 & 0.0 & 0.0 & 0.7860E\text{-}01 & 0.1089E\text{-}01 & -0.1751E{+}00 \\ 0.0 & 0.0 & 0.0 & 0.2146E{+}00 & 0.2525E\text{-}02 & -0.2158E{+}00 \\ 0.8972E{+}00 & 0.3577E{+}00 & -0.1054E{+}01 & 0.3484E\text{-}01 & 0.4098E\text{-}03 & -0.3504E\text{-}01 \end{bmatrix}$$

$\underline{K}_1 = \underline{K}_0$

Input Ramp Time: 0.5 second

Command Vector:

$u = 0.0$

$A_{n_p} = 0.0$

$q = 0.0$

$A_{y_p} = 0.1$ g (step)

$p = 0.0$

$r = 0.009641$ radian/second (step)

Table D-38

Sideforce Maneuver: Failed Model,
0.3 Mach at 30 Feet

Sampling Time: T = 0.02 second

$\bar{\alpha} = 1.0$

$\epsilon = 1.0$

$\underline{\Sigma} = \text{diag}\{\ 2.0,\ 1.0,\ 1.0,\ 1.0,\ 1.0,\ 1.0\ \}$

$$\underline{K}_0 = \begin{bmatrix} -0.4171E-16 & 0.8964E-02 & -0.2136E+00 & -0.1236E-01 & -0.1721E-04 & 0.1256E-01 \\ 0.0 & 0.4924E-01 & -0.1333E+00 & 0.1921E-01 & -0.2071E-01 & -0.4001E-01 \\ 0.0 & 0.4645E-01 & -0.6682E-01 & -0.4041E-02 & 0.2073E-01 & 0.2459E-01 \\ 0.1275E-15 & 0.2867E-03 & -0.6833E-02 & 0.7887E-01 & 0.9883E-02 & -0.1764E+00 \\ 0.6509E-15 & 0.6306E-03 & -0.1503E-01 & 0.2152E+00 & 0.2996E-03 & -0.2186E+00 \\ 0.8972E+00 & 0.3578E+00 & -0.1056E+01 & 0.3493E-01 & 0.4863E-04 & -0.3549E-01 \end{bmatrix}$$

$\underline{K}_1 = \underline{K}_0$

Input Ramp Time: 0.5 second

Command Vector:

u = 0.0

A_{n_p} = 0.0

q = 0.0

A_{y_p} = 0.1 g (step)

p = 0.0

r = 0.009641 radian/second (step)

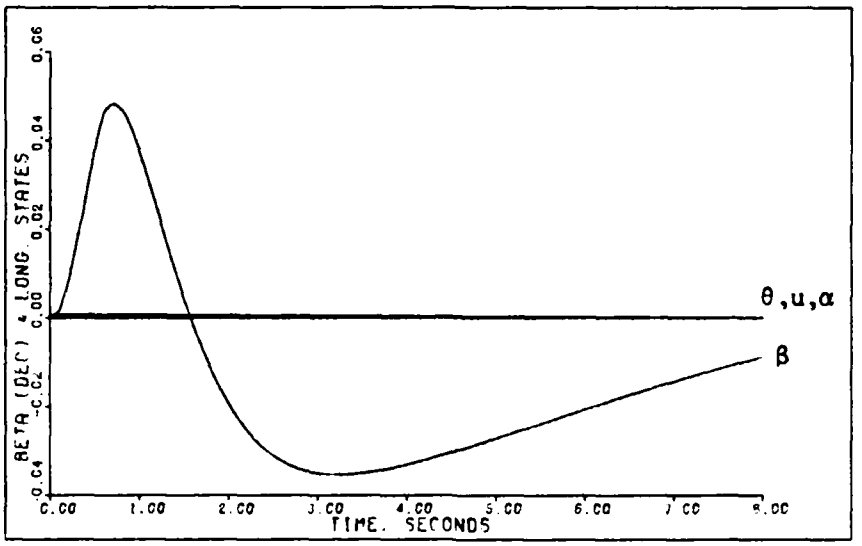

Figure D-139: 0.3M Healthy/Failed Sideforce -- Sideslip Angle, Pitch Angle, Angle of Attack, and Forward Velocity

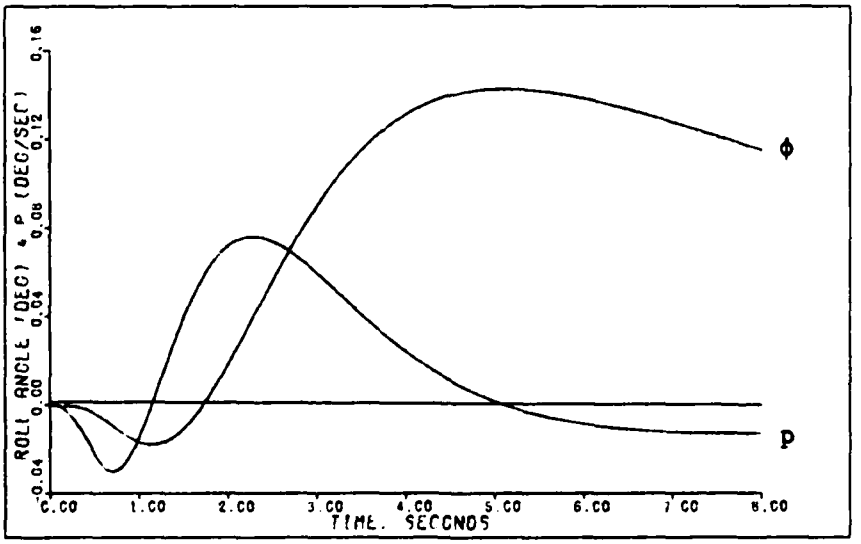

Figure D-140: 0.3M Healthy/Failed Sideforce -- Roll Angle and Roll Rate

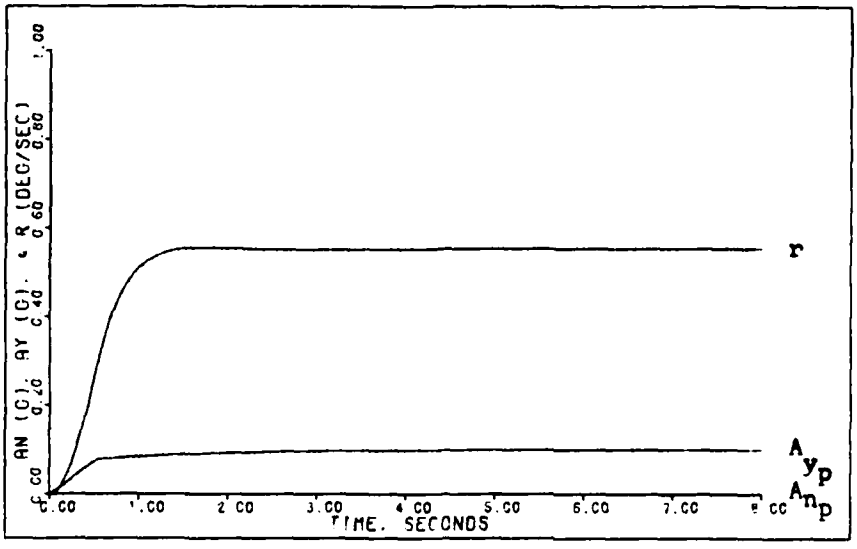

Figure D-141: 0.3M Healthy/Failed Sideforce -- Normal Acceleration, Lateral Acceleration, and Yaw Rate

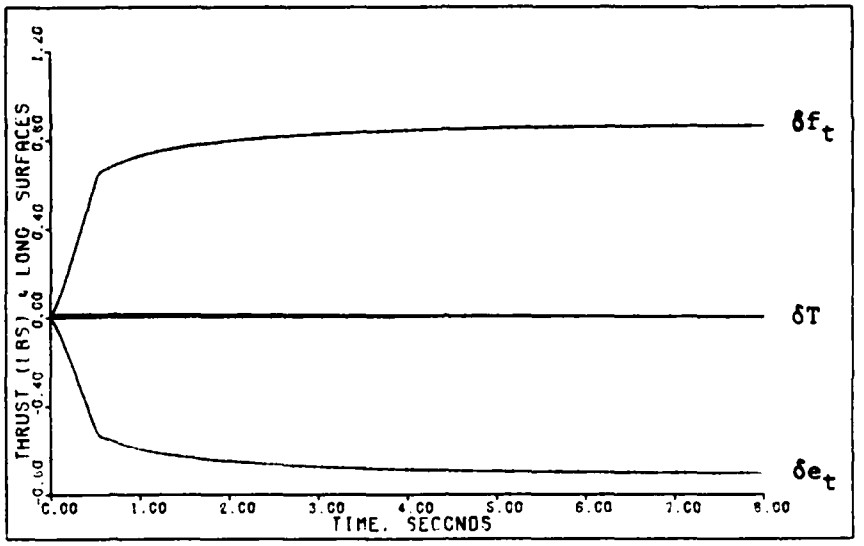

Figure D-142: 0.3M Healthy Sideforce -- Elevator and Flap Deflections and Thrust

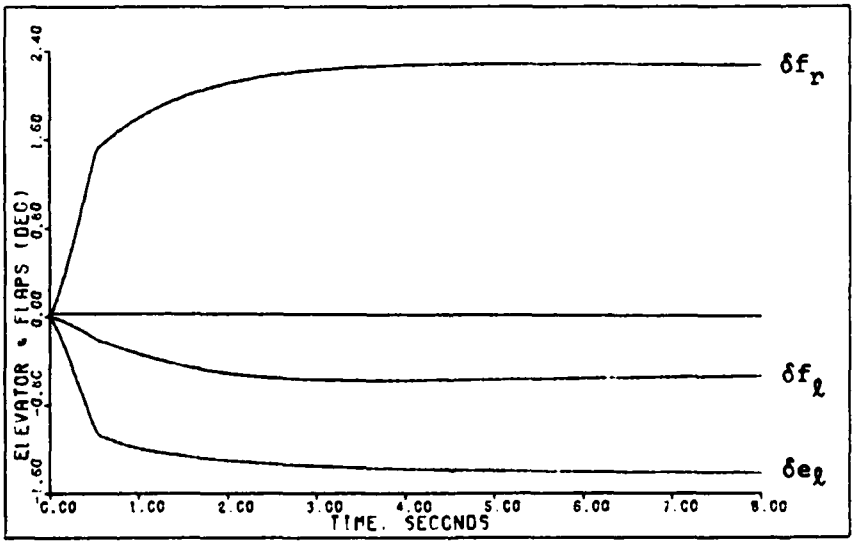

Figure D-143: 0.3M Failed Sideforce -- Left Elevator and Flaperon Deflections

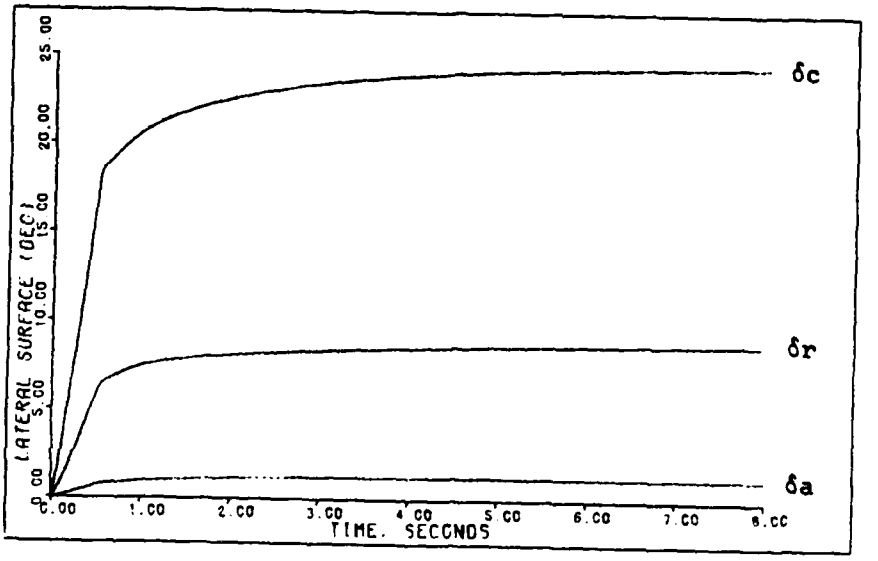

Figure D-144: 0.3M Healthy Sideforce -- Aileron, Rudder, and Canard Deflections

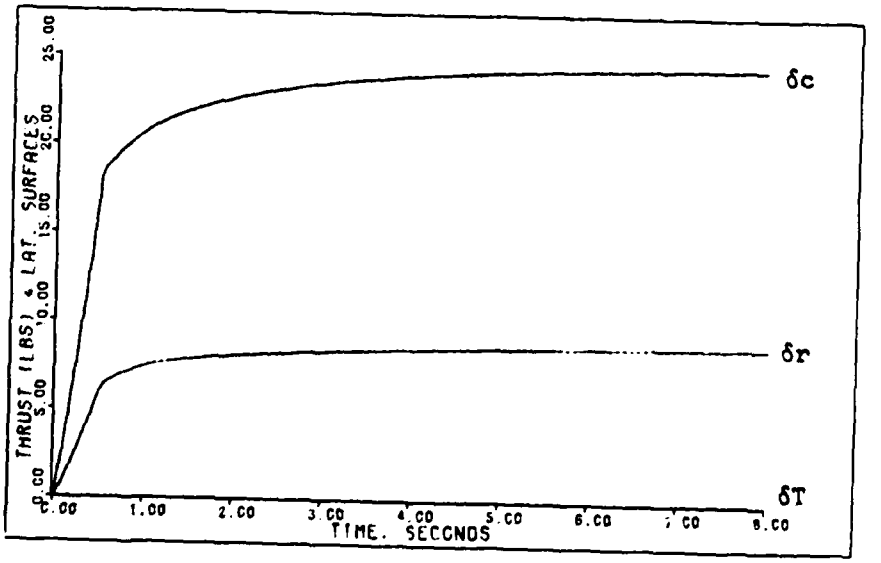

Figure D-145: 0.3M Failed Sideforce -- Rudder and Canard Deflections and Thrust

Yaw Pointing Maneuver. The design parameters for the yaw pointing maneuver are given in Tables D-39 and D-40 for both the healthy and failed models. The parameters are the same for both cases.

Figures D-146 through D-152 present the simulation responses for a three degree yaw pointing command. The maximum angle commanded for this maneuver is limited by the ability to hold the roll angle to a small value. As with the sideforce maneuver Figures D-146 through D-148 give simulation responses for both the healthy and failed aircraft models.

For the yaw pointing maneuver the horizontal tail is used for both pitch and roll control. When the right horizontal tail fails the flaperons take over the roll control and deflect slightly asymmetrically to counter the rolling moment of the left horizontal tail, which deflects for pitch control. The rudder and canard responses are not affected much by the failure for this maneuver.

Table D-39

Yaw Pointing: Healthy Model, 0.3 Mach at 30 Feet

Sampling Time: T = 0.02 second

$\bar{\alpha} = 3.0$

$\epsilon = 1.0$

$\underline{\Sigma} = \text{diag}\{ 2.0, 1.0, 1.0, 1.0, 3.0, 2.0 \}$

$$\underline{K}_0 = \begin{bmatrix} 0.0 & 0.4500E-02 & -0.1072E+00 & -0.6165E-02 & -0.2176E-03 & 0.1240E-01 \\ 0.0 & 0.4782E-01 & -0.9951E-01 & 0.7566E-02 & 0.2670E-03 & -0.1522E-01 \\ 0.0 & 0.0 & 0.0 & 0.1034E-01 & -0.4742E-01 & -0.5225E-01 \\ 0.0 & 0.0 & 0.0 & 0.7860E-01 & 0.3268E-01 & -0.3502E+00 \\ 0.0 & 0.0 & 0.0 & 0.2146E+00 & 0.7574E-02 & -0.4317E+00 \\ 0.8972E+00 & 0.3577E+00 & -0.1054E+01 & 0.3484E-01 & 0.1229E-02 & -0.7007E-01 \end{bmatrix}$$

$$\underline{K}_1 = \begin{bmatrix} 0.0 & 0.1350E-01 & -0.3217E+00 & -0.1850E-01 & -0.6527E-03 & 0.3720E-01 \\ 0.0 & 0.1435E+00 & -0.2985E+00 & 0.2270E-01 & 0.8010E-03 & -0.4565E-01 \\ 0.0 & 0.0 & 0.0 & 0.3101E-01 & -0.1422E+00 & -0.1568E+00 \\ 0.0 & 0.0 & 0.0 & 0.2358E+00 & 0.9805E-01 & -0.1051E+01 \\ 0.0 & 0.0 & 0.0 & 0.6438E+00 & 0.2272E-01 & -0.1295E+01 \\ 0.2692E+01 & 0.1073E+01 & -0.3161E+01 & 0.1045E+00 & 0.3688E-02 & -0.2102E+00 \end{bmatrix}$$

Input Ramp Time: 0.2 second

Command Vector:

$u = 0.0$

$A_{n_p} = 0.0$

$q = 0.0$

$A_{y_p} = 0.0$

$p = 0.0$

$r = -0.05236$ radian/second (1 second pulse)

Table D-40

Yaw Pointing: Failed Model, 0.3 Mach at 30 Feet

Sampling Time: T = 0.02 second

$\bar{\alpha} = 3.0$

$\epsilon = 1.0$

$\underline{\Sigma} = \text{diag}\{ 2.0, 1.0, 1.0, 1.0, 3.0, 2.0 \}$

$$\underline{K}_0 = \begin{bmatrix} -0.4171E-16 & 0.8964E-02 & -0.2136E+00 & -0.1236E-01 & -0.5164E-04 & 0.2512E-01 \\ 0.0 & 0.4924E-01 & -0.1333E+00 & 0.1921E-01 & -0.6214E-01 & -0.8001E-01 \\ 0.0 & 0.4645E-01 & -0.6682E-01 & -0.4041E-02 & 0.6220E-01 & 0.4918E-01 \\ 0.1275E-15 & 0.2867E-03 & -0.6833E-02 & 0.7887E-01 & 0.2965E-01 & -0.3527E+00 \\ 0.6509E-15 & 0.6306E-03 & -0.1503E-01 & 0.2152E+00 & 0.8987E-03 & -0.4372E+00 \\ 0.8972E+00 & 0.3578E+00 & -0.1056E+01 & 0.3493E-01 & 0.1459E-03 & -0.7098E-01 \end{bmatrix}$$

$$\underline{K}_1 = \begin{bmatrix} -0.1251E-15 & 0.2689E-01 & -0.6408E+00 & -0.3709E-01 & -0.1549E-03 & 0.7537E-01 \\ 0.0 & 0.1477E+00 & -0.3998E+00 & 0.5764E-01 & -0.1864E+00 & -0.2400E+00 \\ 0.0 & 0.1394E+00 & -0.2005E+00 & -0.1212E-01 & 0.1866E+00 & 0.1476E+00 \\ 0.3826E-15 & 0.8602E-03 & -0.2050E-01 & 0.2366E+00 & 0.8895E-01 & -0.1058E+01 \\ 0.1953E-14 & 0.1892E-02 & -0.4508E-01 & 0.6456E+00 & 0.2696E-02 & -0.1312E+01 \\ 0.2692E+01 & 0.1073E+01 & -0.3168E+01 & 0.1048E+00 & 0.4376E-03 & -0.2129E+00 \end{bmatrix}$$

Input Ramp Time: 0.2 second

Command Vector:

$u = 0.0$

$A_{n_p} = 0.0$

$q = 0.0$

$A_{y_p} = 0.0$

$p = 0.0$

$r = -0.05236$ radian/second (1 second pulse)

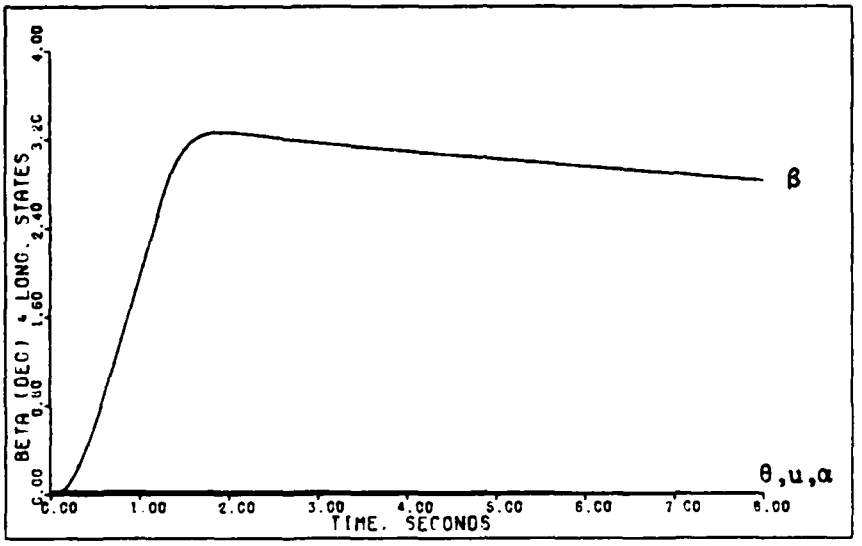

Figure D-146: 0.3M Healthy/Failed Yaw Pointing -- Sideslip Angle, Pitch Angle, Angle of Attack, and Forward Velocity

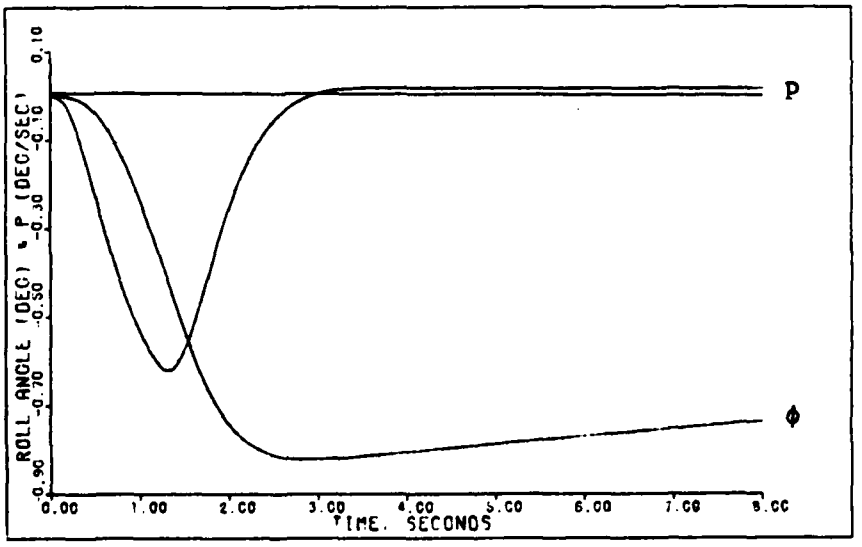

Figure D-147: 0.3M Healthy/Failed Yaw Pointing -- Roll Angle and Roll Rate

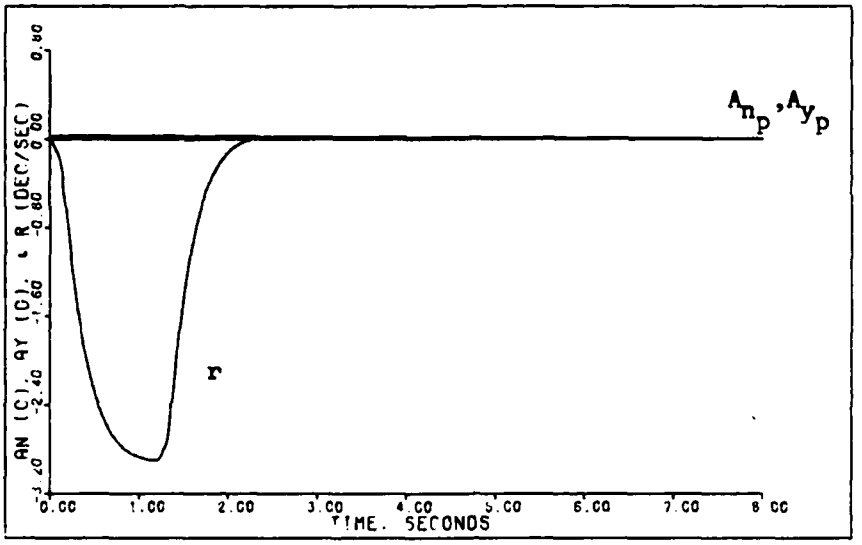

Figure D-148: 0.3M Healthy/Failed Yaw Pointing -- Normal Acceleration, Lateral Acceleration, and Yaw Rate

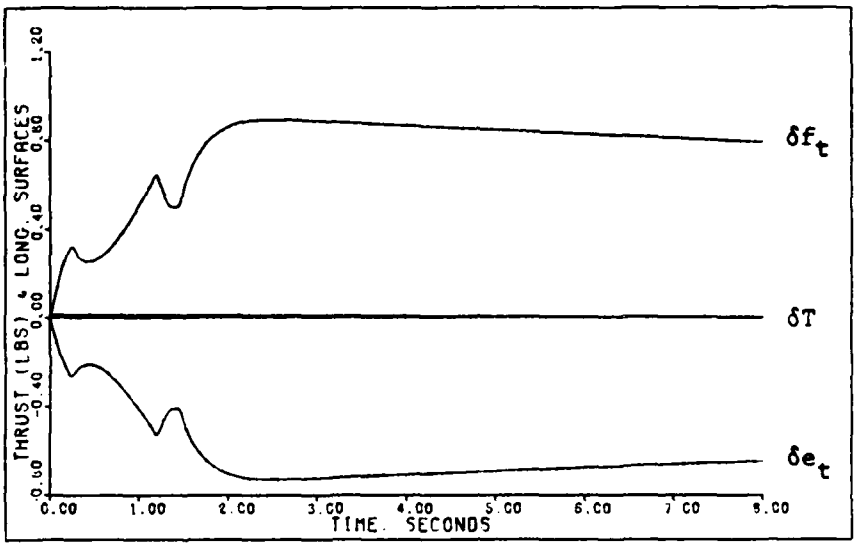

Figure D-149: 0.3M Healthy Yaw Pointing -- Elevator and Flap Deflections and Thrust

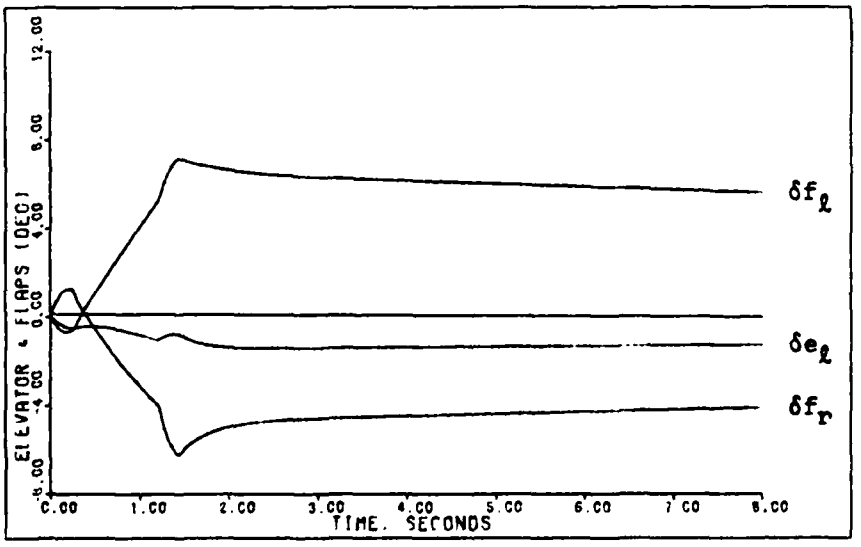

Figure D-150: 0.3M Failed Yaw Pointing -- Left Elevator and Flaperon Deflections

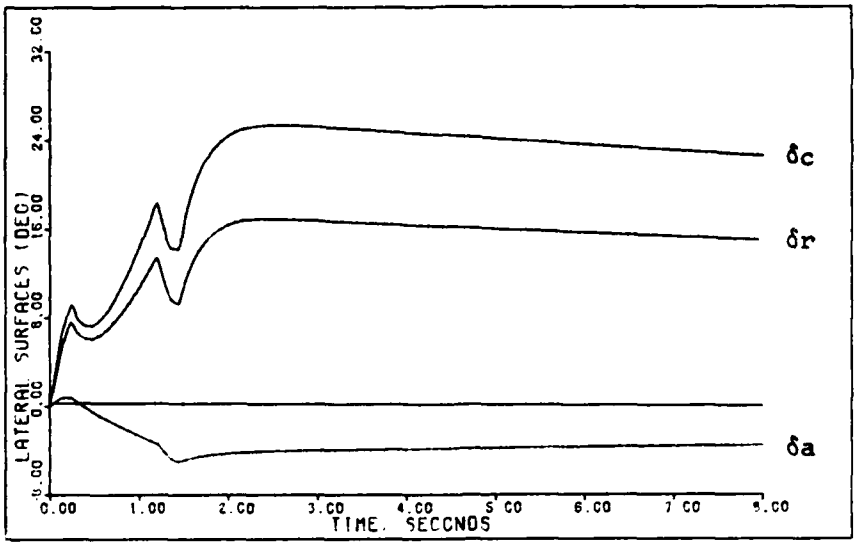

Figure D-151: 0.3M Healthy Yaw Pointing -- Aileron, Rudder, and Canard Deflections

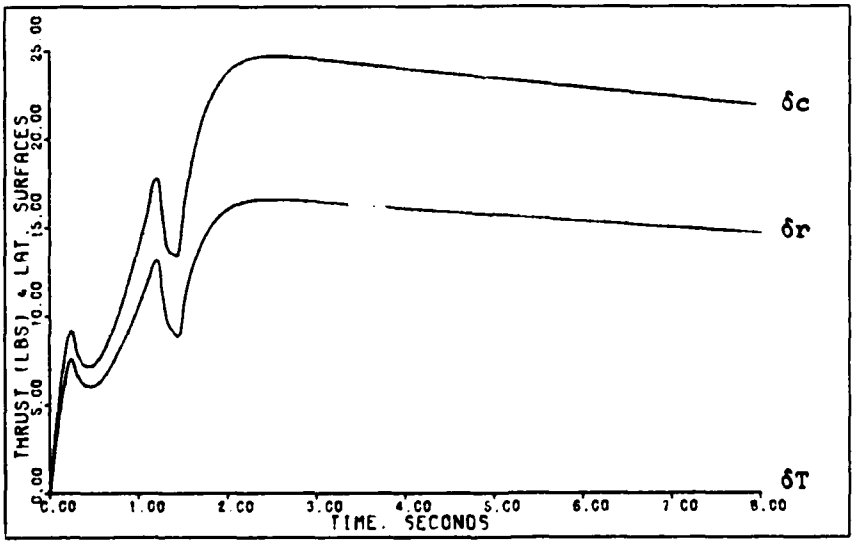

Figure D-152: 0.3M Failed Yaw Pointing -- Rudder and Canard Deflections and Thrust

Lateral Translation Maneuver. Tables D-41 and D-42 give the design parameters for the lateral translation maneuver. As indicated in the tables the same design parameters are used for both the healthy and failed aircraft models.

The simulation responses for a 0.1 g lateral acceleration command, which corresponds to a steady-state lateral velocity value of 4.5 feet/second, are given in Figures D-153 through D-159. The maximum lateral acceleration commanded for this maneuver is limited by the canard deflection. As explained for the sideforce maneuver, Figures D-153 through D-155 give simulation responses for both the healthy and failed aircraft models.

For the lateral translation maneuver the horizontal tail is used mainly as an elevator to counter the small pitch moment generated by the canard deflection. When the right horizontal tail fails the left horizontal tail deflects to approximately twice the elevator deflection of the healthy aircraft simulation, and the flaperons deflect asymmetrically to counter the rolling moment of the left horizontal tail. The rudder and canard responses are not affected much by the failure for this maneuver.

Table D-41

Lateral Translation: Healthy Model,
0.3 Mach at 30 Feet

Sampling Time: T = 0.02 second

$\bar{\alpha} = 1.0$

$\epsilon = 1.0$

$\underline{\Sigma} = \text{diag}\{\ 2.0,\ 1.0,\ 1.0,\ 2.5,\ 1.5,\ 1.0\}$

$$\underline{K}_0 = \begin{bmatrix} 0.0 & 0.4500E-02 & -0.1072E+00 & -0.1541E-01 & -0.1088E-03 & 0.6201E-02 \\ 0.0 & 0.4782E-01 & -0.9951E-01 & 0.1891E-01 & 0.1335E-03 & -0.7609E-02 \\ 0.0 & 0.0 & 0.0 & 0.2584E-01 & -0.2371E-01 & -0.2613E-01 \\ 0.0 & 0.0 & 0.0 & 0.1965E+00 & 0.1634E-01 & -0.1751E+00 \\ 0.0 & 0.0 & 0.0 & 0.5365E+00 & 0.3787E-02 & -0.2158E+00 \\ 0.8972E+00 & 0.3577E+00 & -0.1054E+01 & 0.8709E-01 & 0.6147E-03 & -0.3504E-01 \end{bmatrix}$$

$\underline{K}_1 = \underline{K}_0$

Input Ramp Time: 0.4 second

Command Vector:

$u = 0.0$

$A_{n_p} = 0.0$

$q = 0.0$

$A_{y_p} = 0.1$ g (1 second pulse)

$p = 0.0$

$r = 0.0$

Table D-42

Lateral Translation: Failed Model,
0.3 Mach at 30 Feet

Sampling Time: T = 0.02 second

$\bar{\alpha} = 1.0$

$\varepsilon = 1.0$

$\Sigma = \text{diag}\{ 2.0, 1.0, 1.0, 2.5, 1.5, 1.0\}$

$$\underline{K}_0 = \begin{bmatrix} -0.4171E-16 & 0.8964E-02 & -0.2136E+00 & -0.3091E-01 & -0.2582E-04 & 0.1256E-01 \\ 0.0 & 0.4924E-01 & -0.1333E+00 & 0.4803E-01 & -0.3107E-01 & -0.4001E-01 \\ 0.0 & 0.4645E-01 & -0.6682E-01 & -0.1010E-01 & 0.3110E-01 & 0.2459E-01 \\ 0.1275E-15 & 0.2867E-03 & -0.6833E-02 & 0.1972E+00 & 0.1482E-01 & -0.1764E+00 \\ 0.6509E-15 & 0.6306E-03 & -0.1503E-01 & 0.5380E+00 & 0.4493E-03 & -0.2186E+00 \\ 0.8972E+00 & 0.3578E+00 & -0.1056E+01 & 0.8733E-01 & 0.7294E-04 & -0.3549E-01 \end{bmatrix}$$

$\underline{K}_1 = \underline{K}_0$

Input Ramp Time: 0.4 second

Command Vector:

$u = 0.0$

$A_{n_p} = 0.0$

$q = 0.0$

$A_{y_p} = 0.1$ g (1 second pulse)

$p = 0.0$

$r = 0.0$

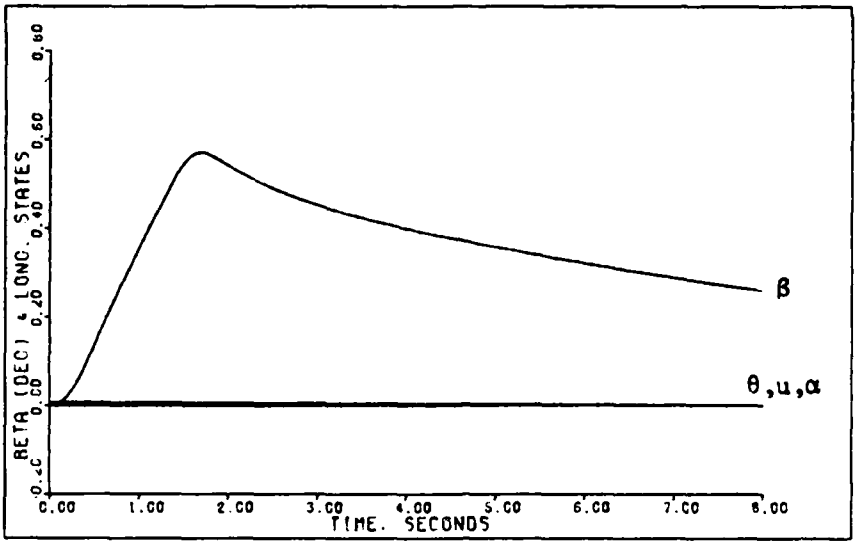

Figure D-153: 0.3M Healthy/Failed Lateral Translation -- Sideslip Angle, Pitch Angle, Angle of Attack, and Forward Velocity

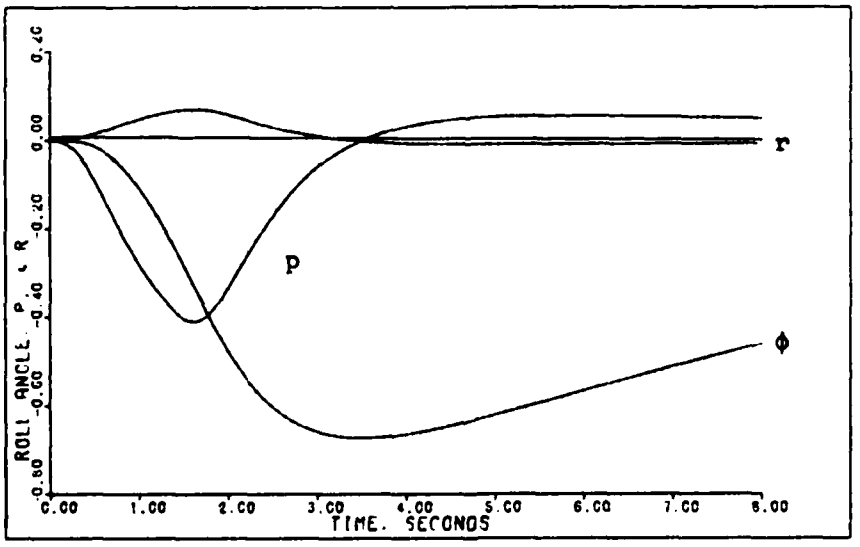

Figure D-154: 0.3M Healthy/Failed Lateral Translation -- Roll Angle, Roll Rate, and Yaw Rate

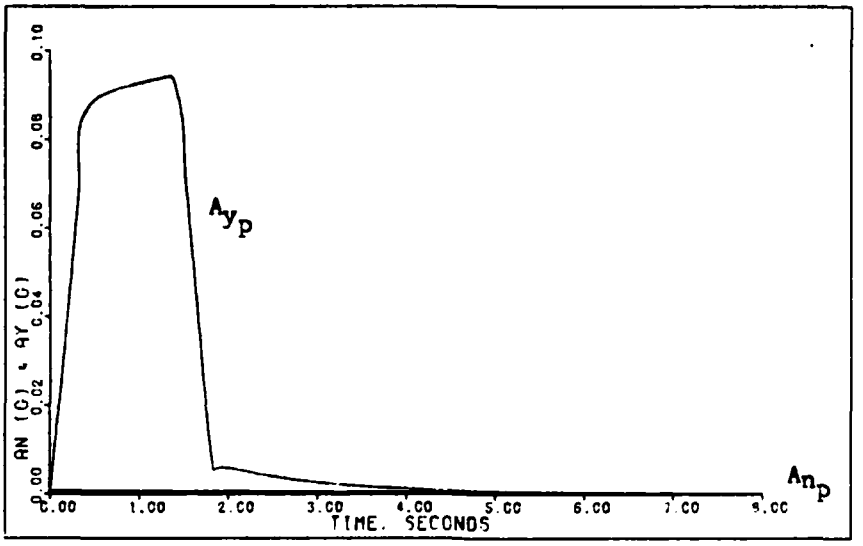

Figure D-155: 0.3M Healthy/Failed Lateral Translation -- Normal Acceleration and Lateral Acceleration

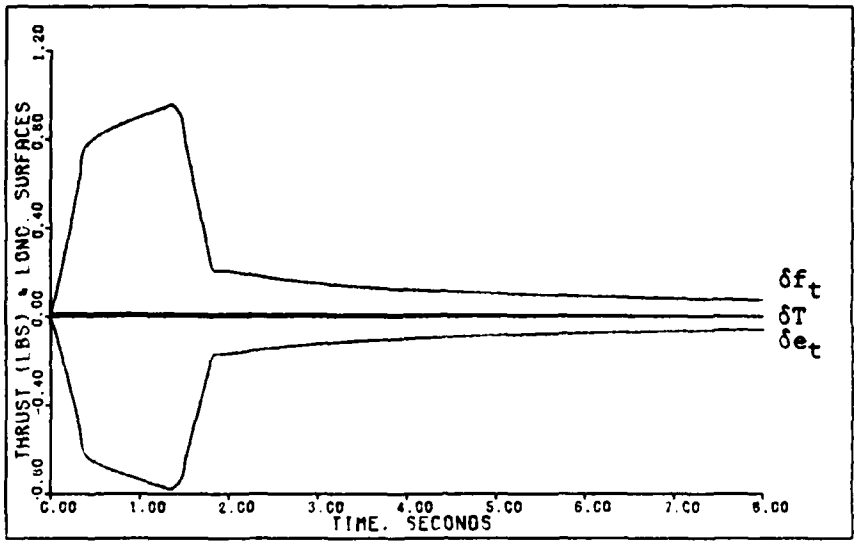

Figure D-156: 0.3M Healthy Lateral Translation -- Elevator and Flap Deflections and Thrust

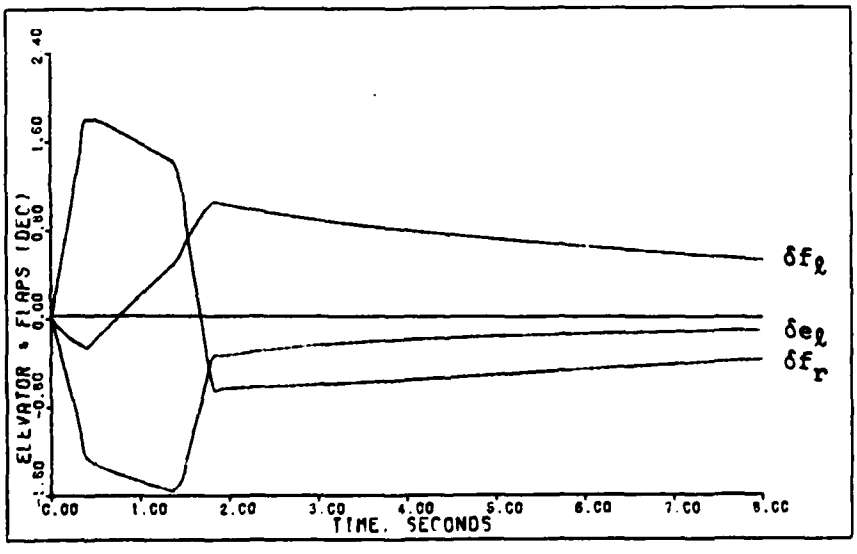

Figure D-157: 0.3M Failed Lateral Translation -- Left Elevator and Flaperon Deflections

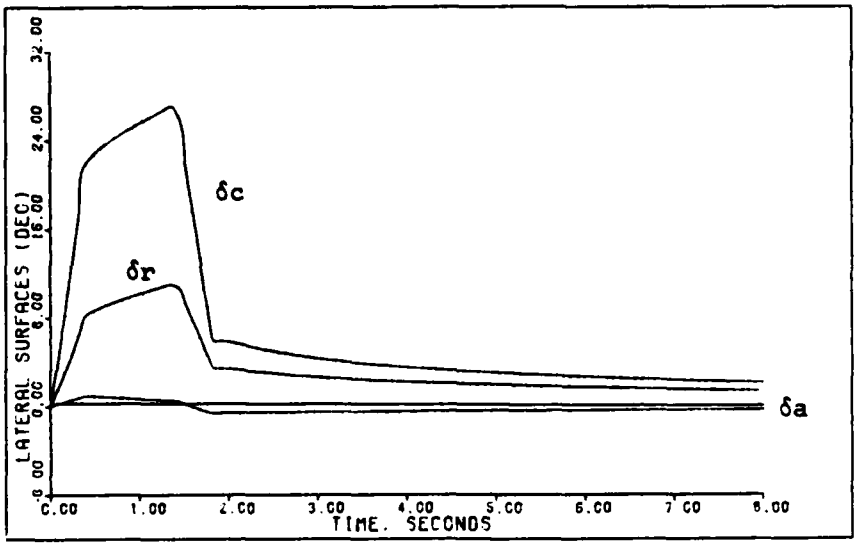

Figure D-158: 0.3M Healthy Lateral Translation -- Aileron, Rudder, and Canard Deflections

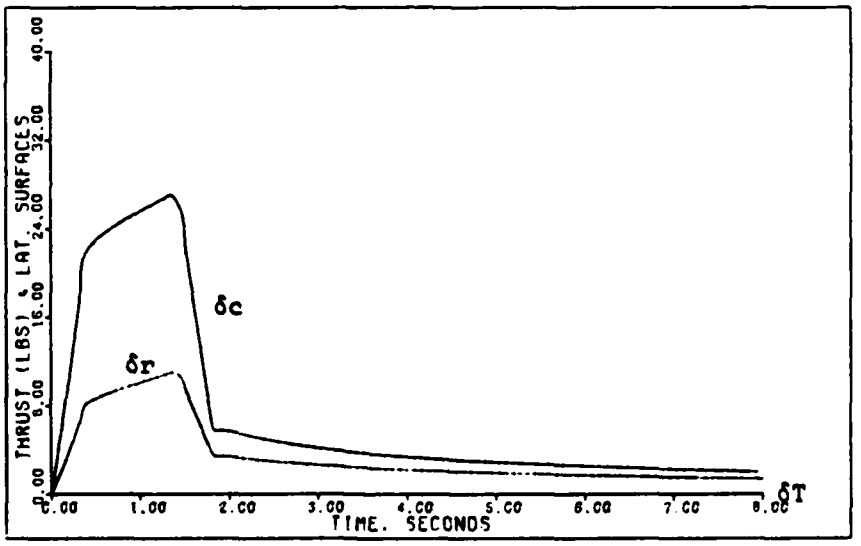

Figure D-159: 0.3M Failed Lateral Translation -- Rudder and Canard Deflections and Thrust

VITA

Second Lieutenant Robert A. Eslinger was born 14 October 1961 in Chambersburg, Pennsylvania. He graduated from the Chambersburg Area Senior High School in 1979 and attended the Pennsylvania State University from which he received the degree of Bachelor of Science in Electrical Engineering in May 1983. Upon graduation, he received a commission in the USAF through the ROTC program. He entered the School of Engineering, Air Force Institute of Technology, in June 1983.

Permanent Address: 620 Stanley Avenue
Chambersburg, PA 17201

UNCLASSIFIED

SECURITY CLASSIFICATION OF THIS PAGE

REPORT DOCUMENTATION PAGE

1a. REPORT SECURITY CLASSIFICATION: UNCLASSIFIED	1b. RESTRICTIVE MARKINGS
2a. SECURITY CLASSIFICATION AUTHORITY	3. DISTRIBUTION/AVAILABILITY OF REPORT: Approved for public release; distribution unlimited.
2b. DECLASSIFICATION/DOWNGRADING SCHEDULE	
4. PERFORMING ORGANIZATION REPORT NUMBER(S): AFIT/GE/ENG/84D-28	5. MONITORING ORGANIZATION REPORT NUMBER(S)
6a. NAME OF PERFORMING ORGANIZATION: School of Engineering; 6b. OFFICE SYMBOL (If applicable): AFIT/ENG	7a. NAME OF MONITORING ORGANIZATION
6c. ADDRESS (City, State and ZIP Code): Air Force Institute of Technology, Wright-Patterson AFB, Ohio 45433	7b. ADDRESS (City, State and ZIP Code)
8a. NAME OF FUNDING/SPONSORING ORGANIZATION: AFTI/F-16 ADPO; 8b. OFFICE SYMBOL (If applicable): AFWAL/FII	9. PROCUREMENT INSTRUMENT IDENTIFICATION NUMBER
8c. ADDRESS (City, State and ZIP Code): Wright-Patterson AFB, Ohio 45433	10. SOURCE OF FUNDING NOS. — PROGRAM ELEMENT NO. / PROJECT NO. / TASK NO. / WORK UNIT NO.
11. TITLE (Include Security Classification): See Box 19	
12. PERSONAL AUTHOR(S): Robert A. Eslinger, B.S., 2d Lt, USAF	
13a. TYPE OF REPORT: MS Thesis; 13b. TIME COVERED: FROM _____ TO _____; 14. DATE OF REPORT (Yr., Mo., Day): 1984 December; 15. PAGE COUNT: 347	
16. SUPPLEMENTARY NOTATION	

17. COSATI CODES		
FIELD	GROUP	SUB. GR.
01	03	

18. SUBJECT TERMS (Continue on reverse if necessary and identify by block number): Flight Control Systems, Failure, Control Theory, Damage Control, Fly By Wire Control, Self Organizing Systems.

19. ABSTRACT (Continue on reverse if necessary and identify by block number)

Title: MULTIVARIABLE CONTROL LAW DESIGN FOR THE AFTI/F-16 WITH A FAILED CONTROL SURFACE

Thesis Chairman: John J. D'Azzo, Ph.D.

Approved for public release. IAW AFR 190-17.

LYNN E. WOLAVER
Dean for Research and Professional Development
Air Force Institute of Technology (AIC)
Wright-Patterson AFB OH 45433

20. DISTRIBUTION/AVAILABILITY OF ABSTRACT: UNCLASSIFIED/UNLIMITED ☒ SAME AS RPT. ☐ DTIC USERS ☐	21. ABSTRACT SECURITY CLASSIFICATION: UNCLASSIFIED
22a. NAME OF RESPONSIBLE INDIVIDUAL: John J. D'Azzo, Ph.D.	22b. TELEPHONE NUMBER (Include Area Code): 513-255-3576; 22c. OFFICE SYMBOL: AFIT/ENG

DD FORM 1473, 83 APR EDITION OF 1 JAN 73 IS OBSOLETE.

UNCLASSIFIED

SECURITY CLASSIFICATION OF THIS PAGE

Two linearized models containing coupled aircraft equations are developed for the AFTI/F-16. The first is a model of the healthy aircraft with all control surfaces intact, and the second is a model of the aircraft with a free-floating right horizontal tail and all other surfaces operational.

The multivariable design technique of Professor Brian Porter and the computer program MULTI are first used to design control laws for the healthy model. The control laws are tailored to perform seven maneuvers at four flight conditions. Maximum maneuvers are commanded to yield maximum control surface deflections.

The same control law designs are then applied to the model with a failed right horizontal tail, and the performance is evaluated. Some maneuvers require modifications to the designs or lowered maximum maneuver requirements to avoid overshooting the deflection limits of the operational control surfaces.

Simulation responses are presented for both the healthy and failure aircraft models. Generally, when the right horizontal tail fails, the left horizontal tail assumes primary pitch control and the flaperons take over complete roll control. The flaperons, rudder, and canards deflect to counter the rolling and yawing moments produced by the left horizontal tail deflection.

The design process used in the study is applicable to other control surface failures. Recommendations are presented for future study.

END

FILMED

4-85

DTIC